MANCHESTER 1824

The University of Manchester

Building a predictive model for PHB production from glycerol

A thesis submitted to The University of Manchester for the degree of Doctor of Philosophy in the Faculty of Science & Engineering

Cristina Pérez Rivero

School of Chemical Engineering and Analytical Sciences

2017

Table of contents

LIST OF FIGURES **7**

LIST OF TABLES **13**

NOMENCLATURE **14**

ABSTRACT **16**

DECLARATION AND COPYRIGHT STATEMENT **17**

ACKNOWLEDGMENTS **19**

CHAPTER 1 *DESCRIBING MICROBIAL KINETICS FOR BIOPROCESS DESIGN* **21**

1.1 THE INCREASING IMPORTANCE OF BIOPROCESSING 23

1.2 THE CHALLENGE OF BIOPROCESSING 25

1.3 CONSIDERATIONS FOR DESIGN 27

1.3.1 Classification of models *27*

1.3.2 Kinetics of biomass production, product formation and substrate utilization in cell cultures *29*

1.3.3 Other factors affecting the design *34*

CHAPTER 2 *PHB PRODUCTION: A REVIEW OF THE LITERATURE* **37**

2.1 INTRODUCTION 39

2.1.1 Carbon storage in living organisms *39*

2.1.2 Storage compounds of current interest *41*

2.2 POLYHYDROXYBUTYRATE, A TYPICAL PHA WITH INTERESTING PROPERTIES 42

2.3 INTEGRATING PHB PRODUCTION WITH BIODIESEL INDUSTRY 45

2.4 MICROBIOLOGY, METABOLISM & ENZYMATIC REGULATION OF *C. NECATOR* 48

2.5 FACTORS AFFECTING PHB PRODUCTION 51

2.5.1 Culture medium *51*

2.5.2 The importance of Carbon to Nitrogen ratio (C/N) *52*

2.5.3 Physical operational variables *54*

2.5.4 Mode of operation *55*

2.6 KINETIC MODELS: CAN THEY BE TOOLS FOR PHA OPTIMIZATION? 56

2.6.1 Description of formal kinetics for PHB production *56*

2.6.2 Application of formal kinetics for optimization of PHB production *59*

2.7 PROJECT AIMS AND OBJECTIVES 62

CHAPTER 3 *PROGRAMME, MATERIALS AND METHODS* **65**

3.1 RESEARCH PROGRAMME 67
3.2 MATERIALS AND METHODS 68
3.2.1 Microorganism 68
3.2.2 Media preparation 72
3.2.3 Cultivation techniques 72
3.2.4 Analytical techniques 74
3.2.5 Data interpretation 80
3.2.6 Error analysis 82
3.2.7 Computational methods 83

CHAPTER 4 *ADAPTATION OF C. NECATOR FOR GLYCEROL CONSUMPTION* 85

4.1 INTRODUCTION 87
4.2 METHODOLOGY 88
4.2.1 Serial sub-cultivation 89
4.2.2 Bio-training 89
4.3 RESULTS 90
4.3.1 Effect of serial sub-cultivation on growth and glycerol utilization 90
4.3.2 Stability of the adaptation 93
4.3.3 Post adaptation growth on a glucose-glycerol mixture 93
4.3.4 A potential mechanism for adaptation 94
4.3.5 Bio-training 96
4.4 CONCLUSIONS 98

CHAPTER 5 *BUILDING A PRELIMINARY MACROSCOPIC MODEL* 101

5.1 INTRODUCTION 103
5.1.1 PHB production process 103
5.1.2 Microbial PHB production and detection during cultivation 104
5.1.3 Measurement of cell concentration in suspension by optical density 105
5.1.4 Example of a simple batch culture for PHB production 107
5.2 STUDIES ON THE INFLUENCE OF GLYCEROL CONCENTRATION ON PHB PRODUCTION 109
5.2.1 Effect on growth rate 109
5.2.2 Effect on PHB accumulation 110
5.2.3 Glycerol consumption 111
5.2.4 Overall yields and mass balances 112
5.2.5 Discussion 114
5.3 STUDIES ON THE INFLUENCE OF NITROGEN CONCENTRATION ON GROWTH AND PHB PRODUCTION 115
5.3.1 Effect on growth rate 115
5.3.2 Effect on PHB accumulation 118
5.3.3 Nitrogen consumption 120
5.3.4 Test with an organic source 121

5.4 DEVELOPING A BIOMASS PRODUCTION HYPOTHESIS 122
5.5 FORMULATING THE MODEL EQUATIONS 123

CHAPTER 6 *TESTING AND DEVELOPING THE MODEL FOR DIFFERENT MODES OF OPERATION* **127**

6.1 INTRODUCTION 129
6.2 SHAKE FLASK FERMENTATION 129
6.2.1 Determination of kinetic constants *129*
6.2.2 Model limitations *131*
6.2.3 Introducing the carrying capacity concept *133*
6.2.4 Model evaluation *135*
6.2.5 Exploring the behavior of the system through model-based simulations *137*
6.3 BIOREACTOR STUDIES 140
6.3.1 Sensitivity analysis *142*
6.3.2 Studies on the mode of operation *143*
6.4 DISCUSSION 153

CHAPTER 7 *PRELIMINARY STUDIES INTO THE INFLUENCE OF AERATION* **155**

7.1 INTRODUCTION AND THEORETICAL BACKGROUND 157
7.1.1 Oxygen transfer rate *158*
7.1.2 Oxygen uptake rate *161*
7.1.3 Kinetics of specific oxygen consumption *162*
7.2 METHODOLOGY: DYNAMIC METHOD 162
7.3 RESULTS AND DISCUSSION 163
7.3.1 Determination of OUR by dynamic method *163*
7.3.2 Relationship between specific oxygen consumption and dissolved oxygen *166*
7.3.3 Determination of k_La *167*
7.3.4 Variation of k_La with agitation and flow rate *171*
7.4 CONCLUSIONS 172

CHAPTER 8 *CONCLUSIONS AND RECOMMENDATIONS* **175**

8.1 INTRODUCTION 177
8.2 CONCLUSIONS 177
8.3 RECOMMENDATIONS 182

ASSOCIATED PUBLICATIONS **185**

BIBLIOGRAPHY **189**

Word count: 54259

List of figures

FIGURE 1-1:TRENDS IN NUMBER OF PUBLICATIONS RELATED TO BIOBASED POLYMERS OVER RECENT YEARS (SCOPUS 2016). 24

FIGURE 1-2: A MODEL GIVES THE RELATIONSHIP BETWEEN INPUTS AND OUTPUTS OF A DETERMINED SYSTEM. LT CAN BE USED TO DETERMINE THE OUTPUT BASED ON A CERTAIN INPUT OR TO FIND AN INPUT THAT WOULD GIVE THE DESIRED OUTPUT (OPTIMIZATION).....26

FIGURE 1-3: DEGREES OF COMPLEXITY IN FERMENTATION MODELS (BAILEY 1998).....28

FIGURE 1-4: DEPENDENCE OF SPECIFIC GROWTH RATE ON SUBSTRATE CONCENTRATION REPRESENTED THROUGH A MONOD EXPRESSION WITH DIFFERENT VALUES FOR K_S: 0.13 MM (DASHED-PINK LINE), 0.28 MM (BLUE LINE) AND 0.69 MM (X-GREEN LINE) FOR A CONSTANT VALUE OF μmax (0.4 H^{-1}).....30

FIGURE 1-5: REPRESENTATION OF MONOD AND TESSIER MODELS FOR DESCRIBING GROWTH RATE AS FUNCTION OF THE LIMITING SUBSTRATE WITH μmax= 0.4 H^{-1} AND KS = 0.13 MM. 31

FIGURE 2-1: CELLULAR FUNCTIONS OF STORAGE PRODUCTS INFLUENCING BACTERIAL FITNESS (PRIETO *ET AL.,* 2014).....40

FIGURE 2-2: DIFFERENT SPECIES FROM FILAMENTOUS FUNGI, YEAST AND MICROALGAE CAN ACCUMULATE LIPIDS WITHIN THE CYTOPLASM (DISALVO 2010; BIOENERGY GENOME CENTER 2011). THESE ORGANISMS ARE CALLED OLEAGINOUS WHEN THEY CAN ACCUMULATE MORE THAN 20% OF THEIR DRY WEIGHT AS OIL (MENG *ET AL.,* 2009). 41

FIGURE 2-3: POLYHYDROXYALKANOATE CHEMICAL STRUCTURE. THE CARBON DENOTED AS C* IS THE CHIRAL CENTRE OF THE PHA BUILDING BLOCK (TAN *ET AL.,* 2014). 42

FIGURE 2-4: DEGRADATION PROCESS AFTER A 2 MONTHS INCUBATION IN SOILS SUSPENSION UNDER DIFFERENT CONDITIONS: ORIGINAL PHB FILM (A) , ANAEROBIC CONDITIONS WITHOUT NITRATE (B), MICROAEROBIC CONDITIONS WITHOUT NITRATE (C), MICROAEROBIC CONDITIONS WITH NITRATE (D) (IORDANSKII *ET AL.,* 2014). 43

FIGURE 2-5: PROCESS INTEGRATION WITHIN A BIODIESEL PLANT. CRUDE GLYCEROL CO-GENERATED ALONG WITH THE BIODIESEL CAN BE USED AS BACTERIAL FERMENTATION FEEDSTOCK FOR THE PRODUCTION OF CHEMICALS. 46

FIGURE 2-6: SCHEMATIC REPRESENTATION OF A PHB GRANULE CONSISTING OF A POLYMER CORE AND A SURFACE LAYER OF STRUCTURAL AND FUNCTIONAL PROTEINS (BRESAN *ET AL.,* 2016) 48

FIGURE 2-7: METABOLIC PATHWAY INVOLVED IN THE SYNTHESIS AND BREAKDOWN OF PHB IN *C. NECATOR* (*R. EUTROPHA)* (LEE 1996). 49

FIGURE 2-8: RELATIONSHIP BETWEEN C/N AND PHB (SQUARES) AND CELLULAR PROTEIN (CIRCLES) CONCENTRATION ACCORDING TO DUCHARS & ATTWOOD (1989).....53

FIGURE 2-9: CONTROL OF GROWTH AND PHB PRODUCTION COULD BE ACHIEVED BY MANIPULATING NITROGEN AND OXYGEN CONCENTRATIONS. THE DIRECTION OF THE ARROWS INDICATES INCREASING CONCENTRATION. 55

FIGURE 2-10: ITERATIVE PROCESS FOR THE DEVELOPMENT AND IMPROVEMENT OF THE MODEL. ONCE THE MODEL PARAMETERS HAVE BEEN DETERMINED, THE PROPOSED METHODOLOGY CAN BE SIMPLIFIED SO THAT EXPERIMENTS TO TEST THE MODEL RESULTS ARE NOT REQUIRED EVERY TIME (DISCONTINUOUS LINE).....63

FIGURE 3-1: *CUPRIAVIDUS NECATOR* DSM 545 AFTER TWO DAYS CULTIVATION ON SOLID CULTURE MEDIUM. 69

FIGURE 3-2: PROCEDURE FOR CREATING WORKING STOCKS FOR CELL BANKING (BIONIQUE® TESTING LABORATORIES 2016). 69

FIGURE 3-3: MICROSCOPE IMAGE FROM *C. NECATOR* CELLS AFTER THE GRAM STAINING TEST. 70

FIGURE 3-4: *C. NECATOR* CELLS STAINED WITH SUDAN BLACK FOR THE OBSERVATION OF PHA GRANULES (JARI *ET AL.* 2015). 71
FIGURE 3-5: TEM IMAGE (FROM THIS WORK) OF A *C. NECATOR* CELL CONTAINING NUMEROUS PHB GRANULES. 72
FIGURE 3-6: SCHEMATICS OF INOCULUM DEVELOPMENT PROGRAMME FOR *C. NECATOR* CULTURE IN BIOREACTOR. 73
FIGURE 3-7: SCHEMATIC REPRESENTATION OF THE EXPERIMENTAL SET-UP FOR BIOREACTOR FED-BATCH FERMENTATIONS. 73
FIGURE 3-8: CHROMATOGRAM OBTAINED DURING GLYCEROL ANALYSIS IN A HPLC. THE GLYCEROL PEAK EMERGED AT T=13 MIN OF RUN. 75
FIGURE 3-9: CALIBRATION CURVE USED FOR CONVERTING HPLC MEASUREMENTS TO GLYCEROL CONCENTRATIONS..... 76
FIGURE 3-10: CALIBRATION CURVE USED FOR CONVERTING HPLC MEASUREMENTS TO GLUCOSE CONCENTRATIONS..... 76
FIGURE 3-11: STEPS IN THE SAMPLE PREPARATION FOR PHB ANALYSIS BY GC. THE DRIED BIOMASS (PICTURE ON THE LEFT) IS WEIGHTED AND A TRANSESTERIFICATION REACTION CONVERTS THE PHB INTO A MORE SOLUBLE FORM (PICTURE IN THE MIDDLE), WHICH IS EXTRACTED IN THE ORGANIC PHASE AFTER THE ADDITION OF WATER (PICTURE ON THE RIGHT). 78
FIGURE 3-12: SAMPLE PREPARATION FOR DETERMINATION OF POLYHYDROXYBUTYRATE (PHB) BY GAS CHROMATOGRAPHY. 79
FIGURE 3-13: TYPICAL CHROMATOGRAM OBTAINED DURING PHB ANALYSIS IN A GC-FID. THE PHB PEAK EMERGED AT T=15.875 MIN OF RUN..... 79
FIGURE 3-14: CALIBRATION CURVE USED FOR OBTAINING THE MASS VALUES OF PHB FROM GC-FID AREA MEASUREMENTS..... 80
FIGURE 3-15: LOGARITHMIC PLOT OF GROWTH CURVE, NATURAL LOG OF BIOMASS CONCENTRATION (*E.G.* OD) VERSUS TIME IN A BATCH CULTURE. 81
FIGURE 3-16: GROWTH CURVES FOR CONSECUTIVE RUNS IN GLYCEROL RICH MEDIUM. 82
FIGURE 4-1: MEMBRANE PERMEABILITY COEFFICIENT OF DIFFERENT COMPOUNDS ACROSS THE MEMBRANE OF AN ALGAL SPECIES (*CHARA*). PERMEABILITY CORRELATES WELL WITH LIPID SOLUBILITY, REPRESENTED BY THE OIL-WATER PARTITION COEFFICIENT. ADAPTED FROM COLLANDER (1937)..... 88
FIGURE 4-2: SCHEMATIC REPRESENTATION OF THE SERIAL SUB-CULTIVATION PROCESS FOR CELL ADAPTATION. 89
FIGURE 4-3: SCHEMATIC REPRESENTATION OF THE BIO-TRAINING PROCESS FOR CELL ADAPTATION. 89
FIGURE 4-4: BIOMASS CONCENTRATION PROFILES FOR THE DIFFERENT SUB-CULTIVATIONS (RUN 1 TO 6) OF *C.NECATOR* 545 IN 20 G/L GLYCEROL..... 90
FIGURE 4-5: CHARACTERISTIC TIMES FOR THE DIFFERENT SUBCULTURES PERFORMED DURING THE ADAPTATION OF *C. NECATOR* 545 TO GLYCEROL. TI1, TI5 AND TI10 REPRESENTS THE TIME NEEDED TO REACH AN ASSOCIATED BIOMASS CONCENTRATION OF TWO, FIVE AND TEN-FOLD INCREASE RESPECT TO THE INITIAL CONCENTRATION IN EACH CULTURE. 91
FIGURE 4-6: RATE OF CHANGE OF THE NUMBER OF GENERATIONS OCCURRED DURING THE EXPONENTIAL PHASE FOR THE DIFFERENT SUBCULTURES PERFORMED DURING THE ADAPTATION *OF C. NECATOR 545* TO GLYCEROL. 92
FIGURE 4-7: OVERALL GLYCEROL UPTAKE RATE TIMES FOR DIFFERENT SUBCULTURES PERFORMED DURING THE ADAPTATION OF *C. NECATOR 545.* THE DATA SHOWS THE AVERAGES OF 3 SAMPLES WITH THEIR RESPECTIVE STANDARD ERROR. 92
FIGURE 4-8: COMPARISON BETWEEN ADAPTED AND ORIGINAL CELLS AFTER STORAGE PERIOD. THE PHOTOGRAPH SHOWS CULTURES INOCULATED WITH ORIGINAL CELLS (FLASK ON THE LEFT) AND ADAPTED CELLS (RIGHT). THE GRAPH SHOWS PROFILES FROM ORIGINAL (RED) AND ADAPTED CELLS (BLUE) THROUGHOUT THE CULTIVATION TIME. THE FILLED SYMBOLS CORRESPOND TO PHB MEASUREMENTS..... 93
FIGURE 4-9: GLYCEROL, GLUCOSE AND BIOMASS PROFILES OBTAINED FROM THE FERMENTATION CONDUCTED WITH A MIXTURE OF GLUCOSE AND GLYCEROL USING GLYCEROL-ADAPTED CELLS OF *C. NECATOR 545*. 94
FIGURE 4-10: ASSOCIATED BIOMASS PROFILES FOR THE FIRST FOUR SUB-CULTIVATIONS. THE SYMBOLS REPRESENT EXPERIMENTAL DATA AND THE SOLID LINES CORRESPOND TO THE MODEL PREDICTION. THE INHIBITION CONSTANT, K_I, WAS THE ONLY KINETIC

PARAMETER VARIED FOR THE DIFFERENT EXPERIMENTS: 4.5 G/L (RUN 1), 5.5 G/L (RUN 2), 20 G/L (RUN 3) , 120 G/L (RUN 4). THE VALUES FOR μ_M, KS AND Y WERE KEPT CONSTANT AT 0.125 H^{-1}, 1 G/L AND 0.07 G/G RESPECTIVELY. 95

FIGURE 4-11: VALUES FOR THE GROWTH INHIBITION CONSTANT DUE TO GLYCEROL OBTAINED FOR THE DIFFERENT SUBCULTURES PERFORMED DURING THE ADAPTATION OF *C. NECATOR* 545. 96

FIGURE 4-12: TIMES AT WHICH CELL CULTURES REACHED CELL DENSITIES EQUAL TO 2 (T_2), 5 (T_5), 10 (T_{10}), 15 (T_{15}) AND 20 (T_{20}) FOLD OF ITS INITIAL CONCENTRATION FOR THE FERMENTATIONS CONDUCTED THROUGHOUT THE BIO-TRAINING PROCESS. 96

FIGURE 4-13: TRENDS IN GLYCEROL PROFILES AT THE BEGINNING OF THE FERMENTATION FOR CULTURES PERFORMED IN SERIES WITH INCREASING INITIAL GLYCEROL CONCENTRATION. 97

FIGURE 4-14: COMPARISON BETWEEN THE CHARACTERISTIC TIMES T_{10} OF *C. NECATOR* CELLS UNDERGOING THE BIO-TRAINING ADAPTATION PROCESS (DIAMOND) AND CELLS ADAPTED TO 20 G/L GLYCEROL THAT WERE DIRECTLY GROWN IN 30, 50, 70 AND 90 G/L OF GLYCEROL, WITHOUT UNDERGOING THE GRADUALLY-INCREASING CONCENTRATION METHOD (TRIANGLES). 98

FIGURE 5-1: PHB RECOVERED FROM GLYCEROL FERMENTATIONS BY *C. NECATOR* USING THE CHLOROFORM METHOD.....103

FIGURE 5-2: UNSTAINED (LEFT) AND STAINED (RIGHT) CELLS OF *C. NECATOR* ON PETRI DISHES. THE BLACK COLORATION INDICATES PRESENCE OF PHB.....104

FIGURE 5-3: OBSERVATION OF PHB GRANULES UNDER TRANSMISSION ELECTRON MICROSCOPE. ON THE RIGHT, THE CENTRAL CELL WAS CHOSEN TO ESTIMATE PHB CONTENT BASED ON COLOUR DIFFERENCE:.....105

FIGURE 5-4: THE CHANGING RELATIONSHIP BETWEEN CELL DRY MASS AND OPTICAL DENSITY AS FERMENTATION PROGRESSES FOR DIFFERENT SETS OF DATA FROM DIFFERENT CULTURES OF *C. NECATOR*.....106

FIGURE 5-5: CORRELATION DEVELOPED TO CONVERT OPTICAL DENSITY MEASUREMENTS INTO ESTIMATED CELL DRY MASS VALUES FOR GLYCEROL FERMENTATIONS BY *C. NECATOR*. 106

FIGURE 5-6: PROFILES OF GLYCEROL FERMENTATIONS BY *C. NECATOR* OVER THE COURSE OF A BATCH CULTURE CONDUCTED WITH EXCESS OF CARBON OVER NITROGEN AT AN INITIAL C/N RATIO OF 32. 107

FIGURE 5-7: EVOLUTION OF BIOMASS, PHB AND ASSOCIATED BIOMASS PRODUCTION RATES OVER THE COURSE OF A GLYCEROL FERMENTATIONS BY *C. NECATOR*. THE OBSERVED MAXIMUM PRODUCTION RATE OCCURRED AT THE 33RD HOUR.....108

FIGURE 5-8: STOICHIOMETRIC DIVISION OF GLYCEROL UTILIZATION DURING A GLYCEROL FERMENTATIONS BY *C. NECATOR* CONDUCTED WITH 30 G/L GLYCEROL. 108

FIGURE 5-9: SPECIFIC GROWTH RATE OBSERVED DURING EXPONENTIAL PHASE FOR DIFFERENT INITIAL GLYCEROL CONCENTRATIONS IN SIMPLE BATCH FERMENTATIONS OF *C. NECATOR*. ERROR BARS REPRESENT DATA FROM REPEAT EXPERIMENTS. 109

FIGURE 5-10: SPECIFIC GROWTH RATE OBSERVED IN *C. NECATOR* CULTURES FOR A RANGE OF INITIAL GLYCEROL CONCENTRATIONS AND FITTED BY EQ. 5- 1 WITH $\mu m = 0.27\ 1/\mathrm{H}, kM = 1.5\ \mathrm{G/L}, kI = 31\ \mathrm{G/L}$. 110

FIGURE 5-11: PHB CONCENTRATION AND PROPORTION OF PHB AND ASSOCIATED BIOMASS OBTAINED FOR BATCH FERMENTATIONS BY *C. NECATOR* CONDUCTED WITH DIFFERENT GLYCEROL AMOUNTS. ERROR BARS REPRESENT DATA FROM REPEAT EXPERIMENTS. 110

FIGURE 5-12: DYNAMICS OF GLYCEROL CONSUMPTION FOR *C. NECATOR* FERMENTATION CONDUCTED WITH VARIOUS INITIAL GLYCEROL CONCENTRATIONS. THE LINES REPRESENT THE EXPONENTIAL DECAY EQUATION FOR EACH INITIAL CONCENTRATION AND AN EXPONENTIAL DECAY CONSTANT OF 0.02 H^{-1}. 111

FIGURE 5-13: (A) GLYCEROL CONCENTRATION LEFT AT THE END (APPROXIMATELY 120 H) OF *C. NECATOR* FERMENTATIONS CONDUCTED WITH DIFFERENT AMOUNTS OF GLYCEROL. (B) TOTAL AMOUNT OF GLYCEROL CONSUMED DURING THE SAME. ...112

FIGURE 5-14: OVERALL YIELDS OF THE MAIN FERMENTATION PRODUCTS, CELLS (x_A) AND PHB FOR *C. NECATOR* FERMENTATIONS CONDUCTED WITH DIFFERENT INITIAL GLYCEROL CONCENTRATIONS. 113
FIGURE 5-15: EXPERIMENTAL AND CALCULATED VALUES OF THE GLYCEROL CONSUMED BY *C. NECATOR* IN FERMENTATIONS WITH DIFFERENT INITIAL GLYCEROL CONCENTRATIONS. CALCULATED VALUES REPRESENT THE GLYCEROL THAT WOULD BE REQUIRED JUST TO PRODUCE CELLS AND PHB BASED ON STOICHIOMETRIC REACTIONS. 113
FIGURE 5-16: RANGE OF TURBIDITY FOUND IN SAMPLE BROTHS FROM GLYCEROL FERMENTATIONS BY *C. NECATOR* CULTURES STARTED WITH DIFFERENT INITIAL NITROGEN CONCENTRATION. THE CONCENTRATIONS USED IN THE RESPECTIVE FLASKS, FROM LEFT TO RIGHT, WERE 0.1, 0.25, 0.5, 0.75 AND 3 G/L. 115
FIGURE 5-17: VARIATION OF CELL DRY MASS WITH TIME FOR GLYCEROL FERMENTATIONS BY *C. NECATOR* WITH INITIAL CONCENTRATIONS OF AMMONIUM SULPHATE (AS) FROM 0.1 G/L TO 3 G/L. 116
FIGURE 5-18: ASSOCIATED BIOMASS CONCENTRATION PRODUCED BY 100 HOURS OF GLYCEROL FERMENTATIONS BY *C. NECATOR* FERMENTATION FOR DIFFERENT INITIAL AMOUNTS OF AMMONIUM SULPHATE. 116
FIGURE 5-19: SEMI-LOGARITHMIC PLOT FOR CELL DRY MASS AGAINST TIME FOR DETERMINATION OF SPECIFIC GROWTH RATE OF *C. NECATOR* AT THE DIFFERENT AMMONIUM SULPHATE CONCENTRATIONS. 117
FIGURE 5-20: VARIATION IN THE MAXIMUM SPECIFIC GROWTH RATE OBSERVED, AT EXPONENTIAL PHASE, AS A FUNCTION OF THE INITIAL AMOUNT OF NITROGEN (AMMONIUM SULPHATE) IN GLYCEROL FERMENTATIONS BY *C.NECATOR*. 117
FIGURE 5-21: SPECIFIC GROWTH RATE OBSERVED FOR A RANGE OF INITIAL AMMONIUM SULPHATE CONCENTRATIONS IN GLYCEROL FERMENTATIONS BY *C.NECATOR* AND FITTED BY EQ. 5- 1 WITH $\mu m = 0.2\ \mathrm{H} - 1, kM = 0{,}5\ \mathrm{G/L}, kI = 5{,}25\ \mathrm{G/L}$ (kM AND kI ARE BASED ON NITROGEN). 118
FIGURE 5-22: BIOMASS AND PHB CONCENTRATION PROFILES FROM GLYCEROL FERMENTATIONS BY *C. NECATOR* CONDUCTED WITH VARIOUS AMOUNTS OF NITROGEN AND THE SAME INITIAL GLYCEROL CONCENTRATION (30 G/L). 119
FIGURE 5-23: PHB CONTENT ON A TOTAL BIOMASS BASIS FOR GLYCEROL FERMENTATIONS BY *C. NECATOR* CONDUCTED WITH VARIOUS AMOUNTS OF INITIAL AMMONIUM SULPHATE CONCENTRATION. 120
FIGURE 5-24: EVOLUTION OF PH FOR GLYCEROL FERMENTATIONS BY *C. NECATOR* CONDUCTED WITH DIFFERENT AMOUNTS OF INITIAL AMMONIUM SULPHATE (AS). 120
FIGURE 5-25: PH AND BIOMASS EVOLUTION FOR A GLYCEROL FERMENTATION BY *C. NECATOR.* 121
FIGURE 5-26: EVOLUTION OF BIOMASS CONCENTRATION FOR GLYCEROL FERMENTATIONS BY *C. NECATOR* CONDUCTED WITH RELATIVELY HIGH INORGANIC (AMMONIUM SULPHATE) AND ORGANIC (PEPTONE) NITROGEN SOURCES. INITIAL CONCENTRATIONS WERE 3 G/L (AS3 AND P3) AND 6 G/L (AS6 AND P6). 121
FIGURE 5-27: MASS FLUXES AND REGULATORY MECHANISMS THAT COULD EXPLAIN PHB PRODUCTION BY *C. NECATOR* FERMENTATION. 123
FIGURE 6-1: PREDICTIONS OBTAINED FROM THE PRELIMINARY MODEL (LINES) AND EXPERIMENTAL DATA (SYMBOLS) FOR A FERMENTATION CONDUCTED WITH 20 G/L GLYCEROL AND 1 G/L AMMONIUM SULPHATE BY *C. NECATOR* IN SHAKE FLASK..... 130
FIGURE 6-2: PREDICTIONS OBTAINED FROM THE PRELIMINARY MODEL (LINES) AND EXPERIMENTAL DATA (SYMBOLS) FOR A FERMENTATION CONDUCTED WITH 30 G/L GLYCEROL AND 1 G/L AMMONIUM SULPHATE BY *C. NECATOR* IN SHAKE FLASK..... 131
FIGURE 6-3: PREDICTIONS OBTAINED FROM THE PRELIMINARY MODEL (LINES) AND EXPERIMENTAL DATA (SYMBOLS) FOR A FERMENTATION CONDUCTED WITH 30 G/L GLYCEROL AND 2 G/L AMMONIUM SULPHATE BY *C. NECATOR* IN SHAKE FLASK..... 132
FIGURE 6-4: PREDICTIONS OBTAINED FROM THE PRELIMINARY MODEL (LINES) AND EXPERIMENTAL DATA (SYMBOLS) FOR A FERMENTATION CONDUCTED WITH 30 G/L GLYCEROL AND 3 G/L AMMONIUM SULPHATE BY *C. NECATOR* IN SHAKE FLASK..... 132

FIGURE 6-5: PREDICTIONS OBTAINED FROM THE UPDATED MODEL (LINES) AND EXPERIMENTAL DATA (SYMBOLS) FOR A FERMENTATION CONDUCTED WITH 20 G/L GLYCEROL AND 1 G/L AMMONIUM SULPHATE BY *C. NECATOR* IN SHAKE FLASK. 134
FIGURE 6-6: PHB AND TOTAL BIOMASS EXPERIMENTAL DATA (SYMBOLS) ALONG WITH PREDICTIONS (LINES) OBTAINED WITH THE UPDATED MODEL FOR GLYCEROL FERMENTATIONS BY *C. NECATOR* IN SHAKE FLAKS AND FOR DIFFERENT CONDITIONS: (A) 20 G/L GLYCEROL, 1 G/L AMMONIUM SULPHATE; (B) 30 G/L GLYCEROL, 2 G/L AMMONIUM SULPHATE; (C) 30 G/L GLYCEROL, 3 G/L AMMONIUM SULPHATE. 135
FIGURE 6-7: VALUES AT 120 HOURS OF ASSOCIATED BIOMASS, PHB AND TOTAL BIOMASS ACCORDING TO THE MODEL SIMULATIONS FOR SHAKE FLASK GLYCEROL FERMENTATION BY *C. NECATOR* UNDER DIFFERENT NITROGEN CONCENTRATIONS AND 30 G/L GLYCEROL. 136
FIGURE 6-8: CONTOUR PLOT OF THE MAXIMUM PHB CONCENTRATION ACHIEVABLE AS A FUNCTION OF THE INITIAL NITROGEN AND CARBON CONCENTRATIONS, PREDICTED USING THE UPDATED MODEL. 138
FIGURE 6-9: CONTOUR PLOT OF PREDICTED SPECIFIC GROWTH RATE FOR *C. NECATOR* AS A FUNCTION OF THE NITROGEN AND CARBON CONCENTRATIONS IN THE FERMENTATION BROTH. 138
FIGURE 6-10: SIMULATIONS OF PHB PRODUCTION DURING GLYCEROL FERMENTATION BY *C. NECATOR* STARTED WITH X_A=0.15 G/L, AS=0,25 G/L, GLY=30 G/L. 139
FIGURE 6-11: SCHEMATIC REPRESENTATION OF MODEL PREDICTIVE CONTROL APPLIED TO A GENERIC INDUSTRIAL PROCESS. 140
FIGURE 6-12: MODEL RESULTS FROM THE BIOREACTOR MODEL (LINES) AND EXPERIMENTAL DATA (SYMBOLS) FOR A BATCH GLYCEROL FERMENTATION BY *C. NECATO*R CONDUCTED IN BENCH-TOP REACTOR. EXPERIMENTAL RESULTS SERVED TO ESTIMATE THE MODEL PARAMETERS. 141
FIGURE 6-13: SENSITIVITY ANALYSIS ON THE OBJECTIVE FUNCTION BY 5% VARIATION AROUND THE STATED VALUE FOR THE KINETIC PARAMETERS. 142
FIGURE 6-14: MODEL PREDICTIONS (LINES) AND EXPERIMENTAL RESULTS (SYMBOLS) FOR A GLYCEROL FERMENTATION BY *C. NECATOR* IN WHICH A PULSE OF NUTRIENTS WAS ADDED JUST PRIOR TO THE 100TH HOUR OF CULTURE IN BIOREACTOR. 144
FIGURE 6-15: SIMULATIONS OF GLYCEROL FERMENTATIONS BY *C. NECATOR* IN WHICH AN INJECTION OF GLYCEROL WAS DONE AT DIFFERENT TIMES 145
FIGURE 6-16: SIMULATIONS OF GLYCEROL FERMENTATIONS BY *C. NECATOR* CONDUCTED WITH DIFFERENT FEEDING STRATEGIES FOR THE NITROGEN: (A) NITROGEN FEEDING AT A FLOW RATE OF 0.0025 L/H; (B) NITROGEN FEEDING AT A FLOW RATE OF 0.001 L/H; (C) SINGLE PULSE OF NITROGEN. 146
FIGURE 6-17: SUMMARY OF RESULTS OBTAINED FROM FERMENTATIONS SIMULATED WITH DIFFERENT FEEDING STRATEGIES FOR THE SUPPLY OF NITROGEN. 147
FIGURE 6-18: MODEL PREDICTIONS (LINES) AND EXPERIMENTAL RESULTS (SYMBOLS) FOR A GLYCEROL FERMENTATION BY *C. NECATOR* IN WHICH PULSES OF NUTRIENTS WERE DONE DURING FERMENTATION. FERMENTATION WAS STARTED WITH 33 G/L GLYCEROL AND 0.68 G N. 148
FIGURE 6-19: EXPERIMENTAL RESULTS FOR A GLYCEROL FERMENTATION BY *C. NECATOR* IN WHICH PULSES OF NUTRIENTS WERE DONE DURING FERMENTATION. PHB DEGRADATION WAS INDUCED AFTER THE 100^{TH} HOUR BY THE ADDITION OF NITROGEN. RESULTS WITHIN THIS PERIOD ARE INSIDE THE BOX. 149
FIGURE 6-20: MODEL PREDICTIONS (LINES) AND EXPERIMENTAL RESULTS (SYMBOLS) FOR A GLYCEROL FERMENTATION BY *C. NECATO*R WITH CONTINUOUS FEEDING OF NUTRIENTS. 151

FIGURE 6-21: COMPARISON IN TERMS OF PHB, ASSOCIATED BIOMASS AND TOTAL BIOMASS AND PHB CONTENT (% OF TOTAL BIOMASS) OF THREE EXTENDED BATCHES WITH DIFFERENT FEEDING SCHEMES. THE TIME IN BRACKETS ON THE X-AXIS INDICATES THE MOMENT AT WHICH THE MEASUREMENTS OF CONCENTRATIONS WERE MADE. 152
FIGURE 6-22: PREDICTED FERMENTATION RATES FOR GLYCEROL FERMENTATIONS BY *C. NECATOR* CONDUCTED WITH DIFFERENT FEEDING REGIMES. THE ARROWS INDICATE THE TIMES WHEN THE INJECTIONS WERE MADE (PLOT ON THE LEFT) AND THE INTERVAL DURING WHICH THE CONTINUOUS FEEDING TOOK PLACE (PLOT ON THE RIGHT). 152
FIGURE 7-1: SPECIFIC BIOMASS GROWTH RATE (RCC) AND SPECIFIC PHB PRODUCTION RATE (PHB) AS FUNCTION OF THE DISSOLVED OXYGEN IN THE BULK MEDIUM (MOZUMDER *ET AL.,* 2016). 158
FIGURE 7-2: OVERVIEW OF STEPS IN THE OVERALL TRANSFER OF OXYGEN FROM A GAS BUBBLE TO THE REACTION SITE INSIDE THE INDIVIDUAL CELL (GARCIA-OCHOA & GOMEZ 2009). 159
FIGURE 7-3: GRAPH OF EXPERIMENTAL DATA OBTAINED DURING DYNAMIC GASSING-OUT TECHNIQUE FOR OUR AND OTR DETERMINATION. BLUE SYMBOLS REPRESENT THE REGION WHERE THE AIR SUPPLY IS OFF AND GREEN, WHERE IT IS ON. 160
FIGURE 7-4: OXYGEN UPTAKE RATES (OUR) AND EXPERIMENTAL VALUES FOR TOTAL BIOMASS CONCENTRATION (SYMBOLS) AND PREDICTED BIOMASS PROFILES (LINES) FOR TWO BIOREACTOR FERMENTATIONS BY *C. NECATOR* WITH DIFFERENT INITIAL GLYCEROL CONCENTRATIONS :(A) 45 G/L AND (B) 30 G/L FOR THAT ON THE RIGHT 164
FIGURE 7-5: OUR EXPERIMENTAL VALUES (SYMBOLS) AND MODEL PREDICTIONS USING EQ. 7- 9 AND $YoxA = 1.1\ \mathrm{G/G}$ AND $m = 0.04\ \mathrm{H}-1$ IN A AND $YoxA = 1.7\ \mathrm{G/G}$ AND $m = 0.0225\ \mathrm{H}-1$ FOR B. 165
FIGURE 7-6: RELATIONSHIP BETWEEN SPECIFIC OXYGEN UPTAKE AND DISSOLVED OXYGEN CONCENTRATIONS FOR TWO BIOREACTOR FERMENTATIONS BY *C. NECATOR* WITH DIFFERENT INITIAL GLYCEROL CONCENTRATIONS: (A) 45 G/L AND (B) 30 G/L 166
FIGURE 7-7: EVALUATION OF K_LA USING VARIOUS METHODS. VALUES ARE PRESENTED FOR DIFFERENT TIMES, DURING GLYCEROL FERMENTATION BY *C. NECATOR*, FOR TWO SEPARATE SYSTEMS WITH DIFFERENT INITIAL GLYCEROL CONCENTRATIONS (A) 45 G/L AND (B) 30 G/L .AS CAN BE SEEN, FOR BOTH FERMENTATIONS, MOST OF THE DATA FALL WITHIN A BROAD HORIZONTAL BAND. 168
FIGURE 7-8: PLOT OF THE LN((C*-CL)/(C*-CO)) AGAINST TIME OF AERATION, THE SLOPE OF WHICH EQUALS – K_LA. 169
FIGURE 7-9: REYNOLD NUMBER-POWER NUMBER CURVE FOR DIFFERENT TYPES OF IMPELLERS (PADRON 2001). 170
FIGURE 7-10: K_LA ESTIMATIONS BASED ON THE OUR VALUES OBTAINED BY THE GRAPHICAL METHOD FOR DIFFERENT OPERATIONAL CONDITIONS. 171
FIGURE 7-11: EXPERIMENTAL (GASSING-OUT) AND CALCULATED VALUES (CORRELATION) FOR DIFFERENT OPERATIONAL CONDITIONS. 171
FIGURE 8-1: SCHEMATICS OF AN INTEGRATED BIOREFINERY FOR THE CO-PRODUCTION OF BIODIESEL AND PHB FROM RAPESEED OIL. THE MASS FLOW RATES ARE BASED ON THOSE FROM A SMALL BIODIESEL PLANT. 183

List of tables

TABLE 1-1: MODELS OF SUBSTRATE INHIBITION IN MICROBIAL GROWTH. THE NUMBER OF PARAMETERS ACCOUNT FOR THE NUMBER OF CONSTANTS ADDED TO THE ALREADY EXISTENT K_S AND μ_{MAX} *IN* MONOD EXPRESSION. 32

TABLE 2-1 PROPERTIES OF PP, PHB AND PHB COPOLYMERS (DATA ADAPTED FROM LEE 1996. PEREIRA *ET AL.,* 2008; KOLLER *ET AL.*, 2010) 43

TABLE 2-2: CURRENT AND POTENTIAL LARGE VOLUME MANUFACTURERS OF PHAS (CHANPRATEEP 2010) 45

TABLE 2-3: COMPOSITION OF CRUDE GLYCEROL ADAPTED FROM (LUO *ET AL.* 2013) 46

TABLE 2-4: VALUES OF C/N REPORTED IN SIMPLE BATCH STUDIES FOCUSING PARTICULARLY ON THIS ASPECT OF MEDIUM OPTIMIZATION. 52

TABLE 3-1: RETENTION TIMES IN HPLC-UV DETECTION OF COMMON ORGANIC ACIDS OBTAINED AS FERMENTATION BY-PRODUCTS..78

TABLE 3-2: RESULTS OBTAINED FROM ONE-FACTOR ANOVA ANALYSIS OF GROWTH CURVES CORRESPONDING TO CONSECUTIVE CULTURE RUNS ON GLYCEROL. 83

TABLE 6-1: EQUATIONS AND COMPUTED PARAMETER VALUES FOR THE PRELIMINARY MODEL FOR SHAKE FLASK FERMENTATION. 130

TABLE 6-2: EQUATIONS AND COMPUTED PARAMETER VALUES FOR THE REFORMULATED MODEL FOR SHAKE FLASK FERMENTATION. 133

TABLE 6-3: OPTIMIZATION RESULTS PERFORMED AT DIFFERENT OBJECTIVE FUNCTIONS: MAXIMIZATION OF PHB AND TOTAL BIOMASS. 139

TABLE 6-4: EQUATIONS AND COMPUTED PARAMETER VALUES FOR THE MODEL ADAPTED TO FERMENTATIONS CONDUCTED IN BIOREACTOR. 142

TABLE 6-5: EQUATIONS AND COMPUTED PARAMETER VALUES FOR THE MODEL ADAPTED TO FED-BATCH OPERATION. 150

TABLE 7-1: OXYGEN REQUIREMENT FOR SOME BACTERIA AND CARBON SUBSTRATES. 157

TABLE 7-2: CRITICAL DISSOLVED OXYGEN VALUES FOR CERTAIN MICROBIAL STRAIN (HELDMAN 2003). 157

TABLE 7-3: CORRELATIONS FOR THE CALCULATION OF VOLUMETRIC MASS TRANSFER COEFFICIENT; COPIED FROM GILL *ET AL.,* (2008). 161

Nomenclature

α	Growth associated constant
β	Non growth associated constant
μ	Specific growth rate
μ_{max}	Maximum specific growth rate
AS	Ammonium sulphate
B	Apparent Contois constant
c_i	Concentration of the species *i*
C_{crit}	Critical concentration
F	Flow rate
Gly	Glycerol
k_{cd}	Constant of cellular death
k_d	Apparent dissociation constant
k_G	Half saturation constant for glycerol
k_I	Inhibition constant
k_{IG}	Inhibition constant due to glycerol
k_{IN}	Inhibition constant due to nitrogen
k_{INP}	Inhibition constant for product formation due to nitrogen
k_G	Half saturation constant for glycerol
$k_L a$	Volumetric mass transfer coefficient
k_N	Half saturation constant for nitrogen
k_P	Half saturation constant for the product
K_S	Saturation constant
K_x	Carrying capacity
m_s	Maintenance coefficient
n	Hill coefficient
N	Nitrogen
N_g	Number of generations
Np	Power number
Re	Reynold number
P	Product concentration
P_g	Power in aerated system
P^{max}	Maximum PHB content
q_i	Rate of production of the species *i*
r_i	Rate of conversion of the species *i*
S	Substrate concentration
t	Time
TB	Total biomass

V	Volume
W	Weight
x	Biomass concentration
x_A	Associated biomass concentration
$Y_{P/S}$	Yield of product based on substrate
$Y_{P/x}$	Yield of product based on biomass

Building a predictive model for PHB production from glycerol

In recent years, the potential of biological routes to replace fossil fuel-based technologies in the drive towards sustainable production of chemicals and energy has been explored and demonstrated. Biodegradable polymers derived from renewable resources could contribute to the global production of plastics (300 million tons per year) currently derived mainly from crude oil refining. However, an efficient design and optimization is required if bioprocesses are to be competitive with oil-based equivalents and describing microbial kinetics is an essential element of the necessary process development for this transition towards a bio-based economy. Polyhydroxybutyrate (PHB) is a storage compound, which accumulates in various microorganisms, with properties comparable to those of oil-derived plastics. For the case of the wild type bacterial strain *Cupriavidus necator*, PHB synthesis occurs in situations when there is a lack of an essential nutrient for growth but an excess of carbon. In such cases, carbon is stocked inside insoluble inclusion bodies in the form of PHB. The intracellular polymer can later be mobilized by the cell with favourable energy outcomes. This mechanism of product formation decoupled from growth challenges PHB production in simple batch systems. Thereby a careful evaluation of the feeding of nutrients is essential to enhance productivities. In this study, PHB production from glycerol by *C. necator* has been investigated with the objective of building a macroscopic model that could assist the process evaluation.

Glycerol, an inherent by-product of the biodiesel industry, has been used throughout the research presented in this thesis as it is a potential low-cost industrial feedstock for PHB production. However, cells exhibit a long lag phase and slow growth when cultivated in glycerol for the first time. To overcome these problems, an adaptation procedure was carried out. By the 15^{th} generation of cells grown on glycerol, the doubling time had been reduced from 22 to 1.5 h and the normal preference for glucose over glycerol (catabolic repression effect) was reversed. A further adaptation process with higher glycerol levels showed an improved tolerance up to 100 g/l, which enabled future fermentations with large amounts of glycerol.

The fermentation kinetics were determined from batch studies and a relatively simple model was gradually refined and improved with each successive series of experiments. Kinetic constants extracted from the experimental data were treated as absolute constants rather than adopting best fit values each time. The resultant model, a double-substrate multiple-inhibition Monod-type set of equations, was then used to search for the best initial conditions of substrates, solve optimization problems and analyse different scenarios based on these fixed constants. The dual effect of carbon and nitrogen were examined and it was found that absolute amounts, not just ratios, determine the fate of the system. In this way, the fraction of biomass that is not PHB, called in this thesis 'associated biomass', was determined to be linearly related to the amount of nitrogen provided up to a certain level (3 g/l ammonium sulphate). Nitrogen concentrations above a low level were found to inhibit PHB formation while large excesses of carbon were channelled towards by-product (organic acids) formation. Also, the PHB production rate was seen to be influenced by total biomass concentration, to which both PHB and associated biomass contribute. Studies involving forced aeration showed that oxygen availability sets a threshold on the amount of biomass that can be formed in non-aerated systems, *e.g.* flasks, but did not affect the results in bioreactors as long as the dissolved oxygen was maintained above 20 % of saturation level.

Using the model to predict conditions and mode of operation under which PHB production could be maximized, high density cultures (>30 g/l) with high PHB content (almost 80 %) were successfully achieved through nutrient feeding. To maintain an uninterrupted product formation rate, feeding of a complete medium with specified composition was found to be best in both experimental and computational studies. The development of the model and its later application in predicting fermentation profiles have therefore been instrumental in acquiring a macroscopic understanding of a complex system while significantly reducing experimental burden. In an industrial process, separation costs and the cost of PHB itself will ultimately determine whether it is PHB or total biomass that should be maximized. In this way, the work presented in this thesis improves the possibility of the integration of PHB production within a biodiesel plant to reduce the gap between petroleum-based chemicals and the bio-based future.

Declaration and Copyright Statement

I hereby declare that the thesis is based on my original work except for quotations and citations, which have been duly acknowledged. I also declare that it has not been previously or currently submitted for any other degree at University of Manchester or other institutions of learning.

Cristina Pérez Rivero

i. The author of this thesis (including any appendices and/or schedules to this thesis) owns certain copyright or related rights in it (the "Copyright") and s/he has given The University of Manchester certain rights to use such Copyright, including for administrative purposes.

ii. Copies of this thesis, either in full or in extracts and whether in hard or electronic copy, may be made only in accordance with the Copyright, Designs and Patents Act 1988 (as amended) and regulations issued under it or, where appropriate, in accordance with licensing agreements which the University has from time to time. This page must form part of any such copies made.

iii. The ownership of certain Copyright, patents, designs, trademarks and other intellectual property (the "Intellectual Property") and any reproductions of copyright works in the thesis, for example graphs and tables ("Reproductions"), which may be described in this thesis, may not be owned by the author and may be owned by third parties. Such Intellectual Property and Reproductions cannot and must not be made available for use without the prior written permission of the owner(s) of the relevant Intellectual Property and/or Reproductions.

iv. Further information on the conditions under which disclosure, publication and commercialisation of this thesis, the Copyright and any Intellectual Property University IP Policy (see http://documents.manchester.ac.uk/display.aspx?DocID=24420), in any relevant Thesis restriction declarations deposited in the University Library, The University Library's regulations (see http://www.library.manchester.ac.uk/about/regulations/) and in The University's policy on Presentation of Theses.

Acknowledgments

I wish to thank the University of Manchester for the provision of a *President's Doctoral Scholarship Award* that allowed these studies. I am especially thankful - and I believe, extremely lucky - to have had Prof. Colin Webb as supervisor. He has been of incredible help throughout the last years. I have greatly enjoyed all the meetings and discussions we have had, which are, without doubt, the things I am going miss the most from the PhD.

I would also like to express my gratitude to my co-supervisor Konstantinos Theodoropoulos for all his guidance. I am also very thankful to Carol Lin for welcoming me in her lab and gave me chance of having an amazing experience in Hong Kong.

I cannot forget here all my colleagues from the CPI and SCGPE which made this time a very special period of my life. A special gratitude goes to all the staff and PhD students in the CEAS that somehow contributed to the project. Special thanks to Chenhao Sun, working with him has been a rewarding experience.

To my family and friends who encouraged me all the way until here. Without them, this would have been much harder. To my dad who taught me about never giving up, you are my role model. Finally I want to thank Pablo for standing beside me throughout this thesis, and specially, the end of it. His faithful support and advice are greatly appreciated. His assistance at the latest stages of preparation has been priceless.

Chapter 1

Describing microbial kinetics for bioprocess design

1.1 The increasing importance of bioprocessing

Biotechnology is the application of scientific and engineering principles to the processing of materials by biological agents (OECD 2005). Although this word is being heard today more than ever, the use of living organisms (or their components) to generate desired products has been practiced since the dawn of civilization. It is known that ancient Egyptians were regular consumers of fermented beverages, such as beer, wine or mead. Other fermented products, tofu, tempeh, natto, bread, kefir and cheese have been essential for the diet of eastern and western regions for centuries.

The basis for those processes was, however, unknown until Pasteur, in the 19th century, began working with yeasts and proved they were living organisms. The later discovery of *Escherichia coli* and the isolation of pure strains boosted the research in biotechnology and development of bioproducts which continued in the 20th century, driven by context of wars. For example the industrial acetone-butanol-ethanol (ABE) fermentation process was developed at Manchester University and was extensively used in munitions products and later in paint varnish production (Venkataramanan & Scholz 2014) . The availability of other bioproduct, antibiotics, within the Allies is argued to have changed the fate of World War II.

Successfully first achieved in 1973 by Cohen *et al.*, the possibilities of joining together DNA molecules from different species opened the door to molecular biology and genetic engineering. The studies on recombinant technology have made tremendous progress in recent decades and there is no doubt that it will play a major role in the future (to breed high yielding crops, provide diagnostic kits and tailor more efficient biocatalysts). However, there is still a long way to go before knowledge of metabolism can be translated into process models.

The range and types of products derived from bioprocesses has also increased throughout history. Whereas food and beverages were the main products in the past, the molecules that can nowadays be synthesized biologically range from fine chemicals to textiles, including all types of products currently derived from petroleum (Gavrilescu & Chisti 2005). This feature of microbes being versatile living "factories" allows new synthesis routes for the production of everyday products which, moreover, could constitute greener technologies.

As with energy, if the production of chemicals is to be sustainable, this would require a sustainable (renewable) supply of raw material. Apart from CO_2 and water, the only renewable feedstocks for chemical production are based on biomass. Biomass is biological material derived from living or recently living organisms. This means that it can refer to the substrate (reactive) of a bioprocess or to the biocatalyst used. Different types of biomass can be converted into a wide spectrum of products by

numerous microorganisms under normally mild conditions, in terms of temperature, pH and pressure, and producing biodegradable waste waters. Products include bulk and fine chemicals, solvents, fibres, fuels, catalysts and even plastics (De Jong *et al.*, 2012). It is therefore clear that as the world focuses on sustainable growth, bioprocessing will play an ever more important role in the development of new and more sustainable chemical industry products.

In recent years, the plastics industry has become one of the largest manufacturing industries. Conventional plastics are either burnt after use, releasing toxic fumes and bulk pollutants, or they accumulate in landfills and oceans. Although environmental politics aim to increase the recycling levels and favor energy recovery over waste sent to landfill, the limited number of cycles that a plastic can be recycled and the impossibility of incinerating every plastic, make plastic accumulation an inescapable reality. Because they are rarely biodegradable, they can remain in the environment for many years without decomposing. Bioplastics on the other hand, are generally biodegradable and can be converted to carbon dioxide and water under aerobic conditions over much shorter time periods. Consequently, there is much interest in bioplastics and research into these bio-counterparts has risen exponentially over the past decade or so, as can be seen in Figure 1-1.

There are many different bioplastics, but most of them fall within three basic categories. These include: naturally occurring bioplastic polymers, such as polyhdroxyalkanoates (PHAs) of which polyhdroxybutyrate (PHB) is the most common; other naturally occurring polymers, such as starch and cellulose, that can be converted into plastics; and monomeric products of metabolism, such as lactic acid (LA), which can be polymerized to produce plastics (*e.g.* PLA). Those three types are biodegradable plastics; however, there are also bio-based plastics which are not biodegradable (*e.g.* polyethylene derived from sugar cane). For a plastic to be considered biodegradable it has to break down relatively quickly and safely into harmless compounds, and eventually into very simple compounds such as carbon dioxide and water, by the action of microorganisms such as fungi and bacteria (Rivero *et al.* 2017).

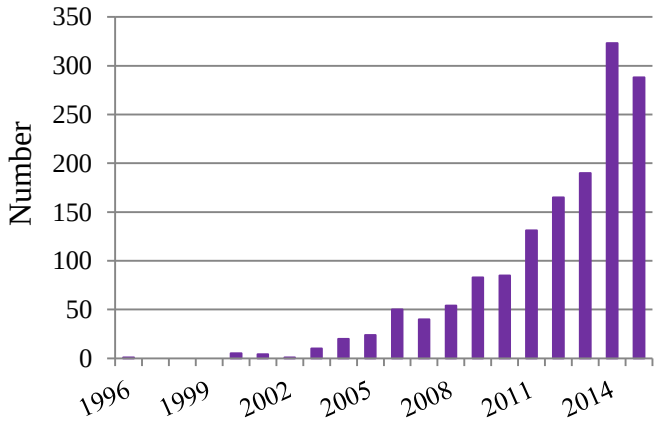

Figure 1-1:Trends in number of publications related to biobased polymers over recent years (Scopus 2016).

The legislation in residues related to the EU circular economy package is changing in response to the need for reducing the carbon dioxide emissions and enhancing the recycling taxes and using of resources. For instance, in France, modification on the Waste Framework Directive have replaced light plastic bags for bioplastic-based bags for fruits and vegetables and biodegradable or biocompostable bags for residues. This and similar measurements adopted by other counties in Europe will strength the bioplastic market (European Bioplastics e.V. 2015).

1.2 The challenge of bioprocessing

Despite the bright prospects for bioprocessing, the reality is that biotechnology lags behind the development of petrol-based chemicals. The transition of bioproducts from the laboratory to a manufacturing scale is often a very long process which ultimately depends on economic factors. Consequently, the idea of biofuels, bulk biochemicals and biopolymeric materials partially replacing conventional chemicals is still far from being realized.

Some of the reasons that could explain why the commercialization of bioprocesses has not been as fast as expected are the fall in petrol prices, the discovery of new reserves of oil and gas, the higher cost of agricultural raw materials compared to the former and the quite ineffective utilization of cellulosic materials by microorganisms. The traditional strategy of 'low volume and high price' applies to the biomedical field, chiral monomers and drug development, but it cannot be the approach for many other bioproducts. Instead, we should aim for a high volume and low price strategy that can compete with the chemical industry.

Synthetic biology can contribute to foster industrial biotechnology by applying new techniques (*i.e.* assembling pathways that can metabolize mixed substrates, removing unnecessary pathways consuming substrates) but it is also important to imitate chemical industry on some engineering fundamentals (continuous and open processes, heat integration, by-product synergy). Going back to the bioplastics example, and specifically to PHB as the most representative type, metabolic engineering cannot be directly applied to suppress the pathways competing with product synthesis, and continuous operation cannot be the operation mode to yield high product concentrations. Still, industry can take advantage of inexpensive substrates, process optimization and process integration.

The challenge then is to understand and analyse bioprocesses so that they can be designed and operated in a rational way. Considering that a fermentation process involves a multicomponent and multiphase environment interacting with a (often heterogeneous) cell population with internal controls (metabolic flexibility) and thousands of individual biochemical reactions, it seems intuitive that fermentation profiles would reflect the very complex growth dynamics. That is why modelling bioprocesses often comes with many assumptions that can scarcely be verified.

Nonetheless, models can be powerful tools for the design of fermentations, a task that when done experimentally can be very tedious. A model, on the other hand, is an image of a real system that shows analogous behavior in the important properties and that allows, within a limited region, a prediction of the behavior of the original system (Bellgardt 2000). In this way, experimental studies can be replaced by the model with many advantages. The first one is economic: it is much cheaper (and faster) using the model to predict data than obtaining those results empirically. For research and development purposes and because the model is less complex than the real system, some effects can be suppressed in order to emphasize others. Last but not least, the exercise of modelling helps to clarify the understanding of the process being described.

The model can be seen as a calculation rule that relates the pattern observed in the output variables to a certain pattern given in the input variables. Other components of the model are the parameters, which are fixed entities of the system. Once these parameters are known and the model validated, the model can be used for other purposes as indicated in Figure 1-2.

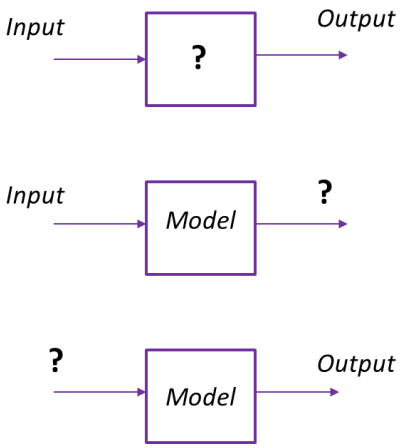

Figure 1-2: A model gives the relationship between inputs and outputs of a determined system. lt can be used to determine the output based on a certain input or to find an input that would give the desired output (optimization).

The process of building a model is seldom a single-step exercise. Instead, it can be seen as an iterative procedure that starts by taking advantage of existing models and elemental knowledge translated into equations that could be adjusted to the nature of the phenomenon being modelled. These basic notions need to be tested in order to find where the discrepancies between the preliminary version of the model and the system of study lie. To do so, empirical data from the real system is required. The formulation of the model can then be tweaked based on the latest information available. Higher levels of complexity, new variables or factors affecting the system can be also incorporated to achieve a better representation of real-life situations, bearing in mind that the more sophisticated a model is, the more difficult it would be to gather the data to validate it and the more computationally intensive it will be. That is why the first thing to know is the purpose for which the model is intended.

Throughout this thesis, the development of mathematical model is described for the fermentation dynamics of a particular bioprocess in order to guide the process optimization of the lab-scale fermentation by using a systematic approach. A theoretical introduction to bioprocess modelling is discussed next.

1.3 Considerations for design

Process design is the conceptual work normally done prior to building, expanding or retrofitting a process plant (Petrides *et al.*, 2015). Process design and, specifically bioprocess design, requires the integration of knowledge from many different scientific and engineering disciplines (biology, microbiology, chemistry, chemical engineering, mathematics, physics). The bioreactor or "fermenter" is the vessel where the bioreaction that leads to the synthesis of the product takes place and it is considered to be the heart of the process. The function of a properly designed bioreactor is to provide a suitable environment (subject to control) for the growth and/or optimal formation of the product within a particular cellular system. It is important to note that optimal usually refers to overall economics and not necessarily to maximum conversion of substrate into product.

1.3.1 Classification of models

Once the type of reactor is chosen, the sizing of the fermenter would be a crucial aspect in the design and, as for any other piece of equipment in a chemical plant, it involves solving mass balances. The mass balance for a variable A, in liquid form, is calculated from Eq. 1-1:

$$V\frac{dc_A}{dt} + c_A\frac{dV}{dt} = F_{inlet}\cdot c_{A_{inlet}} - F_{outlet}\cdot c_{A_{outlet}} + r_A\cdot V \qquad \textbf{Eq. 1-1}$$

where V is the liquid volume inside the bioreactor, c_A the concentration of the variable inside the bioreactor; F_{inlet} is the flow rate entering the bioreactor, $c_{A_{inlet}}$ is the concentration of the variable in the flow entering the bioreactor, F_{outlet} is the flow rate exiting the bioreactor; $c_{A_{outlet}}$ is the concentration of the variable in the flow exiting the bioreactor and r_A the rate of conversion of A (<0 if A is consumed, >0 if A is produced).

For batch and fed-batch configuration, the expression is simplified and the flow terms disappear for the former and only the inlet (feeding) remain for the latter. Depending on the expression for r_A, we find different types of models that can assist in the task of sizing the fermenter. The most complex type of model considers differences in the cells within the population inside the reactor (segregated) and also structuring at the cell level, so that intracellular events are taken into account (structured). Alternatively, we find unsegregated and unstructured models, in which it is assumed that all cells in

the population are identical (unsegregated) and biomass be represented by one state variable (unstructured). Between these two extremes, other combinations can be found as illustrated by Figure 1-3:

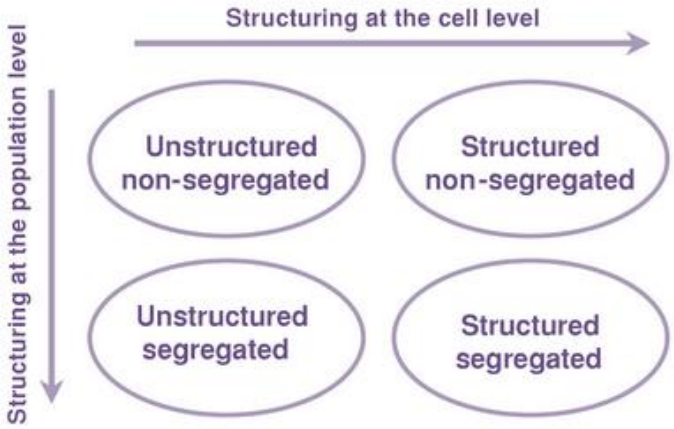

Figure 1-3: Degrees of complexity in fermentation models (Bailey 1998).

An entirely different type of model is that based on the metabolic network of cells, so-called, metabolic model. Although such models should describe the system perfectly, to achieve this, the kinetics of each metabolic reaction would be required. The experimental difficulty of measuring intracellular compounds throughout the course of a fermentation together with the very large number of reactions taking place inside the cell challenges this particular modelling exercise. The information revealed is often aimed at identifying bottlenecks and biochemical constraints which could potentially be relieved by the application of genetic engineering tools (Smolke 2010).

Although the two different approaches, which could be referred to as macroscopic and intracellular modelling, have different outputs and serve different purposes, it is worth questioning whether they could be combined to enlarge the predictive capabilities of the resultant model. For doing so, while keeping a model structure with a low complexity level, two strategies have been attempted (Sengupta & Pike 2013). In the top-down approach, only the preponderant intracellular mechanism (having an impact at the cell population level) is included in detail in a macroscopic model. For the bottom-up approach, on the other hand, intracellular mechanisms are simplified and linked to the macroscopic scale. In other words, joining macroscopic and metabolic scale (without greatly increasing the level of computational complexity) has been done at the expense of over-simplifying, and sometimes neglecting, phenomena from either scale.

In the research reported in this thesis, the purpose of the mathematical model to be constructed was the process development of a particular bioproduct. The ultimate goal of the model was to be used for design (*e.g.* equipment sizing) and not for searching for efficient pathways as in the case of metabolic modeling. As neuronal network modeling dismisses the insights of the bioprocess reactions, it was not

considered the best option to achieve a deep understanding of the fermentation basis. Hence, macroscopic modelling was the approach chosen and conventional macroscopic kinetics are reviewed below with the purpose of establishing the basis on which the computational studies have been built.

1.3.2 Kinetics of biomass production, product formation and substrate utilization in cell cultures

Biomass production

Together with suitable environmental conditions, in terms of pH, temperature, aeration or exclusion of oxygen, the microorganisms require the provision of (specific) substrates for growth. Sources of carbon and nitrogen are essential for microbial growth, and to achieve optimal performance, the medium is normally completed with minerals and salts which provide inorganic elements to act as minor nutrients and/or enzymatic cofactors.

Although it is intended that the microorganism grows in optimal conditions, it is rare that substrates are just provided in large excess. This is because the same substrate that favors growth is inhibitory when surpassing a certain concentration. Also, cell metabolism can lead to undesirable products when growth is too vigorous and substrates can be "wasted" into undesirable products as a natural mechanism to cope with large amount of some chemicals.

In practise, all the nutrients that compose the medium are supplied within a range and one of them is considered to limit growth, since its depletion occurs before the others. As the microorganism catalyzes its own growth, it is expected that the biomass concentration, represented by *x*, appears in the growth rate equation, Eq. 1-2:

$$r_x = \frac{dx}{dt} = \mu \cdot x \qquad \textbf{Eq. 1-2}$$

where μ is the specific growth rate. Specific variables, obtained when dividing the variable by the biomass concentration, are very useful to avoid the effect of the number of cells in the actual variable. The most popular the expression for specific growth rate is the Monod equation (Eq. 1-3).

$$\mu = \frac{\mu_{max} \cdot S}{K_S + S} \qquad \textbf{Eq. 1-3}$$

This formulation is analogous to the Michaelis Menten equation for enzymatic kinetics and also to the adsorption isotherm model proposed by Langmuir. In this case, μ_{max} represents the maximum growth rate that the microorganism can possible achieve when growing on the limiting substrate (*S*). K_s, or the

saturation constant, represents the concentration of the substrate that results in half of the maximum specific growth rate. The effect of the saturation constant on μ is illustrated in Figure 1-4.

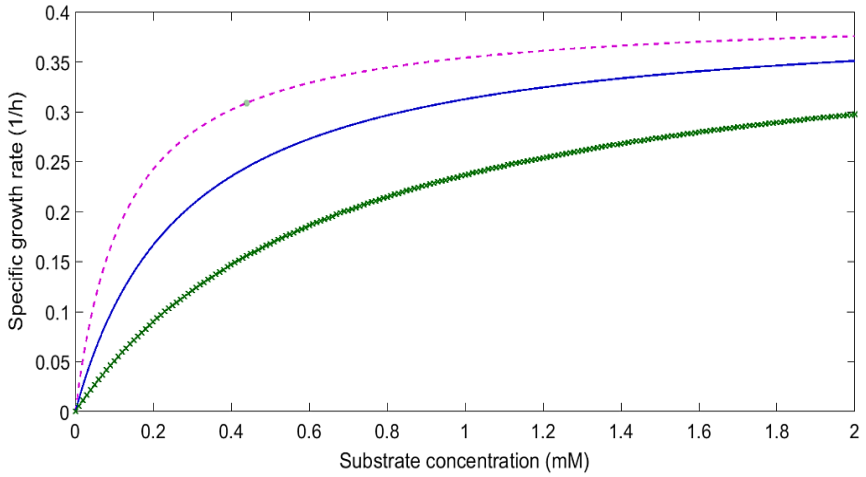

Figure 1-4: Dependence of specific growth rate on substrate concentration represented through a Monod expression with different values for K_s: 0.13 mM (dashed-pink line), 0.28 mM (blue line) and 0.69 mM (x-green line) for a constant value of μ_{max} (0.4 h^{-1}).

For low concentration of *S*, growth rate is highly dependent on *S* and the relationship becomes almost linear (first order). For very high concentrations on the other hand ($S >> K_s$), μ tends to μ_{max} and its value does not change even if the concentration of S keeps increasing (zero order). The Monod equation has been extensively used to describe population growth in bioprocesses. However, this simple equation has several limitations that other forms of the model try to address.

Another formulation with two parameters (μ_{max} and K_s) is the Tessier equation (1936) shown in Eq. 1-4. However, this form of the model has not been taken up widely. The conceptual meaning of K_s is different to that in the Monod equation.

$$\mu = \mu_{max} \cdot \left(1 - e^{-\frac{S}{K_S}}\right) \qquad \textbf{Eq. 1-4}$$

Figure 1-5 shows a comparison between the Monod and Tessier models using the same values for the kinetic constants. It can be seen that the Tessier model saturates much quicker than the Monod model.

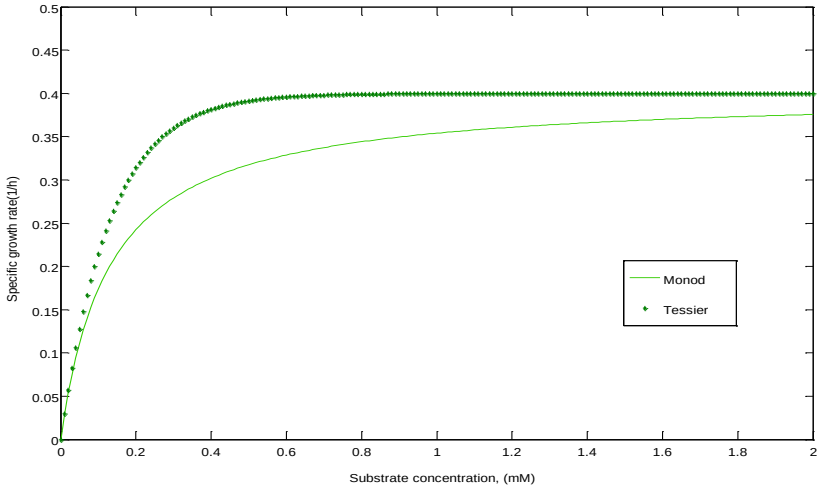

Figure 1-5: Representation of Monod and Tessier models for describing growth rate as function of the limiting substrate with μ_{max}= 0.4 h^{-1} and K_S = 0.13 mM.

Contois (1959) introduced a new constant, B, (the apparent Contois constant) proportional to biomass concentration (Eq. 1-5):

$$\mu = \frac{\mu_{max} \cdot S}{B \cdot x + S} \qquad \textbf{Eq. 1-5}$$

The term $(B \cdot x)$ causes the specific growth rate to decrease as the population increases. The same idea is found in the logistic-type equation (Eq. 1-6) which was actually formulated as a general model of population growth, where N is the number of individuals in a population and K, the carrying capacity.

$$\frac{dN}{dt} = r \cdot N \cdot \frac{K - N}{K} \qquad \textbf{Eq. 1-6}$$

The above models are rather simplistic, being based on a single limiting substrate. It could be that growth rate is simultaneously affected by more than one substrate, and thus, a multiple-substrate model is required. Eq. 1-7 shows a model for a two-substrate system in which one substrate limits the extent of growth while the other controls the rate (Bader 1978). This type of model is computed by simply multiplying the expression for two single-substrate (Monod) models together.

$$\frac{\mu}{\mu_{max}} = \frac{S_1}{K_{S_1} + S_1} \cdot \frac{S_2}{K_{S_2} + S_2} \qquad \textbf{Eq. 1-7}$$

As previously commented, not only can the substrate positively influence growth rate but can also be inhibitory. Several models adapted from enzyme kinetics have been used to describe substrate inhibition in microbial growth and are presented inTable 1-1.

Table 1-1: Models of substrate inhibition in microbial growth. The number of parameters account for the number of constants added to the already existent k_s and μ_{max} *in* Monod expression.

Name	Model	No. parameters
Haldane (uncompetitive)	$\mu = \frac{\mu_{max} \cdot S}{K_S + S \cdot \left(1 + \frac{S}{K_i}\right)}$	1
Ierusalimsky (non-competitive)	$\mu = \frac{\mu_{max} \cdot S}{K_S + S} \cdot \frac{1}{1 + \frac{C_s}{K_i}}$	1
Teisser	$\mu = \mu_{max}\left(e^{(-S/K_i)} - e^{(-S/K_s)}\right)$	1
Aiba	$\mu = \frac{\mu_{max} \cdot S \cdot e^{(-S/K_i)}}{K_S + S}$	1
Hill (allosteric)	$\mu = \frac{\mu_{max} \cdot S^n}{{K_S}^n + S^n}$	1
Webb	$\mu = \frac{\mu_{max} \cdot S \cdot \left(1 + \frac{\beta \cdot S}{K_i}\right)}{K_S + S + \frac{S^2}{K_i}}$	2
Yano & Koga	$\mu = \frac{\mu_{max} \cdot S}{K_S + S + \frac{S^2}{K_i} + \frac{S^3}{K_i}K}$	2
Luong	$\mu = \frac{\mu_{max} \cdot S}{K_S + S} \cdot \left(1 - \frac{S}{S_m}\right)^n$	2
Tseng & Wayman	$\mu = \frac{\mu_{max} \cdot S}{K_S + S} - K_i \cdot \ (S - S_m)$	2
Chen (toxic substrate)	$\mu = \mu_{max} \cdot \left(1 - \frac{S}{K_i}\right) \cdot \frac{S}{K_S + S - (K_{S2} \cdot S)^2}$	3
Han and Levenspiel	$\mu = \frac{\mu_{max} \cdot S}{K_S \left(1 - \frac{S}{S_m}\right)^m + S} \cdot \left(1 - \frac{S}{S_m}\right)^n$	4

The generalized model of Han-Levenspiel aims to cover most of the inhibition cases. The cost in terms of meaningfulness is the increased number of parameters, which gives more degrees of freedom to artificially fit to experimental data.

As well as growth, there can also be reductions in the population due to reactions that consume cellular material (endogenous metabolism). This is normally expressed by an extra term that reduces the net growth as presented in Eq. 1-8.

$$r_x = \mu \cdot x - k_{cd} \cdot x$$ **Eq. 1-8**

where k_{cd} is the constant for cellular death. The equation is analogous to that which accounts for endogenous metabolism.

Product formation

Kinetic models for product formation parallel descriptions for growth kinetics. Although it is accepted that a robust model should be a close representation to the biochemical events taking place, there is little development of structured kinetic models for product formation (Bailey 1976) . The simplest way of expressing the kinetics of product (P) formation is to relate it to cellular growth or substrate formation as Eq. 1-9 and Eq. 1-10 indicate.

$$r_p = \frac{dP}{dt} = Y_{P/x} \cdot r_x$$ **Eq. 1-9**

$$r_p = -Y_{P/S} \cdot r_S$$ **Eq. 1-10**

where $Y_{P/x}$ is the yield of product from biomass and $Y_{P/S}$ is the yield of product based on substrate. When those relationships hold true, as in the case of alcoholic fermentation, the products are often called growth-associated products. Some other products are generated with a delay over growth or even when stationary phase has been reached, these are called secondary metabolites and many antibiotics such as penicillin exhibit this pattern. Then, the rate is assumed to be proportional to the number of cells instead of the rate of growth (non-growth associated models). The Luedeking and Piret model presented in Eq. 1-11 is a good catch-all and often suffices for product formation in the case of extracellular products.

$$r_p = \alpha \cdot r_x + \beta \cdot x$$ **Eq. 1-11**

where α and β represent the growth and non-growth associated constant respectively.

A certain type of fermentation product not described by any particular model is the group of bulky intracellular products, such as polymers and oils. These products accumulate over the fermentation time course, inside the cells, so that biomass is composed of both conventional cell components and fermentation product, which is not excreted to the medium.

Substrate consumption

The substrate, consumed from the medium, can be assimilated by the cells through different metabolic routes and directed to cell growth, product formation or to generate energy that supports cellular maintenance. In cell cultures where there are no extracellular products, apart from CO_2 and H_2O, it can

be assumed that the whole substrate is utilized for growth and maintenance purposes. Then, the rate of consumption can be expressed as shown in Eq. 1-12:

$$r_s = -\frac{dS}{dt} = \frac{r_x}{Y_{x/S}} + m_s \cdot x \qquad \textbf{Eq. 1-12}$$

where $Y_{x/S}$ represents the real or theoretical yield of biomass based on substrate and m_s is known as the maintenance coefficient.

Energy can be required by the cell for activities other than growth and product formation such as keeping concentration gradients and electrical potential across membranes, futile cycles, turnover of macromolecules. These maintenance requirements vary with the type of cell and might not be constant for all growth rates. Whenever m_s is very small (0.01-0.04), the substrate consumption rate can be approximated by Eq. 1-13:

$$r_s = -\frac{r_x}{Y_{x/S}} \qquad \textbf{Eq. 1-13}$$

Other authors prefer including the substrate consumption for maintenance in that associated with growth and refer to an apparent yield, $Y'_{x/S}$.

This short review does not aim to cover all existing models but present some basic expressions for describing macroscopic kinetics. Adaptations of these forms are common in the literature and specific equations are normally developed for describing a particular fermentation. Developing new and more general expressions, which can be appropriately adjusted to apply in different systems, would be preferable to the current practice of developing highly specific model on a case by case basis and could be of benefit to the scientific community.

1.3.3 Other factors affecting the design

Besides the reaction kinetics, other aspects such as microbiology, fluid dynamics and heat and mass transfer can play a significant role in many bioprocesses. When this is the case, they should be carefully evaluated as they could influence the choice of reactor and will definitely have an effect on fermentation results; thus, their study and understanding would enable better interpretations of the data obtained.

The task of designing a bioreactor should not be done without considering the requirement for aseptic conditions, control of fermentation indicators and implications for the separation and purification stages (downstream). The downstream operation would depend on the type of product (intracellular/ extracellular) and the degree of purity sought. Waste materials can have positive or negative value and

would be treated accordingly. Although it goes beyond the work done for this project, frequently the success of a design also relies on its scalability. Traditional methods to do this are based on keeping constant critical parameters in both scales (*e.g.* power requirement, impeller tip speed, volumetric mass transfer coefficient). More recently, computational studies on fluid dynamics have shown its efficiency for scaling-up despite the complexity of the task.

Once a process flowsheet has been drawn and stream data and equipment sizes have been calculated, the utilities design can be carried out. An economic evaluation and environmental impact studies would then determine the feasibility of the project. It is important to have and keep a holistic approach; bearing in mind that, changes in any of the stages would have an effect on the overall behaviour (*i.e.* a new by-product formed due to very large substrate input would affect the separation stages).

For in-depth understanding of the culture dynamics and for suitable reactor design, a mathematical model is developed throughout this thesis using PHB production as a model process. The product of interest, PHB, belongs to the intracellular macromolecules that microorganisms can synthesize. Unlike primary metabolites (ethanol, acetate, lactate) or even secondary metabolites (*e.g.* penicillin), the field of intracellular macromolecules has not received much attention in recent reviews on the modelling of microbial processes. Thus PHB has been chosen as the target product for the studies conducted here because it is a potential representative of the paradigm for this group and is also of important commercial interest. To prepare for this, the following chapter reviews the literature on PHB production.

Chapter 2

PHB production: a review of the literature

2.1 Introduction

2.1.1 Carbon storage in living organisms

Living organisms have a limited set of exergonic (energy releasing) pathways (normally glucose catabolism during cellular respiration) and a multitude of pathways that require energy (endergonic). Adenosine triphosphate (ATP) is a direct link between these two types of reactions (Lehninger 1959). In this way, the energy released from exergonic processes and that cannot be stored as free energy without increasing too much the temperature inside the cell, is stored in the form of ATP. When energy is abundant, cells can produce energy-rich molecules to deal with such excess (Brigham & Kurosawa 2011).

Organisms from all across the living kingdoms have developed the ability to synthesize storage molecules (Radakovits *et al.*, 2010). These compounds act as energy or material reservoirs and can be chemically transformed to release energy, carbon or some other element (S, P, N) abundant in their composition and required by the organism (*e.g.* volutin granules of polyphosphate (Pallerla *et al.*, 2005)). Starch, glycogen or triglycerides are examples of storage compounds that provide carbon, whereas creatine phosphate is only an energy sink (Thauer *et al.*, 1977). Storage compounds can be accumulated within intracellular bodies (*e.g.* starch) or be dispersed throughout the cellular cytoplasm (*e.g.* glycogen) and, while they differ in nature and chemistry, they have some common features. Their molecular weight is normally high and they have a high energy density so that they do not cause an increase in the osmotic pressure and are relatively easy to transport, especially when present in motile organisms (Society for General Microbiology 1992).

Storage materials in plants and animals have been known since ancient times. However, their presence in bacteria was not confirmed until recently. It was doubted that unicellular organisms would require storage compounds as, unlike higher organisms, they do not need energy for activities such as muscular movements, hormonal production and temperature maintenance. According to Wilkinson (1959), to demonstrate that a compound has an energy-storage function, it has to verify the following three criteria:

- *The compound accumulates whenever there is an excess of energy from exogenous sources over that needed by the cells for growth and growth related processes.*
- *When energy from exogenous sources is scarce for growth (division) and growth related processes (maintenance of viability), the same compound is utilised by the cell to provide the carbon or energy required for the maintenance of the cell.*
- *The breakdown of the substance to intermediates and energy in sub-optimal conditions, gives a biological advantage to the cell over other cells not so well endowed. It is this last feature that Wilkinson argues to be the most important criterion to evaluate a storage function, since organisms may utilise essential constituents under prolonged starvation conditions.*

These criteria are important since, for example, fungi, when growing in carbohydrate-rich media also accumulate substances that they do not synthesize when the environmental conditions are not so privileged. The excess of sugars causes the enzymes dealing with their oxidation to become saturated leading to the generation of incompletely oxidised products, such as organic acids. The products of this faulty metabolism are either excreted, accumulated or shunted to secondary subsidiary enzyme systems that slightly modify the substance for accumulation. Foster (1947) compared these products, resulting from a carbon overflow, with storage compounds. However, as commented, a shunt product may be excreted and not accumulated intracellularly and there is no energy requirement for its synthesis. It is also only generated in media containing very high sugar concentrations and is often toxic to the organism. Storage compounds on the other hand require high carbon to nitrogen ratio and can be formed even in poor media (Brigham & Kurosawa 2011).

The utilization of the storage compound by the cell, also called mobilization or *in situ* degradation, responds to one of the following requirement: cell growth in the absence of an external energy source; maintenance of cell integrity and viability; adaptation to a different medium (by supplying the additional energy that might be needed); or for special mechanisms of survival such as sporulation. Examples of cellular functions for the group of storage compounds PHAs are given in Figure 2-1.

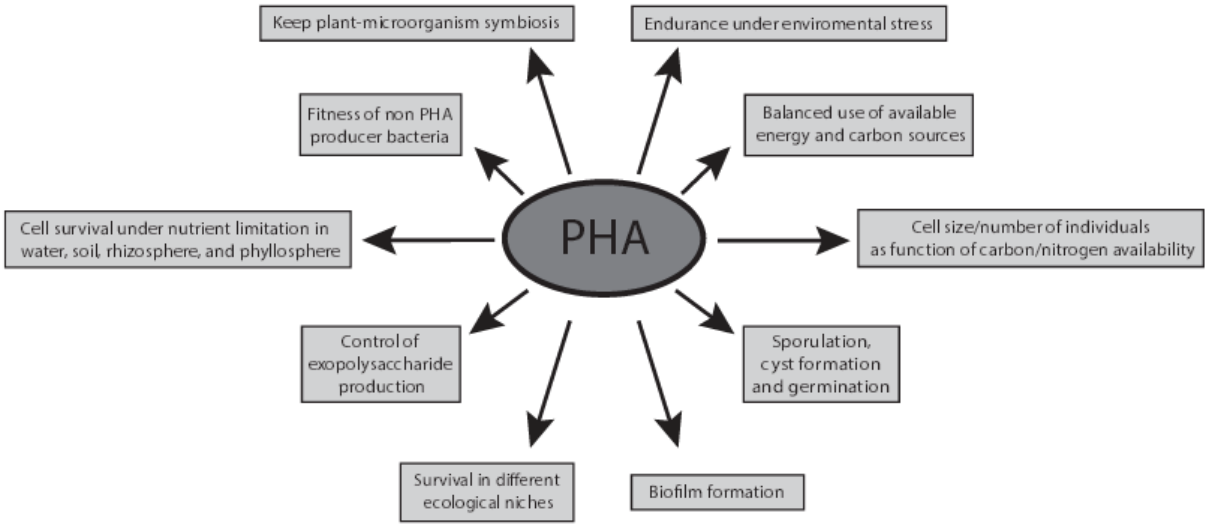

Figure 2-1: Cellular functions of storage products influencing bacterial fitness (Prieto *et al.*, 2014)

The value of the storage compound might vary depending on its concentration inside the cell and the rate of breakdown. For instance, if the concentration is low, it is unlikely that the product will allow the net synthesis of essential proteins and nucleic acids (growth) but it will probably serve as substrate for endogenous respiration, motility, sporulation or adaptation.

2.1.2 Storage compounds of current interest

Single cell oil

Single cell oil (SCO) is the name given to microbial oil produced by yeast, filamentous fungi and microalgae species as shown in Figure 2-2. The initial interest in producing SCO is linked to its use as a potential replacement for cocoa butter, a product that was rather scarce in the 1980s. SCO composition is similar to rare and high value oils such as γ-linoleic acid (GLA), arachidonic acid (ARA), docosahexaenoic acid (DHA) and eicosapentaenoic acid (EPA), so it can be also seen as a source of polyunsaturated fatty acids with proven benefits to human health (Huang *et al.*, 2013). A more recent SCO application is as an alternative feedstock for biodiesel production that does not compete with food crops and is climate independent (Karamerou *et al.*, 2016).

Figure 2-2: Different species from filamentous fungi, yeast and microalgae can accumulate lipids within the cytoplasm (DiSalvo 2010; BioEnergy Genome Center 2011). These organisms are called oleaginous when they can accumulate more than 20% of their dry weight as oil (Meng *et al.*, 2009).

Polyhydroxyalkanoates

Polyhydroxyalkanoates (PHAs) are a type of polyester naturally produced by different microorganisms. Since the discovery of polyhydroxybutyrate (PHB) by Lemoigne (1926), more than 100 monomeric units (constituents of PHA) have been identified in more than 300 microorganisms (Dias *et al.*, 2006). PHAs are sought after as potential replacements for oil-derived plastics. Research into their production has become a hot topic due to their biocompatibility and biodegradability properties, which could significantly reduce accumulation of plastics in landfills. PHAs, compared to other biodegradable plastics synthesized by bacteria, present a wide range of applications due to the broad range of compositions (Bugnicourt *et al.*, 2014).

Over the last decade, more plastics have been produced than during the past 100 years. The current production of SCO and PHA is however negligible when compared to that of petroleum and plastics in the world. By 2018, a production capacity of 6.7 million tonnes of bioplastics is expected, which would correspond to a 2% of the total production. For an economic, and thus competitive, industrial production of storage compounds, there is a need for fast growing microorganisms (that would reduce fermentation times), capable of accumulating large amounts of the product (reducing extraction costs), and able to utilize low cost feedstocks. In addition, if microorganisms are to be used as sources of

biofuels and bioplastics, it is also essential to establish optimal nutrient-dependent conditions for the maximum production of plastics and/or lipids during the cultivation stage.

2.2 Polyhydroxybutyrate, a typical PHA with interesting properties

In the chemical structure of PHAs, the composition of the side chain *R* and the value of *n* determine the identity of the monomeric unit (Braunegg *et al.,* 1998) as represented in Figure 2-3. Side chains can be saturated or unsaturated and, although they are normally aliphatic, certain bacteria can synthesize PHAs with aromatic functions, halogens, pseudo halogens or even alcohols (Koller *et al.,* 2010). Due to its simple skeleton (*n* =1 and *R*, a methyl group) and multiple synthesis pathways, polyhydroxybutyrate (PHB) is the most abundant of polyhydroxyalkanoates. PHB belongs to the short chain length PHAs (scl-PHA), composed by monomers with a number of carbons between 3 and 5. The monomers containing a longer carbon chain (C6→C14) constitute the medium chain length category (mcl-PHA). PHAs have molecular weights in the order of 100 to 1000 kDa. Microorganism (due to the specificity of PHA synthase), cultivation conditions (pH, nature and concentration of the carbon source), fermentation time and extraction methods are factors that affect the molecular weight of the polymer (Anderson & Dawes 1990).

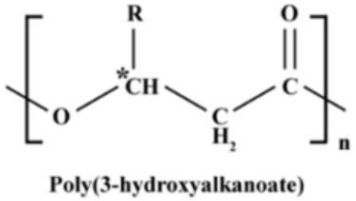

Poly(3-hydroxyalkanoate)

R group	Carbon no.	PHA polymer
methyl	C_4	Poly(3-hydroxybutyrate)
ethyl	C_5	Poly(3-hydroxyvalerate)
propyl	C_6	Poly(3-hydroxyhexanoate)
butyl	C_7	Poly(3-hydroxyheptanoate)
pentyl	C_8	Poly(3-hydroxyoctanoate)
hexyl	C_9	Poly(3-hydroxynonanoate)
heptyl	C_{10}	Poly(3-hydroxydecanoate)
octyl	C_{11}	Poly(3-hydroxyundecanoate)
nonyl	C_{12}	Poly(3-hydroxydodecanoate)
decyl	C_{13}	Poly(3-hydroxytridecanoate)
undecyl	C_{14}	Poly(3-hydroxytetradecanoate)
dodecyl	C_{15}	Poly(3-hydroxypentadecanoate)
tridecyl	C_{16}	Poly(3-hydroxyhexadecanoate)

Figure 2-3: Polyhydroxyalkanoate chemical structure. The carbon denoted as C* is the chiral centre of the PHA building block (Tan *et al.,* 2014).

Biodegradability is a key property of PHB and refers to the rupture of its macromolecule into smaller units by microbial enzymes from filamentous fungi, bacteria or algae. In nature, the products yielded from depolymerisation reactions can be converted into carbon and energy inside the host cell and are ultimately transformed into carbon dioxide and water (Tokiwa *et al.,* 2009). Objects fabricated from PHB will similarly degrade. The time for degradation depends on environmental conditions (type and amount of microorganisms, temperature) and geometry of the object. Degradability of PHB and its copolymer, PHBV, has been shown in aerobic (Marchessault *et al.,* 1994; Jendrossek *et al.,* 1996) and anaerobic conditions (Abou-Zeid *et al.,* 2001). Figure 2-4 shows the effect of nutrients and oxygen availability on the degradation process. Fortunately, PHBV does not degrade in humid air, which guarantees a long shelf life for packaging application. Microbial attack is more prone to happen in amorphous regions of the molecule and for lower molecular weight polymers.

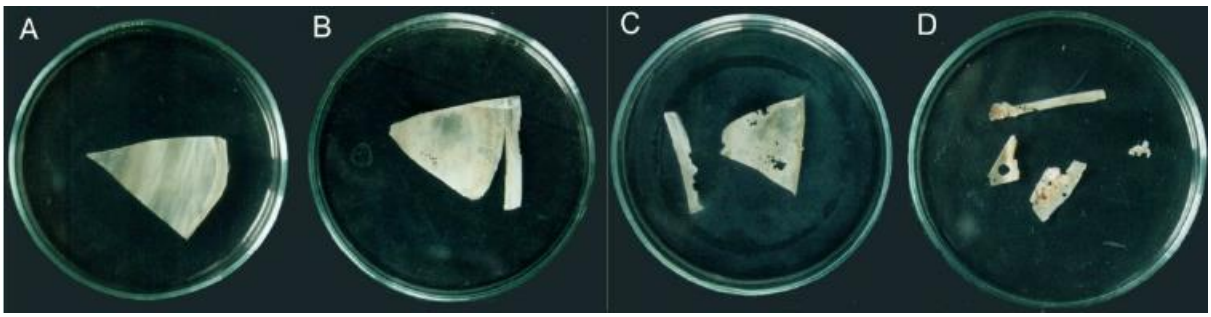

Figure 2-4: Degradation process after a 2 months incubation in soils suspension under different conditions: original PHB film (A) , anaerobic conditions without nitrate (B), microaerobic conditions without nitrate (C), microaerobic conditions with nitrate (D) (Iordanskii *et al.*, 2014).

To be classified as biodegradable, products must be completely degraded and decomposed in composting facilities within a specific time frame (e.g. according to the standards set by EN 13432 , a 90 % degradation is required within 180 days) without leaving any toxic residue or harmful effect (Kalia 2017).

PHB can also degrade by hydrolysis, mechanical, thermal, oxidative or photochemical destruction. It is the hydrolysis rupture which enables its use in medical applications. PHB is also non-toxic, does not cause inflammatory response and their intermediate (CoA-derivative intermediates) and ultimate products (CO_2 and water) can be metabolized and cleared by the body (Valappil *et al.*, 2006), *i.e.* it is biocompatible. The fact that PHB degrades thermally can limit its processability in molten state and additives are sometimes used to prevent this (Asrar & Gruys 2011).

PHB has similar characteristics when compared to polypropylene (PP) regarding melting temperature, degree of crystallinity, glass transition temperature or tensile strength (Hrabak 1992) as presented in Table 2-1

Table 2-1 Properties of PP, PHB and PHB copolymers (data adapted from Lee 1996. Pereira *et al.*, 2008; Koller *et al.*, 2010)

Property	Polypropylene	Commercial PHB	Commercial P (3HB-co-HV)	Commercial P (3HB-co-3HHx)
Density (g/cc)	0.91-0.94	1.17-1.25	1.25	1.20
Crystallinity (%)	60	60-70	50-60	N/A
Tensile strength (MPa)	34.5	18-27	25-40	10-20
Elongation (%)	400	6-17	2.5-30	10-100
Tensile modulus (GPa)	1.4	N/A	1.2-3.0	N/A
Melting temperature (°C)	171-186	N/A	147-175	N/A
Estimated price ($/m^3)	1055	4320	N/A	N/A

Nevertheless, PHB is stiffer and more fragile, partly due to the spherulites formed during the cooling of molten form. It is enantiomerically pure and steroregular (Marchessault *et al.*, 1988); these optical properties enable its use in isomer separation. Due to its water insolubility and low permeability to oxygen and carbon dioxide, it is an ideal candidate for food packaging material (5 times less permeable to CO_2 than PET). It is also piezoelectric (which is a rare property for a plastic) and hence finds application in bone scaffold prosthesis (Mendenhall *et al.*, 2007).

The low elongation to break and stiffness make natural PHB unsuitable for standing impact. To improve flexibility, ductility or tenacity, plastifiers or blends with other, not exclusively renewable, molecules are often used. The natural co-production of different monomers occurring in some bacteria growing in various carbon sources is also exploited for the synthesis of tailor-made plastics. PHB-co-HV for example has better mechanical properties than the homopolymer: the hydroxyvalerate content increases the flexibility and resistance and decreases the melting point without varying the degradation temperature (Shino Yamada *et al.*, 2001). Also cheap macromolecules and organic polymers (*e.g.* starch, wood) can be mixed with PHB to produce active bio-based packaging to extend its use in agriculture applications (Schué 2000).

Currently, PHB serves in the manufacture of commodity products such as shampoo and cosmetic bottles or single-use articles like cups and food containers (Philip *et al.*, 2007). The first artificial esophagus has been generated based on polyhydroxybutyrate; treatment for cardiovascular diseases, use as drug carrier and for nerve and tissue regeneration are only few of the examples for which PHB emerges as perfect candidate (Chen & Wu 2005). Beyond the medical or pharmaceutical field, PHB is expected to fight for its own place within electronic components as replacement of conventional plastics such as low-density polyethylene.

The biodegradable and biocompatible features of this polymer make it an attractive substitute for chemo-synthetic petroleum plastics. In addition, the utilization of renewable materials and agricultural/food wastes for its production, has encouraged the research on the production of this polymer. Since the late eighties, industrial biotechnology research has investigated the natural capacity of certain microorganisms to accumulate PHA via microbial fermentation of pure cultures using wild and genetically modified strains (bacteria). Although a large number of PHAs have been discovered, only a few of them have been produced in large scale. The major commercial producers are listed in Table 2-2.

Table 2-2: Current and potential large volume manufacturers of PHAs (Chanprateep 2010)

Polymer	Trade names	Manufacturers	Capacity (tons)	Price (kg^{-1}) (in 2010)
PHB	Biogreen®	Mitsubishi Gas Chemical Company Inc. (Japan)	10	€2.5–3.0
PHB	Mirel™	Telles (US)	50	€1.50
PHB	Biocycle®	PHB Industrial Company (Brazil)	50	n/a
PHBV and PHB	Biomer®	Biomer Inc. (Germany)	50	€3.0–5.0
PHBV, PHBV + Ecoflex blend	Enmat®	Tianan Biologic, Ningbo (China)	10	€3.26
PHBH	Nodax™	P&G (US)	20,000–50,000	€2.50
PHBH	Nodax™	Lianyi Biotech (China)	2000	€3.70
PHBH	Kaneka PHBH	Kaneka Corporation (Japan)	1000	n/a
P (3HB-*co*-4HB)	Green Bio	Tianjin Gree Bio-Science Co/DSM	10	n/a
Polyhydroxyalkanoate from P&G	Meredian	Meredian (US)	272,000 (2013)	n/a

2.3 Integrating PHB production with biodiesel industry

The international fuel market has traditionally experienced great fluctuation since 2008, when the price of Brent crude reached a record peak of US$147 per barrel. Since then, prices have fallen dramatically such that it is hard to predict what can happen in the future. For example, on the 27th September 2016, the price was exactly $100 less per barrel (Oil-price.net 2016). Biofuels development is strongly supported by subsidies offered by the governments in conjunction with tax reduction. But for biorefineries to provide viable alternatives to petroleum oil, they need to be competitive from a financial point of view even when non-renewable feedstock are as cheap as they currently are (Erickson & Winters 2012).

In the biodiesel industry, one of the main production costs is that of raw materials, which could be minimized by using inexpensive and high yield crops, algae cultures, cooking oils, animal fats or municipal wastes. But for a real enhancement of the biodiesel production, by-products need to be valorized to its maximum potential. An example of this strategy is illustrated in Figure 2-5.

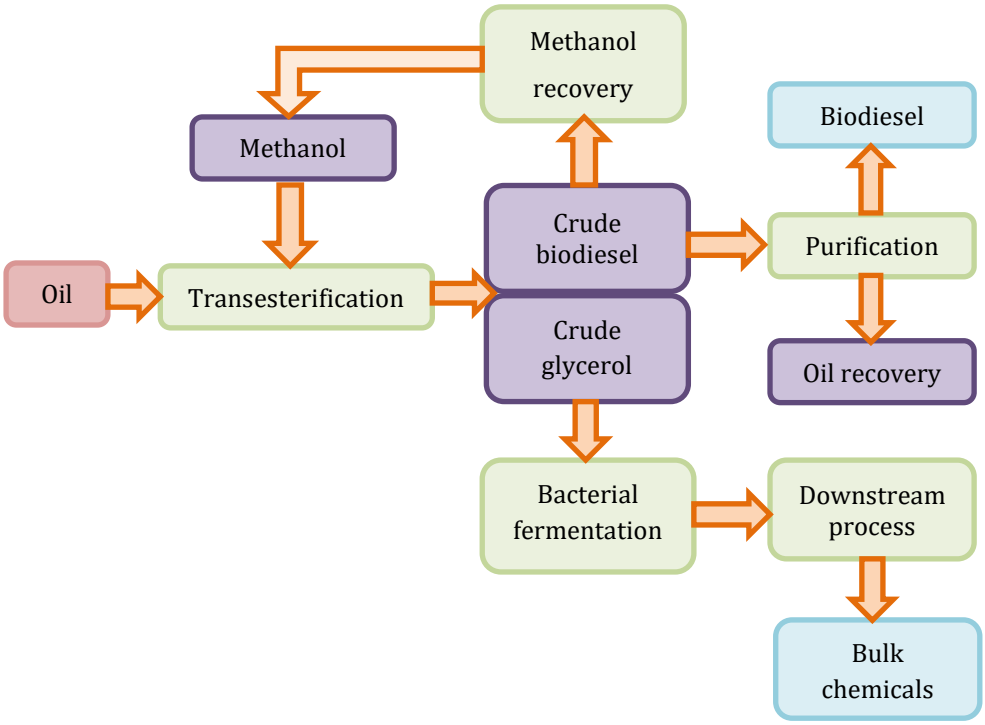

Figure 2-5: Process integration within a biodiesel plant. Crude glycerol co-generated along with the biodiesel can be used as bacterial fermentation feedstock for the production of chemicals.

Glycerol is produced in a transesterfication reaction that converts triglycerides to methyl esters as the main reaction in biodiesel production and accounts for a 10 % wt of the original oil (Meher *et al.*, 2006). Glycerol finds application in a wide range of industries. It can serve in drug and cosmetics manufacturing, food preservation, or paper and textiles conditioning for example. However, the glycerol obtained during the biodiesel production is contaminated with methanol, soaps, salts, heavy metals and residual fatty acids (Pagliaro & Rossi 2010). The composition of crude glycerol can be found in Table 2-3. Those impurities make this crude glycerol unsuitable for the applications mentioned. In order to improve the profitability of the biodiesel production and deal with the large amount of glycerol generated, researchers have explored different options for converting this waste into a valuable product.

Table 2-3: Composition of crude glycerol adapted from (Luo *et al.* 2013)

Compound	Content (wt.%)
Free glycerol	22.9 ± 0.2
Methanol	10.9 ± 0.2
Water	18.2 ± 0.1
Soap	26.2 ± 0.2
FAMEs	21.3 ± 0.2
FFAs	1.0 ± 0.1
Monoglycerides	0.7 ± 0.1
Diglycerides	0.5 ± 0.1

The surplus of glycerol in the market has made the prize as low as $0.1 per kilogram (Quispe *et al.*, 2013) so purification process is no longer a viable option especially for small and medium biodiesel producers. Other attempts at utilizing the glycerol include composting, combustion or feeding to animals. Combustion requires extremely high temperatures and if incomplete, produces acrolein fumes (Steinmetz *et al.,* 2013). Composting or using glycerol in animal feeding is a simpler option, but it does not add much value nor solves the problem of the growing excess of glycerol.

Glycerol based biorefineries appear as the most promising alternative. Such biorefineries would provide for the sustainable and integrated production of biofuels, promoting the utilization of readily available by-product glycerine (glycerol) for the generation of energy and/or chemicals. In this way, glycerol could serve as feedstock for biopolymer production through biological fermentation (Cavalheiro *et al.*, 2009).

Pilot scale glycerol fermentation in a 42 l reactor achieved high PHB productivities and yields of approximately 1 g/(l·h) and 0.25 g/g when using *Zobellella denitrificans* in fed-batch mode; self-flotation of cell debris after extraction with chloroform served as purification method (Ibrahim & Steinbüchel 2009). Productivity and molecular weight are lower than the ones obtained with glucose. The binding of the hydroxybutyrate polymer to the secondary hydroxyl groups of glycerol is believed to explain the reduction in length of the chain. Apart from this, there is no significant difference in other properties between the glycerol-based PHB and the glucose counterpart (Tanadchangsaeng & Yu 2012). Techno-economic studies demonstrated that glycerol-based PHB could be produced at industrial scale with a selling price of 2.6 US$/kg (Naranjo *et al.,* 2013).

Different strains have been tested for PHB production from glycerol and *Cupriavidus necator*, which can accumulate 80% of its mass as PHB, is one them (Mothes *et al.,* 2007; Posada *et al.,* 2011; Cavalheiro *et al.,* 2009). This microorganism, the first to be used in the manufacture of a commercial product by Biopol (Shively 2006), has been known by different names as research developed (Vandamme & Coenye 2004). Although *C. necator* was the first name to be published to refer to a copper resistant bacteria isolated from oil by Makkar & Casida (1987), they did not conduct 16s RNA studies in order to examine its phylogenetic positions, a current standard procedure in prokaryoric taxonomy. There has however been proliferation of other different names (*Wautersia eturopha*, *Ralstonia eutropha*, *Alcaligenes eutrophus*) to refer to the same strain. According to the rules of the International Code of Nomenclature of Bacteria, “each taxon above a species can bear only a name that is the earliest in accordance with the rules of the code” (Lapage *et al.,* 1992), *i.e.* it should be *C. necator*.

Since the beginning of the studies on glycerol performed by the Satake Centre for Grain Process Engineering, the perspectives on biofuels have changed. It is impossible to predict how the alternative fuel market will continue, but it is still important to conduct research in the by-products of this type of industry so that the maximum potential of biorefineries can be met.

2.4 Microbiology, metabolism & enzymatic regulation of *C. necator*

PHB appears as granules of different sizes (0.2 to 0.5 μm diameter) in the cellular cytoplasm of the producer organism. These granules, illustrated in Figure 2-6, are coated by a protein layer and can merge to form bigger inclusions (Shively 1974). They can be found in Gram negative and Gram positive bacteria. The first group is the most common and includes species such as *Cupriavidus necator*, *Alcaligenes latus*, *Pseudomonas putida*, *P. olevarans*, *Aztobacter vinealandii* or recombinant *E. coli* (operon *C. necator).* Within the gram positive group, the genus *Bacillus*, with species such as *B. megaterium* or *B. cereus*, is gaining popularity. The genus *Streptomyces* has also been evaluated as a potential producer of PHB.

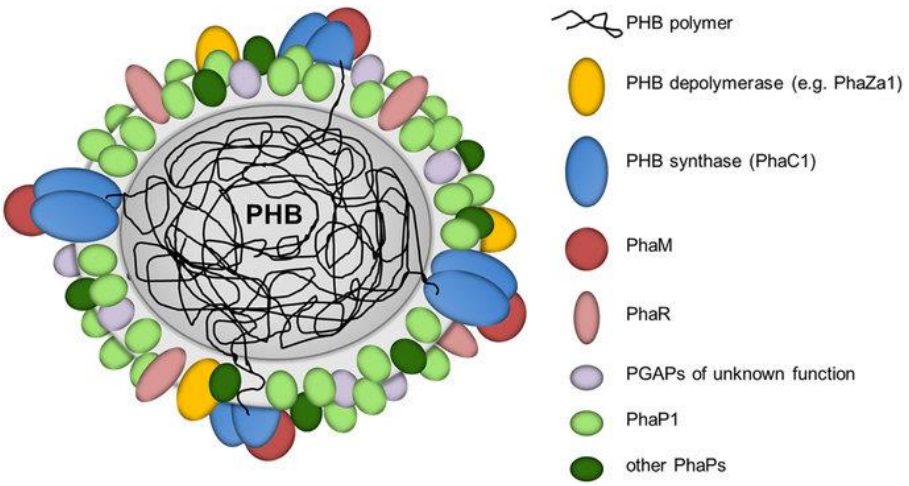

Figure 2-6: Schematic representation of a PHB granule consisting of a polymer core and a surface layer of structural and functional proteins (Bresan *et al.*, 2016)

The thick wall of Gram positive bacteria is thought to complicate the extraction process, thus the limited number of studies. On the other hand, PHB produced by Gram negative organisms might contain endotoxins found in the outer membrane lipopolysaccharide, which put at risk the biocompatibility of the polymer. Bacteria from the genus *Bacillus* have demonstrated promising performance. However, the conditions for triggering PHB are the same as those for sporulation, which could lead to complications and lower yields (Wu *et al.,* 2001).

There are aerobic and anaerobic bacteria as well as chemoautotrophs (inorganic oxidation as single source of carbon) and chemoheterotrophs that can utilize diverse carbon sources (Solaiman *et al.,*

2006). The original strain from the species *C. necator* cannot utilize glucose, whereas the strain used throughout this thesis has achieved that ability due to natural mutation (Grousseau *et al.,* 2013). This big diversity can be explained by the fact that PHB is started from acetyl-CoA and the activated acetic acid is a central intermediate in all living organisms. A general classification of PHB producer is often made according to the conditions required for the synthesis of the polymer (Chee *et al.,* 2010):

•*Biosynthesis coupled to cellular growth: the polymer accumulation takes place during growth under normal conditions as in the case of the genera* Rhodococcus*,* Nocardia*,* Rhizobium*,* Corynebacterium *(Anderson & Dawes 1990).*

•*Biosynthesis decoupled from cellular growth: the polymer accumulation is favored by the availability of the carbon source whenever there is growth limitation due to the lack of nutrients, such as N, P,* O_2 *or microelement including S,* K^+*,* Fe^{2+}*,* Mg^{2+}*. This is the case of* C. necator *and certain* Pseudomonas*.*

In the case of *C. necator*, PHB synthesis starts when two molecules of acetyl- CoA condense with a thiolase encoded by phaA to form acetoacetyl-CoA, which is subsequently reduced by the action of a reductase encoded by phaB (NADPH) to 3-hydroxybutyl-CoA (Khanna & Ashok K. Srivastava 2005) as represented in Figure 2-7. The elongation of the chain (polymerization) is achieved with a synthase encoded by phaC.

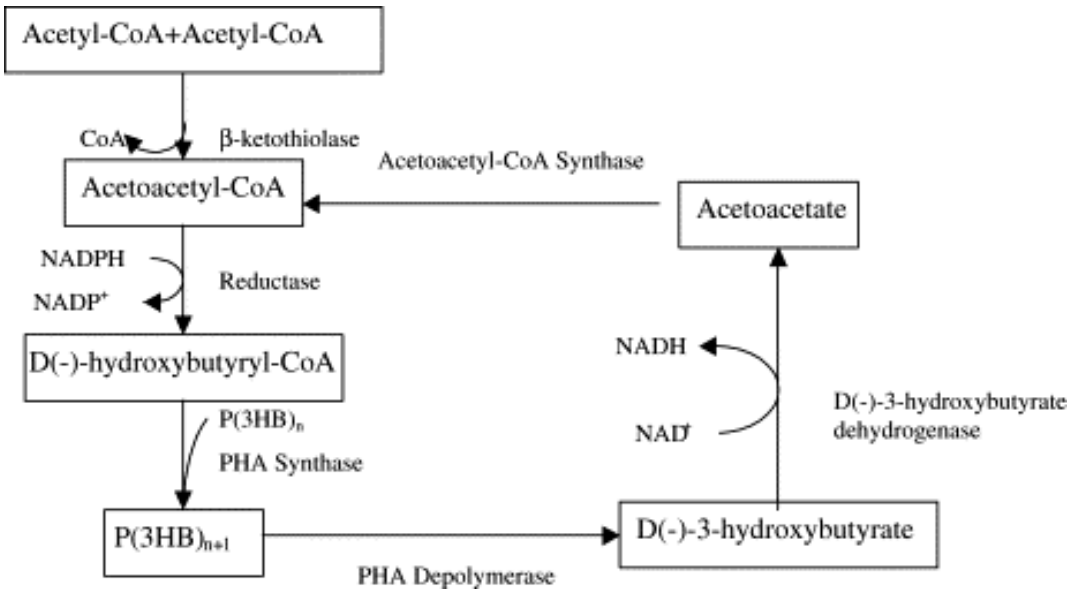

Figure 2-7: Metabolic pathway involved in the synthesis and breakdown of PHB in *C. necator* (*R. eutropha)* (Lee 1996).

PHB is not an essential cellular component and it is not synthesized under every circumstance. Despite not being a taxon-related characteristic nor a particular ecophysiological feature, its ubiquitously occurrence and the fact that a number of environmental stimuli triggers its formation suggest that PHB has a major physiological role. It was noted early on its development that the rate of production increased with the ratio of carbon to nitrogen (glucose to ammonia) (Macrae & Wilkinson 1958), but the accumulation could also be enhanced by the nutritional limitation of phosphorous or oxygen.

PHB formation is often treated as a switch response to suboptimal conditions for growth and multiplication characterized by imbalanced supply of nutrients (Stal 1992). This response of microorganisms to overcoming internal bottlenecks (when external limitations are imposed) is known as "overflow metabolism". A lack of nitrogen, phosphorous, oxygen, sulfate or even K^+, Mg^{2+}, Fe^{2+} can all lead to a similar response and this implies underlying common mechanisms. As a rule, concentration of acetyl-CoA must be high to lead to the synthesis of acetoacetyl-CoA and reducing equivalents must be available to withdraw the acetoacetyl-CoA generated (Babel *et al.,* 2001). The most common trigger mechanisms for PHA production are described next:

•*Nitrogen limitation: Nitrogen is involved in the synthesis of proteins, nucleotides and coenzymes. When there is a lack of N, NADPH cannot be consumed for reductive synthesis, such as amino acids production so it remains available and starts inhibiting the citrate synthase. Being the TCA cycle inhibited, acetyl-CoA becomes available to flow into the PHB pathway. In other words potential applications of acetyl-CoA and NAD (P)H are restricted.*

•*Phosphorous limitation: Phosphorous is essential for the conversion of the energy provided by the substrate in the form of ATP. In the absence of P, ADP cannot be phosphorylated to form ATP. It is believed that the reducing power that does no flow away and acetyl-CoA that becomes available can be assimilated for PHB as in the case of nitrogen limitation. A decrease in the ATP synthase activity and a repression in the Krebs cycle can be observed during P limitation (Marzan & Shimizu 2011).*

•*Oxygen limitation: O_2 acts as acceptor of electrons in the respiratory chain. Whenever there is lack oxygen, reduced cofactors cannot be oxidized via respiratory chain. The effect of the reducing power (metabolic control) and the lack of oxygen itself put a stop in the TCA (which would become endergonic in anaerobic conditions) and the same consequences follow as in the N and P limitation cases.*

If all (macro and micro) nutrients are present, in amounts which do not constitute a deficit, cells will grow and multiply and have no other major metabolic product than CO_2, water and heat. In this perfect situation, which could happen for only a short time, if at all, intermediates are formed in simple catalytic amount so that cells will possess a determined composition. Microorganisms cope with shortcomings and environmental fluctuations of diverse extension and intensity and have developed different strategies to deal with these, one for them is overflow metabolism. PHB is produced when more reducing power than can be consumed is generated due to limitation of other factors. In the words of Babel *et al.,* (2001), "… it is an investment for the future as it can be mobilized in conditions of starvation…".

PHB can be mobilized by the cells under stressful conditions as mentioned earlier in the chapter. PHB depolymerase (PhaZ) hydrolyzes the polymer to yield 3-hydroxybutyric acid. This can be then metabolized to obtain carbon or energy or excreted. For metabolizing 3-hydroxybutyrate, it needs to be converted into acetoacetate or activated to CoA derivatives by various enzymes like acyl-CoA synthetase or thioesterase. Acetoacetate can be broken into two molecules of acetyl-CoA by the action of β-ketothiolase and these molecules enter the tricarboxylic acid (TCA) or glycoxylate cycles. (R)-3-hydroxybutyl-CoA can immediately be epimerized to the (S)-isomer and catabolized with the

consequent energy release through the β-oxidation pathway (Wang *et al.,* 2009).

2.5 Factors affecting PHB production

2.5.1 Culture medium

Within the culture medium, the factor that has been most extensively studied is the carbon source. This is not only because of its direct influence in PHB production but also due to its contribution to total operating costs, which can reach the 40% (Choi & Lee 1997). Thereby, numerous cheap carbon sources have been tested including solid and liquid residues from cereal processing such as wheat and rice bran (Van-Thuoc *et al.,* 2008; Ramadas *et al.,* 2009; Huang *et al.,* 2006), by-products from dairy industry such as molasses (Solaiman *et al.,* 2006; Gouda *et al.,* 2001; Santimano *et al.,* 2009; Albuquerque *et al.,* 2007), other vegetable residues (Haas *et al.,* 2008) and waste oils (Verlinden *et al.,* 2011). Autotrophic culture for PHB production from carbon dioxide (Ishizaki & Tanaka 1991) is another alternative for exploiting inexpensive raw materials that could act as an interesting CO_2 capture technology.

Opposed to one factor at a time strategy, attempts to optimize the culture medium in a less time consuming manner have been done using statistical based experimental design, *e.g.* response surface methodology (Ramadas *et al.,* 2010; Mokhtari-Hosseini *et al.,* 2009; Khanna & Ashok K Srivastava 2005b; Nikel *et al.,* 2010; Grothe *et al.,* 1999). Although the optimal recipe for the culture medium is strain dependent, some of the most sensible parameters were found to be the carbon and nitrogen source, phosphates and some trace elements.

Identification, isolation and genetic engineering of strains that can grow and produce PHB at relatively high yields from these or other inexpensive substrates is also subject of several investigations (Li *et al.,* 2007). Low-cost nitrogen sources such as urea and corn steep liquor have also been utilized in an attempt of replacing expensive and undefined yeast extract (Kulpreecha *et al.,* 2009; Gouda *et al.,* 2001). But it is actually the relation between the amount of carbon and nitrogen (limiting nutrient to trigger PHB) what has attracted more discussion. It seems clear that conditions in which carbon is supplied in excess of nitrogen are required for PHB synthesis since cells grown in nitrogen-free conditions favour growth and maintenance functions over PHB accumulation.

According to Khanna & Srivastava (2008), "N/C was indicated to be a more comprehensive term reflecting the true impact on growth and product formation". PHB is stimulated at high ratios in favor of growth, as cells are deprived of essential nutrients to grow, but at very high ratios though, growth can be inhibited. Nonetheless, there is not agreement on an optimal value for this term and authors claim different ratios for each particular case.

2.5.2 The importance of Carbon to Nitrogen ratio (C/N)

According to Spoljarić *et al.,* (2013) it is "…critical to assess optimum C/N ratio for best production of non-growth conditions". There are many studies in the literature that aim to determine the 'optimal' value (based on different criteria) for PHB fermentations using different microorganisms and substrates. The reported optimal value could be the ratio that leads to the highest concentration, highest production, highest yield or, rarely, highest productivity. Table 2-4 illustrates the variety of ratios reported in the literature as optimum values for PHB production.

Table 2-4: Values of C/N reported in simple batch studies focusing particularly on this aspect of medium optimization.

Organism	**Carbon source**	**Nitrogen source**	**C/N (molar)**	***Reference***
Bacillus subtilis ATCC 6633	D-mannitol	L-glycine	2.5	(Tamdoğan & Sidal 2011)
Rhodobacter sphaeroides N20	Acetate	Ammonium sulphate	6	(Sangkharak & Prasertsan 2008)
Bacillus megaterium	Sucrose	Ammonium sulphate	8	(Faccin *et al.,* 2009)
Cupriavidus taiwanensis	Gluconic acid	NH_4Cl	8	(Wei *et al.,* 2011)
Protornonas extorquens	Methanol	Ammonia	10	(Suzuki *et al.,* 1986)
Bacillus Megaterium	Various	Various	16	(Sharma & Dhingra 2015)
Pseudomonas stutzeri	Sucrose medium	Ammonium sulphate	20	(Belal 2013)
Bacterium isolated from soil	Glucose	Ammonium sulphate	20	(Lathwal *et al.,* 2015)
Paracoccus denitrificans DSMZ 413	Glycerol	Yeast extract	21.4	(Kalaiyezhini & Ramachandran 2015)
Alcaligenes latus ATCC 29713	Sucrose	Ammonium sulphate	28.3	(Grothe *et al.,* 1999)
Cupriavidus sp. USMAA2-4	Oleic acid	Ammonium sulphate	30	(Aziz *et al.,* 2012)
Ralstonia eutropha	Condensed corn solubles	Ammonia	50	(Chakraborty *et al.,* 2009)
Azotobacter chroococcum 6B	Glucose	Ammonium sulphate	137.7	(Quagliano & Miyazaki 1997)

As can be seen in the table, the range is wide and it appears that there is no pattern to what might be the optimum C/N ratio in any particular system. However, on closer inspection, some general observations can still be made when mapping the results.

Considering the type of microorganism, those that exhibit growth associated production kinetics are more likely to have low optimum values, as for the case of *Bacillus subtilis*. On the other hand, if production is non-growth associated, an excess of carbon would probably be beneficial and hence, optimum C/N would be higher (*Ralstonia eutropha*). There are also effects based on the substrate. For fermentations performed with inhibitory nitrogen sources, C/N cannot be very low. In the same way, if the carbon source is inhibitory, such as methanol, the ratio will not take very high values. Also, if the criterion chosen for defining the optimum is growth, the ratio tends to be low compared to when PHB accumulation is the objective.

What seems applicable in all cases is that when using relative low ratios, carbon is directed to growth and anabolic reactions so that less is prone to be utilized for PHB formation. The flow of carbon into the PHB synthesis is stimulated for relative high ratios.

Duchars and Attwood (1989) studied the influence of the C/N ratio in a chemostat. They found that at low C/N ratios, no PHB was produced and growth (indicated by cellular protein concentration) stayed approximately constant for a certain range. For ratios higher than this, PHB production started and was gradually increased as the ratio increased. At the same time, the concentration of cellular components started decreasing until it became barely stable, matching the time at which PHB also reached a plateau, as schematized in
Figure 2-8.

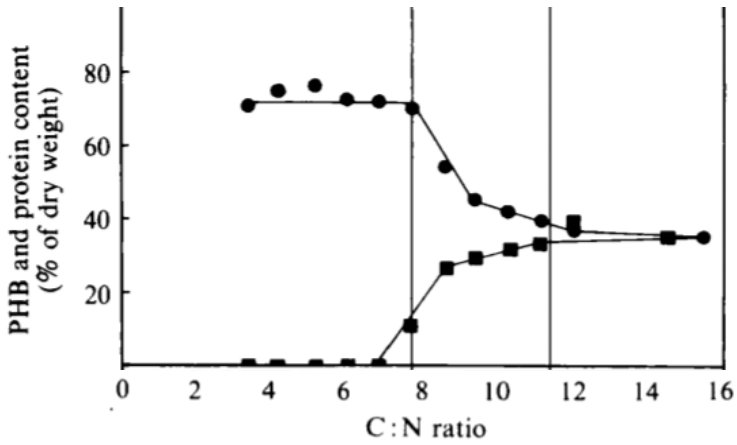

Figure 2-8: Relationship between C/N and PHB (squares) and cellular protein (circles) concentration according to Duchars & Attwood (1989).

Wang & Yu (2001) stated that low C/N, *i.e.* nitrogen rich media, led to increased reproduction and acetate (carbon source) utilization but decreased PHB formation. At very high acetate concentrations, an inhibitory effect on growth, PHB production and acetate consumption was noted. Most of the studies focused on growth and production but there are also indications that C/N might affect the product quality.

2.5.3 Physical operational variables

Besides the type and concentration of substrates, environmental conditions can also make a difference in the success of PHB fermentation. Again, these conditions are particular to the strain used, however, there are not so many studies as for the case of medium components. Krishna and Van Loosdrecht (1999) reported that kinetics of the process were strongly influence by temperature. In general terms, it can be said that the optimum condition for PHB fermentation ranges from 30 to 37℃. This could be related to activity of the enzyme synthase which is induced above 30℃ and decreases above 40℃ (Tripathi *et al.,* 2013). Accordingly, Grothe *et al.,* (1999) found that the optimal temperature for batch culture of *Alcaligenes latus* is 33℃. The PHB production process is normally carried out at pH values between 6 and 7.5. Studies with different set values and no control for pH demonstrated that a value of 7 was better that either 6, 8 or no control for growth and PHB production (Kulpreecha *et al.,* 2009). A pH of 6.9 was found optimum for growth and PHB production by *Alcaligenes eutrophus* (Palleroni & Palleroni 1978).

Agitation, essential to achieve an homogeneous culture and avoid diffusion phenomena being the rate limiting step of the biological process, has a great influence in the availability of a low soluble gas such as O_2 in the medium. Dissolved oxygen is critical for growth of many aerobic bacteria and is often maintained at high values during growth phase; in special cases, enriched air or pure oxygen can be necessary. Decreasing the agitation speed can serve to induce PHB synthesis (by decreasing the dissolved oxygen and thus, imposing oxygen limitation) at a more advanced stage of the fermentation, once good cell growth has been achieved, but a severe shortage of oxygen can have the contrary effect and delay PHB biosynthesis (Patnaik 2008). When maintaining a constant value for aeration, Quagliano & Miyazaki (1997) showed that an aeration of 2.5 vvm led to the highest biomass concentration when compared to lower rates, but 0.5 vvm resulted in maximum PHB content. Very high agitation speeds can lead to excessive shear stress on cells, which can in turn affect the viability of the culture.

The importance of aeration

It is known that oxygen can act as the limiting substrate to enhance PHB production. What is less often reviewed is the role that oxygen has as a secondary limiting nutrient, *i.e.* when another nutrient is already limiting, *e.g.* N. Combined effects of nitrogen and oxygen have not been reported but, during the accumulation stage, as growth slows down or even stops, dissolved oxygen is often set to a lower value. The critical value for PHB formation seems to be significantly lower than that required for full growth (Mozumder *et al.,* 2016). It might even be that there are synergistic effects between the two limitations such that overall productivity is higher than if just one limitation is imposed. The limitation effects are illustrated schematically in Figure 2-9.

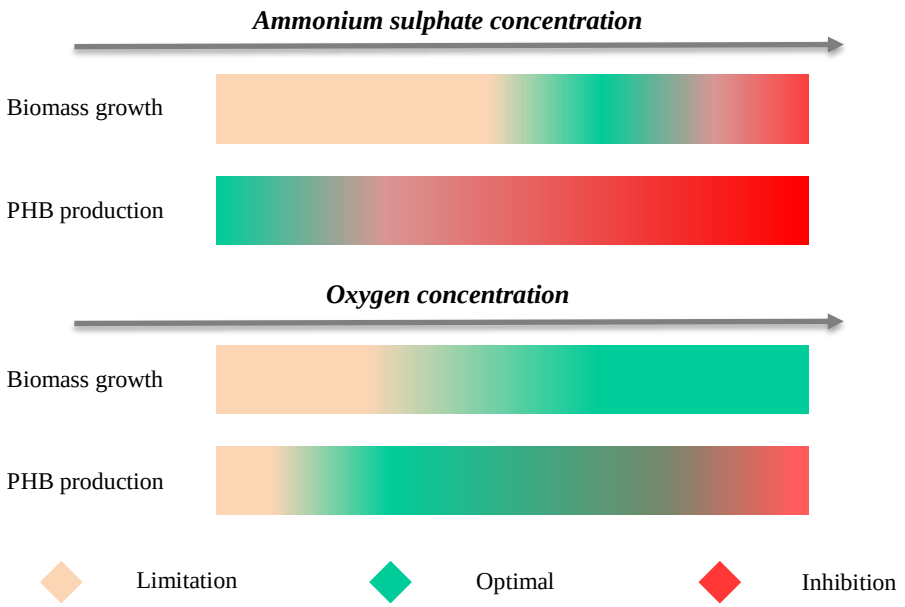

Figure 2-9: Control of growth and PHB production could be achieved by manipulating nitrogen and oxygen concentrations. The direction of the arrows indicates increasing concentration.

2.5.4 Mode of operation

Typically, PHB production is carried out in discontinuous operation with an approximate duration between 38 and 72 hours. In this way it is easy to stablish the nutrient limiting conditions required for synthesizing the polymer. Two stages are distinguished within a discontinuous process:

- *Growth phase to achieve the desired cellular density and finish off the nutrient that triggers the production*
- *Production phase triggered by the limitation at which cellular growth is stopped.*

Batch processes are limited by the initial amount of substrates and they are discouraged for substrates that can inhibit growth at high concentrations. Fed-batch allows a better control of the two cultivation stages and the use of potential toxic substrates such as volatile fatty acids (acetic, lactic, propionic, butyrique) which can be gradually added.

Feeding strategies

Besides the feeding of the carbon source, essential at the production stage, some studies have reported the importance of maintaining a "sustained growth" over the accumulation phase by feeding some nitrogen together with the carbon. The C/N ratio in the feeding has been investigated by Suzuki *et al.,* (1986). The way in which the feeding should be carried out (for a more efficient PHB fermentation)

has been evaluated by Hafuka *et al.,* (2011) where a pulse, a stepwise and continuous feeding were compared in terms of PHB production. A common fermentation practice is to use a solution of NH_4OH to control the pH and provide additional N in the first hours of fermentation. When the nitrogen limiting conditions are to be imposed, that solution is replaced for NaOH (base function only) and the feeding of carbon/carbon and nitrogen in a determinate ratio starts.

Enhanced PHB production by dense biomass cultures conducted in fed-batch mode is widely practiced. In such systems, the preliminary batch time is critical not only for defining (in most cases) the cell mass concentration yielded but also the productivity of the overall process. As the product of interest is accumulated intracellularly, it becomes crucial to evaluate not only PHB content but also the total production regarding the amount of biomass present. The trade-off between growth and product formation should then be optimized so that the yield of PHB based on carbon is maximum.

Feeding responds to a need to supply additional carbon (that cannot be supplied at the beginning as it can hamper growth or be utilized in anabolic processes). The addition of nitrogen or some other minor nutrients together with the carbon has also been employed by some authors. It is then important to define the feeding composition and the profile at which they will be fed to assure there are no bottlenecks in the polymer metabolic pathways.

The shortcomings of the fed-batch fermentation (non-productive time for reactor revamping, irregular product quality, insufficient productivity) can be theoretically improved by continuous fermentation (Koller & Braunegg 2015). However, the fundamental differences between the possibilities of running continuous fermentation for the production of extracellular products and doing it for PHB, or any other intracellular product from the carbon storage group, need to be highlighted. A significant number of cells have to be firstly achieved so that, later on, these cells can accumulate the biopolymer. This means that PHB production cannot happen in steady state. Continuous fermentation for PHB production and for bacteria such as *C. necator* (production is non-growth associated) have to be conducted in multistage fermentation at reactors operated at different dilution rate or under different conditions at each stage have been tested (Atlić *et al.,* 2011; Koyama & Doi 1995; Yu *et al.,* 2005). An airlift reactor with in situ cell retention has been design for growth associate production of PHB (Gahlawat *et al.,* 2012). To date, continuous fermentation has been more employed as tool for studying kinetics or as enrichment step of PHA producers in mixed cultures.

2.6 Kinetic models: can they be tools for PHA optimization?

2.6.1 Description of formal kinetics for PHB production

Bioprocess modelling can be attempted from very different approaches, which take different names

depending on the authors. Formal kinetics refers here to unstructured or low-structured models, also called mechanistic models, embedded in the macroscopic modelling strategy defined in Chapter 1. To represent the dynamics of a fermentation, they usually consist of ordinary differential equations that express the evolution/profiles (rates) of the variables of interest against time. The interaction between variables is formulated by different functions (kinetic expressions) including several parameters that need to be identified. As illustration, the formulation of a model with three state variables (biomass, product and substrate) is presented below:

$$r_x = \frac{dC_x}{dt} = f_1(c_x, c_{p,} c_s) \quad \textbf{Eq. 2-1}$$

$$r_p = \frac{dC_p}{dt} = f_2(c_x, c_p, c_s) \quad \textbf{Eq. 2-2}$$

$$-r_s = \frac{dC_s}{dt} = f_3(c_x, c_p, c_s) \quad \textbf{Eq. 2-3}$$

For practical engineering purposes, unstructured kinetic models are useful process optimization tools. However, the first mathematical models of this type were not conceived for optimization (Mulchandani *et al.,* 1988; Sonnleitner *et al.,* 1979). There was not yet distinction between the storage polymeric material (inert fraction of biomass) and the biological active part consisting of the membrane, cytosolic proteins, glycolipids, phospholipids, glycoproteins and nucleic acids, *i.e.* anything that is not PHB (residual biomass). Fermentations, to establish the relationships between substrates and products, were conducted with excess of all substrates except for the carbon source. Growth rate was described following the Monod equation based on carbon. Equations for substrate consumption and product formation were constructed upon stoichiometric coefficients or yields. The first breakthrough was the development of the still used "two-main compartments" strategy by Heinzle & Lafferty (1980) in which PHB and residual biomass were considered two separate variables.

Growth kinetics

In fermentations planned to produce significant amounts of PHB, the carbon source is rarely the limiting nutrient. Thereby, growth rate has been widely expressed in terms of the nitrogen source and phosphorous (Shang *et al.,* 2007). To account for the effect of more than one substrate, double substrate kinetics were also employed and were later extended to multi-substrate Monod kinetics for the cases of complex media:

$$\frac{\mu}{\mu_m} = \mu(S_1) \cdot \mu(S_2) \cdot \mu(S_3) \quad \textbf{Eq. 2-4}$$

The observation that growth stops when biomass reaches a certain concentration, independently of the concentration of the substrate considered to be limited, was reported by several authors and the use

of a logistic type equation has become a common practice to describe biomass self-inhibition (Luong 1987).
With the increasing range of substrates came the incorporation of inhibitory terms to growth kinetics. Some of them, developed for different biological systems (*e.g.* hemoglobin, alcohol fermentation) were adapted to express the effect of different nutrients in cell proliferation. Also product inhibition has been considered as in the Luong equation (1988). However, other factors such as catabolic repression, also known to affect growth, have hardly been translated to mathematical expressions.

Product kinetics

The Luedeking-Piret equation (1959) is the most extensively applied model to describe product formation and has also been used for PHB production. It is however questionable whether it is suitable for microorganisms where production is not simply linked to either primary or secondary metabolism. For the case of *C. necator*, non-growth associated with and without growth associated production have all been reported and different authors have contradictory views concerning appropriate models. (Atlić *et al.,* (2011) considered PHB formation to be a non-growth associated synthesis, whereas (Mozumder *et al.,* (2014) assumed both growth and non-growth associated kinetics.

Modifications of the Leudeking-Piret model have been made by including an inhibitory term to represent the effect that nitrogen or phosphorous has on repressing PHB formation. Product inhibition is also reported by some authors to account for the effect that PHA granules have on biomass growth due to the large volumes they can occupy of the intracellular space (Mulchandani *et al.,* 1989).

Although the influence of dissolved oxygen on growth and PHB production was already noticed by Sonnleitner *et al.,* (1979), this variable is very rarely included in kinetic models. Despite the apparent difficult, Tohyama *et al.,* (2002) managed to include the effect of oxygen in their mixed culture model. Another model adaptation was the incorporation of a maintenance term in the description of substrate consumption. The Guthke equation presents this energy of maintenance in the form of a saturation relationship, similar to the Monod equation itself (Novak 2015).

The fact that research in PHB is so dispersed throughout many subjects might explain that some models do not go beyond a descriptive purpose, for which the ultimate goal is obtaining a good fitting to the experimental data. For doing this, constant kinetics are frequently tuned until a minimum error between theoretical and experimental results is achieved. The applicability of the model to conditions different to those used to obtain the parameters may be thus compromised. Some studies conducted on batch kinetics served to determine the parameter constants. However those models are often not extrapolated to fed-batch fermentation, which is the regular operation regime.

After testing different equations against a set of experimental data, Dhanasekar *et al.,* (2003) found

that logistic, "logistic incorporated Leudeking–Piret" (LLP), and "logistic incorporated modified Leudeking–Piret" (LMLP) models were the ones that better described growth, product formation and glucose consumption by the mutant strain *Actinobacillus vinelandii*. LMLP is the name given by the authors to express substrate consumption for growth product formation, which kinetics were described by the mentioned expressions, and for maintenance.

In a similar manner to Dhanasekar *et al.,* (2003), Mozumder *et al.,* (2014) studied PHB production by *C. necator* DM 545 under N limitation, when oxygen was supplied in large excess. Production was considered to be growth and non-growth associated, although the first term was inhibited by N. The product itself also inhibited the process and they included three parameters to represent it. Three different models, based on previous works by different research groups, were used for parameter estimation in fed batch cultivation. The simplest model considered only growth on substrate (glucose). Biomass growth on PHB, based on the findings of Luong *et al.,* (1988), was also considered in a second model. An extension of this included a self-limited population term and was applied for biomass growth on the carbon source and on PHB through the logistic equation (Mulchandani *et al.,* 1989). The most comprehensive model gave the smallest difference between simulations and empirical data for a set of experiments and was then used for simulating a PHB fermentation on glycerol after a new stage of calibration (recalculation of the kinetic constants).

It was stated in their report that "during the two-phase fermentation processes, cell growth and PHB production need to be balanced to obtain a higher productivity, avoiding incomplete production because of late shifting to stress conditions, at a high biomass concentration or because of premature shifting at a too low biomass concentration". However, there was no discussion about the times at which feedings should start or any evaluation of the compromise between biomass and production to achieve high productivities.

2.6.2 Application of formal kinetics for optimization of PHB production

A different and maybe a more interesting approach was taken by Raje & Srivastava (1998). They firstly studied the kinetics of *Alcaligenes eutrophus* in batch culture in order to develop a model that could then be used to simulate suitable nutrient feeding profiles in semi-continuous operation. A novel expression was proposed for growth rate composed of two additive terms, Monod and Sigmoidal growth kinetics, which were multiplied by an inhibitory factor to account for high ratios of N/C (ammonium chloride/fructose). PHB production was computed as growth and non-growth associated. For the non-growth associated production, PHB inhibition was accounted for by a subtractive term, and nitrogen inhibition in the usual form. A minimum amount of catalytic biomass was considered necessary for PHB production to initiate.

The model was then updated for fed-batch operation by the addition of the various flow terms. Feeding

of nitrogen was applied to strengthen growth associated PHB production whereas carbon concentration was maintained above a certain value by the feeding of fructose. Regimes in which nitrogen was supplied at a constant rate, maintained at a particular value and a feeding profile time dependent necessary to maximize PHB production were tested. This work shows a greater applicability of kinetic models. However, aspects such as when to start feeding were chosen arbitrarily and not yet theoretically evaluated.

The two feeding streams present in fed-batch operation were nitrogen feed (F_1) and fructose feed (F_2). Following the recommendations of Mulchandani *et al.,* (1988), the fructose concentration was not allowed to fall below 10 g/l and F_1 was optimized for maximum PHB production through three different strategies. The optimization function was defined as:

$$F_{max} = \frac{P \cdot V}{T_{finish}} \qquad \textbf{Eq. 2-5}$$

where P is the total amount of PHB and T_{finish}, total time of fermentation. Three different feeding strategies were evaluated :

- *Constant feeding strategy: F_1 and the concentration of nitrogen in the feeding were changed in discrete step sizes until the maximum value of the function was reached. This occured at 6 ml/h and 300 g/l respectively.*
- *Constant nitrogen concentration: different concentrations of nitrogen inside the bioreactor were tested and F_1 was calculated to satisfy that for a fixed concentration in the feeding. Although, F seemed to take higher values for high nitrogen concentrations, this strategy was not implemented as they felt it would increase the reactor volume too much.*
- *Generalized flow profile: flow rate was variable with time and the parameter A, B and C were calculated for maximum F_{max}:*

$$F_1 = A + B \cdot t + C \cdot t^2 \qquad \textbf{Eq. 2-6}$$

This was the strategy with better results (F_{max}= 1.3), for both simulations and experiments conducted in a 2 l reactor. As in the first case, the optimum nitrogen concentration in the feeding was found to be 300 g/l, and in this case, the optimum feeding time at which the feed started was mathematically defined and equal to 19 h. Fed batch fermentations improved significantly the productivity compared to the batch system (F_{max}= 0.1976).

In later work (Patwardhan & Srivastava 2004), the same model was employed (although new values for kinetic constants were calculated) with the intention of testing those conditions that the simulations showed to be promising. Again two different feeding strategies were tested:

- *Constant nitrogen strategy. Contrary to what was found in the previous paper, the concentration in the medium was aimed to be as low as possible and this was difficult to implement due to the variable flow with time.*

•*A constant feeding of N and fructose was a simpler strategy but with lower productivity than the previous, although still better that batch.*

Khanna & Srivastava (2008) developed a new model with an increased number of parameters. For instance, the new equation for the growth rate had 9 kinetic constants. Production was described by a Leudeking-Piret term. Kinetic values were fitted to the experimental work presented in the publication but also to experiments conducted by Raje & Srivastava (1998) and Mulchandani *et al.,* (1988) (different values). Beyond improving the mathematical descriptions, as the publication claims, there is little application to their findings as results were not tested predictively just fitted retrospectively.

Especially relevant to the research presented in the current thesis are the works of Špoljarić *et al.,* (2013) leading with by-products stemming from biodiesel production. In the latest publication, they present two models for fermentations conducted with two carbon sources each, glucose and glycerol in the first case and FAME and valeric acid in the second. In this latter case, PHBV is yielded as the main fermentation product and the authors distinguished between the two monomers, treating them as different variables. The lag phase is captured by the definition of time intervals. They consider residual mass is produced from glucose and during exponential phase, PHB production is growth associated and also comes from glucose. During stationary phase, production is obviously non growth associated and, in the model, activated by nitrogen depletion. Synthesis of PHB from glycerol is completely non growth associated and inhibited by glucose. The energy for maintenance is assumed to come from glucose. To enhance production from glycerol, in silico fermentations were conducted in which the feeding of glucose, glycerol and nitrogen was evaluated. Glucose even in small amounts appeared to block glycerol consumption in experiments and was catered for in the model.

Very recently Mozumder *et al.,* (2016) presented a model able to describe heterotrophic-autotrophic PHB production and reported optimal values for nitrogen and oxygen. The above review summarizes the principal semi-structured or unstructured models for PHB production. Other, more sophisticated models have also been published but are generally of limited use for prediction or design purposes. For example Koller *et al.,* (2006) developed low structured models for different microorganisms and substrates whenever pathways were known, so that they can for example describe changes in intracellular metabolite pools.

The more sophisticated a model is the more demanding the building and validating processes will be. Also, the more degrees of freedom, the least absolute are the constant. In fact, one of the most difficult tasks when building a model is to balance the level of sophistication and that of practicability. There is a need for versatile models, which are easy to populate with consistent values for constants, readily comparable with experimental data and yet robust enough to be used over a wide range of conditions due to meaningful kinetics.

2.7 Project aims and objectives

Energy storage molecules in microorganisms (lipids and polyesters) have become bio-products of commercial interest in recent years. As detailed above, cells synthesize these intracellular products when cultured under conditions that not necessarily favor growth. Therefore, the selection of the operational conditions that yield high productivities is not trivial. PHB is a bioplastic that accumulates in high amounts inside bacteria and that can be used as case study to understand the phenomena governing the synthesis process so that better fermentation designs can be implemented. The numerous factors affecting growth and production make the empirical optimizing of PHB fermentation very complicated in a short timeframe.

The use of modelling and, furthermore, of computer assisted control can be powerful tools for improving bioprocesses. Formal kinetic models are necessary in order to have a solid basis for the design of fermentation processes, economic calculations and control, and experiments to study the dynamics of the system are fundamental for the development of a mathematical model able to describe the behavior of the system.

The main goal of the project was to develop a mathematical model that guides the process development for the case of PHB production from glycerol by *C. necator* and that, ultimately, allowed a model-based design of the fermentation. To achieve this goal, the objective was to progressively derive a mass balance model, based on a set of biological reactions, able to describe the dynamics of the fermentation process and assess the potential of improving performance metrics.

As reported in the above literature review, there is not a unique model for bacterial production of PHB. Rather, models tend to be specific to the system of study. The model developed in the research reported in this thesis was not be based on any particular existing model but instead built from the knowledge and understanding gained by the researcher during preliminary experimentation and it was conceived as an optimizing tool.

Aspects that had not previously been fully examined but which are considered to be critical for design (*e.g.* cell adaptation, absolute amount of nutrient *vs.* ratios, competition between growth and product formation, feeding regimes, importance of aeration) were carefully evaluated using a systematic approach with the assistance of a predictive model that reduced the experimental burden.

With the intent to propose a preliminary mathematical description of the system, fermentations were conducted and conditions that stimulate PHB production were identified (*e.g.* C/N). The first model hypothesis were compared against experimental data and contributed to the fundamental knowledge of the system. Decoupling growth and production was necessary to understand the main factors affecting

each phenomenon and, thus, to be in a better position to further evaluate the compromise between cell proliferation and product formation.

The discrepancies between empirical and simulated data were used in view to redefine the model in an iterative process as illustrate in Figure 2-10. A wide range of condition were tested while keeping the same values for the kinetic constants and relatively easy formulation (*e.g.* number of parameters) to assess the robustness and versatility of the model.

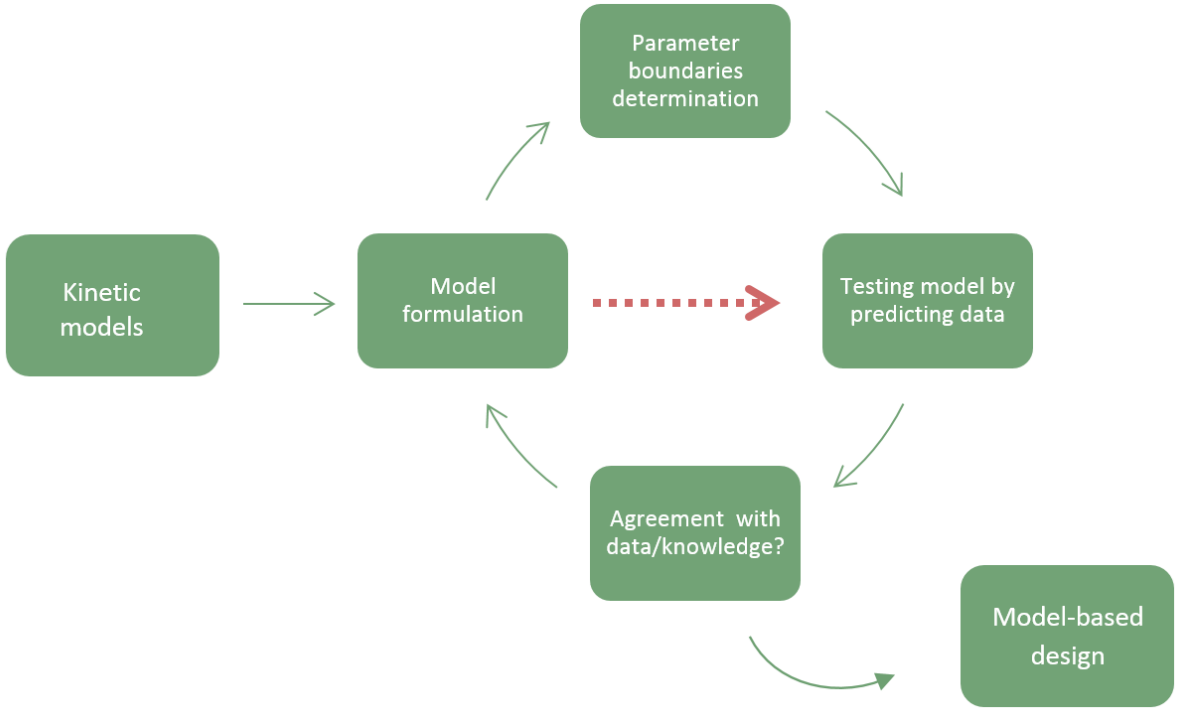

Figure 2-10: Iterative process for the development and improvement of the model. Once the model parameters have been determined, the proposed methodology can be simplified so that experiments to test the model results are not required every time (discontinuous line).

To fully examine the applicability of the model, different operational modes were tested, both through simulation and experiments. Those with greater potential were further examined regarding operational times and stream composition as part of scenario analysis exercises. Variables that can be used for control purposes, such as aeration, were considered and relevant physical values such as oxygen transfer rate and oxygen uptake rate calculated.

Chapter 3

Programme, materials and methods

3.1 Research programme

As highlighted in chapter 2, the methodology implemented in this project integrated experimental and computational studies, which complemented each other in the task of describing the macroscopic kinetics. The development of an experimental programme enabled meeting the specific objectives mentioned in the last section of the previous chapter.

For the sake of establishing a lab-scale fermentation system (from which kinetic information could be extracted), the first experiments were planned to test growth and PHB production by the chosen bacterial strain, *C. necator* DSM 545, when cultivated in the selected carbon source, *i.e.* glycerol. In this way, the conditions where the polymer of interest is produced as main fermentation product could be identified.

With the intention of enhancing growth and PHB production on glycerol, a series of sub-cultivation stages were planned for cells to progressively acclimatize to glycerol first, and then to explore the feasibility of increasing initial glycerol concentrations (once cells were used to it). Therefore, the first milestone in the programme was to establish an adaptation procedure to ensure an optimal growth of *C. necator* in glycerol that could be replicated in all the experiments that would follow.

In order to build the first mathematical equations that would compose the model, a series of fermentations were arranged for systematic study of the effects of individual variables, *e.g.* one medium component was gradually increased in the range considered applicable (non-toxic effect by substrates) while other variables were maintained constant. The factors having a major effect on the fermentation performance would thus be identified as the key model variables. Production needed to be confirmed as either growth or non-growth associated and conditions favoring production over growth and vice versa needed to be established.

For testing the model predictions, a sequence of fermentations under different conditions were anticipated. By comparing simulations and empirical data, the applicability of the model could be evaluated in conditions that differ from those used to develop the equations. Discrepancies between the two (predictions and experiments) could serve for refining the model whenever new insights enabled a more realistic representation of the biological system.

With a view to improving the fermentation outcomes, the model was used to optimize fermentation parameters (initial concentrations, fermentation time) and to predict the results in various operational regimes. Those that improved the results achieved in simple batch fermentation were then incorporated into the experimental plan. Other variables (agitation, oxygen supply), that had not yet

been considered in the model description, but that were revealed to have an important role in the bioprocess, were studied by a series of specific experiments.

By comparing results from non-aerated and aerated systems, the importance of oxygen became clear; this created a new sub-objective: studying the role of oxygen in PHB production as a potential parameter for control. Fermentations to conduct studies on oxygen transfer and uptake rate were thus foreseen.

Throughout the studies conducted in this thesis, standard techniques were used for the different aspects related to a fermentation process (cell identification, cell propagation, sterilization, inoculation, metabolite analysis, etc.). Full details of each are presented in the following section.

3.2 Materials and methods

3.2.1 Microorganism

The microorganism used throughout this work, *Cupriavidus necator* DSM 545 was obtained from the German Collection of Microorganisms and Cell Cultures (Deutsche Sammlung von Mikroorganismen und Zellkulture Gmb) in freeze dried form. *C. necator* 545 is a spontaneous mutant from DSM 529 which has acquired the ability to grow on glucose.

Descriptive characteristics of *C. necator*

Firstly isolated from soil, this non-obligate bacterial predator was incorporated in the genus *Cupriavidus*, making reference to the fact that copper stimulates its growth. The name of this bacterial strain has changed many times since its identification. Current *Cupriavidus necator* was initially named as *Hydrogenomonas* eutropha in 1958 by Wittenberger and Repaske . A study signed by Davis et al. (1969) proposed the name of *Alcaligenes eutrophus* ten years later. In 1995, a new gender was defined and *Ralstonia eutropha* became its official name (Yabuuchi *et al.* 1995). Based on evidence exposed by Vaneechoutte *et al.* (2004), *R. eutropha* was transferred as *Wausteri*a *eutropha* in 2004 for a short period.

C. necator is a Gram negative bacteria of coccoid rod shape and dimensions of 0.7-0.9 x 0.9-1.3 μm. It moves by peritrichous (projected in all directions) flagella and obtains energy from oxidation of organic and inorganic compounds (chemoheterotrophic or chemolithotrophic). According to other identification techniques, it is classified as catalase and oxidase positive, *i.e.* catalase and oxidase activity is produced (American Society for Microbiology 1964). Colonies on nutrient agar look off-white, glistening, mucoid, smooth and have entire edge and around 2-4 mm in diameter (See Figure 3-1).

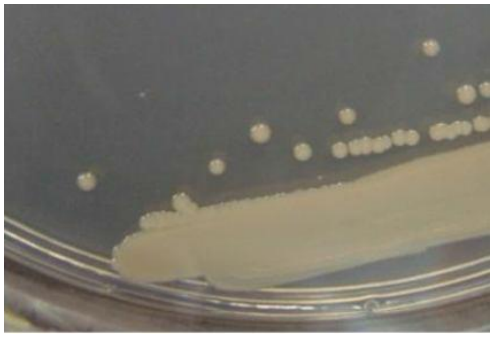

Figure 3-1: *Cupriavidus necator* DSM 545 after two days cultivation on solid culture medium.

Microorganism reactivation and storage

Upon receipt of the master culture from the DSM, a cell bank was developed to ensure the experimental reproducibility and avoid any genetic drift derived from frequent sub-culturing. Cells in freeze dried form were reactivated by culture in a nutrient rich medium (5 g/l peptone and 3 g/l beef extract) to ensure a good proliferation. Cells from a dense culture were later harvested and stored in a cryopreservative agent at cryogenic condition. Before the seeding lot created from the initial (master culture) was finished, a first generation working lot was created from it and so on as illustrated in Figure 3-2:

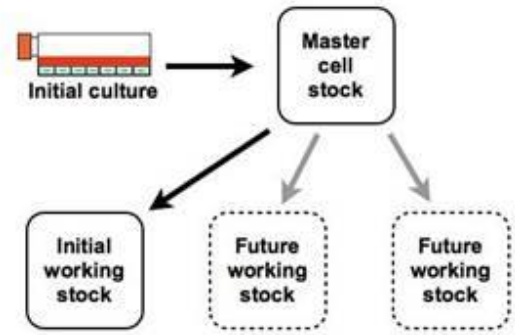

Figure 3-2: Procedure for creating working stocks for cell banking (Bionique® Testing Laboratories 2016)**.**

For creating a working lot from a liquid culture, the following protocol was used:

1. Prepare several sterile Eppendorf tubes. Label them and place in order in a suitable rack.
2. Aseptically pipette 1 ml culture into each of the sterile tubes.
3. Place the tubes into a centrifuge with the lid tabs facing inwards. Centrifuge at 14,000 × g (*i.e.* 13,000 rpm in the Hermle Z160M) for 5 min.
4. Aseptically decant or aspirate the supernatant (*e.g.* inside a laminar flow cabinet) from each of the tubes without disturbing the sediment.

5. If more cells are required, repeat steps 1 to 3 (up to a maximum of 3 times) using the same Eppendorf tube.
6. Pipette 0.5 ml of sterile medium into the Eppendorf tube containing the final pellet of cells. To this, add 0.5 ml of sterile glycerol solution.
7. Re-suspend the cells using the pipette. It is important not to allow the liquid to come into contact with the pipette, which has not been autoclaved (only soaked in ethanol). Alternatively the re-suspension can be achieved using a vortex mixer.
8. Place the Eppendorfs tubes in the freezer (-80℃) in a period of 15-60 min after adding the glycerol solution.

Staining techniques

Gram staining

Gram staining is a common technique in microbiology that allows differentiating Gram positive and Gram negative bacteria. To conduct this test, cells were firstly stained with crystal violet dye. A drop from a liquid culture was fixed by heating on a microscope slide. Next, iodine solution was added (covering the sample) so that a large complex could be formed between the crystal violet and iodine. Acetone was then used, for a short period, as decolourizer. This dehydrates the peptidoglycan layer of cells, which shrinks and becomes tight. For Gram positive bacteria, this layer is so thick that the complex cannot pass through and, hence, gets trapped. On the other hand, Gram negative layer is thinner enough for the complex to trespass it and cells do not retain the colour due to the dye. Safranin was then added to the sample. It stains red the Gram negative but does not disturb the Gram positive cells which remain violet. As shown in Figure 3-3, *C. necator* cells have a red colour after the test.

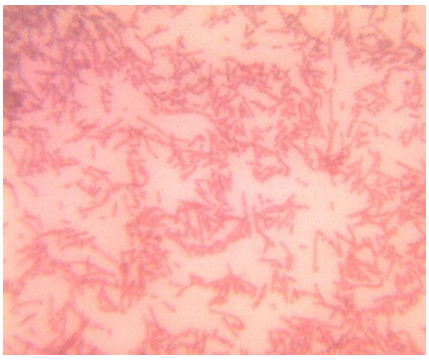

Figure 3-3: Microscope image from *C. necator* cells after the Gram staining test.

Sudan black

To identify PHAs granules, sudan black staining was regularly carried out. A drop of culture was placed on a microscope slide and spread with a loop and let it dry. The slide was introduced in a sudan

solution (0.3 % w/v sudan black in an aqueous solution of ethanol at 70%) for at least 15 min and a maximum 45 minutes. It was then rinsed with an aqueous solution of ethanol 60% and left it to dry. The slide was subsequently introduced in a safranine solution (0.5 g safranine in 100 ml distilled water) for 10 seconds. Last, it was rinsed with abundant distilled water and left to dry naturally before observation. PHB granules appear dark blue/black while the cytoplasm and membrane look pink as can be seen in Figure 3-4. The coloration with black sudan can be also done in petri dishes where cells have been grown.

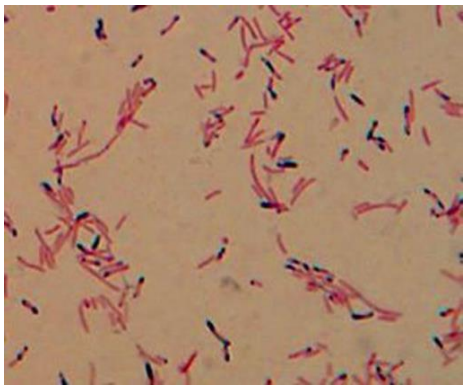

Figure 3-4: *C. necator* cells stained with sudan black for the observation of PHA granules (Jari *et al.* 2015).

Cells, with or without staining, were observed in an optic light microscope (Olympus BH-2 BHTU) using 1000 times magnification. In addition to the eyepiece, a digital camera was connected to the computer and enabled the recording of images taken at different times of the fermentation. In this way, changes in the microorganism morphology could be evaluated by comparing the camera captions.

PHB granule observation using transmission electron microscopy

Observation of PHB granules was also made using a transmission electron microscope (TEM). The principles of operation are similar to those of a light microscope but a beam of electrons, instead of light, is passed in this case through a very thin sample. Since the wavelength of electrons is much smaller than that of light, a much higher resolution can be achieved. This enables revealing features of internal structure, such as the granules of PHB. In order to prepare the sample that would be observed, 0.5 ml of a fresh high cell-density culture were mixed with an equal volume of a fixative solution provided by the School of Life Science at The University of Manchester, were the samples were further processed and the observation and acquisition of images were made. One of the pictures obtained is shown as example in Figure 3-5:

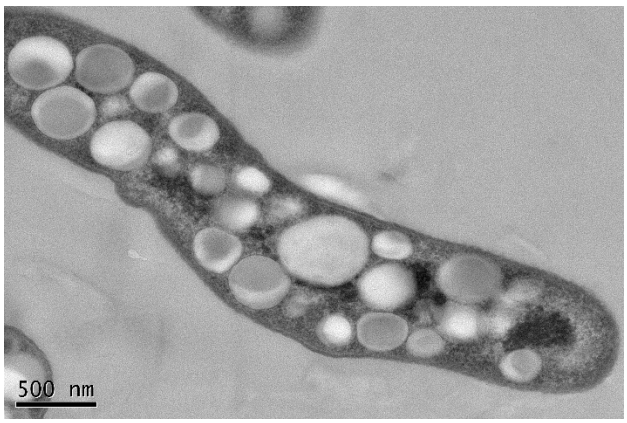

Figure 3-5: TEM image (from this work) of a *C. necator* cell containing numerous PHB granules.

3.2.2 Media preparation

Liquid culture medium

The mineral medium used for cultivation is based on that developed by Kim *et al.* (1994), and contains (per litre): KH_2PO_4, 1.5 g; $Na_2HPO_4 \cdot 12H_2O$, 9g; $MgSO_4 \cdot 7H_2O$, 0.2 g; $CaCl_2 \cdot 2H_2O$, 0.02 g; NH_4Fe(III) citrate, 0.05 g and trace element solution, 1 ml. The trace element solution was composed (per litre) by $ZnSO_4 \cdot 7H_2O$, 2.25 g; $CuSO_4 \cdot 5H_2O$, 1 g; $MnSO_4 \cdot 5H_2O$, 0.5 g; $(NH_4)_6Mo_7O_{24}$, 0.1 g; 35% HCl, 10 ml. The concentrations of nitrogen and carbon, in the form of ammonium sulphate and glycerol respectively, have been adapted in the different experiments performed depending on particular objectives. $CaCl_2$ and NH_4Fe(III) citrate (0.05 g in 20 ml H_2O) were autoclaved separately from the rest of chemicals and added aseptically to the medium after sterilisation to avoid precipitation. Pure glycerol is the carbon source employed in this work, mimicking the biodiesel co-product stream. Considering that the main impurities of crude glycerol have previously been studied by the research group (Salakkam 2012), using the pure form was considered still a good representation of the industrial waste and it provided a model system to generate fundamental knowledge without introducing too many disturbances from unknown chemical/biological interactions.

Solid culture medium

The solid media consisted on mineral medium supplemented with glycerol (30 g/l) and agar (15 g/l).

3.2.3 Cultivation techniques

Inoculum preparation

Before starting any experiment, a preculture from fresh agar plates, was prepared in order to avoid excessive long lag phases or poor growth. Agar plates were incubated for two day at 30℃ before using for inoculating the preculture flasks, a 500 ml flask with 50 ml of working volume. This was incubated at 30℃ and in an orbital shaker with an agitation speed of 250 rpm. The preculture was then used for

inoculating the flasks for study (10% vol.). Cotton plugs were used as closure of the flasks intending to have some oxygen diffusion through it. Yeast extract (1 g/l) was just included in the preculture to promote a rapid growth but was absent from the cultivation medium due to its variable composition. For the case of bioreactor experiments, these were inoculated from cultures made on flask as illustrated in Figure 3-6:

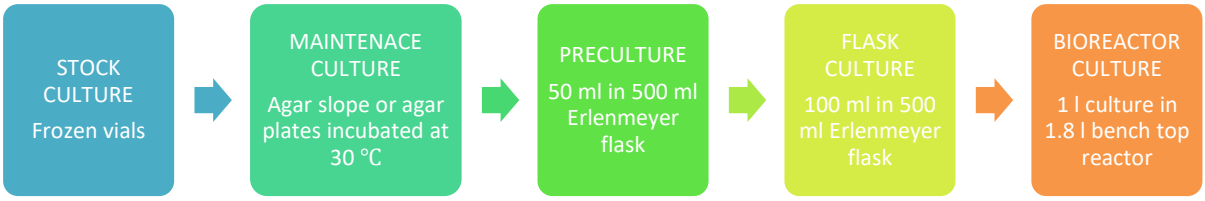

Figure 3-6: Schematics of inoculum development programme for *C. necator* culture in bioreactor.

Fermentation in flask

For studies conducted in flask, 500 ml Erlenmeyer flasks were used. The air-liquid ratio was maintained constant for all the experiments conducted by maintaining a fixed working volume of 100 ml for all the cultures conducted. Flasks were inoculated using preculture broth (10% vol.) and cultivated under the same conditions. Samples were aseptically withdrawn in a laminar cabin flow.

Fermentation in bioreactor

Bioreactor studies were conducted in a 1.8 l bench-top bioreactor containing a working volume of 1.0 l. A schematic configuration of the experimental apparatus is shown in Figure 3-7:

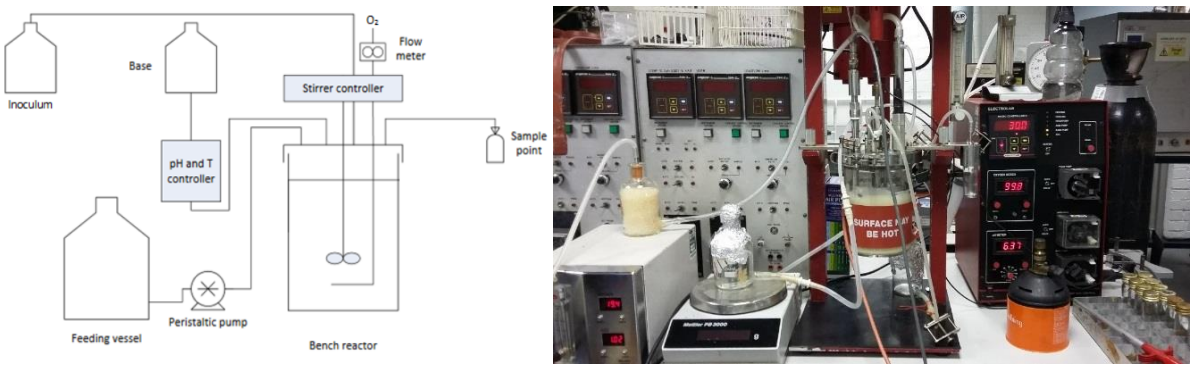

Figure 3-7: Schematic representation and picture from the experimental set-up for bioreactor fed-batch fermentations.

The agitation was provided through a turbine with six flat plane blades. Baffles were used to reduce vortexing. The air supply was achieved by a sparger at the bottom of the reactor. The gas was filtered when entering and exiting the vessel with a 0.2 µm pore size membrane filter. Temperature and pH probes were connected to a controller unit. Heating was achieved by a jacket that surrounded the vessel. A control valve deviated water flow into an internal coil if the temperature inside the reactor exceeded the set point or to the condenser otherwise. A sampling point inside the reactor allowed periodic sample collection. Temperature was maintained at 30°C and the agitation was varied between

250 and 600 rpm for different experiments. Whenever a dissolved oxygen probe was to be used, this was polarized overnight after sterilization and before the reactor was inoculated. The bioreactor was inoculated with 100 ml culture grown on the flask. The inoculation time was intended to match the exponential growth phase of cells. Agar streak plates were regularly made to check the purity of the culture. All biological wastes were autoclaved before disposal.

3.2.4 Analytical techniques

pH measurements

The pH of the culture samples was measured using pH meter (HANNA Instruments HI 221, UK).

Biomass quantification

Cell dry mass (CDM)

1 ml culture was centrifuged in a 1.5 ml Eppendorf tube for 5 minutes at 13,000 rpm. The supernatant was decanted into a new tube and stored in a freezer for subsequent glycerol and total nitrogen analysis. Following that, the pellet was re-suspended with 1 ml distilled water and the tube was centrifuged for 5 minutes at 13,000 rpm. The supernatant from this was discarded and the pellet was again re-suspended in distilled water and poured into a pre-weighed aluminium dish. The dish was placed in an oven at 60℃ until constant weight in order to determine biomass concentration. CDM measurements were made in triplicate and biomass concentrations, in g/l, were obtained using Eq. 3-1:

$$CDM = \frac{W_2 - W_1}{V} \qquad \textbf{Eq. 3- 1}$$

where W_2 and W_1 are the weights, in grams, of the dried aluminium dish after and before adding the culture. V corresponds of the volume, in l, of culture used for the measurement.

Optical density: The culture was diluted with distilled water to measure absorbance at 600 nm in a UV-VIS Shimadzu® UV-mini 1240 spectrophotometer. The dilution factor changed throughout the fermentation to ensure a resulting absorbance value lower than 1. Optical density was correlated with growth and was used in the first hours of fermentation as an indicator of growth.

Substrate quantification

HPLC Analysis of glycerol content

Glycerol consumption was determined using a High Performance Liquid Chromatograph (Dionex Ultimate 3000, Thermo Scientific) equipped with an Aminex HPX-87H, 300 x 7.8 mm (BIO-RAD) column and coupled with and refractive index detector (Thermo Scientific) operating at 50℃. The mobile phase consisted of an aqueous solution of 5 mmol sulphuric acid previously sonicated in a sonicator Decon F5100b. The temperature in the column was also set at 50℃ and the flow rate was 0.6 ml/l. Samples were diluted ten times and filtered through 0.45 µm prior to analysis. An example of the chromatograms obtained is presented in Figure 3-8:

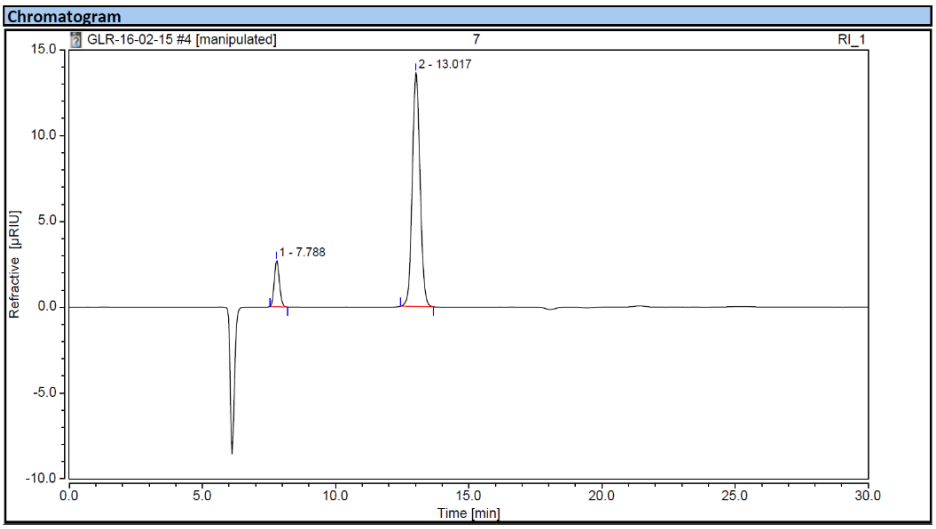

Figure 3-8: Chromatogram obtained during glycerol analysis in a HPLC. The glycerol peak emerged at t=13 min of run.

The concentrations of glycerol in the samples were calculated with the linear regression shown in Figure 3-9 and applying the corresponding dilution factor. Results were processed with the Chromeleon 7.2 Chromatography Data System software.

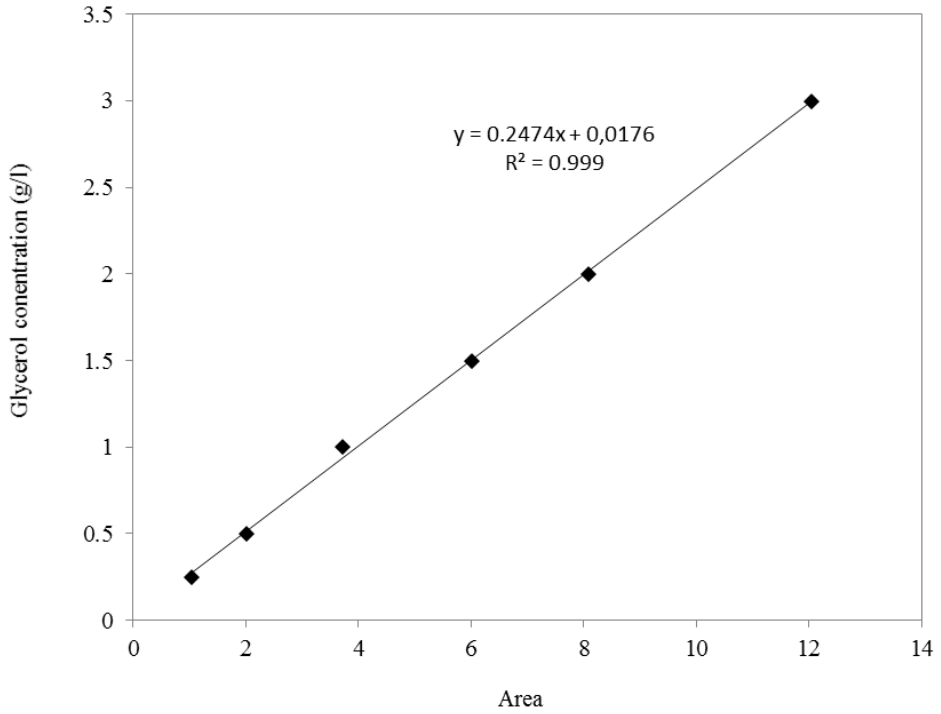

Figure 3-9: Calibration curve used for converting HPLC measurements to glycerol concentrations.

Glucose was used as co-substrate together with glycerol in a specific experiment. The concentration of glucose in the medium was also measured by HPLC. For calibration purposes (See Figure 3-10), the analytical standard form was used.

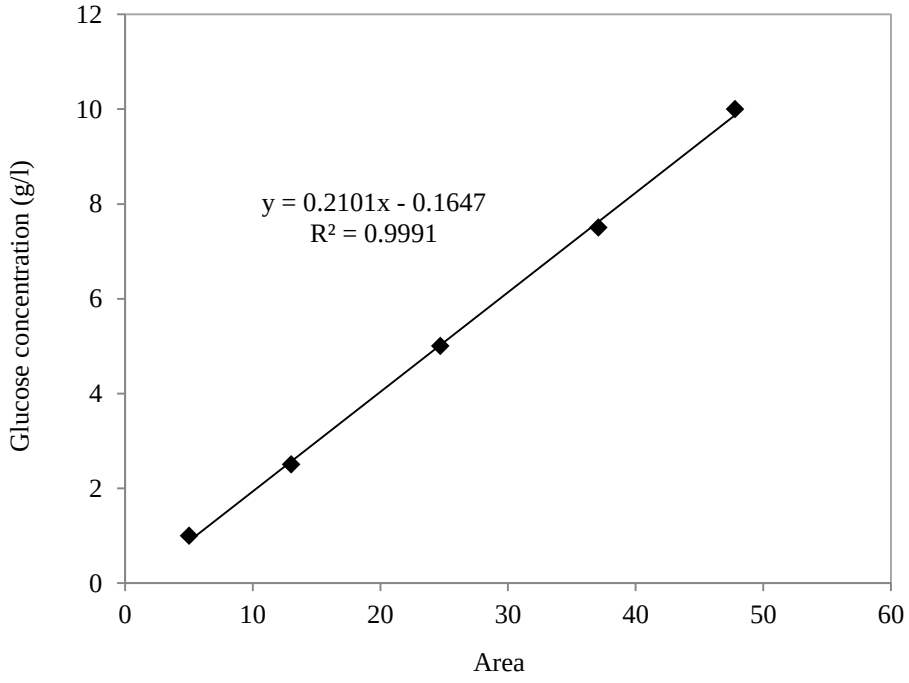

Figure 3-10: Calibration curve used for converting HPLC measurements to glucose concentrations.

Nitrogen Analyser

Total nitrogen in the media was determined using a Total Organic Carbon / Total Nitrogen Analyser (TOC-VCSH/TNM-1 Shimadzu). After a catalytic combustion, the nitrogen oxide species react with ozone and form excited states. The light emitted when those forms return to ground state is measured with a chemiluminiscence detector. The light energy emitted is proportional to the amount of total nitrogen. Solutions of ammonium sulphate were used as standards.

Free amino acids quantification

The ninhydrin colorimetric method (Abernathy *et al.* 2009) was used to estimate the amount of free amino acids (FAN) in yeast extract. The ninhydrin, originally yellow, turns purple after reacting with amino acids according to the following reaction:

$$\alpha - amino\ acid\ +\ 2\ ninhydrin \rightarrow CO_2\ +\ aldehyde\ +\ final\ complex\ (blue)\ +\ 3H_2O$$

For carrying out this analysis, the ninhydrin colour reagent, the dilution reagent and the stock standard solution were prepared. The ninhydrin colour reagent contains, per litre of distilled water, 40 g of $NaHPO_4$, 60 g KH_2PO_4, 5 g of ninhydrin and 3 g of fructose. The dilution reagent solution is composed of 2 g KIO_3 in 600 ml of distilled water and 400 ml of ethanol at 96%. The stock standard solution was made by dissolving 107.2 mg of glycine in 100 ml of distilled water, what gives a concentration of 200 mg amino- nitrogen/l.

1 ml of sample was diluted in 50 ml water, and 2 ml of such solution were transferred into a test tube. 1 ml of ninhydrin colour reagent was added to the tube and this was placed in a water bath at 100 ℃ for 16 minutes. The tube is allowed to reach room temperature and then 5 ml of the dilution reagent were added. The absorbance at 575 nm was measured immediately thereafter against a blank prepared with the culture media.

Product quantification

Fermentation products, essentially organic acids (succinic, formic, acetic acid) were analysed by HPLC coupled with an UV-Vis diode array detector. The column was the same that the one used for the glycerol analysis.The most polar compounds elute earlier meanwhile as polarity decreases and the aliphatic chain increased, compounds are retained longer in the column. The column was protected with a guard column and the mobile phase employed consisted of a solution 0.1% (v/v) trifluroacetic acid previously sonicated. The operation conditions were set for the system to operate with a flow rate of 0.6 ml/min, a temperature in the column of 60°C and a pressure of 70 bars. The wavelength used in the detector was 210 nm.

For the preparation of the samples, stored in the freezer once the cell pellet was removed, 300 µl were diluted in 1200 µl of double distilled water and filtered (regenerated cellulose, 0.45 µm pore size) to prevent blockages in the column. The different interaction strength of the components with the stationary phase of the column is the reason that some compounds elute faster than others, and it is just this retention time that makes identification possible. The retention times for different organic acids are listed in Table 3-1:

Table 3-1: Retention times in HPLC-UV detection of common organic acids obtained as fermentation by-products

Compound	Chemical formula	Retention time (min)
Malic	$C_4H_6O_5$	10.50
Succinic acid	$C_4H_6O_4$	12.55
Lactic acid	$C_3H_6O_3$	13.17
Formic acid	CH_2O_2	14.10
Acetic acid	$C_2H_4O_2$	15.26
Fumaric acid	$C_4H_4O_4$	15.85
Propionic acid	$C_3H_6O_2$	18.30
Butyric acid	$C_4H_8O_2$	22.40

PHB recovery and analysis

Biomass was harvested by centrifugation (between 10 and 40 ml depending on the cell density) at 4500 rpm for 15 min. The pellet was dried in oven at 60℃ and the supernatant was either stored for further analysis or discarded. To be able to analyse the PHB in GC-FID, this needed to be extracted in a volatile form. The experimental procedure is summarized in Figure 3-11:

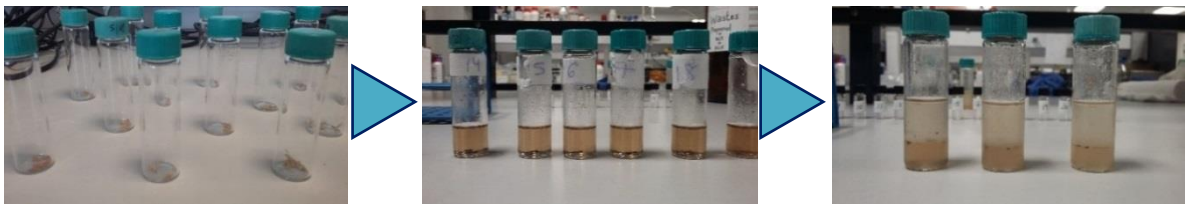

Figure 3-11: Steps in the sample preparation for PHB analysis by GC. The dried biomass (picture on the left) is weighted and a transesterification reaction converts the PHB into a more soluble form (picture in the middle), which is extracted in the organic phase after the addition of water (picture on the right).

To achieve this, a determined amount of dry cell mass was mixed with 2 ml of acidified n-propanol (1 vol HCl: 4 vol n-propanol) and 2 ml dichloroethane and heated for two hours at 100℃. The acid was responsible for the hydrolysis of the cell wall and acted as catalyst of the reaction esterification reaction between the polyhydroxybutric acid and the alcohol. Water (2 ml) was added, when the reaction was finished (after 2 h) and the mixture has cooled to room temperature, to favour the separation. The polyhydroxybutyrate stays in the organic phase (dichloroethane) which separated from

the aqueous phase with the rest of organic compounds. Figure 3-12 shows the key principles of the procedure for measuring PHAs by GC.

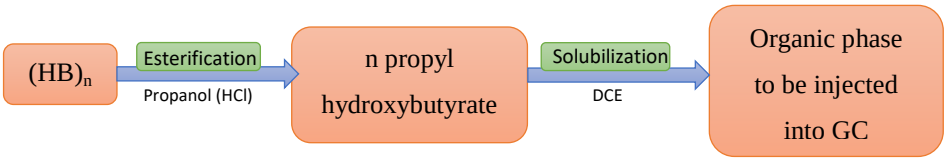

Figure 3-12: Sample preparation for determination of polyhydroxybutyrate (PHB) by gas chromatography.

The organic phase obtained from the extraction process described by Riis and Mai (1988) was filtered and injected into a gas chromatograph (GC) Varian model CP-3800 assembled with autosampler Combi/Pal and coupled with a flame ionization detector (FID).The temperature of the oven where the Paraplot Q-HT column was placed was 120℃ at the time of injection, and increased to 230℃ after three minutes. The sample was volatilized and passed through a slightly polar column using helium as carrier gas. A hydrogen / air flame oxidised organic molecules and ionized them. The ions were collected and the signal produced was measured as an indicator of concentration. Samples and standards were prepared following the same procedure described elsewhere by Riis and Mai (1988). Chemicals were obtained from Sigma-Aldrich (UK) and were of the highest grade available. The normal chromatogram obtained in the GC-FID can be seen in Figure 3-13:

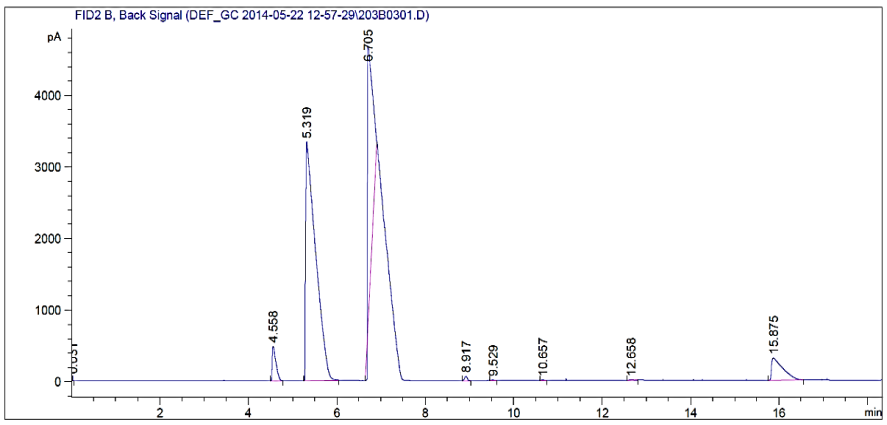

Figure 3-13: Typical chromatogram obtained during PHB analysis in a GC-FID. The PHB peak emerged at t=15.875 min of run.

Contents of PHB were obtained using Eq. 3- 2 in which the mass of PHB was obtained using the calibration curve presented in Figure 3-14. Concentrations of PHB were simply calculated by applying the percentage of PHB to the total biomass concentration at that particular time.

$$\%\, PHB = \frac{Mass\ PHB}{Mass\ of dried\ biomass\ used\ for\ extraction} \cdot 100 \qquad \textbf{Eq. 3- 2}$$

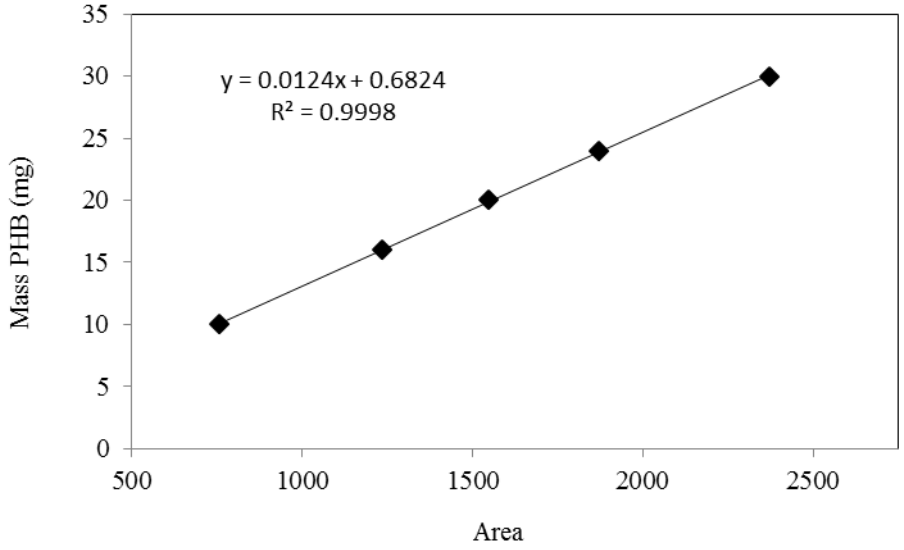

Figure 3-14: Calibration curve used for obtaining the mass values of PHB from GC-FID area measurements.

The difference between CDM and PHB corresponds to the so-called associated biomass (x_A).

Extraction method with chloroform

PHB was recovered using the chloroform method (Hahn *et al.* 1995) to obtain the pure solid form. After fermentation, biomass was dried in the oven and the resulting pellet submerged in a volume of chloroform 50 times higher than that occupied by the dried biomass. The suspension was incubated at 30℃ for 48 h and then filtered. The filtrate was finally washed with a mixture of methanol and water in a proportion of 7 to 3 in volume for the bioplastic precipitation to occur.

3.2.5 Data interpretation

Graphical determination of maximum growth rate

The mass balance applied to the biomass in a batch reactor is given by Eq. 3- 3:

$$\frac{dx}{dt} = \mu \cdot x \qquad \textbf{Eq. 3- 3}$$

where μ is the specific growth rate. Assuming that during the exponential growth phase μ stays approximately constant, the diffential equation can be easily integrated (Eq. 3- 4):

$$\ln x = \mu \cdot t + \ln x_0 \qquad \textbf{Eq. 3- 4}$$

Hence, by plotting the natural logarithm of the cell concentration against time during the exponential phase, the maximum specific growth rate can be obtained from the slope of the curve as illustrated by Figure 3-15. The length of the lag phase can also be obtained from this type of plot. For doing so, a horizontal line crossing the y-axis at the value of the initial cell concentration is extended until intersecting with the exponential phase straight line. The value on the x-axis at which the lines crossed each other indicates the lag time of the culture.

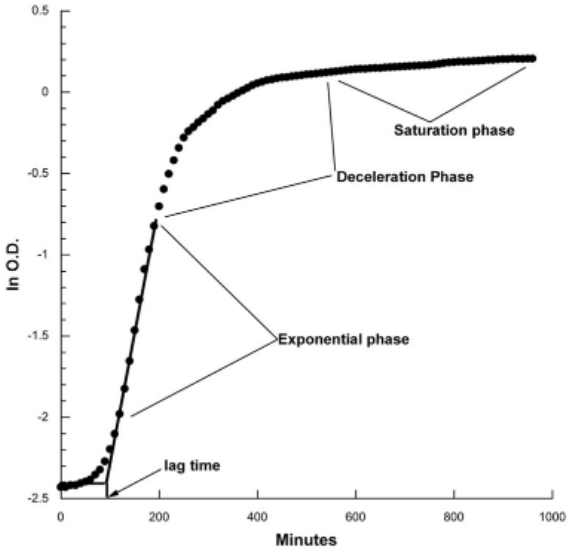

Figure 3-15: Logarithmic plot of growth curve, natural log of biomass concentration (*e.g.* OD) versus time in a batch culture.

Calculation of yields

Overall yields from a fermentation are calculated as the change in product concentration occurred over the total substrate consumed during cultivation, see Eq. 3- 5:

$$Y_{P_i/S_i} = \frac{\Delta P_i}{|\Delta S_i|} \qquad \textbf{Eq. 3- 5}$$

Mass balances

The simplified mass balance to glycerol in a batch system can be written as follows:

Initial glycerol - remaining glycerol = glycerol consumed for cell formation + glycerol consumed in PHB synthesis + glycerol converted to CO_2

Heterotrophic biomass growth of *C. necator* on an organic substrate (typically) takes place according to Eq. 3- 6 (Mozumder *et al.* 2016):

$$C_3H_8O_3 + O_2 + NH_4{}^+ \rightarrow CH_{1.74}O_{0.46}N_{0.19} + CO_2 + H_20 \qquad \textbf{Eq. 3- 6}$$

Under stress conditions, *i.e.* under nutrient limitation, the organic carbon source is used for PHB production according to Eq. 3- 7 (Akiyama *et al.*, 2003):

$$C_3H_8O_3 + O_2 \rightarrow C_4H_6O_2 + CO_2 + H_20 \qquad \textbf{Eq. 3- 7}$$

3.2.6 Error analysis

Most of the measurements presented in this thesis were made in triplicate. The average was the value reported here and the standard deviation (SD), defined Eq. 3- 8, was calculated to evaluate how much the different measurements deviated from the mean:

$$SD = \sqrt{\frac{(X - \bar{X})^2}{n - 1}} \qquad \textbf{Eq. 3- 8}$$

where X refers to individual data points, $\bar{X}$ is the average (mean) of individual data points for the n measurements.

Statistical tests

One way analysis of variance (ANOVA) was applied to test if experimental results were significantly different (at a specified level of confidence). This test compares means of two or more number samples based on the F distribution. In the example below, ANOVA was used to compare the optical density values obtained during growth of *C. necator* in glycerol rich medium for consecutive runs. Figure 3-16 displays the data used for the analysis, k=1 corresponds to the first run, k=2 to the second run and so on.

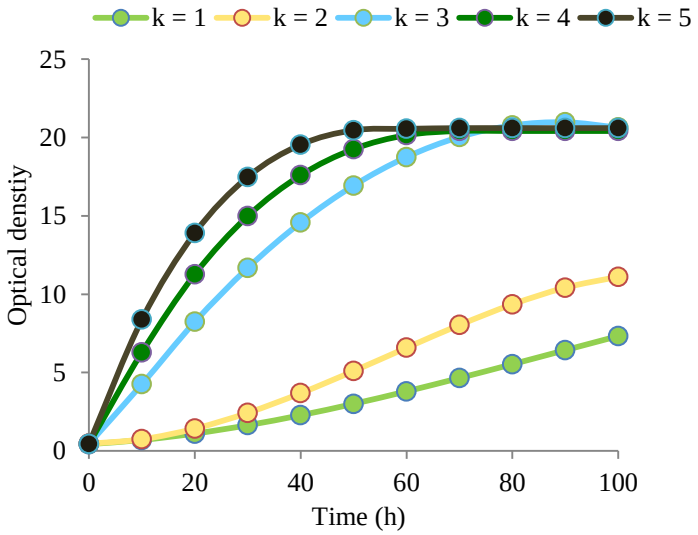

Figure 3-16: Growth curves for consecutive runs in glycerol rich medium.

The results of ANOVA were obtained using the statistical table tool from Excel and the normal display is shown in Table 3-2 where F test is used to determine statistical significance.

Table 3-2: Results obtained from one-factor ANOVA analysis of growth curves corresponding to consecutive culture runs on glycerol.

Groups	*Number of samples*	*Sum*	*Average*	*Variance*
k =1	11	36.9006	3.3546	5.680785
k =2	11	59.3373	5.3943	15.57097131
k =3	11	157.315	14.30136364	52.2810502
k =4	11	171.6892	15.60810909	46.62111263
k =5	11	183.193	16.65390909	43.96883389

Source of variations	*Squared sum*	*Degrees of freedom*	*Squared averages*	*F*	*Probability*	*Critical F value*
Between groups	1693.52	4	423.38	12.89	2.74E-07	1.55
Within groups	1641.22	50	32.82			
Total	3334.75	54				

The fact that the value of F calculated exceeds the value of F_{crit} implies that the set of data are significantly different at a level of confidence of $\alpha = 0.05$.

3.2.7 Computational methods

Matlab was used to produce all the simulations presented in this thesis. ODE23s was used to solve the system of differential equations of the model. To obtain kinetic parameters, a stochastic optimization based on a Simulated Annealing (SA) algorithm coupled with a deterministic method that uses the 'fmincon' function was used (Vlysidis *et al.* 2011). The objective function for the optimisation was the minimum sum of squared errors between predicted and experimental values of the four state variables. The optimization of other function was done in the same way.

Chapter 4

Adaptation of C. necator for glycerol consumption

4.1 Introduction

Non-conventional fermentative substrates, such as lignocellulosic materials and food/industrial wastes are increasingly sought as alternatives to refined sugars to reduce production costs. However, their complexities very often mean that the utilization of these cheap materials results in a sub-optimal performance by the biocatalyst. To represent a real economic benefit, the yield of the microorganism on a particular source has to be taken into account as proposed by Yamane (1993) when formulating an expression for the cost of raw materials:

$$RC = \sum_{i=1}^{n} \frac{k_{S_i}}{Y_{P/S_i}} \qquad \textbf{Eq. 4-1}$$

where k_s is the price of the ith nutrient and Y_{P/S_i} is the yield of the metabolite from it.

On the positive side, microorganisms, and in particular bacteria, are known for their ability to adapt to new environments and new substrates. The natural adaptation may involve fine-tuning of the biophysical properties of cell membranes (*e.g.* modification of the lipid membrane composition or membrane fluidity), the induction of proteins and enzymes synthesis, changes in gene expressions, morphological changes and accumulation of organic acids (Roy *et al.,* 2009; Buzzini & Margesin 2014; Giannattasio *et al.,* 2005; Cavalheiro *et al.,* 2009; Cavalheiro *et al.,* 2013). By mimicking this natural behaviour, under controlled cultivation conditions, cellular phenotypes can be shaped. Such in vitro adaptation processes are normally aimed at increasing the tolerance of a strain to common toxins found in the feedstock, reducing lag phases and enhancing substrate uptake.

An effective way to achieve cell adaptation is by continuous fermentation. The chemostat has a long history as a device used in adaptation studies, cell physiology and mutation (Ferenci 2007). In this configuration, the microbial selection is achieved through the feeding of a substrate, which favours growth of a specific sub-group of the population. In addition, the pressure imposed by the dilution rate ensures that only those cells that proliferate at a rate higher than the dilution rate remain as an effective population in the chemostat. In this way, cells that are not able to metabolize the substrate or that do not reproduce fast enough are lost from the system.

Landaeta *et al.,* (2013) performed a cell recycle batch fermentation for 39 days to adapt a strain of *Saccharomyces cerevisiae* to lignocellulosic hydrolysate medium containing inhibitory compounds. For the case of *Skeletonema costatum* and *Dunaliella tertiolecta*, two species of marine phytoplankton, Falkowski & Owens (1980) used a light shade adaptation strategy to promote more effective processes when harvesting and transferring light energy to reaction centres.

Glycerol is an example of a non-conventional fermentation feedstock. However, due to its simple chemical structure, it is readily metabolized into an intermediate of the glycolysis. Even though it can be utilized by a number of bacteria, high concentrations of this substrate frequently have an inhibitory effect on cell growth (Szymanowska-Powałowska 2015). The three hydroxyl groups in its molecule make glycerol a polar compound for which the phospholipid layer of cells has a low permeability as illustrated in Figure 4-1.

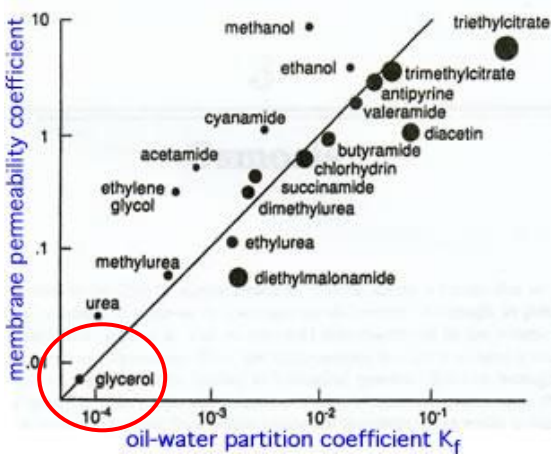

Figure 4-1: Membrane permeability coefficient of different compounds across the membrane of an algal species (*Chara*). Permeability correlates well with lipid solubility, represented by the oil-water partition coefficient. Adapted from Collander (1937).

As glycerol is unable to diffuse through the lipid bilayer, it is incorporated into the cytosol through facilitated diffusion, specifically, mediated by the facilitator protein GlpF (Lopar *et al.*, 2014). Several authors have reported the practice of serial subcultivations of *Cupriavidus necator* cells during the propagation stage (Cavalheiro *et al.*, 2009; García *et al.*, 2013) in order to adapt cells to glycerol rich environments. Increases to the number of facilitators (Lopar *et al.*, 2014) or a decrease in the degree of saturation of the protein (Cavalheiro *et al.*, 2013) are suggested as possible mechanisms for the adaptation.

Glycerol was the carbon source utilized throughout the research reported in this thesis. Due to the nature of the bioprocess studied, glycerol was always provided in excess to trigger product formation. Therefore, cell adaptation was a key requirement in order to achieve a fit for purpose strain. There was little description in literature regarding the implications of the adaptation or the ´standard´ procedure to conduct it. For this reason, further investigation into adaption process (minimum number of sub-cultivations required, stability of the change, impact on growth/glycerol tolerance/substrate preference) was carried out alongside the adaptation itself.

4.2 Methodology

The adaptation was carried out by serial sub-cultivation and bio-training as described next.

4.2.1 Serial sub-cultivation

Cells coming from a working lot made directly for the master culture (obtained from the German Collection of Microorganisms and Cell culture, DSM) were used as inoculum of a seeding medium prepared as described in Section 3.2.2 and supplemented with 20 g/l glycerol. An aliquot of this culture (5% vol.) was transferred to a second flask of fresh media (with the same concentrations of glycerol as the first one) at the time during which cells were at exponential growth phase. The transferring process was repeated until similar growth curves were obtained. Periodic samples were withdrawn from the flasks to monitor growth and substrate consumption. Figure 4-2 illustrates the serial sub-cultivation process.

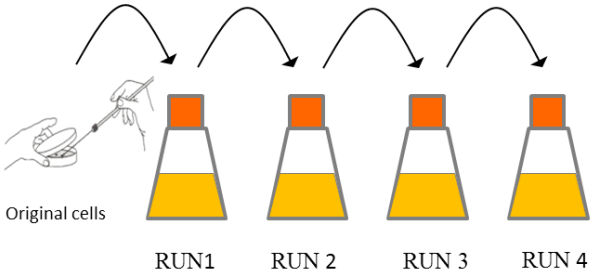

Figure 4-2: Schematic representation of the serial sub-cultivation process for cell adaptation.

4.2.2 Bio-training

The adaptation strategy followed for the serial sub-cultivation was repeated for glycerol concentrations ranging from 30 to 100 g/l. Cells adapted to 20 g/l glycerol were used to inoculate a flask of defined medium supplemented with 30 g/l of the mentioned carbon source. Once the culture was in the exponential growth phase, an aliquot of broth was used to inoculate fresh medium of the same initial glycerol concentration. This step, of sub-cultivating cells at constant glycerol concentration, was repeated until reproducible growth curves were obtained. Only then, cells were transferred to a higher concentration to repeat the adaptation sequence, until a maximum concentration of 100 g/l was reached. Cultivation conditions and medium composition were the same as those reported in section 3.2.2. An illustration of the bio-training experimental procedure is presented in Figure 4-3.

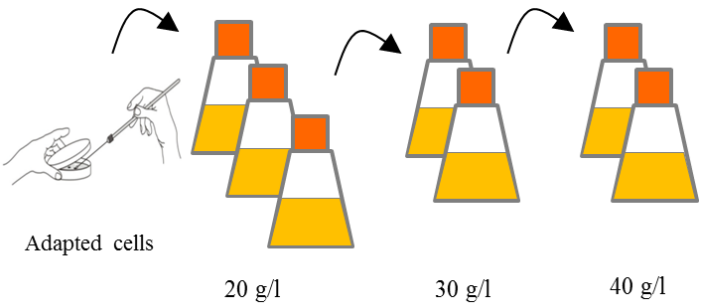

Figure 4-3: Schematic representation of the bio-training process for cell adaptation.

4.3 Results

4.3.1 Effect of serial sub-cultivation on growth and glycerol utilization

Figure 4-4 shows the evolution of the total biomass concentration during the serial subcultivation process (run 1 corresponds to first cultiavation). It can be seen in the figure that for the first two runs, biomass increased relatively slowly and required more than 250 h to reach the levels of biomass that were expected. Growth rate became steeper with each subsequent subcultivation until a relatively constant value was obtained. For the latest runs, approximately 4.5 g/l of biomass was achieved in less than 50 h. Run 5 and 6 exhibited very similar growth curve and thus, the subcultivation was stopped after the latter.

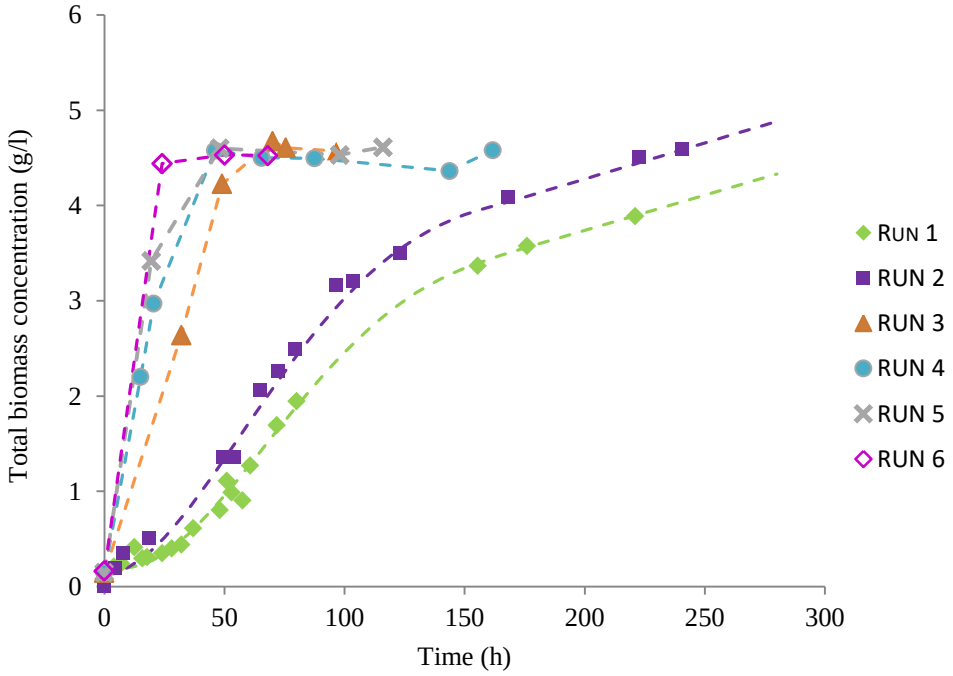

Figure 4-4: Biomass concentration profiles for the different sub-cultivations (run 1 to 6) of *C.necator* 545 in 20 g/l glycerol.

The generation number was used as a characteristic parameter of the adaptation process. A time t_0, there exists a defined microbial population with low capability for utilising glycerol. The gene expressions for metabolising glycerol seem to be activated by the presence of glycerol, therefore with an adequate nitrogen source, the corresponding number of cells (z_1) would divide with variation into enzyme activities (adaptation). At t_1, the offsprings of *Generation 0* form *Generation 1*, which can utilise glycerol at a faster rate. *Generation 1* undergoes the same process to form Generation *2* and so on. In general, the total number of generations required for initial number of cells to evolve to a certain different number (z_2) is:

$$N_g = \log_2(\frac{Z_2}{Z_1}) \qquad \textbf{Eq. 4-2}$$

The number of cells can usually be replaced with the concentration of active biomass x_A in the culture. The active biomass corresponds to the biomass concentration substrated from PHB. The number of generation at a particular time (t) can be calculated as follows:

$$N_g = \log_2(\frac{x_{A2}}{x_{A1}}) \qquad \textbf{Eq. 4-3}$$

where x_{A1} is the concentration of active biomass at the beginning of the subcultivation and whereas x_{A2} is the concentration of active biomass at that particular time, t. Hence, the overall number of generation achieved over a series of subcultivations is the sum of the number of generations achieved in each one of them. If there is a faster glycerol uptake resulting from adaptation, the biosynthesis would be accelerated as cells become more efficient in utilising the carbon source with the number of generations. To investigate this, the times when the culture reached cell densities equal to 2, 5 and 10 fold of its initial concentration (newly inoculated) were plotted against the number of generations in Figure 4-5. To facilitate explanation, these characteristic times were denoted as t_{i2}, t_{i5} and t_{i10}.

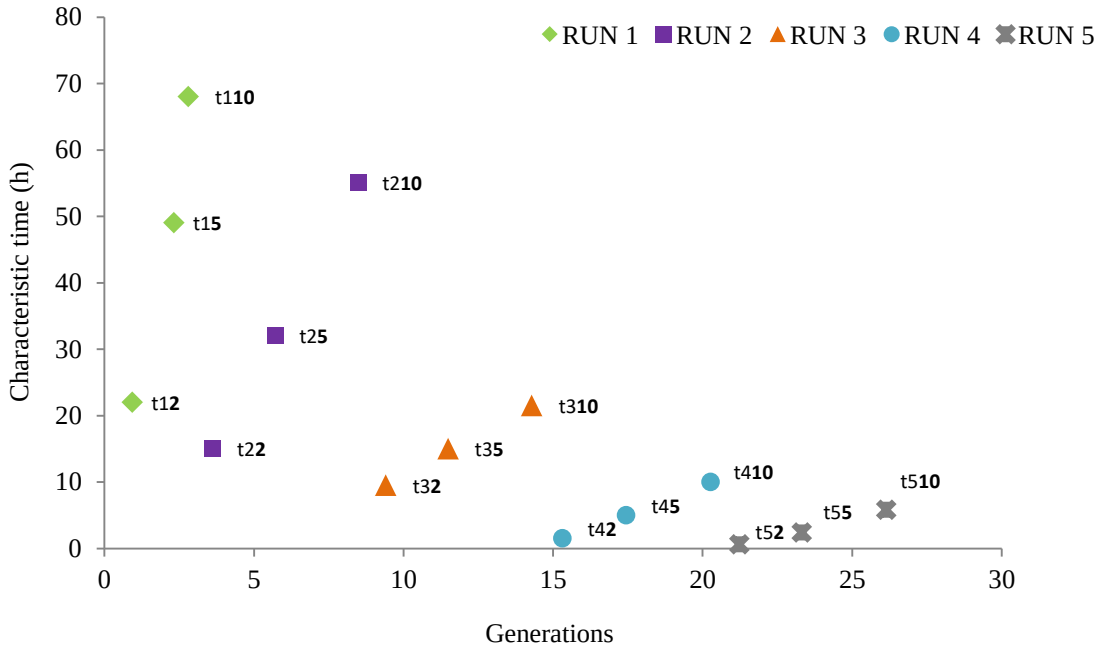

Figure 4-5: Characteristic times for the different subcultures performed during the adaptation of *C. necator* 545 to glycerol. ti1, ti5 and ti10 represents the time needed to reach an associated biomass concentration of two, five and ten-fold increase respect to the initial concentration in each culture.

Looking at the values of t_{i2}, the doubling times throughout the adaptation process can be compared: this number was significantly reduced from 22 h in the first run to only 1.5 h in the fourth cultivation. Figure 4-6 shows the number of generations over time that occurred during the exponential growth phase in each sub-cultivation.

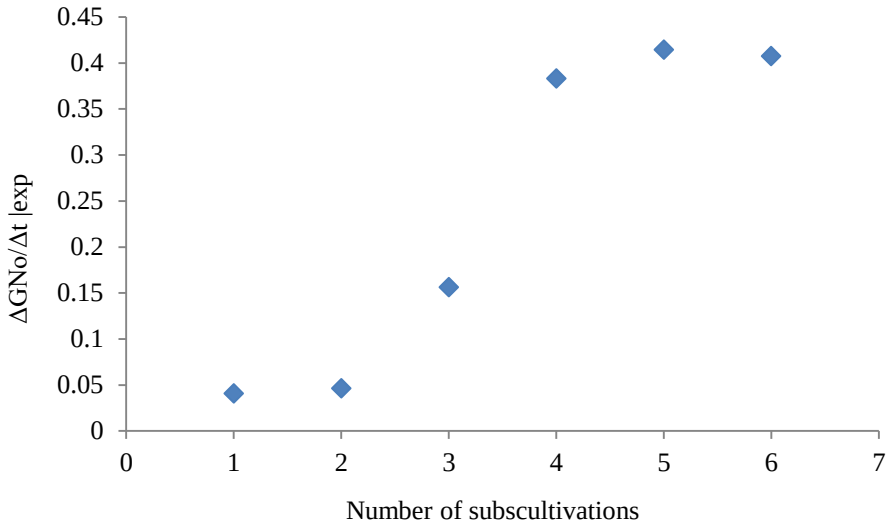

Figure 4-6: Rate of change of the number of generations occurred during the exponential phase for the different subcultures performed during the adaptation *of C. necator 545* to glycerol.

In addition to the carbon source, nitrogen is a vital constituent of cellular components. Without sufficient external nitrogen supply, many microorganisms can hardly achieve any adaptation due to inability to synthesis the enzymes required (Stanier 1951) . Protein turnover of cellular constituents can, to some degree, permit synthesis of new enzymes using internal reserves of nitrogen. However, this mechanism is negligible when the enzymatic adaptation takes place with ample nitrogen supply.

As can be seen from Figure 4-7, the glycerol uptake rate increased with the number of sub-cultivations. The fact that extracellular nitrogen was probably already scarce by the time cell started consuming glycerol in run 2 could contribute to the low value on glycerol uptake rate.

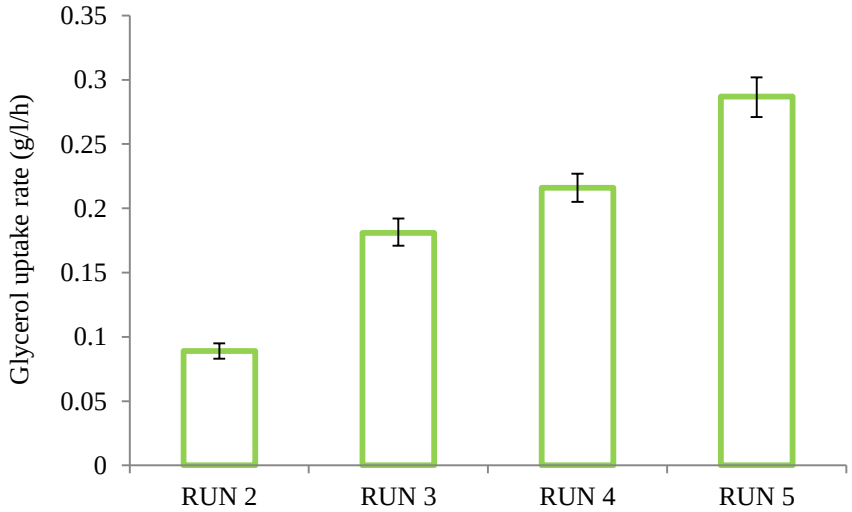

Figure 4-7: Overall glycerol uptake rate times for different subcultures performed during the adaptation of *C. necator 545.* The data shows the averages of 3 samples with their respective standard error.

4.3.2 Stability of the adaptation

The broth from the last run of the serial sub-cultivation was centrifuged and cells were stored in frozen form as specified in section 3.2.1. With the purpose of evaluating the stability of the changes over the storage period, a vial from the master culture was compared to a vial from adapted cells stock. Each of them was used to inoculate a flask containing defined media supplemented with 60 g/l. Flasks were incubated and periodic samples were withdrawn to monitor growth and PHB was measured for one sample towards the end of the batch. A dramatic difference was seen between the flask inoculated with adapted cells and the one seeded with non-adapted cells (see Figure 4-8). This confirms that the changes occurred during adaptation can be preserved throughout storage periods and therefore there is a degree of permanence to the changes. Subsequently, a working lot of adapted cells can be generated to avoid repeating the serial sub-cultivation process before every fermentation experiment.

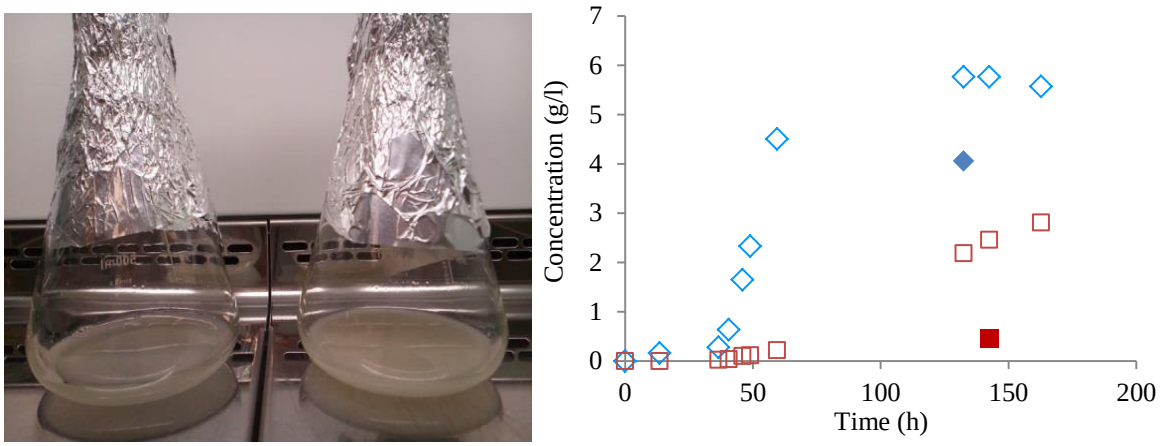

Figure 4-8: Comparison between adapted and original cells after storage period. The photograph shows cultures inoculated with original cells (flask on the left) and adapted cells (right). The graph shows profiles from original (red) and adapted cells (blue) throughout the cultivation time. The filled symbols correspond to PHB measurements.

4.3.3 Post adaptation growth on a glucose-glycerol mixture

As final test, bacteria coming from the serial sub-cultivation in glycerol, were grown in media containing both glucose and glycerol in such a way that each of them provides the same amount of carbon (equivalent to 30 g/l of glycerol). The results are presented in Figure 4-9. Interestingly, glycerol was clearly the preferred substrate while glucose was barely consumed. The amount of cells is similar to the one achieved during the sub-cultivation and, as expected, the amount of PHB is smaller (just half of the carbon was consumed here).

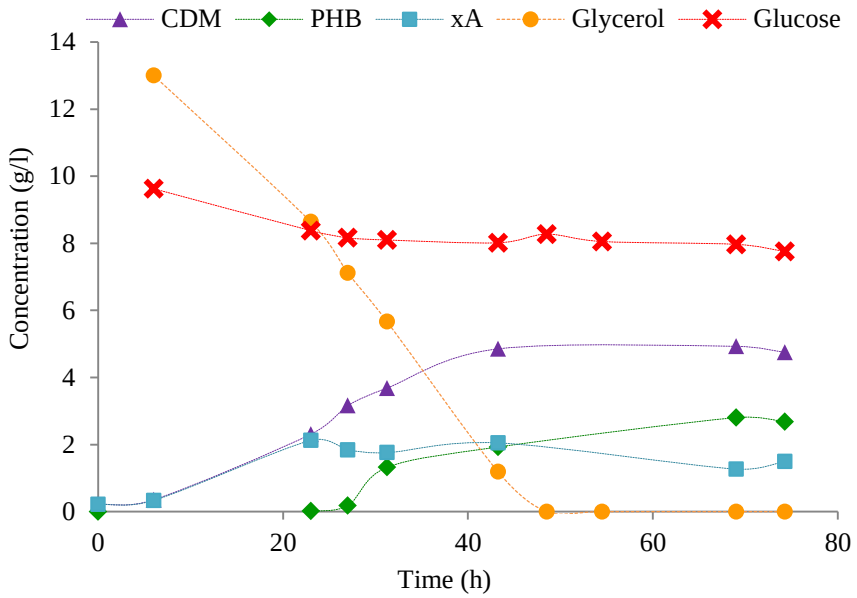

Figure 4-9: Glycerol, glucose and biomass profiles obtained from the fermentation conducted with a mixture of glucose and glycerol using glycerol-adapted cells of *C. necator 545*.

In the literature, it is frequently reported that when *C. necator* cells are cultivated on media containing both glucose and glycerol as carbon sources, the glycerol consumption is inhibited by the presence of glucose (Špoljarić *et al.*, 2013). The authors suggest that this phenomenon is related to high sensitivity of glycerol kinase and glycerol-3-phosphate dehydrogenase on intracellular metabolites originated from glucose and that the problem could be perhaps solved by improvement of capacity of transport system for glycerol. From Figure 4-9, it appears that the adaptation process can reverse the natural trend. In this way, it appears that there is a certain irreversibility of the adaptation process. To return to a glucose preference, cells may require re-adaptation.

Interestingly in this study, in contrast to carbon catabolite repression (CCR), glycerol uptake became constitutive while glucose uptake was inhibited in the presence of glycerol this time. In this phenomenon, known as reverse catabolite repression (RCR) (Collier *et al.*, 1996; Inui *et al.*, 1996; Parche *et al.*, 2006), glycerol replaced glucose to become the primary carbon source. Thus, *C. necator* DSM 545 not only acquired the ability to utilise glycerol efficiently via adaptation but also successfully inverted CCR to RCR, which implies that the strain possesseses a global regulatory system with remarkable flexibility.

4.3.4 A potential mechanism for adaptation

The data collected from the serial sub-cultivation was fitted with a convention model to show the decreasing apparent inhibition due to glycerol throughout adaptation. Initial glycerol concentration was 20 g/l for all consecutive runs. The variation in the associated biomass, x_A, was formulated based on a Monod equation with substrate inhibition. Glycerol was included as the only substrate to focus on

its particular influence on growth (Eq. 4-4). A constitutive relationship between glycerol and associated biomass was also assumed (Eq. 4-5).

$$\frac{dx_A}{dt} = \mu_m \cdot \frac{S}{S + k_s + \frac{S^2}{k_I}} \cdot x_A \qquad \textbf{Eq. 4-4}$$

$$-\frac{dS}{dt} = \frac{r}{Y} \qquad \textbf{Eq. 4-5}$$

The equations were solved simultaneously for the initial conditions of the batches 1 to 4.The kinetic parameters, μ_m, *ks* and *Y*, were calculated to obtain a good fit of the latest runs (4,5,6) and kept constant at 0.125 h^{-1}, 1 g/l and 0.07 g/g respectively and the inhibition constant was varied to achieve a suitable fitting for each set of experimental data. Results are shown in Figure 4-10.

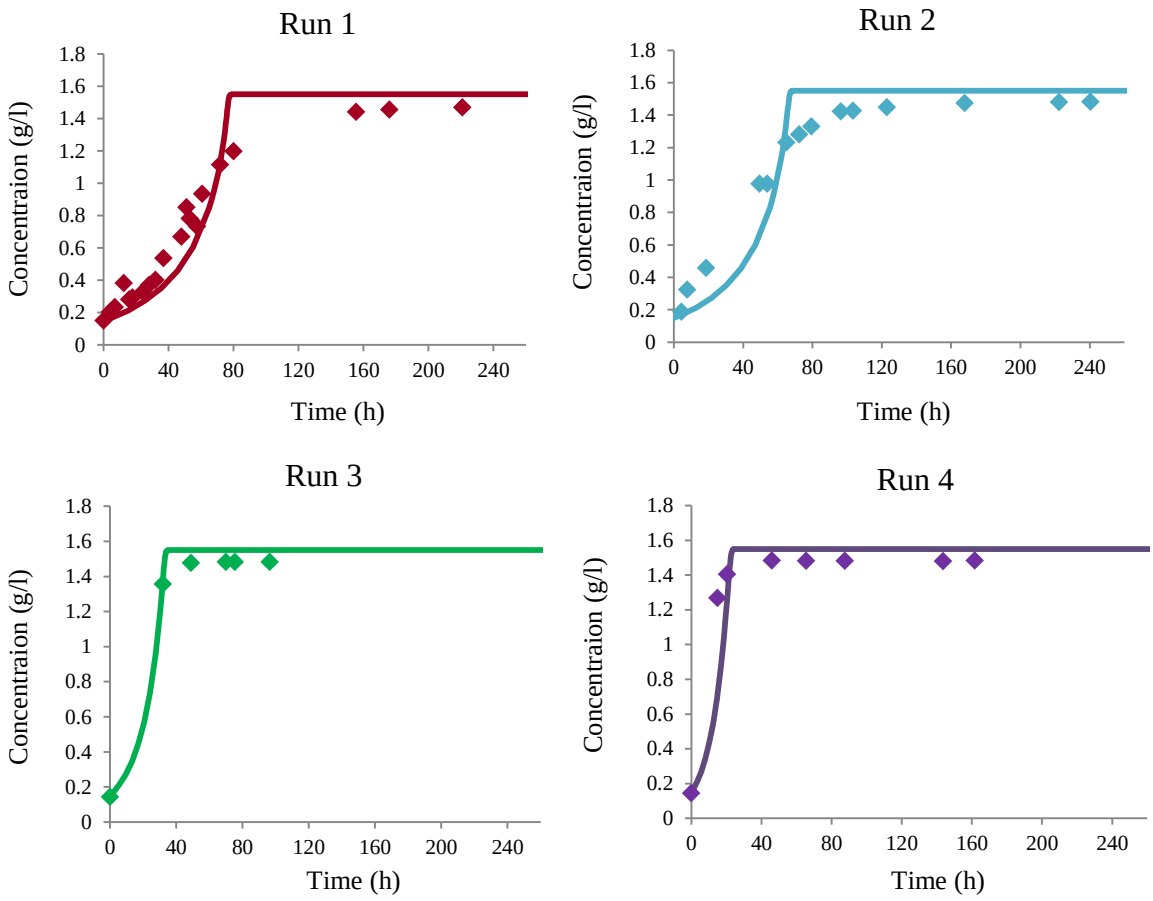

Figure 4-10: Associated biomass profiles for the first four sub-cultivations. The symbols represent experimental data and the solid lines correspond to the model prediction. The inhibition constant, k_I, was the only kinetic parameter varied for the different experiments: 4.5 g/l (Run 1), 5.5 g/l (Run 2), 20 g/l (Run 3) , 120 g/l (Run 4). The values for μ_m, Ks and Y were kept constant at 0.125 h^{-1}, 1 g/l and 0.07 g/g respectively.

The exposure time of cells to glycerol (*e.g.* number of sub-cultivations) seems to influence the detrimental effect of glycerol on growth. This mechanism could be described by a reduction of an inhibitory constant in the growth rate equation (responsible for decreasing the specific growth rate whenever glycerol exceeds certain critical concentration) with the number of sub-cultivations. The

trend in the variation of k_I is presented in Figure 4-11. The higher the value, the less the inhibition effect is observed, such that with no inhibition at all, k_I tends to infinity. The figure clearly shows that the k_I value that starts quite low reaches a level where there is effectively no glycerol inhibition by the fourth run.

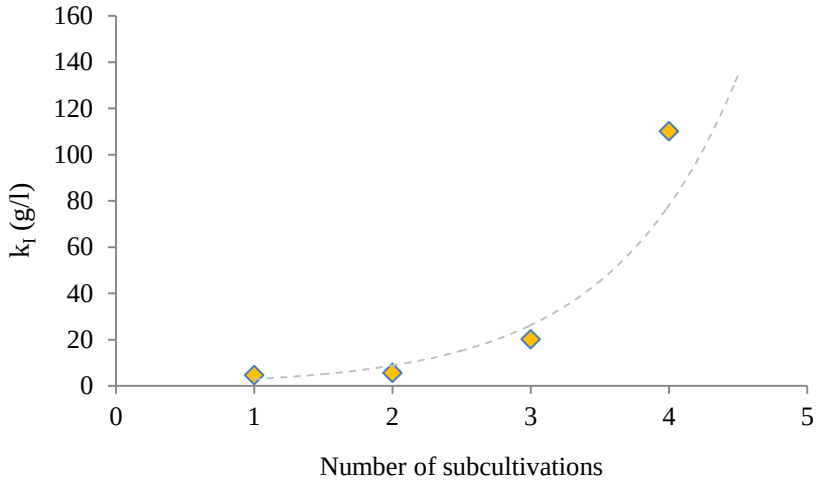

Figure 4-11: Values for the growth inhibition constant due to glycerol obtained for the different subcultures performed during the adaptation of *C. necator* 545.

4.3.5 Bio-training

Following the success of the adaptation process, which greatly reduced the doubling time of cells that were cultivated in glycerol rich medium (20 g/l) for 10 to 15 generations, an analogous procedure, a so-called bio-training, was implemented with the aim of increasing glycerol tolerance to higher concentrations. As previously, characteristic times were calculated for each subculture and for every glycerol concentration tested. Characteristic times, t_5, t_{10}, t_{15}, t_{20}, corresponded to those times required to reach a biomass concentration 5, 10, 15 and 20 times the inoculum concentration respectively.

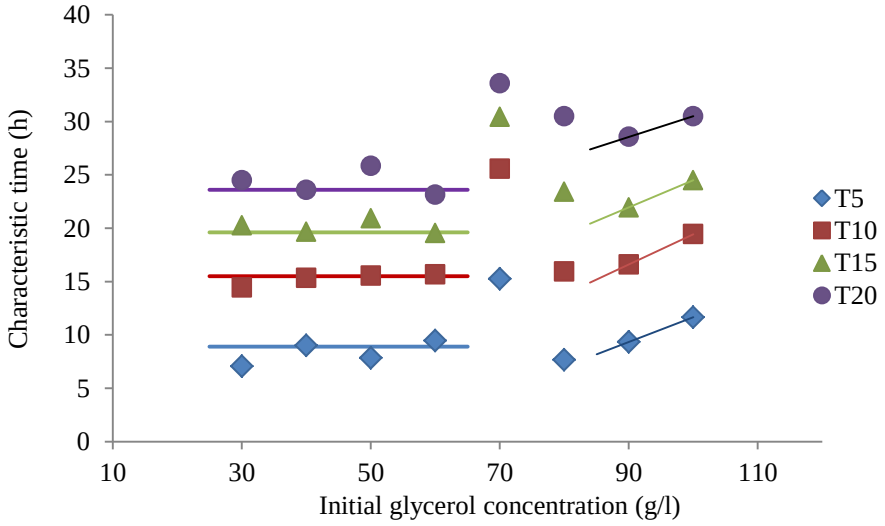

Figure 4-12: Times at which cell cultures reached cell densities equal to 2 (t_2), 5 (t_5), 10 (t_{10}), 15 (t_{15}) and 20 (t_{20}) fold of its initial concentration for the fermentations conducted throughout the bio-training process.

As result of the training procedure, the growth curve of cells cultured at different glycerol exhibited very little variation until they were exposed to 90 g/l glycerol, where all characteristic times increased. Curiously, the data obtained during the sub-cultivation at 70 g/l glycerol did not follow the same pattern. It could be that the inoculum used to transfer cells from 60 to 70 g/l glycerol was weak or too old and resulted in a longer lag phase than expected. Another possible explanation is that there is a second phase for the adaptation when cells were firstly exposed to 70 g/l. This would explain that the distance between the points in the graph (characteristic times for 70 g/l) gradually decreases as cells adapted during cultivation.

Besides growth, residual glycerol concentration in the medium was also measured, as described in section 3.2.4. Results are shown as simple linear trend lines in Figure 4-13. The improved capability of *C. necator* cells to tolerate glycerol (and grow almost equally fast in the range of 20 to 90 g/l) can be related to an increased initial uptake rate as observed in Figure 4-13, where the slope of the lines increases with the initial glycerol concentration until this one reaches 90 g/l.

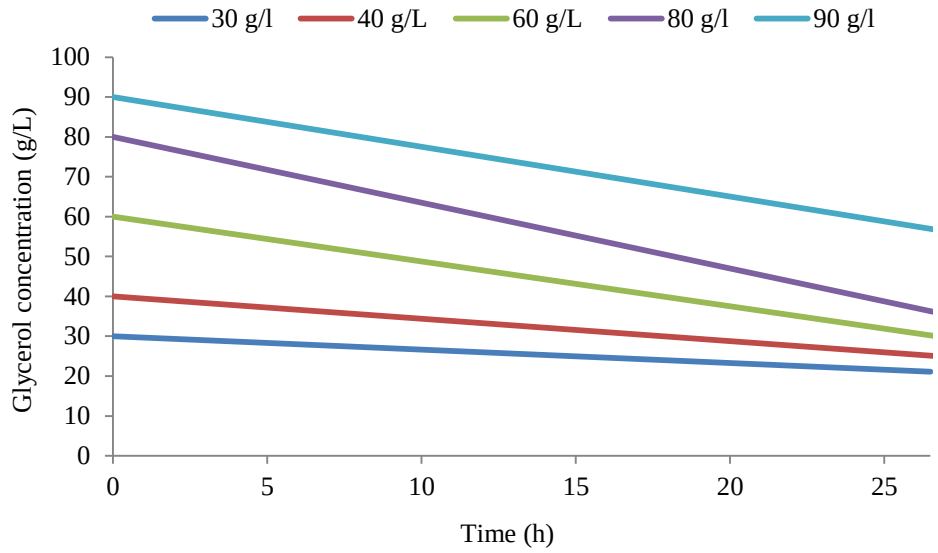

Figure 4-13: Trends in glycerol profiles at the beginning of the fermentation for cultures performed in series with increasing initial glycerol concentration.

Following the good response of cells cultivated under high glycerol concentrations, adapted cells were directly transferred to four separate flasks containing 30, 50, 70, 90 g/l glycerol in order to investigate if the same results would have been obtained without the bio-training process. The differences between them are presented in Figure 4-14:

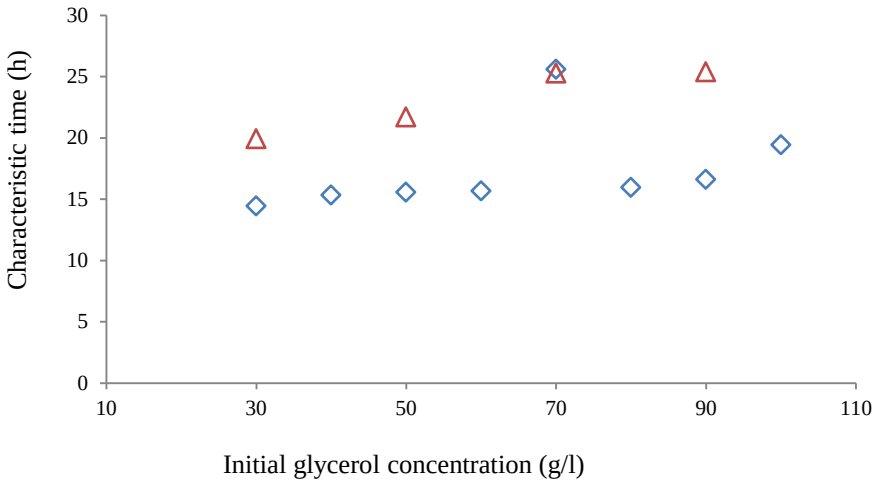

Figure 4-14: Comparison between the characteristic times t_{10} of *C. necator* cells undergoing the bio-training adaptation process (diamond) and cells adapted to 20 g/l glycerol that were directly grown in 30, 50, 70 and 90 g/l of glycerol, without undergoing the gradually-increasing concentration method (triangles).

Compared to cells which were not progressively transferred from low to high glycerol concentration, trained cells exhibit a faster response as can be seen in Figure 4-14, This difference can represent a delay in reaching end of exponential phase as long as 11.7 h if cells have not being "trained".

4.4 Conclusions

According to Brooks *et al.,* (2011)), an organism has adapted when it has evolved molecular mechanisms that allow it to grow optimally under spatiotemporally varying physicochemical conditions of its surroundings. The microbial strategies of adaptation to a particular environment can occur at phenotypical or genotypical level. The former are characterised by temporary changes whereas the latter involve long lasting changes (van Gemerden & Kuenen 1984). For instance, a change in lipid composition of microbial cells, increasing proportion of unsaturated acids, allows the membrane to retain fluidity when incubating in low temperatures (Russell *et al.,* 1990). When grown in a more viscous environment, certain bacteria such as *Vibrio parahaemolyticus* can adapt by forming swarmer cells; these cells adopt a more efficient means of movement which confers them an advantage for moving over a more solid surface. Another example is the phenotypic characteristics developed by biofilm bacteria for evolving from free swimming microorganisms to be part of a surface attached community (O'Toole *et al.,* 2000).

Researchers have taken advantage of this natural behavior of cells being adaptable to improve the performance of the biocatalysts at the target working conditions by following different strategies. The pre-exposure of the microorganisms to normally inhibitory compounds/sub-optimal conditions can improve the later performance in a bioreactor containing such components/carried out at similar conditions. *Vibrio parehaemolyticus* has demonstrated a greater tolerance to acidity and temperature stresses following growth in media containing 3% NaCl (Whitaker *et al.,* 2010).

Preliminary studies showed that, without adaptation and in comparison to glucose, glycerol is not the preferred substrate for bacterial growth and carries additional inhibitory effects. When *C. necator* cells were grown on glycerol for the first time in the present study, they exhibited a long lag phase followed by a slow growth, derived from a poor glycerol uptake rate. A series of experiments were therefore planned in order to overcome this low performance and to ensure a reproducible behavior in subsequent fermentations.

Adaptation of *C. necator* cells to glycerol-rich environments was achieved by serial sub-cultivation in media containing glycerol as sole carbon source. After 4 or 5 consecutive cultivations, biomass growth rate had significantly improved and a maximum (observable) specific growth rate of 0.46 h^{-1} was achieved. This result is in agreement with the typically reported range for number of sub-cultivations to reach adaptation (Salakkam 2012; Cavalheiro *et al.*, 2009; Naranjo *et al.*, 2013).

In fact, the number of subcultivations will depend to some extent on the length of those cultivations. The number of generations might be a more meaningful measure and so this was calculted in the present study. Using this measure, the adaptation can be fully achieved between 10-15 generations regardless the number of sub-cutivations.

The reason behind the cellular adaptation to glycerol is linked to the glycerol uptake and intracellular metabolism of it. Considering that glycerol is normally used as cryogenic preservative agent, it is unlikely that diffusion would be a limiting resistance for glycerol utilization. It is more likely that a switch in the enzymatic machinery to synthesize those enzymes required for the consumption of glycerol occurred during extended cultivation.

Studies in literature show that when glucose and glycerol were both used as carbon sources, a strong inhibition of glycerol consumption by glucose occurred (Špoljarić *et al.*, 2013). The fact that when, in the present work, adapted cells were cultivated in a mixture of glucose and glycerol, they did not consume glucose is rather interesting. This could because of catabolic repression (CCR), where enzymes necessary for the utilization of various other substrates are not longer synthesized. In the metabolic pathway, glycerol is closer to the end-product than glucose, so it could be the case that once the enzymes involved in their metabolism are synthesised, glycerol becomes the preferred substrate. This switch in the enzymatic machinery makes other forms of adaptation less efficient. In the same research group, parallel studies on cell subcultivation in media containing glucose and glycerol with decreasing amounts of the former in favour of the latter have shown an increased time to reach adaptation. In fact, adaptation barely occurred while glucose was still present. Therefore, there is an element of pre-programming in the metabolism of the organisms that prevents it to adapt to a different substrate while it has the preferred element. Once adapter however, the situation is reversed.

In conclusion, *C. necator* can be trained to tolerate and grow on glycerol concentrations of up to 90 g/l with little deviation from the profiles obtained for growth when using 20 g/l. This is very important considering that once the carbon required for cell formation is provided, the rest can be used for PHB synthesis. Also, the final doubling time of adapted cells is very close to that for cells growing on glucose, suggesting that glycerol is capable of substituting glucose as a substrate for cell growth.

Chapter 5

Building a preliminary macroscopic model

5.1 Introduction

This chapter presents the process of setting up a preliminary macroscopic model for describing glycerol-based PHB production by *C. necator* DSM 545. Once glycerol had been shown to be a suitable carbon source for growth (after the corresponding adaptation procedure), the next step was to evaluate if it could be also a good feedstock for the synthesis of the biopolymer of interest. Cells adapted to 20 g/l were used in the subsequent experiments. After PHB production was verified, procedures for conducting and following a fermentation process in flask scale were implemented. Studies on different conditions, in terms of carbon and nitrogen concentrations, were then performed in order to enable future kinetic analysis, investigate mechanisms that control PHB production and identify those regions (nutritional conditions) in which PHB is best.

5.1.1 PHB production process

The general procedure for microbial PHB fermentation, involves upstream and downstream operations similar to those normally found in any fermentation system. Media are formulated to supply the required nutrients and minor elements, or as in this case, to impose limiting conditions. Media are autoclaved prior to inoculation, then after fermentation, biomass is separated from it and the cell structure is disrupted to release intracellular products.

After biomass is separated from the culture medium, normally by centrifugation, sedimentation or filtration, PHB is extracted. When designing an industrial process, the selection of an appropriate method of extraction would depend on the microorganism, desired purity and impact of the treatment on the molecular weight. As reviewed by Jacquel *et al.,* (2008), there are different options for each of the downstream operations: pretreatment (thermic, alkaline, salts, freezing), extraction (solvents, chemical/enzymatic digestion, mechanical rupture, supercritical fluids), purification (oxygen peroxide, ozone). However, as these operations were not the focus of this research, a standard extraction method based on solvents (Riis & Mai 1988) was chosen for its practicality for all the lab experiments conducted, as reported in section 3.2.4. If the product were to be characterized, it can be also recovered using the chloroform method (Kunasundari & Sudesh 2011) reported in 3.2.4. Some PHB produced in the current study and extracted by this method, for the purpose of knowing how it appears, is shown in Figure 5-1.

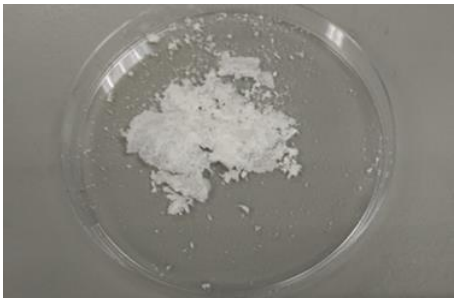

Figure 5-1: PHB recovered from glycerol fermentations by *C. necator* using the chloroform method.

5.1.2 Microbial PHB production and detection during cultivation

Methods for identifying PHB production during fermentation enabled preliminary studies on the capability of *C. necator* cells to accumulate PHB. Sudan black staining and transmission electron microscopy were performed with the view to confirming the presence of PHB granules prior to the extraction stage at the end of the fermentation. The staining technique, detailed in section 3.2.2, is a quick way of detecting PHB within cells grown on solid media (See Figure 5-2).

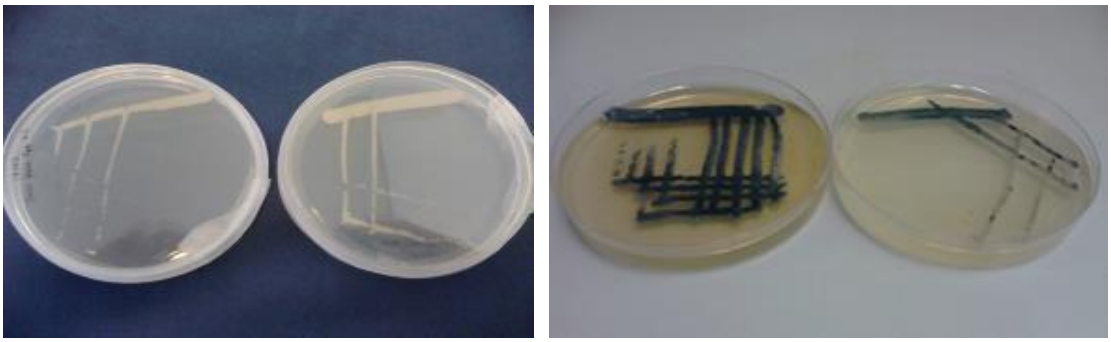

Figure 5-2: Unstained (left) and stained (right) cells of *C. necator* on petri dishes. The black coloration indicates presence of PHB.

Samples from a fermentation performed with large excess of carbon were observed under the transmission electron microscope (TEM) with view to visualize PHB granules in the cell culture. The majority of *C. necator* DSM 545 cells revealed inclusion bodies inside (See Figure 5-3) that appeared similar to those reported in the literature (Anderson & Dawes 1990; Ballard *et al.,* 1987). These granules had a higher density than the rest of cell matter (electron denser) and thus appear as a different colour. Cells were rod shaped and some became large and wider as granule formation progressed. Cells appeared to contain relatively large numbers of granules, but this is consistent with what other authors have reported when conditions are favourable. Where very large granules were observed, these are thought to have come from the fusion of smaller ones.

In early studies, typically around 10 granules per cell were reported for *C. necator* cells (Tian *et al.*, 2005; Silva *et al.,* 2007); more recently, the findings of Mravec *et al.,* (2016) revealed a higher average number of granules, between 10 and 15 per cell. In conditions that favour PHB synthesis, the number of granules rapidly changed from 2-6 to more than 12 in *R. eutropha* H16 (Wahl *et al.,* 2012) and up to 18 to 25 granules per cell were occasionally observed in the same strain (Tian *et al.,* 2005). Coalescence of granules was observed after 73 hours of cultivation. A much lower number was obtained in a fermentation conducted in 5 CSTRs connected in series, where the number rarely exceeded 3 within *C. necator* cells. It was not clear whether the differences come from intrinsic regulation of granule-associated proteins or the cultivation technique (Vadlja *et al.,* 2016).

The different colour of PHB and cellular components in the image allows an estimation of the quantity of PHB within the cell, as shown by the inset of Figure 5-3. The area of the coloured image (represented by the number of pixels) occupied by the granules can be divided by the total area of the cell to express an approximate percentage of the cell occupied by PHB. Clearly, the volumetric effect would mean that the number is an overestimate but it is useful to show trends and comparisons.

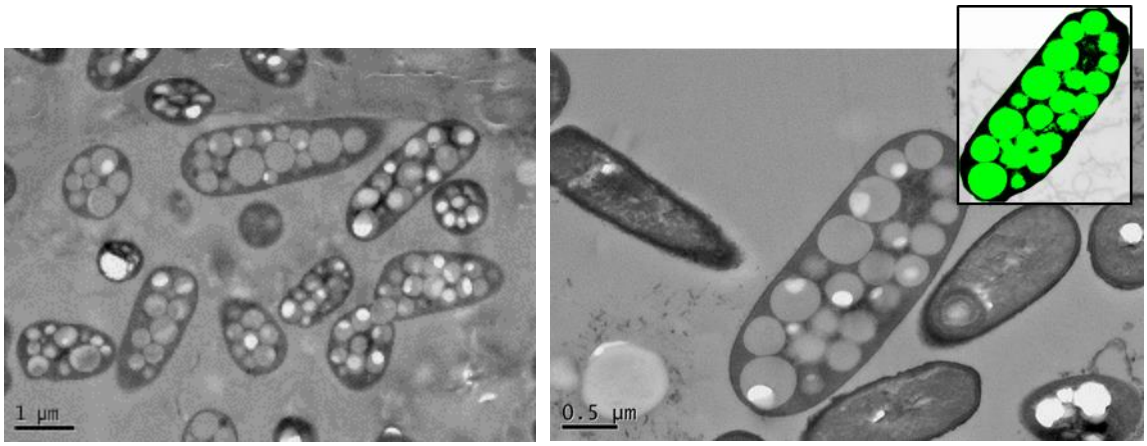

Figure 5-3: Observation of PHB granules under transmission electron microscope. On the right, the central cell was chosen to estimate PHB content based on colour difference:

$$(Area\ occupied\ by\ green\ pixels\ )/(Total\ cell\ area) = 1122057/1664549 \cdot 100 = 67.4\%.$$

Of course, the actual PHB content would not correspond to exactly the 67.4 % calculated. But the number is in the typical range for the content that *C. necator* cells can accumulate and that was found when determining PHB amount by gas chromatography after extraction.

For an accurate quantification, as mentioned, the cellular volume would need to be calculated. For doing this, Tian *et al.*, (2005) used the volume equation of a cylinder. Tomographic models could also be applied to restore 3D figures from 2D images as developed by Beeby *et al.*, (2012) to follow granule genesis and development. It is important to point out the diversity of number and sizes of granules within the cell culture, which makes statistical analysis of the cell population a requirement for obtaining representative results such as those from Vadlja *et al.*, (2016)

5.1.3 Measurement of cell concentration in suspension by optical density

Techniques to monitor biomass concentration based on light scattering have the advantage of being rapid and non-destructive. However, it was questioned if they would be appropriate to follow biomass evolution considering that biomass is integrated by two different compartments that will possible have different absorbance properties. To test the suitability of this technique in this particular case, the relationship between cell dry mass (CDM) and optical density (OD) was plotted against fermentation time for the later cultures of the adaptation process. OD measurements were converted into OD absolute values by multiplying the absorbance readings by the corresponding dilution factor. Results are shown in Figure 5-4.

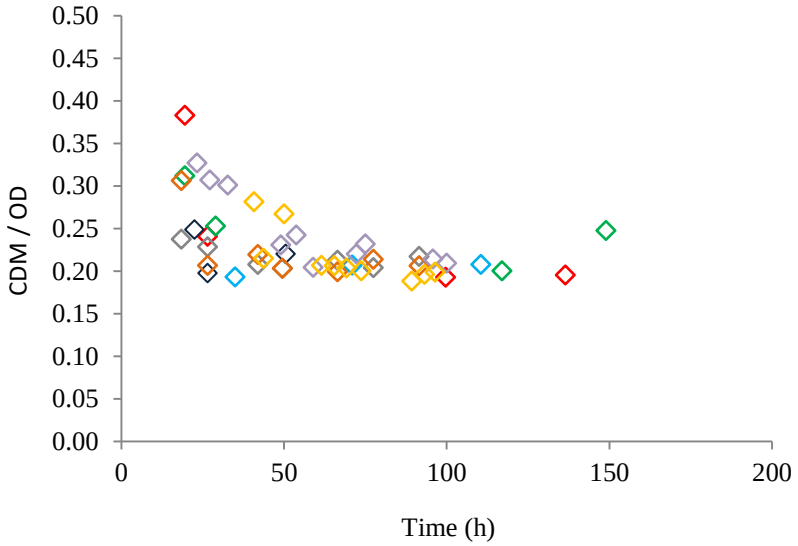

Figure 5-4: The changing relationship between cell dry mass and optical density as fermentation progresses for different sets of data from different cultures of *C. necator*.

Despite the data scattering, it can be observed that the ratio between CDM/OD decreases (non-linearly) for the first 50 hours of fermentation and then stabilizes to a constant value of around 0.2. This means that for younger cells, optical density changes faster than cell dry mass, but both properties tend to vary very similarly as the fermentation progresses. In other words, optical density relates linearly with optical density after a certain point in the fermentation (or a certain value of CDM or OD). It was decided that optical density would be converted into cell dry mass following the two different correlation curves presented in Figure 5-5. For optical densities lower or equal to 10.5, second order polynomial equation would be used, whereas for higher values of OD, a linear curve applies.

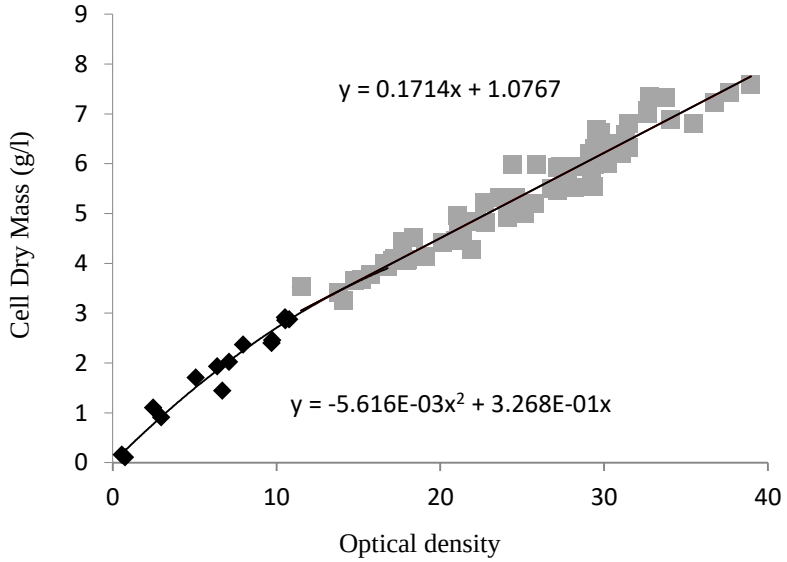

Figure 5-5: Correlation developed to convert optical density measurements into estimated cell dry mass values for glycerol fermentations by *C. necator*.

5.1.4 Example of a simple batch culture for PHB production

Results presented in Figure 5-6 illustrate typical substrate and product profiles obtained when using a relative high C/N ratio (32 mol/mol) in a batch fermentation. Total biomass, PHB, associated biomass (non-PHB biomass) and glycerol concentration are plotted against experimental time. Total biomass concentration, which integrates PHB and associated biomass, increased rapidly in the first hours of fermentation. The fermentation entered stationary phase after 40 h and totally biomass concentration started decreasing by the 75th hour. PHB production was slower than associated biomass accumulation during the first hours of cultivation although, eventually, the amount of PHB reached a higher value than the amount of associated biomass. PHB content began to decline from the time at which glycerol had been exhausted (around 80 h). Nonetheless, associated biomass remained approximately constant.

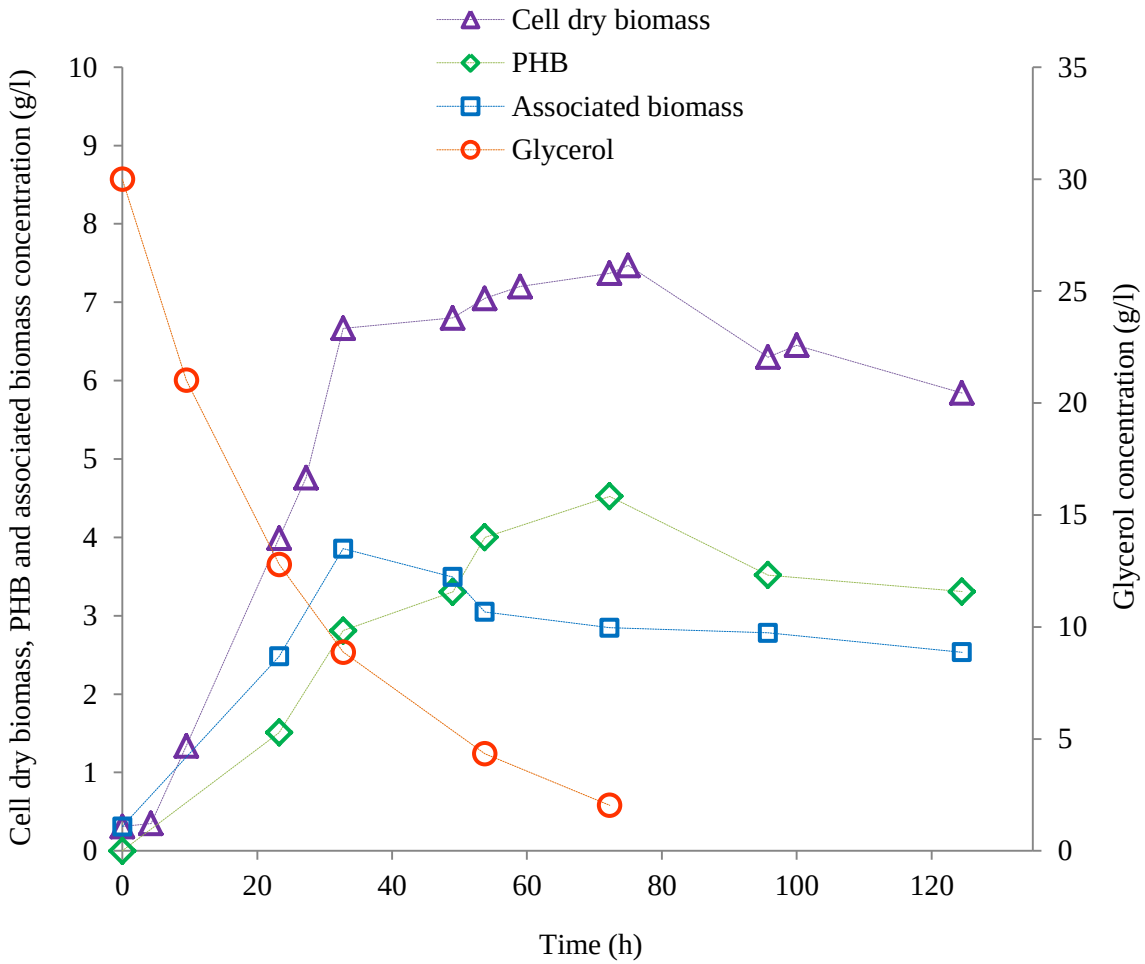

Figure 5-6: Profiles of glycerol fermentations by *C. necator* over the course of a batch culture conducted with excess of carbon over nitrogen at an initial C/N ratio of 32.

The observable maximum growth rate occurred at 9.5 h of fermentation. The maximum production rate however was in the 33rd hour as shown in Figure 5-7:

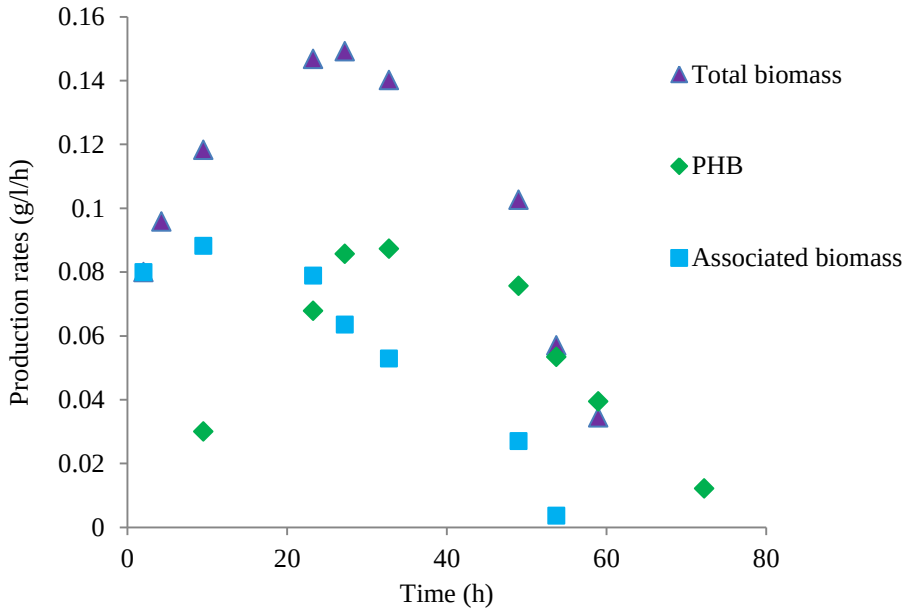

Figure 5-7: Evolution of biomass, PHB and associated biomass production rates over the course of a glycerol fermentations by *C. necator*. The observed maximum production rate occurred at the 33rd hour.

Based on the stoichiometric reaction proposed by Akiyama *et al.*, (2003), every mole of PHB is synthesized from 2 moles of glycerol. Although all glycerol appeared to be consumed by the end of the fermentation, only around 30 % can be accounted for in terms of PHB formation (See Figure 5-8). The remainder is consumed for the purposes of respiration, biomass formation and general metabolism.

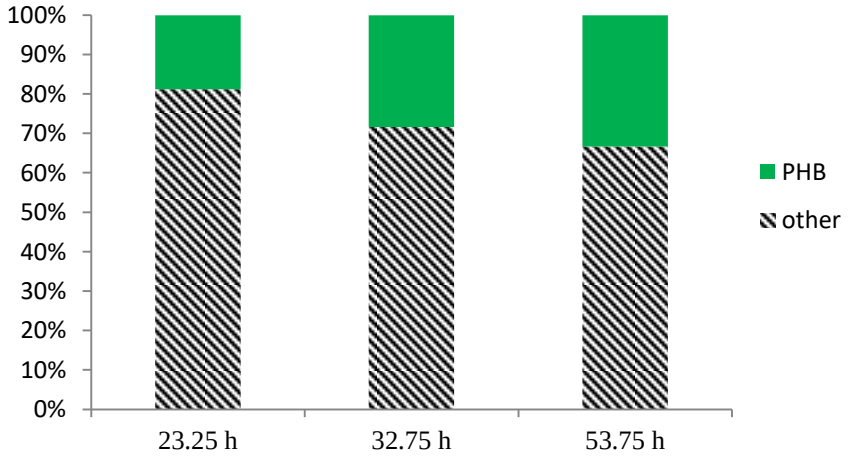

Figure 5-8: Stoichiometric division of glycerol utilization during a glycerol fermentations by *C. necator* conducted with 30 g/l glycerol.

5.2 Studies on the influence of glycerol concentration on PHB production

PHB reserves are mainly accumulated when microorganisms are grown under nutrient-limited conditions with an excess of the carbon source. However, the amount of carbon (glycerol) can have a positive or negative effect on growth, which in turn affects PHB production. Therefore, the maximum concentration of glycerol needs to be carefully evaluated to prevent inhibitory effects and maximize the yield of carbon into PHB. The effect of glycerol on the fermentation results was evaluated using data obtained from experiments with variable initial amounts of glycerol and constant amount of ammonium sulphate (1 g/l).

5.2.1 Effect on growth rate

To study how the presence of glycerol influences the velocity at which cells divide, the specific growth rate during exponential phase was calculated from the logarithmic plot of biomass with time as detailed in section 3.2.5. During the early hours of culture, when nitrogen is plentiful, all biomass is considered to be associated biomass. The error bars shown in Figure 5-9 represent the standard error between this variable calculated for more than one culture (repetition).

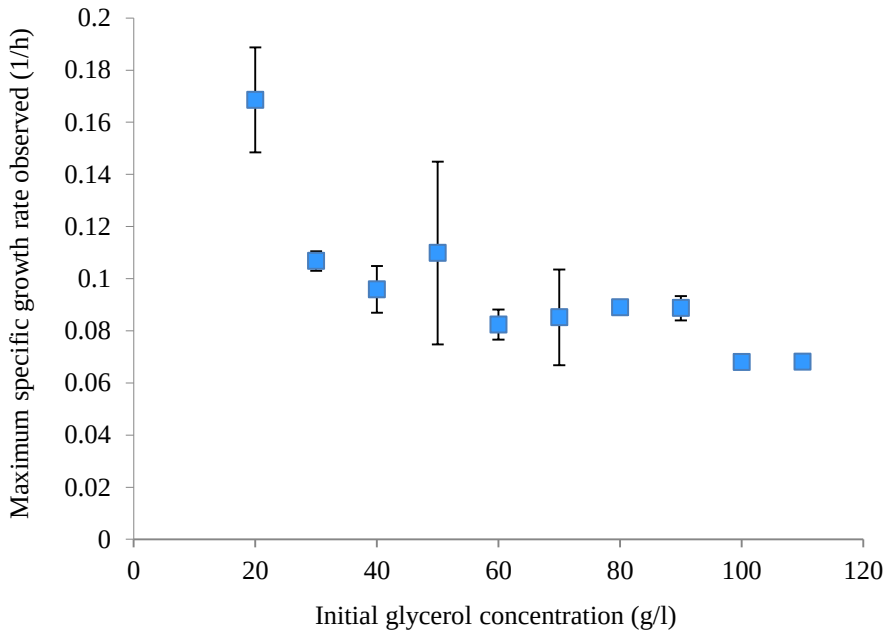

Figure 5-9: Specific growth rate observed during exponential phase for different initial glycerol concentrations in simple batch fermentations of *C. necator*. Error bars represent data from repeat experiments.

The observed maximum specific growth rate decreased as the initial glycerol concentration in the medium increased. Values for the growth rates of the cultures at more than 100 g/l glycerol are less than half of those for 20 g/l. Clearly, there is significant substrate inhibition. A popular model to represent this is the modified form of Monod equation (Eq. 5- 1) which can capture the experimental trend. Using this model with typical but un-optimized parameters values, a curve through the data is represented in Figure 5-10.

$$\mu = \frac{\mu_{max} \cdot [S]}{k_M + [S] + \frac{[S]^2}{k_I}} \qquad \textbf{Eq. 5- 1}$$

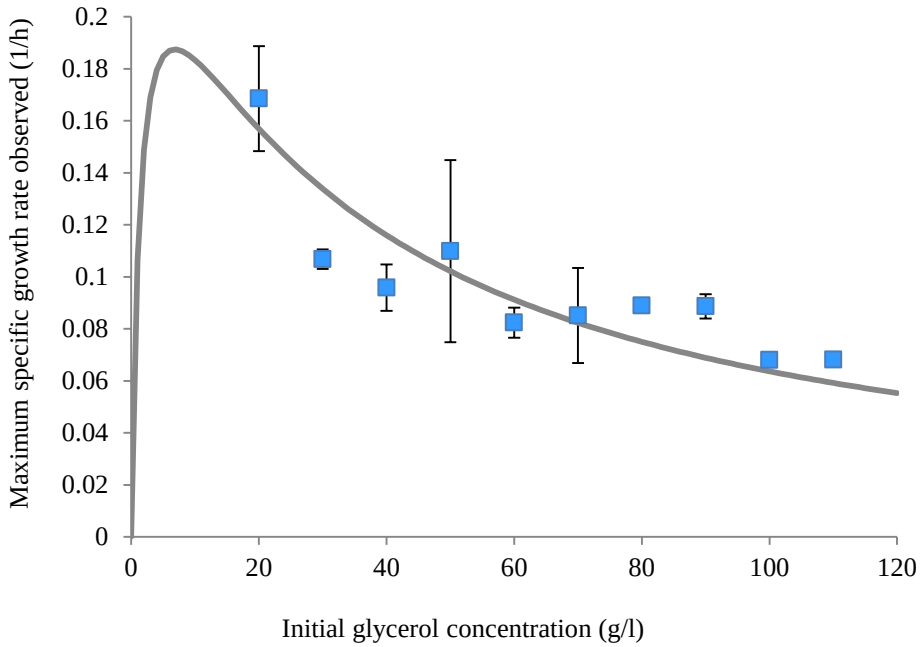

Figure 5-10: Specific growth rate observed in *C. necator* cultures for a range of initial glycerol concentrations and fitted by Eq. 5- 1 with $\mu_m = 0.27\ 1/\mathrm{h}, k_M = 1.5\ \mathrm{g/l}, k_I = 31\ \mathrm{g/l}$.

5.2.2 Effect on PHB accumulation

Volumetric PHB concentration in the vessel is a function of intracellular content of PHB and biomass concentration. PHB content was measured at the end of the fermentation and results, in terms of concentration (by multiplying by the final biomass concentration) are shown in Figure 5-11 by the triangles. The distribution of PHB and associated biomass is shown by the bars.

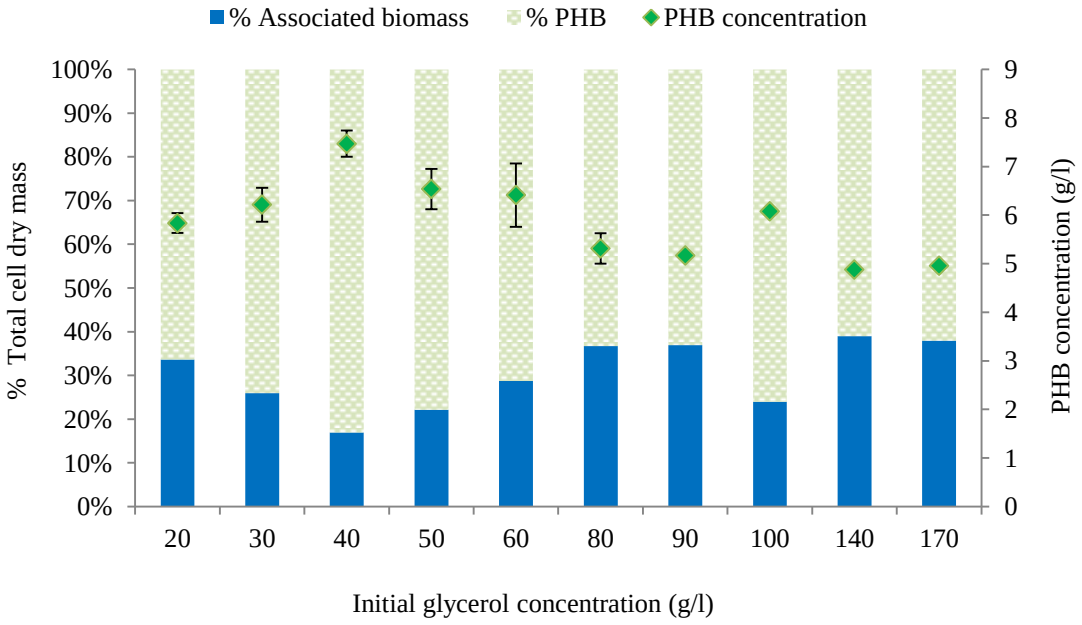

Figure 5-11: PHB concentration and proportion of PHB and associated biomass obtained for batch fermentations by *C. necator* conducted with different glycerol amounts. Error bars represent data from repeat experiments.

Maximum PHB concentration (7.5 g/l) was achieved with 40 g/l of glycerol, which improved the production over the batches conducted with 20 and 30 g/l. Concentrations exceeding 40 g/l did not foster any further increase in PHB concentration and in fact, contents fell to a low value at 80 g/l and appeared to remain (with the exception of 100 g/l) constant thereafter. Associated biomass concentration followed the opposite trend.

The above observations strongly suggests that initial glycerol concentrations regulate the production of PHB and associated biomass during a fermentation and that beyond a certain concentration the carbon source negatively impacts PHB production.

5.2.3 Glycerol consumption

Besides not favouring PHB accumulation, too much glycerol can have detrimental effects: increasing cost in purification stages and/or leading to undesirable metabolic pathways. Glycerol consumption under different initial conditions is illustrated in Figure 5-12. The data were fitted to an exponential decay model (Eq. 5- 2) in which *k* is the decay constant.

$$Gly\ (t) = Gly_0 \cdot e^{-k \cdot t} \qquad \textbf{Eq. 5- 2}$$

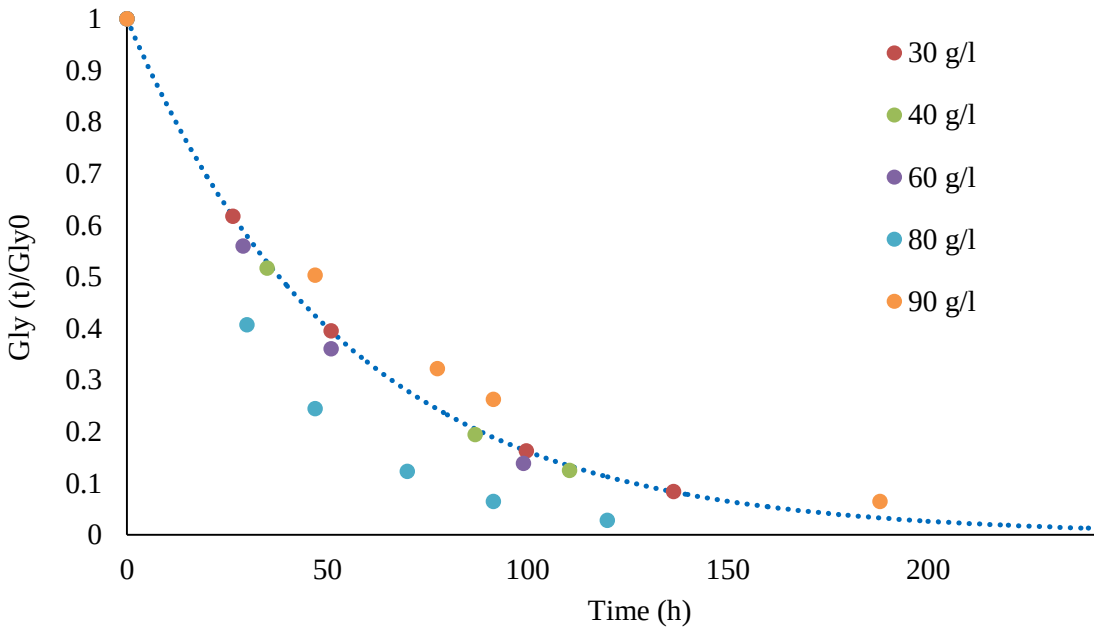

Figure 5-12: Dynamics of glycerol consumption for *C. necator* fermentation conducted with various initial glycerol concentrations. The lines represent the exponential decay equation for each initial concentration and an exponential decay constant of 0.02 h^{-1}.

Figure 5-12 suggests that initial glycerol uptake increases with the initial glycerol amount but not all glycerol gets consumed for the highest initial glycerol concentrations (80, 90 g/l) and for the time range plotted. Although the exponential decay model described well the profiles for the lowest glycerol concentrations is a poor fit for high initial glycerol concentrations. The fact that enzymes involved in glycerol conversion might get saturated could explain the residual glycerol levels.

Remaining glycerol and final consumption of glycerol are presented in Figure 5-13. These confirm the general observation described above. Glycerol consumption was computed taking into account the initial and final values of volume from the culture, as indicated in Eq. 5- 3:

$$Gly\ consumed = Gly_0V_0 - Gly_fV_f \qquad \textbf{Eq. 5- 3}$$

As PHB production did not increase for initial glycerol concentration exceeding 40 g/l, it was expected that the percentage of unused glycerol would increase for larger initial amounts of glycerol. Nonetheless, for concentrations over 80 g/l, glycerol utilization seemed to start rising again. It is speculated that flux of carbon can be redirected towards organic acid formation as a cell mechanism to deal with the excess of substrate. Fermentation by-products (organic acids) were detected on those conditions.

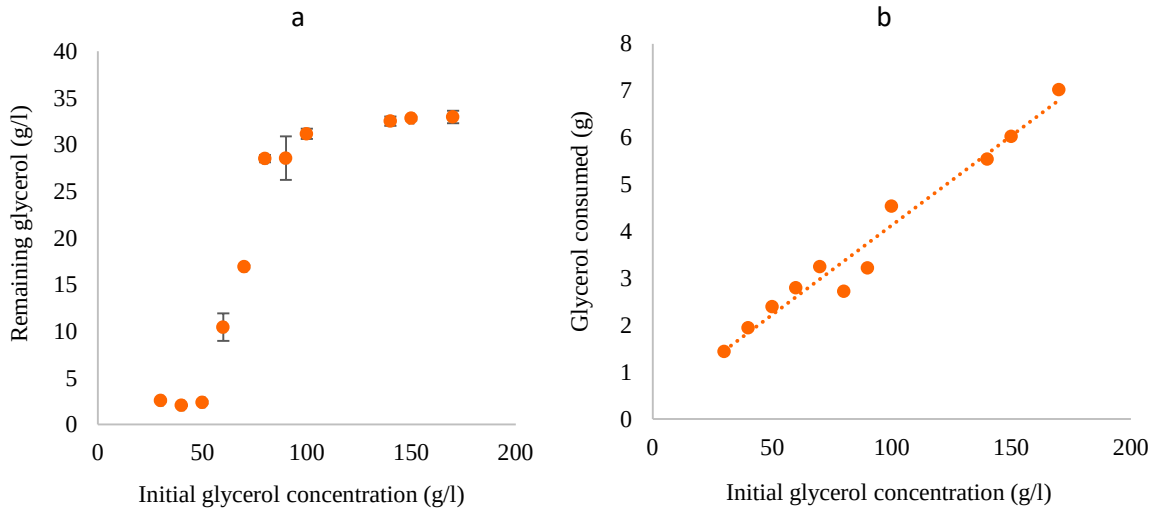

Figure 5-13: (a) Glycerol concentration left at the end (approximately 120 h) of *C. necator* fermentations conducted with different amounts of glycerol. (b) Total amount of glycerol consumed during the same.

5.2.4 Overall yields and mass balances

For a better evaluation of the fermentation performance, yields of associated biomass ($Y_{xA/Gly}$) and PHB ($Y_{PHB/Gly}$) based on total glycerol consumption were calculated for the experiments already presented and these are shown in Figure 5-14.

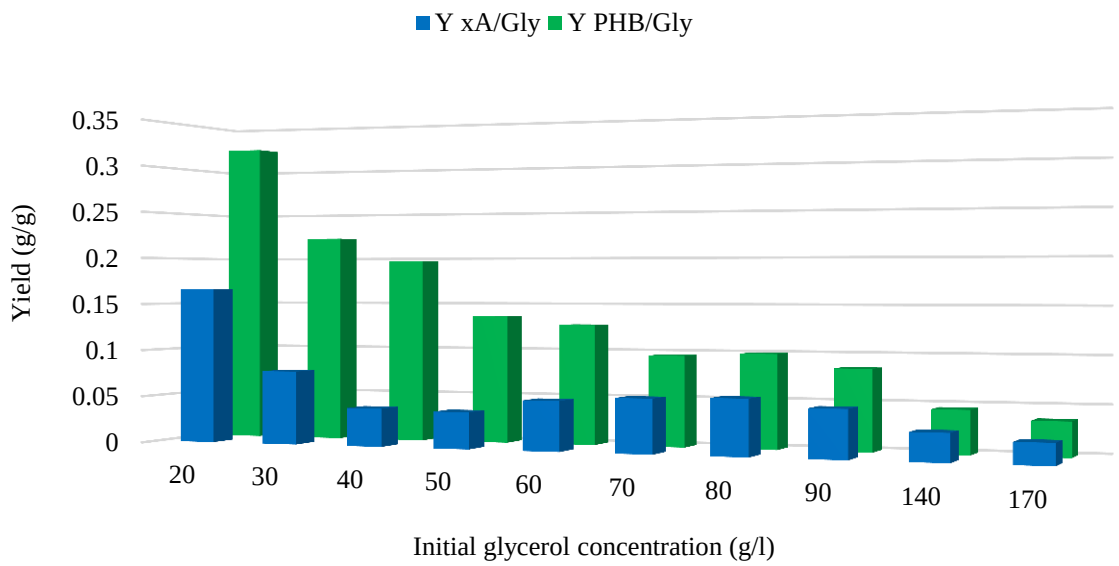

Figure 5-14: Overall yields of the main fermentation products, cells (x_A) and PHB for *C. necator* fermentations conducted with different initial glycerol concentrations.

As presented in section 3.2.5, stoichiometric equations to represent glycerol conversion to biomass and PHB were used to estimate the carbon concentration that would be theoretically required in order to obtain the experimental values of cells and PHB. The difference between the theoretical requirement and the actual consumption is presented in Figure 5-15 and represents carbon utilized for other metabolic purposes.

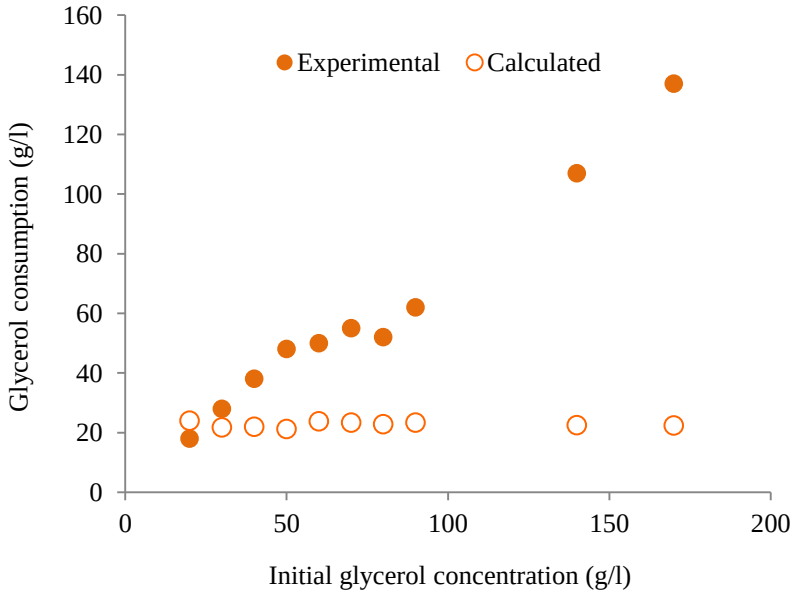

Figure 5-15: Experimental and calculated values of the glycerol consumed by *C. necator* in fermentations with different initial glycerol concentrations. Calculated values represent the glycerol that would be required just to produce cells and PHB based on stoichiometric reactions.

5.2.5 Discussion

From the above results it can be seen that glycerol can be used as the sole carbon source for both growth and PHB production by *C. necator* DSM 545. The PHB produced could be easily identified with staining techniques, such as Sudan Black. Intracellular granules were also detected by observing cells under TEM. Fermentations conducted with excess of glycerol over any other nutrient yielded PHB as main fermentation product, although the proportion of glycerol used in PHB production was only one third of the total consumed. PHB was extracted and recovered using the chloroform method and a white film of polymer was obtained.

Within a typical fermentation culture, the maximum rate of PHB production occurred after the maximum rate of biomass had been achieved, which could indicate a non-growth associated process. PHB production seemed to depend on the presence of glycerol and PHB concentration started decreasing as glycerol was virtually exhausted (in this way, the degradation of PHB could provide essential carbon that the culture lacked). It was thought that a larger excess of glycerol could lead to better results and the outcomes of cultures with higher amounts of glycerol were tested. Final associated concentration did not vary significantly regardless the initial concentration, which implies that glycerol was not limiting growth even at a concentration of 20 g/l. Although cells can grow on very high glycerol concentrations (170 g/l), large amounts of this carbon source seemed to reduce the doubling time of the cells, which agrees with the findings of Zhu *et al.,* (2009), who stated that the specific growth rate of *C. necator* decreased when using either pure glycerol or biodiesel-glycerol as sole sources of carbon at concentrations exceeding 30 g/l. A Monod-based model with substrate inhibition was therefore chosen to model the experimental data.

PHB content improved when the initial glycerol concentration increased from 20 to 40 g/l, reaching 83 % on a total biomass basis. The fact that for this case associated biomass was slightly lower than normal (values for 20 g/l) could suggest that cells did not proliferate to their maximum potential in favour of an over-production of PHB. Larger excesses of glycerol would, therefore, not have any further benefit as no more PHB would be formed. Cultures would take longer (slower growth rate) and some glycerol could remain unconsumed until the end of the fermentation.

In the experiments reported above, the highest PHB concentration was achieved when using 40 g/l of glycerol. However, the highest yield of PHB based on glycerol was attained for the fermentation started with 20 g/l. Even if glycerol is considered to be a very energetically favourable substrate for the formation of acetyl-CoA, the precursor for PHB synthesis, it is speculated that above a certain concentration, it is redirected into different pathways since it was observed that the glycerol consumption increases with increasing initial glycerol concentration. Other metabolites (organic acids) might have been produced as a result of the excess of carbon that cells could not convert into PHB and

accommodate in the cytoplasm (cells might have a maximum capacity for storage). Consequently, there is a gap between stoichiometrically calculated and experimentally observed data in Figure 5-15 leading to a decrease in overall yield.

5.3 Studies on the influence of nitrogen concentration on growth and PHB production

As described in the literature review, carbon and nitrogen concentrations are considered amongst the critical variables for the optimization of PHB production. Clearly, both elements have a major effect on outcomes, but maybe not to the same extent on PHB production and growth. The effect of carbon on the fermentation outcomes was reported in the previous section. The current section describes the results of experimental work performed to understand the effect that nitrogen concentration has on the system.

5.3.1 Effect on growth rate

Batch fermentations with different initial amounts of nitrogen, in the form of ammonium sulphate (AS), and constant amount of glycerol (30 g/l) were carried out in order to establish the impact of this compound. Cultures with larger amounts of nitrogen became turbid sooner than those with less nitrogen. Figure 5-16 shows broth samples taken from cultures started with various amounts of ammonium sulphate.

Figure 5-16: Range of turbidity found in sample broths from glycerol fermentations by *C. necator* cultures started with different initial nitrogen concentration. The concentrations used in the respective flasks, from left to right, were 0.1, 0.25, 0.5, 0.75 and 3 g/l.

Aliquots from flasks, incubated under the same conditions, were periodically withdrawn so that growth curves could be obtained and evaluated. The raw data corresponding to initial concentrations of ammonium sulphate (AS) ranging from 0.1 to 3 g/l are presented in Figure 5-17.

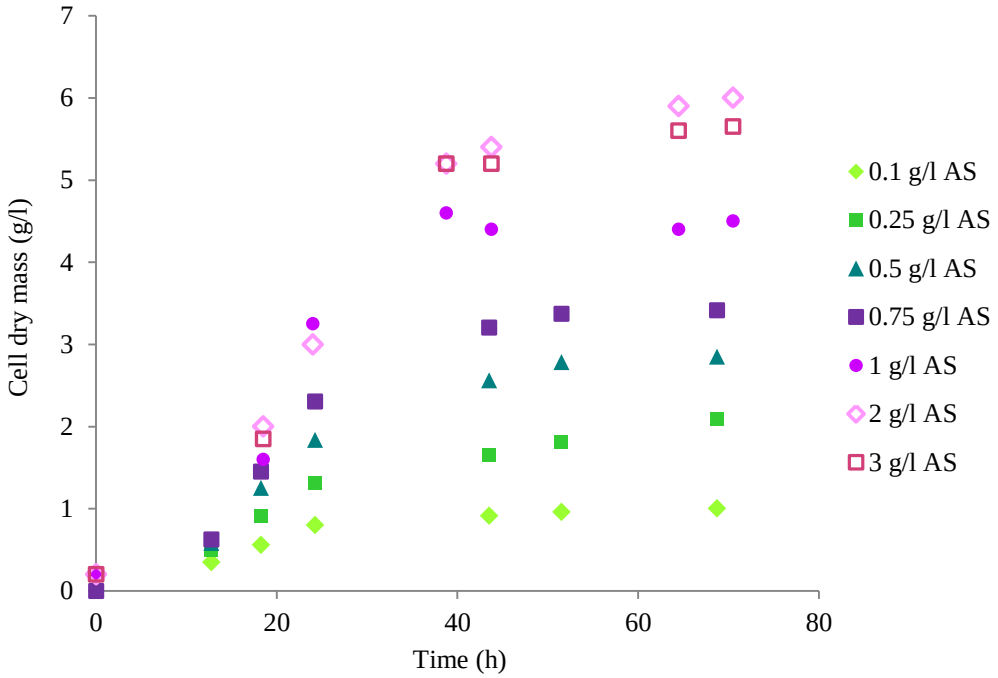

Figure 5-17: Variation of cell dry mass with time for glycerol fermentations by *C. necator* with initial concentrations of ammonium sulphate (AS) from 0.1 g/l to 3 g/l.

Fermentations with higher concentrations of ammonium sulphate (4 and 8 g/l) were conducted with a view to establishing the threshold in terms of cell concentration for this particular system. After PHB was extracted and quantified, the associated biomass, which is the actual indicator of cellular growth, can be deduced. Results at 100 hours of cultivation are plotted in Figure 5-18.

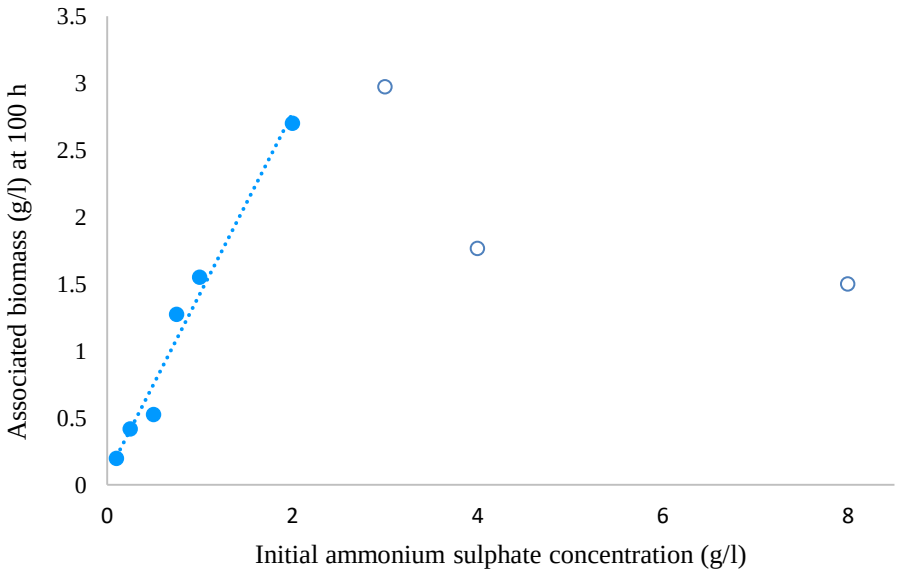

Figure 5-18: Associated biomass concentration produced by 100 hours of glycerol fermentations by *C. necator* fermentation for different initial amounts of ammonium sulphate.

As observed in Figure 5-17, there is an apparent relationship between nitrogen concentration and cell growth. Cultures that had the lowest nitrogen concentration *i.e.* 0.1 g/l also showed the lowest biomass concentration throughout the fermentation. As seen in the graph, cell dry mass increased with initial

nitrogen concentration following a linear trend up to 2 g/l (represented by a dashed line in Figure 5-18).

Unlike glycerol, variations in the nitrogen concentration have a direct impact on the production of associated biomass (as expected for the limiting substrate). It can be seen that final dry cell mass and the production rate of it increased when cells grew in a medium with abundant nitrogen. Specific growth rates for the various N concentrations were graphically calculated from the semi-logarithmic plot of biomass, as illustrated in Figure 5-19:

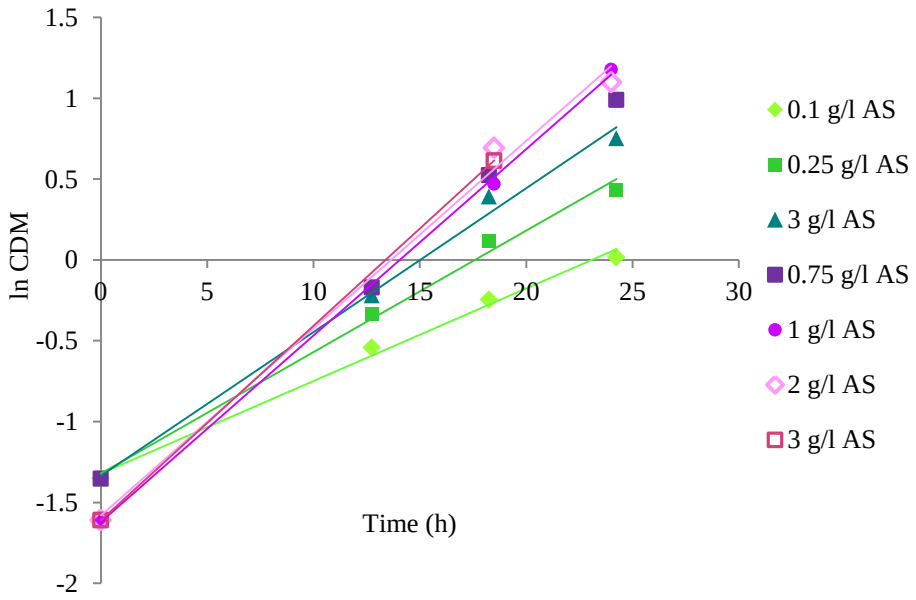

Figure 5-19: Semi-logarithmic plot for cell dry mass against time for determination of specific growth rate of *C. necator* at the different ammonium sulphate concentrations.

In all the data series, the data points corresponding to the first 24 hours of fermentation (exponential phase) follow a linear trend, which becomes steeper as the concentration increases. The slope from these lines corresponds to the specific growth rate. Finally, the plot of specific growth rate *vs.* ammonium sulphate concentration is presented in Figure 5-20:

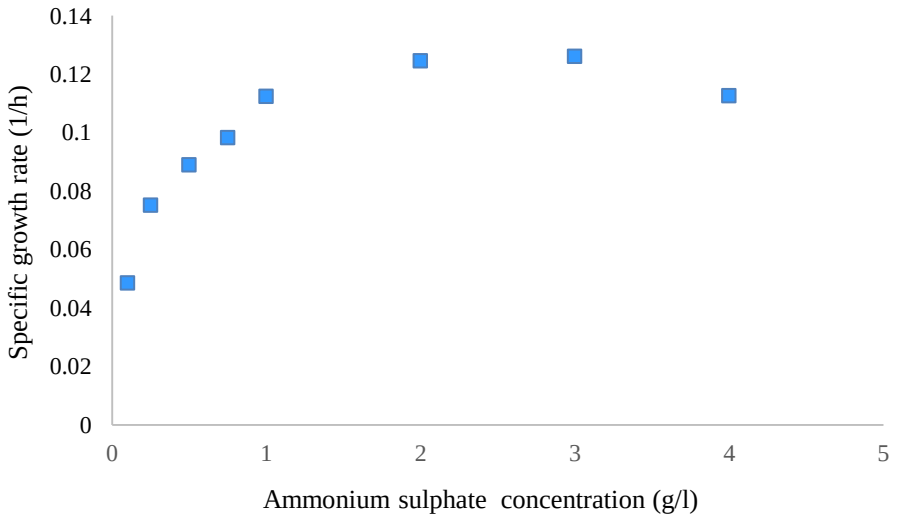

Figure 5-20: Variation in the maximum specific growth rate observed, at exponential phase, as a function of the initial amount of nitrogen (ammonium sulphate) in glycerol fermentations by *C.necator*.

Specific growth rate increased with the concentration of nitrogen until concentrations around 2 to 3 g/l when it started to decrease. This inhibitory effect is consistent with the results obtained in the fermentation conducted with 8 g/l of AS, where only 1.5 g/l of associated biomass had been produced by 100 hours.

As with the glycerol data, growth rates were fitted to a Monod equation coupled with substrate inhibition. In this case, the equation was based on nitrogen as the limiting substrate. The results of un-optimised modelling are presented in Figure 5-21.

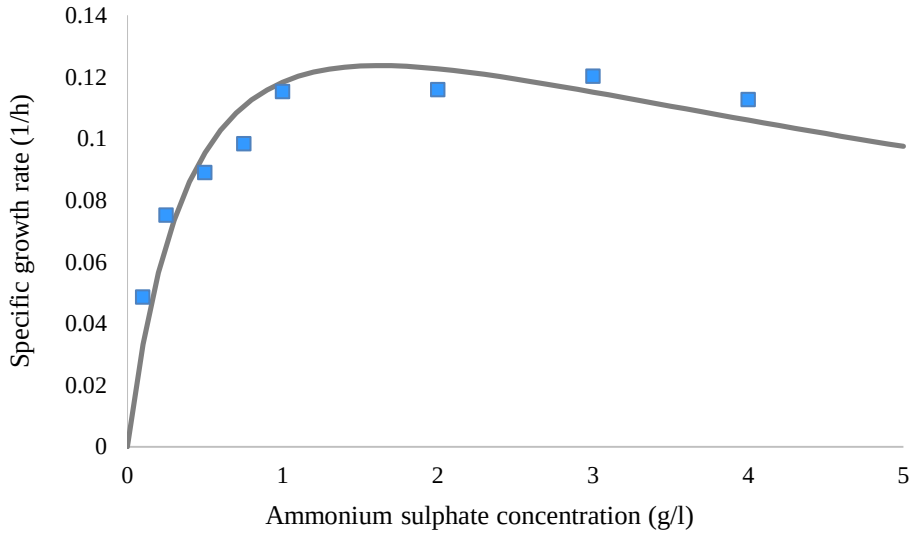

Figure 5-21: Specific growth rate observed for a range of initial ammonium sulphate concentrations in glycerol fermentations by *C.necator* and fitted by Eq. 5- 1 with $\mu_m = 0.2\ \mathrm{h}^{-1}, k_M = 0,5\ \mathrm{g/l}, k_I = 5,25\ \mathrm{g/l}$ ($k_M$and k_I are based on nitrogen).

This indicates that, as expected, specific growth rate is strongly dependent on the amount of nitrogen in the medium, since nitrogen is limited with respect to carbon. The more nitrogen in the medium, the more the cells can grow and they do until a concentrations of 3 g/l, for which extra nitrogen does not lead to higher specific growth rate nor amount of cells produced. In fact, it looks like ammonium sulphate concentrations above 3 g/l have an inhibitory effect on growth, which agrees with the findings reported in literature (Heinzle & lafferty 1980). However, specific growth rate also varied with glycerol concentration for a fixed amount of carbon, which means that both substrates (carbon and nitrogen) impact the rate of cell reproduction, and thus, both need to be incorporated in the equation to describe cellular growth rate (*i.e.* a double substrate model is needed).

5.3.2 Effect on PHB accumulation

Fermentation results, in terms of total biomass and PHB concentrations, for cultures prepared with 1, 2 and 3 g/l of ammonium sulphate and the same initial glycerol concentration (30 g/l) are presented in Figure 5-22.

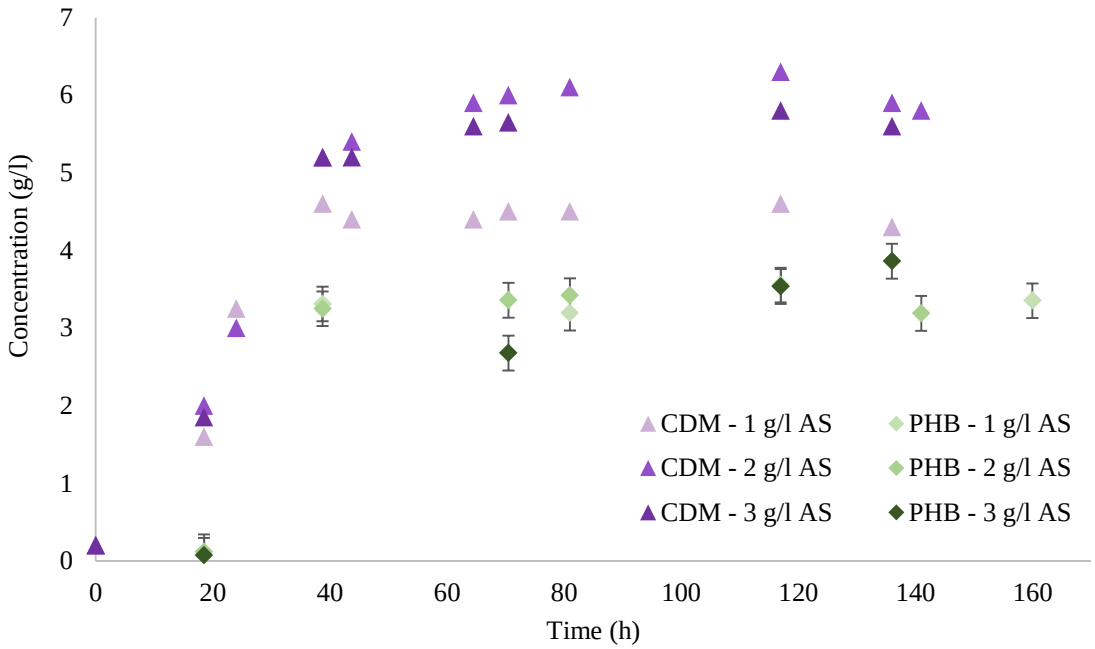

Figure 5-22: Biomass and PHB concentration profiles from glycerol fermentations by *C. necator* conducted with various amounts of nitrogen and the same initial glycerol concentration (30 g/l).

As observed from Figure 5-22, the lowest total biomass concentration by the end of the fermentation corresponded to the culture that contained, at the beginning, 1 g/l ammonium sulphate. As commented earlier, higher nitrogen concentrations yielded higher associated biomass concentrations, and thus, values of total biomass obtained for 2 and 3 g/l were higher. The growth rate seemed to stay rather constant for the three cases based on the time required to reach stationary phase for the different cases. The major difference observed between those set of data is the PHB profile for the culture conduced with 3 g/l initial ammonium sulphate. Production rate was much lower than for the cases with less nitrogen and just reached its maximum value by 136 hours. A higher concentration of nitrogen in the first hours of fermentation is thought to limit the synthesis of PHB, as cells prioritize growth and PHB formation. Figure 5-23 shows that PHB content by the end of fermentation was significantly higher for the culture started with 1 g/l ammonium sulphate than for those cultures that initially contained 2 and 3 g/l.

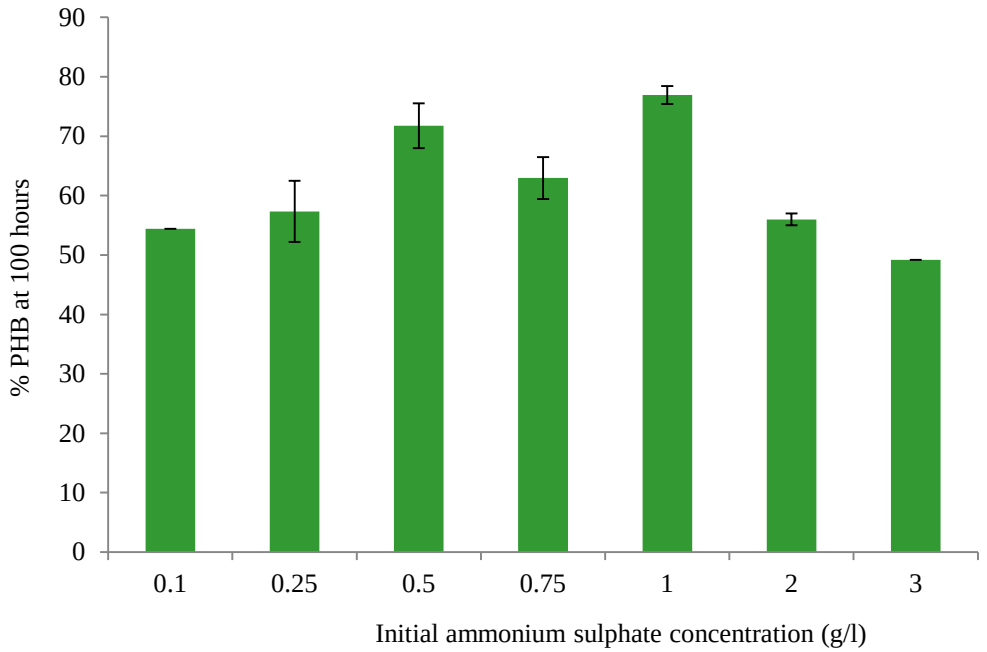

Figure 5-23: PHB content on a total biomass basis for glycerol fermentations by *C. necator* conducted with various amounts of initial ammonium sulphate concentration.

5.3.3 Nitrogen consumption

The uptake of ammonia by the cells liberates a proton from the NH_4^+ molecule, which is (partially) responsible for the acidification of the media. Thus, pH measurements can be an indirect method of following nitrogen consumption over the course of fermentations. Figure 5-24 shows the variation in the pH for cultures started with different amounts of ammonium sulphate.

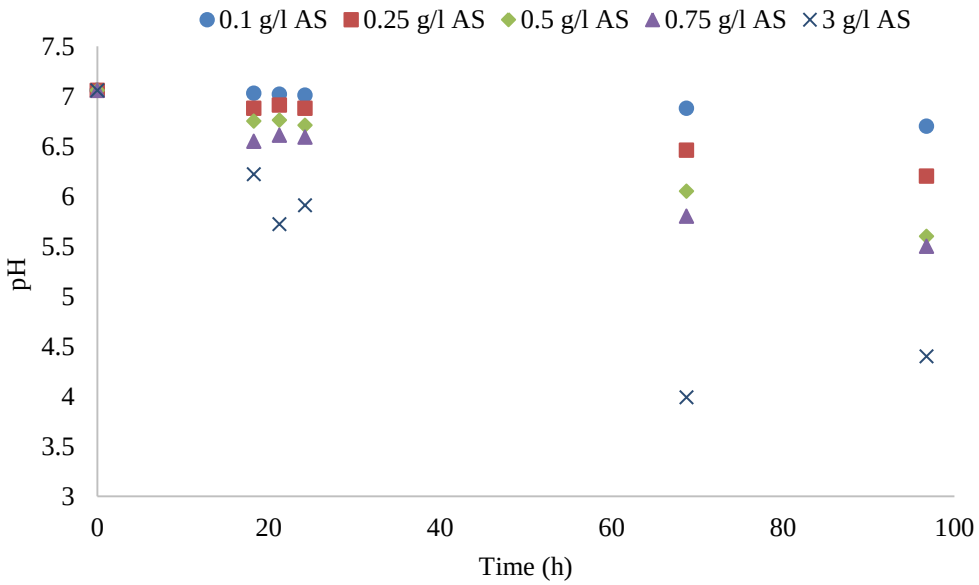

Figure 5-24: Evolution of pH for glycerol fermentations by *C. necator* conducted with different amounts of initial ammonium sulphate (AS).

As expected, the drop in pH is larger for cultures conducted with higher concentrations of ammonium sulphate. By the 18th hour of culture, when the reduction in pH can be assumed to come just from

growth, the decrease was of 0.4, 2.5, 4.4, 7.2 and 11.9 % for fermentation conducted with 0.1, 0.25, 0.5, 0.75 and 3 g/l respectively. The relationship between pH diminution and growth rate is shown in Figure 5-25. The sharpest pH drop matches the exponential growth phase.

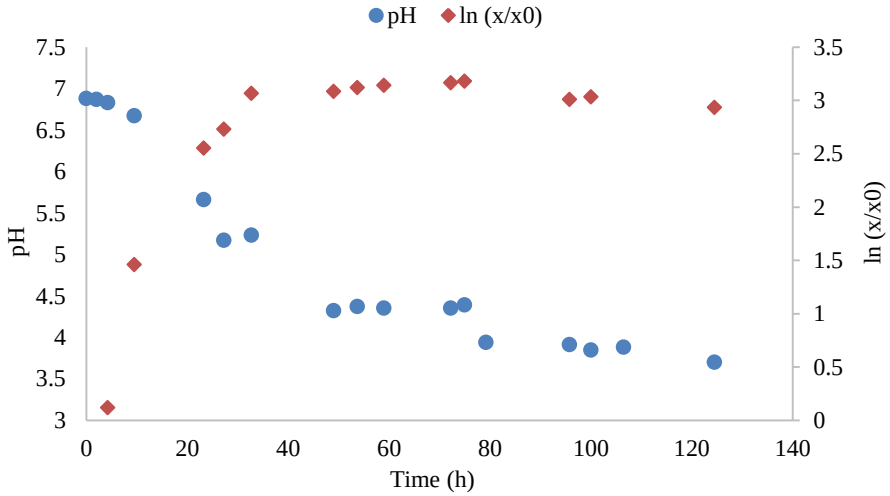

Figure 5-25: pH and biomass evolution for a glycerol fermentation by *C. necator*.

5.3.4 Test with an organic source

In all the experiments conducted during the research, ammonium sulphate was used in order to have a defined composition in the media that could be easily quantified. To evaluate if growth could be improved by using an organic source (peptone), four flasks were prepared with two high nitrogen concentrations, 3 and 6 g/l ammonium sulphate (AS3 and AS6) and the equivalent nitrogen concentrations in the form of peptone (P3, P6) in the other two. The growth curves obtained are presented in Figure 5-26.

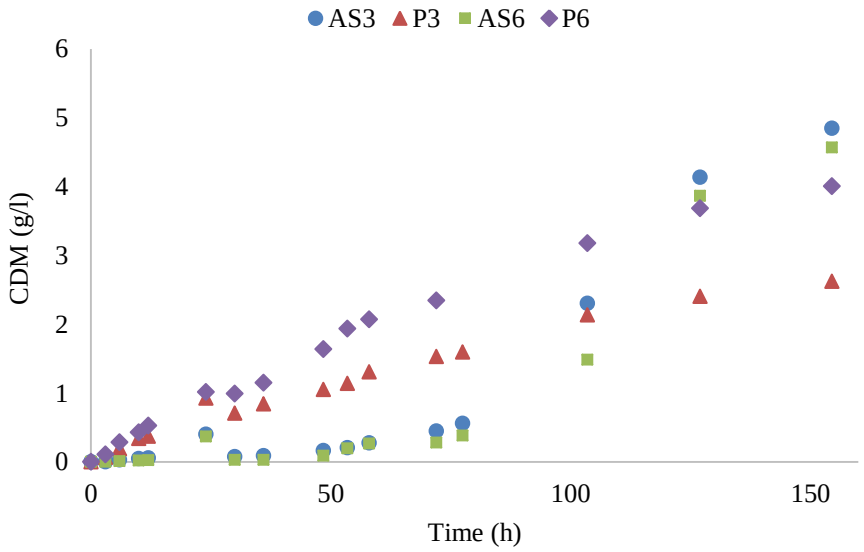

Figure 5-26: Evolution of biomass concentration for glycerol fermentations by *C. necator* conducted with relatively high inorganic (ammonium sulphate) and organic (peptone) nitrogen sources. Initial concentrations were 3 g/l (AS3 and P3) and 6 g/l (AS6 and P6).

Growth on the organic sources looked better as the culture was able to make use of it straight away and cells grew more readily (the inhibition effect for ammonium sulphate concentrations greater than 3 g/l has been reported earlier). Nonetheless, peptone did not yield overall higher yields than ammonium sulphate, which could have led to more PHB production. Thereby, using an organic, more expensive and undefined, nitrogen source did not seem to bring great benefits.

5.4 Developing a biomass production hypothesis

Biomass is the main product of the fermentations conducted and it is composed of two principal components, residual (associated) biomass and PHB. Growth of the active fraction of biomass and PHB production are controlled by different mechanisms. The two factors studied, the carbon and nitrogen source, have shown a large effect throughout the course and on the final values of the fermentations. Glycerol and ammonium sulphate, however, impact the culture dynamics differently. Together with these two substrates, the 'response' variables evaluated, associated biomass and PHB, will constitute the main variables in the model. Using the observations described above the following hypothesis for growth and PHB production is postulated.

Biomass concentration is the sum of associated biomass and PHB concentrations. Growth of the active fractions causes the increase of total biomass during the first hours of fermentation. Consumption of nitrogen, the limiting substrate, is directly proportional to the growth of the non- PHB fraction, at least for concentrations between 0 and 2-3 g/l, and is totally consumed by the time associated biomass growth stops. This implies a constant yield of associated biomass based on nitrogen. The growth rate of associated biomass is enhanced by the presence of ammonium sulphate up to 3 g/l. Growth rate inhibition occurs for concentration exceeding this value. Glycerol concentrations above 40 g/l also inhibit growth, although they do not influence the final value of associated yielded.

PHB production, on the other hand, is directly related to the presence of carbon, and the deficiency of nitrogen. In fact, it is believed that nitrogen depletion activates PHB production. PHB increases with glycerol concentration to a certain extent above which additional glycerol does not result in any more PHB formation. There is a maximum size that cell can reach during PHB accumulation and thus, there is an upper limit in terms of PHB content. If high glycerol concentration is too high, other products (*e.g.* organic acids) are produced. PHB production does not start until nitrogen is depleted (*i.e.* unfavorable conditions for growth). This suggests a non- growth associated production process.

Nitrogen is only consumed for growth associated process and is therefore directly proportional to growth rate, whereas glycerol is utilized both for growth and PHB production. A general representation of the above is given in Figure 5-27 and was used as the basis to construct the model.

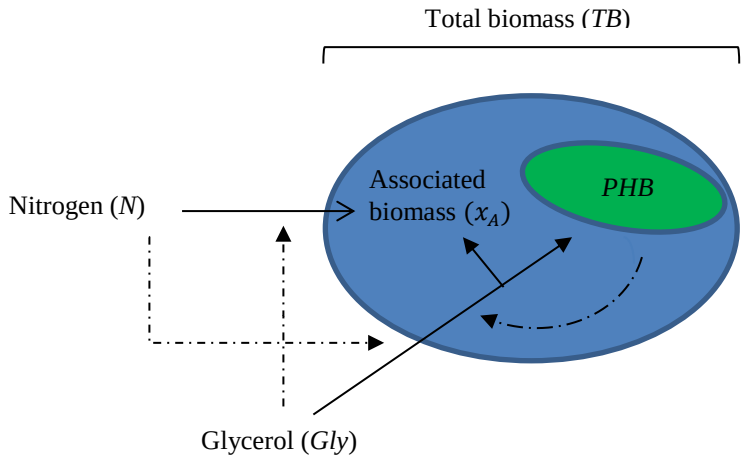

Figure 5-27: Mass fluxes and regulatory mechanisms that could explain PHB production by *C. necator* fermentation.

5.5 Formulating the model equations

The biomass production hypothesis has been translated into mathematical equations to describe the variation of products (PHB and associated biomass) and substrates (glycerol and nitrogen) with time and constitutes the kinetic model, which will be used to predict fermentation outcomes (Eq.5- 4 to Eq.5- 7).

$$\frac{dx_A}{dt} = r_{x_A} = \mu_{x_A} \cdot x_A \qquad \textbf{Eq.5- 4}$$

$$\frac{dP}{dt} = r_P = q_p \cdot x_A \qquad \textbf{Eq.5- 5}$$

$$-\frac{dGly}{dt} = r_{Gly} = q_{Gly} \cdot x_A \qquad \textbf{Eq.5- 6}$$

$$-\frac{dN}{dt} = r_N = q_N \cdot x_A \qquad \textbf{Eq.5- 7}$$

Cells are responsible for creating new cellular matter (x_A) and synthesizing the intracellular biopolymer (PHB), which together form the total biomass (TB), as indicated in Eq.5- 8. Since PHB stays inside the cellular membrane if cells do not lyse, any change in TB is due to an increase or decrease in x_A and/or increase or decrease in PHB. However, neither cell death nor PHB degradation has yet been considered in this model formulation.

$$TB = x_A + PHB \qquad \textbf{Eq.5- 8}$$

The specific rates, value of the rate divided by the associated biomass, were formulated based on the kinetic mechanisms observed. In this way, the fact that the growth rate can be affected simultaneously by more than one substrate is can be mathematically translated into a double substrate model. To

account for the inhibition effect of both substrates, several forms of the Monod equation could be used (Pérez Rivero *et al.,* 2016), but the one that resembles closest to the situation is given in Eq.5- 9.

$$\mu_{x_A} = \frac{\mu_m \cdot N}{k_N + N} \cdot \frac{1}{1 + \frac{N}{k_{IN}}} \cdot \frac{Gly}{Gly \cdot \left(1 + \frac{Gly}{k_{IG}}\right) + k_G} \qquad \textbf{Eq.5- 9}$$

where k_N and k_{IN} are respectively the half saturation constant in Monod model and the inhibitory constant due to (large) nitrogen (N) concentrations and k_G and k_{IG} correspond to the half saturation constant for glycerol (Gly) and its inhibitory constant.

As for growth rate (based on associated biomass), a modified Monod equation with glycerol as limiting substrate was also produced to describe the specific PHB production rate. An excess of glycerol, the sole carbon source, promotes PHB production up to a certain level at which the system becomes "saturated". A term representing the delayed appearance of PHB when nitrogen is still abundant was included in Eq.5- 10:

$$q_p = \frac{\beta \cdot Gly}{Gly + k_P + \frac{N^2}{k_{INP}}} \qquad \textbf{Eq.5- 10}$$

where β can be defined as the non-growth associated specific rate constant for PHB production whereas k_P and k_{INP} are the half saturation constant for PHB production based on glycerol and the inhibition constant based on nitrogen.

PHB production stops when the content inside the cell reaches around 80% of total biomass. Product inhibition has been reported in the literature as the phenomenon causing the cessation of polymer formation (Raje & Srivastava 1998). An inhibitory term that reduces the growth rate by a factor less than 1 if PHB is present was introduced to describe what is believed to be the regulatory mechanism used by the cells.

$$q_p = \frac{\beta \cdot Gly}{Gly + k_P + \frac{N^2}{k_{INP}}} \cdot \left(1 - \frac{PHB^n}{PHB^n + k_d}\right) \qquad \textbf{Eq. 5- 11}$$

where the integer exponent n would be the equivalent to a Hill coefficient and k_d the apparent dissociation constant (Pérez Rivero *et al.,* 2016).

Glycerol is consumed for product formation but also for the synthesis of nucleic acids and other cellular compounds via gluconeogenesis. Acetate, malate, formate or glucose are some of the intermediate metabolites that can be released when glycerol is used in the gluconeogenesis pathway (Tanadchangsaeng & Yu 2012). However, no significant concentrations of organic acids were detected in the experiments conducted with glycerol concentrations below 40 g/l. If high glycerol

concentrations were to be used, other products (organic acids) might have to be accounted for (*e.g.* malic, acetic acid). In any case, it is been shown in section Studies on the influence of glycerol concentration on PHB productionthat high glycerol concentrations are outside of desirable range of conditions for PHB production. Hence, glycerol consumption rate can be related simply and directly to the rate of cell production and product formation through the yields of associated biomass, $Y_{x_A/_{Gly}}$, and PHB based on glycerol, $Y_{PHB/_{Gly}}$:

$$q_{Gly} = \frac{1}{Y_{x_A/_{Gly}}} \cdot \mu_{x_A} + \frac{1}{Y_{PHB/_{Gly}}} \cdot q_p \qquad \textbf{Eq.5- 12}$$

Nitrogen, on the other hand, is considered to be used only for growth of associated biomass. Its consumption is described by Eq.5- 13:

$$q_N = \frac{1}{Y_{x_A/_N}} \cdot \mu_{x_A} \qquad \textbf{Eq.5- 13}$$

where $Y_{x_A/_N}$ is the yield of associated biomass based on nitrogen.

Using this preliminary formulation, the model could be tested against tailored experimental data. Based on the differences between model predictions and experimental outcomes, the model could then be readjusted to cover a wider range of experimental conditions for a set of fixed kinetic constants. Simulations of the experimental system serve to identify optimal initial conditions, including the often sought C/N ratio. Other variables such as fermentation time could also be assessed with the assistance of the model. Thus, the model was tested and further developed as described in the next chapter.

Chapter 6

Testing and developing the model for different modes of operation

6.1 Introduction

Fermentations are routinely conducted in small scale flasks for research purposes. However, industrial fermentation is carried out at a much larger scale and frequently involves intense mixing and forced aeration. The cultivation conditions can be thus quite different and hence so too the dynamics. This might lead to the need for different models to represent each scale.

In this chapter, attempts to use the preliminary model, developed for flask systems, presented in chapter 5 to predict the outcome of tailored experiments are reported. The first objective of this work was to obtain meaningful values for the kinetic constants. These were tested under different conditions and differences between predictions and empirical results were used to modify the model formulation and associated constants to make it a more robust representation of the real system. The next stage was to evaluate whether bioreactor performance is any different from flask fermentations with the objective of finally developing a model that can guide the bioreactor design.

6.2 Shake flask fermentation

6.2.1 Determination of kinetic constants

A single experiment to provide definitive data used to estimate the model parameters was performed using 20 g/l glycerol and 1 g/l ammonium sulphate. To do this, a stochastic optimization based on a Simulated Annealing (SA) algorithm coupled with a deterministic method that uses the 'fmincon' function in MATLAB was employed. The objective function for the optimisation was the minimum sum of squared errors between predicted and experimental values of the four state variables: associated biomass, PHB, glycerol and nitrogen. The addition of associated biomass and PHB concentration constitutes the total biomass concentration plotted in Figure 6-1.

The curves generated using the preliminary model for fermentation conducted with 20 g/l glycerol and 1 g/l ammonium sulphate appear to follow the data well and succed in predicting the dynamics and final values of substrates and products. The model, shown in Table 6-1 was tested for different initial concentrations, glycerol and ammonium sulphate, in order to investigate if the predictions would still be acceptable within the normal range of operational conditions.

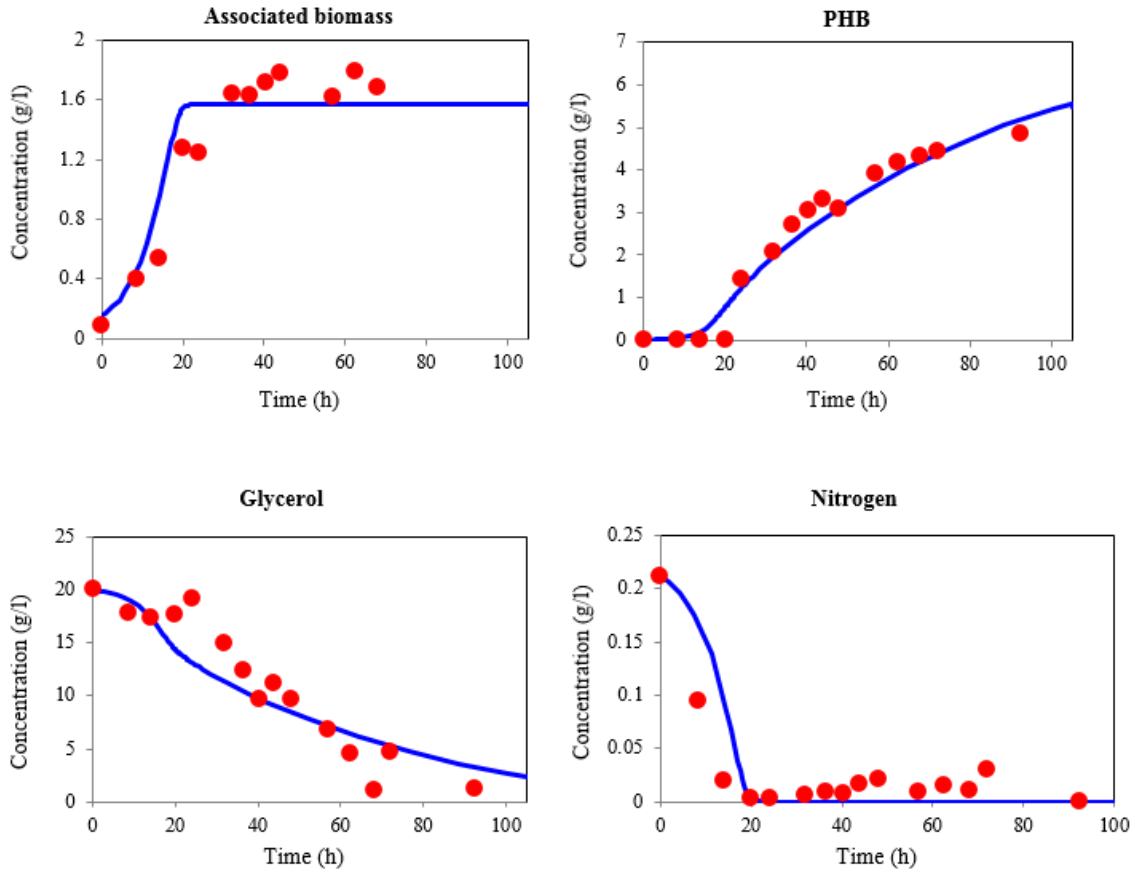

Figure 6-1: Predictions obtained from the preliminary model (lines) and experimental data (symbols) for a fermentation conducted with 20 g/l glycerol and 1 g/l ammonium sulphate by *C. necator* in shake flask.

Table 6-1: Equations and computed parameter values for the preliminary model for shake flask fermentation.

Associated biomass growth rate	$\frac{dx_A}{dt} = \mu_{x_A} \cdot x_A = \left(\frac{\mu_m \cdot N}{k_N + N} \cdot \frac{1}{1 + \frac{N}{k_{IN}}} \cdot \frac{Gly}{Gly \cdot \left(1 + \frac{Gly}{k_{IG}}\right) + k_G} \right) \cdot x_A$	$\mu_m = 0.25\ h^{-1}$ $k_N = 0.04\ g/l$ $k_{IN} = 0.08\ g/l$ $k_{IG} = 70.0\ g/l$ $k_G = 0.18\ g/l$
PHB production rate	$\frac{dP}{dt} = \mu_P \cdot x_A = \frac{\beta \cdot Gly}{Gly + k_P + \frac{N^2}{k_{INP}}} \cdot \left(1 - \frac{PHB^n}{PHB^n + k_d}\right) \cdot x_A$	$\beta = 0.125\ h^{-1}$ $k_P = 2.0\ g/l$ $k_{INP} = 0.0005 (g/l)^2$ $n = 1$ $k_d = 9$
Glycerol consumption rate	$-\frac{dGly}{dt} = \left(\frac{1}{Y_{x_A/Gly}} \cdot \mu_{x_A} + \frac{1}{Y_{PHB/Gly}} \cdot \mu_p \right) \cdot x_A$	$Y_{x_A/Gly} = 0.375\ g/g$ $Y_{PHB/Gly} = 0.4$ g/g
Nitrogen consumption rate	$-\frac{dN}{dt} = \frac{1}{Y_{x_A/N}} \cdot \mu_{x_A} \cdot x_A$	$Y_{x_A/N} = 6.7$ g/g

6.2.2 Model limitations

Fermentation at higher glycerol concentration (30 g/l) and different ammonium sulphate concentration (1, 2, 3 g/l) were simulated and then compared to the experimental results achieved for such conditions. Model prediction together experimental data are presented in Figure 6-2, Figure 6-3 and Figure 6-4.

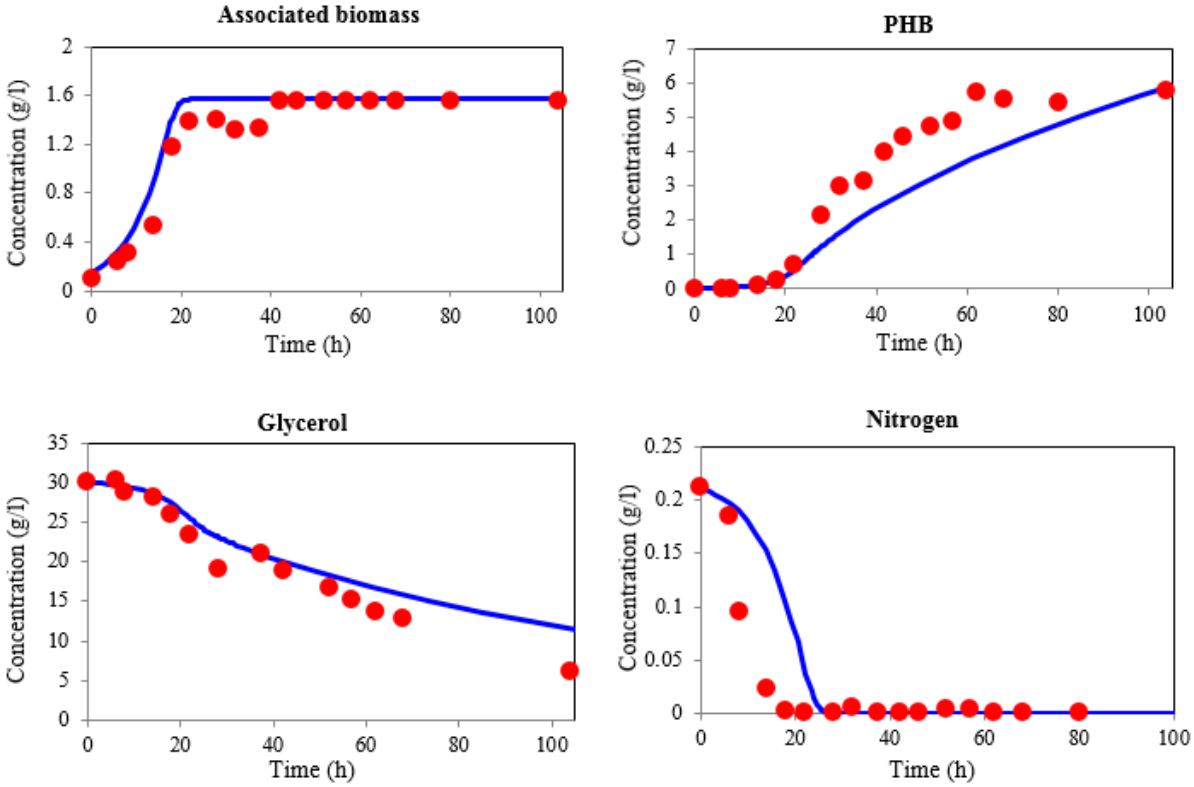

Figure 6-2: Predictions obtained from the preliminary model (lines) and experimental data (symbols) for a fermentation conducted with 30 g/l glycerol and 1 g/l ammonium sulphate by *C. necator* in shake flask.

The predictions obtained when the carbon source was increased (and the nitrogen concentration kept constant) are able to forecast the product concentrations by the end of fermentation, although discrepancies between the shape of the curve for PHB and the measurements can be noted. The simple stoichiometric basis for the model means that the under-prediction of PHB production by the model, from 30 to 90 h, is matched by an under-prediction of glycerol consumption.

For higher nitrogen concentrations, the model presented so far gives a poor description of the fermentation outcomes; see Figure 6-3 and Figure 6-4. PHB production would not stop during the first 120 h of fermentation according to the model, while the PHB measurement indicated that PHB reached a maximum at 46 h and started to decline after that. As result, the total biomass prediction is also very different from the experimental data for the latest hours of fermentation. Glycerol data fell below the model curve, which implies that more glycerol was consumed than is needed for PHB production.

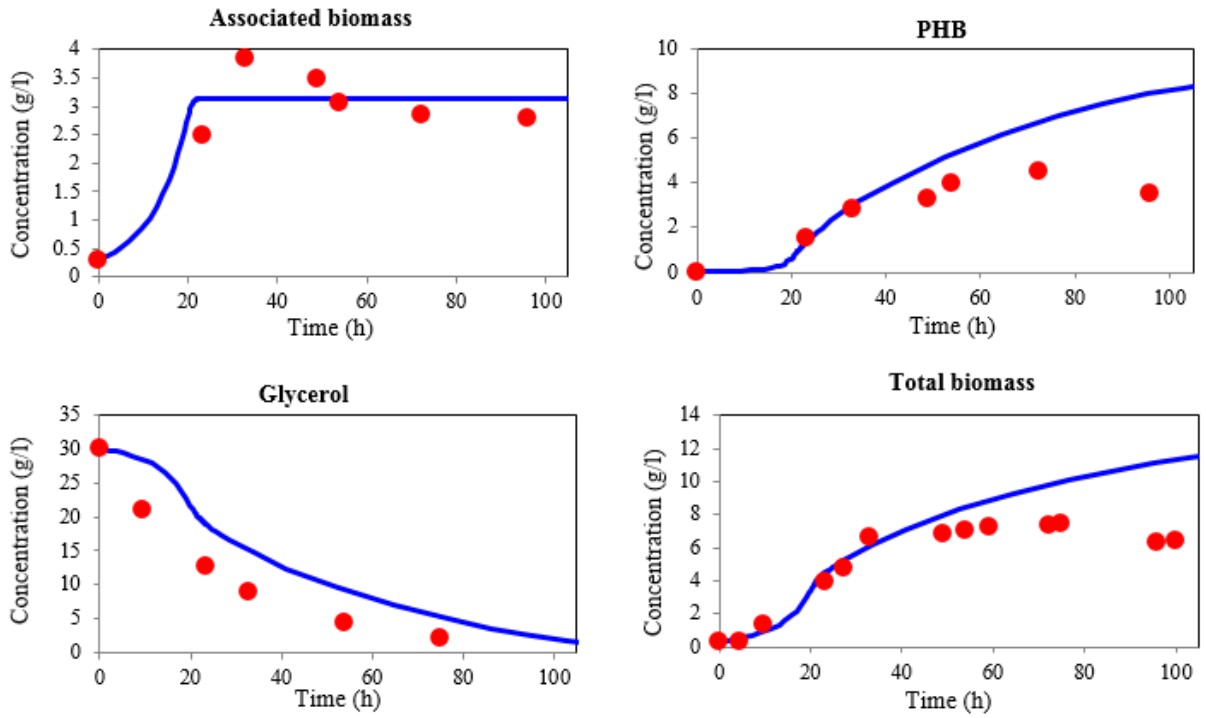

Figure 6-3: Predictions obtained from the preliminary model (lines) and experimental data (symbols) for a fermentation conducted with 30 g/l glycerol and 2 g/l ammonium sulphate by *C. necator* in shake flask.

In Figure 6-4 (3 g/l ammonium sulphate), both PHB and associated biomass are over-predicted. The yields of PHB and x_A are, under these circumstances, much lower than expected.

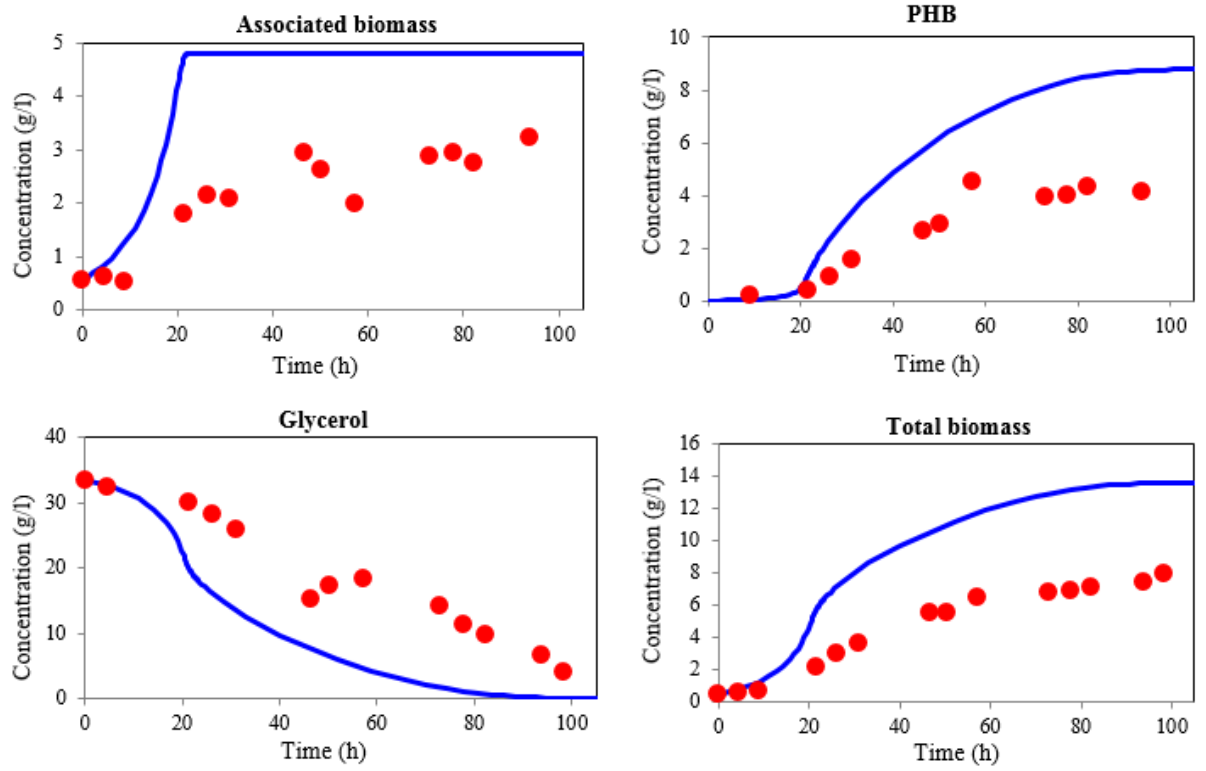

Figure 6-4: Predictions obtained from the preliminary model (lines) and experimental data (symbols) for a fermentation conducted with 30 g/l glycerol and 3 g/l ammonium sulphate by *C. necator* in shake flask.

6.2.3 Introducing the carrying capacity concept

The simulation over-predicts PHB production at higher initial nitrogen concentrations, since the theoretical PHB production does not stop until the carbon source is depleted. However, it is clear that in reality, other components, not accounted for in the model can become exhausted and therefore limit production.

PHB production rate is proportional to the amount of associated biomass and, hence, the amount of PHB that can be formed is limited by the amount of cells. Several studies in the literature have suggested a self-inhibition mechanism that affects growth rate and this has been included in their equations for describing cell growth rate with different formulations, *e.g.* a cell density inhibition coefficient (Tsoularis & Wallace 2002; Mozumder *et al.*, 2014). However, these models in addition to the preliminary model presented earlier, still neglect the effects of PHB on cellular growth. It is only when growth and PHB production are expressed as functions of both compounds that a regulatory effect appears. This can be taken into account through the addition of a term with both variables included, which provides a factor between 0 and 1 to reduce the rates of both growth and PHB formation, as shown in Table 6-2.

Table 6-2: Equations and computed parameter values for the reformulated model for shake flask fermentation.

Associated biomass growth rate	$\frac{dx_A}{dt} = \frac{\mu_m N}{k_N + N} \cdot \frac{1}{1 + \frac{N}{k_{IN}}} \cdot \frac{Gly}{Gly \cdot \left(1 + \frac{Gly}{k_{IG}}\right) + k_G} \cdot x_A \cdot \left(1 - \frac{x_A + PHB}{K_x}\right)$	$\mu_m = 0.35\ h^{-1}$ $k_N = 0.01\ g/l$ $k_{IN} = 0.27\ g/l$ $k_{IG} = 1.05\ g/l$ $k_G = 86.31\ g/l$ $K_x = 8\ g/$l
PHB production rate	$\frac{dPHB}{dt} = \frac{\beta \cdot Gly}{Gly + k_P + \frac{N^2}{k_{INP}}} \cdot x_A \cdot \left(1 - \frac{x_A + PHB}{K_x}\right)$	$\beta = 0.14\ h^{-1}$ $k_P = 0.01\ g/l$ $k_{INP} = 0.001\left(\frac{g}{l}\right)^2$
Glycerol consumption rate	$-\frac{dGly}{dt} = \left(\frac{1}{Y_{x_A/Gly}} \cdot \mu_{x_A} + \frac{1}{Y_{PHB/Gly}} \cdot \mu_p\right) \cdot x_A \cdot \left(1 - \frac{x_A + PHB}{K_x}\right)$	$Y_{x_A/Gly} = 0.35\ g/g$ $Y_{PHB/Gly} = 0.29\ g/g$
Nitrogen consumption rate	$-\frac{dN}{dt} = \frac{1}{Y_{x_A/N}} \cdot \mu_{x_A} \cdot x_A$	$Y_{x_A/N} = 6.00\ g/g$

In this closed system, where nutrients are limited, cell growth and PHB formation compete for some of the same elements. Thus, both affect the rate at which the other occurs, creating a trade-off between cell proliferation and PHB formation. It is worth noting that no other inhibition term needs to be added to the differential equation for PHB, since its own concentration slows down the production rate. The extent to which this occurs is governed by a property of the system that can be defined as its carrying capacity, K_x.

K_x is the upper threshold on growth size for a specific system under certain environmental conditions (Tsoularis & Wallace 2002). In this case, it is a function of the initial composition in the fermenter including inoculum concentration and operational factors such as agitation, which in turn influence dissolved oxygen. The carrying capacity represents the maximum biomass concentration that can be reached. The function of the term added to the differential equations of growth and PHB formation is to reduce the production rate as the system gets close to that upper bound. Although this parameter can be obtained from a given set of data, work needs to be done in order to estimate K_x even when no experimental values are available, *i.e.* before conducting any fermentation.

The final model is formed by the four differential equations corresponding to associated cell matter, PHB, glycerol and ammonium sulphate (see Table 6-2) containing 12 parameters, one less than in the previous version of the model. As previously described, the model parameters were estimated using experimental data corresponding to a representative fermentation conducted with 20 g/l glycerol and 1 g/l ammonium sulphate. Parameter values, estimated using the same methodology described earlier and, once obtained, they were treated as fixed constants for the *C. necator*-glycerol system.

The updated model is able to describe qualitative and quantitative biomass production and PHB formation, which indicates that an accurate distinction between cell biomass and intracellular product has been accomplished. The substrate consumptions can also be predicted throughout the fermentation with little deviation from the experimental data as seen in Figure 6-5. It is important to note that the quality of the model predictions has been improved without increasing the degrees of freedom, *i.e.* number of parameters.

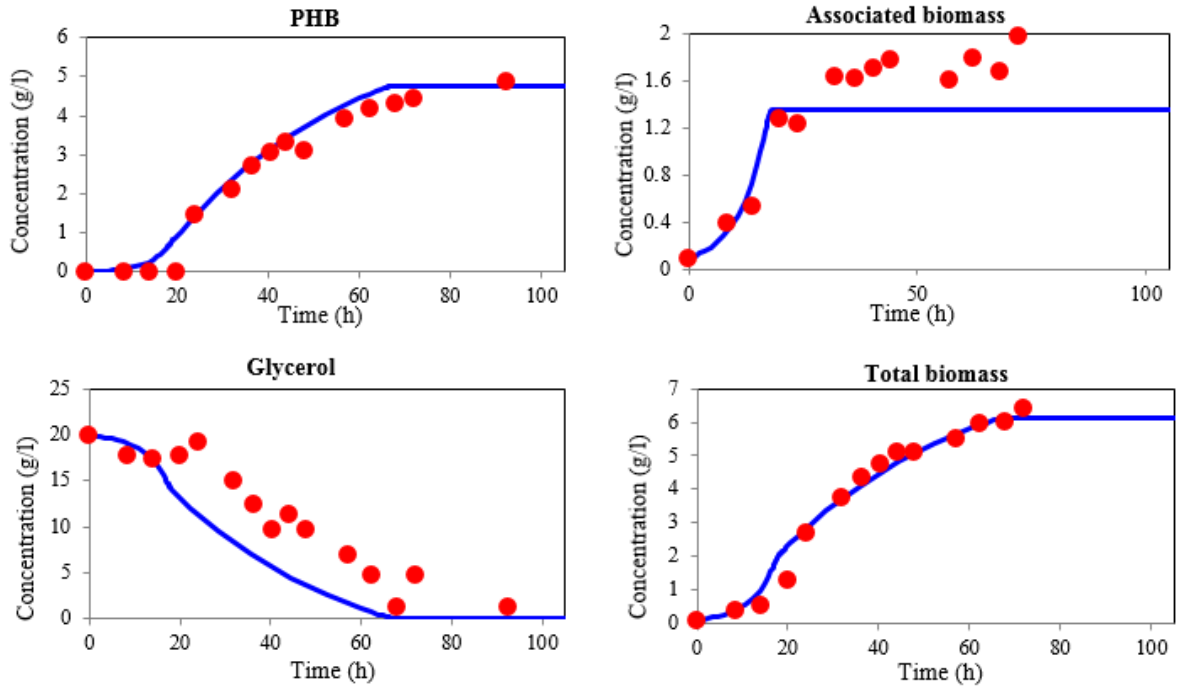

Figure 6-5: Predictions obtained from the updated model (lines) and experimental data (symbols) for a fermentation conducted with 20 g/l glycerol and 1 g/l ammonium sulphate by *C. necator* in shake flask.

6.2.4 Model evaluation

To tests the robustness of the model and the applicability of the constants listed in Table 6-2, simulations of fermentations carried out with different amounts of carbon and nitrogen were run, in the same way as previously. Results are contrasted to experimental data and presented in Figure 6-5 and Figure 6-6. By introducing the carrying capacity in the model formulation, it appears that more realistic yields for PHB and associated biomass are obtained.

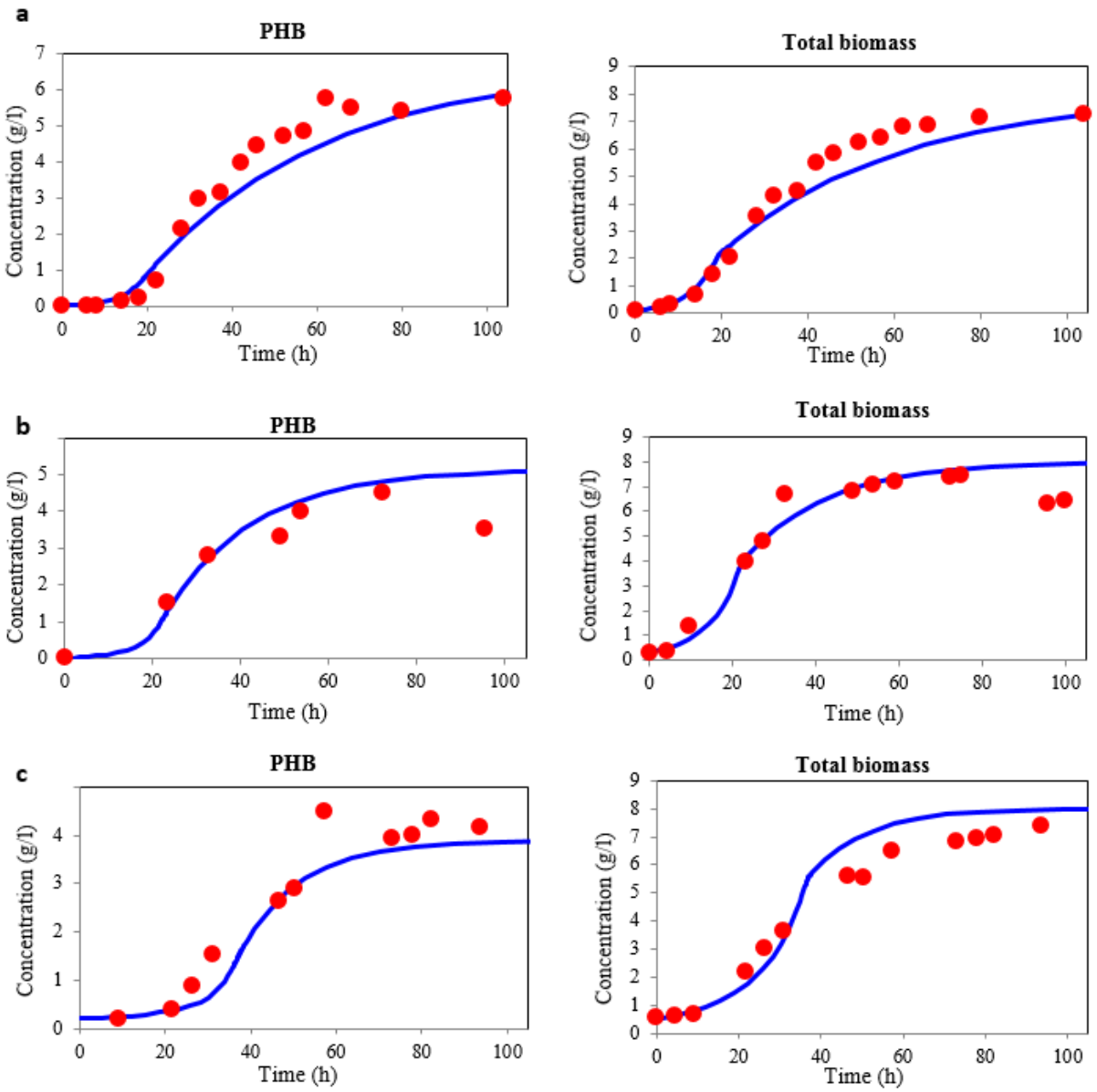

Figure 6-6: PHB and total biomass experimental data (symbols) along with predictions (lines) obtained with the updated model for glycerol fermentations by *C. necator* in shake flaks and for different conditions: (a) 20 g/l glycerol, 1 g/l ammonium sulphate; (b) 30 g/l glycerol, 2 g/l ammonium sulphate; (c) 30 g/l glycerol, 3 g/l ammonium sulphate.

Whenever glycerol is increased and nitrogen keep constant, an increase in PHB production is seen, both in theoretical and empirical results. Associated biomass remains constant as it is mainly governed by the nitrogen source. On the other hand, as the supply of nitrogen is increased but glycerol is maintained constant, associated biomass rises to a maximum level of 3 g/l (inhibition) and PHB

concentration suffers a significant decrease to 3.8 g/l; the difference between this and the model prediction (4.15 g/l) is less than 10%. Through this formulation, production may stop, even if where there is still glycerol present in the medium, so the production curves tend to reach a constant value and concentration does not keep increasing as was the case in the preliminary version of the model. PHB degradation seemed to happen for fermentations conducted with 30 g/l glycerol and 2 g/l ammonium sulphate. This may have been because the glycerol was rapidly consumed for the production of the PHB and associated biomass.

The blue bar in Figure 6-7 represents total biomass and reaches its maximum concentration (K_x) when using between 2 and 4 g/ ammonium sulphate according to the updated model. PHB decreases as nitrogen increases as expected (except from very low nitrogen concentration when the low growth and resulting low x_A can justify the low production). Final associated biomass concentration, on the other hand, increases as more nitrogen is present until the inhibitory effect becomes important (> 4 g/l ammonium sulphate).

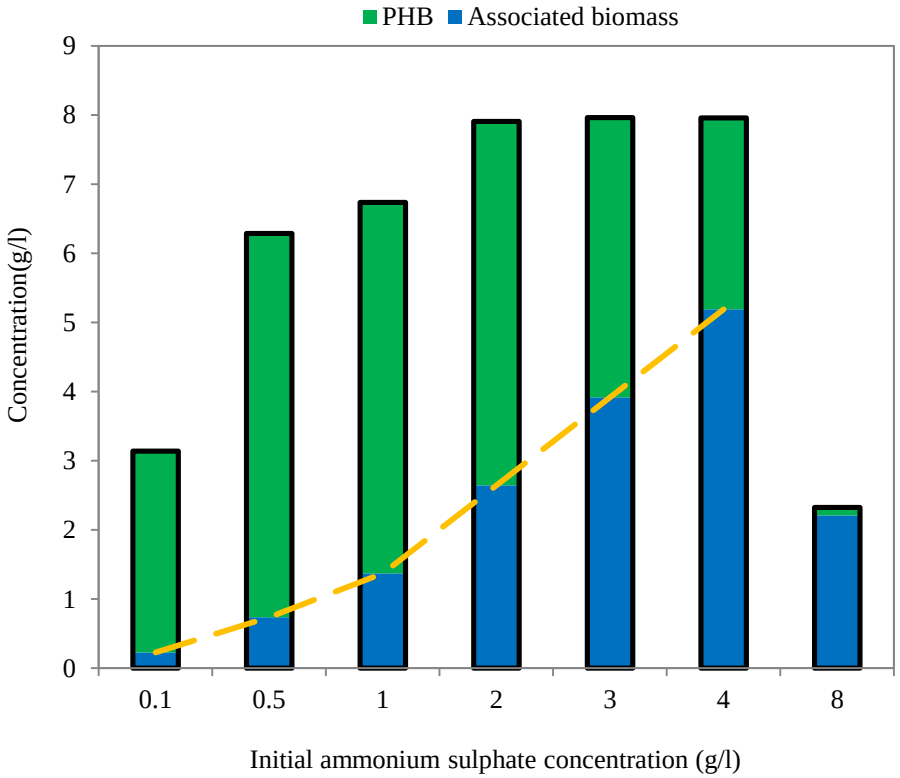

Figure 6-7: Values at 120 hours of associated biomass, PHB and total biomass according to the model simulations for shake flask glycerol fermentation by *C. necator* under different nitrogen concentrations and 30 g/l glycerol.

The kinetic constants shown previously are applicable to PHB formation by *C. necator* when using glycerol as sole carbon source and ammonium sulphate as nitrogen source. They were maintained constant for all the simulations performed to test the model performance and degree of fulfillment under different conditions where the biopolymer can be synthesized. The maximum specific growth

rate reported is higher than the one observed from experimental data due to the fact that the model involves double substrate expression with inhibition terms, but it is actually close to the maximum growth rate for *C. necator* reported in literature, 0.33 h^{-1} (Grousseau *et al.,* 2013). The inhibition constants, k_{IN} and k_{IG} reflect the maximum concentrations that can be used before those compounds become inhibitory. The values of the constants used in the expression for PHB production could be subject to small changes in cases where PHB production associated with growth is not negligible. In this case, PHB accumulation started when nitrogen was almost depleted, which explains the low value of k_{INP}. The carrying capacity, matches the overall concentration obtained experimentally but it is recognized that it may change with bioreactor type and conditions. It is possible to predict the steady state concentration of associated biomass using the given yield of x_A based on nitrogen. However, nitrogen consumption occurs faster than the model predicts, suggesting that this nutrient is used for purposes other than just growth, *e.g.* cell maintenance.

Since the calculation of constants is based on just one experiment, it is important to start with a sensible range for the constants (based on experience), otherwise, values such as those for inhibitory terms would not be significant if obtained in conditions where no inhibition occurs. In this way, these values can be subject to improvement, if more data are available or better ranges for the kinetic constants are predefined. Those are practical values that work on the model under the conditions that have been tested but they may not be the true values. The more data available, the more they can refined to approach the true values.

6.2.5 Exploring the behavior of the system through model-based simulations

The model was also used predictively in order to evaluate the effect of carbon and nitrogen over a wider range of situations than those which could be practically conducted. Maximum product concentration and specific growth rate were two of the variables considered as having a critical impact on the fermentation feasibility. Figure 6-8 shows the maximum concentration of PHB that can be achieved (in the laboratory system) as a function of the two main media components. It is easy to identify those combinations of concentration which promote a higher production and those that do the opposite. The proposed competition effect becomes clear when looking at that region of very high nitrogen concentration. Also, it is important to emphasize that excess glycerol above 60 g/l does not lead to higher PHB accumulation and should be avoided in order not to have unused substrate remaining or undesirable secondary products. The same ratio of carbon to nitrogen can be achieved with numerous combinations and hence, the impact on fermentation outcomes may be expected to differ with different combinations. The effect of carbon and nitrogen are not linearly related.

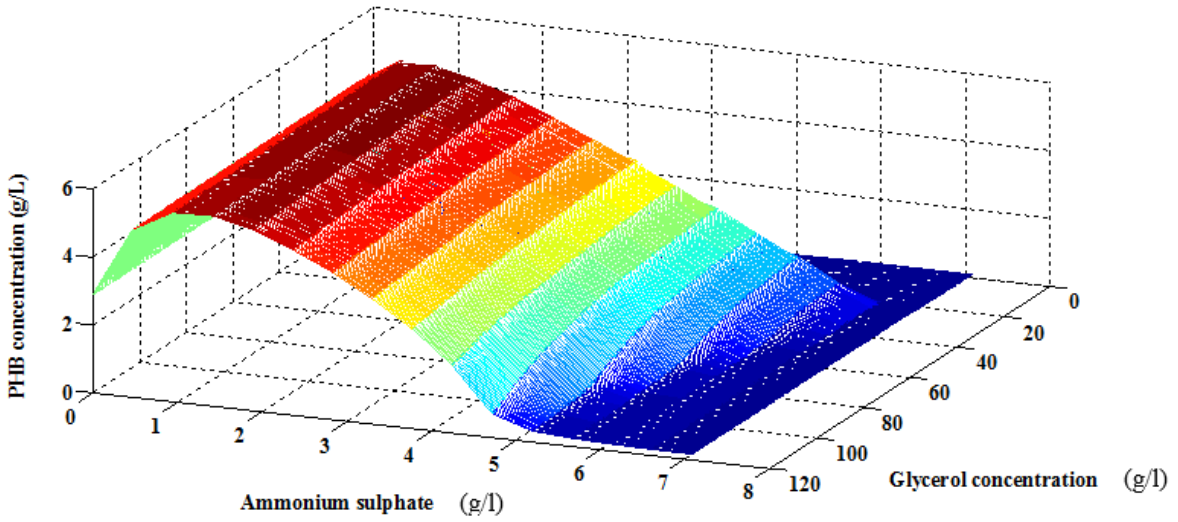

Figure 6-8: Contour plot of the maximum PHB concentration achievable as a function of the initial nitrogen and carbon concentrations, predicted using the updated model.

Specific growth rate is a key factor to ensure good productivities in batch fermenters but also of utmost importance in continuous fermentations where it determines the maximum dilution rate (minimum residence time) that can be used without risking biomass wash-out. The heterologous substrate concept assumes that growth rate can be affected simultaneously by more than one substrate, exactly as happens for this system (Okpokwasili & Nweke 2005) and thus the interest in studying them simultaneously. The initial conditions that should be used to ensure a high specific growth rate or those substrate and nutrient concentrations to be maintained in the reactor in a flow system can be readily predicted through Figure 6-8 plots, such as the one shown in Figure 6-9.

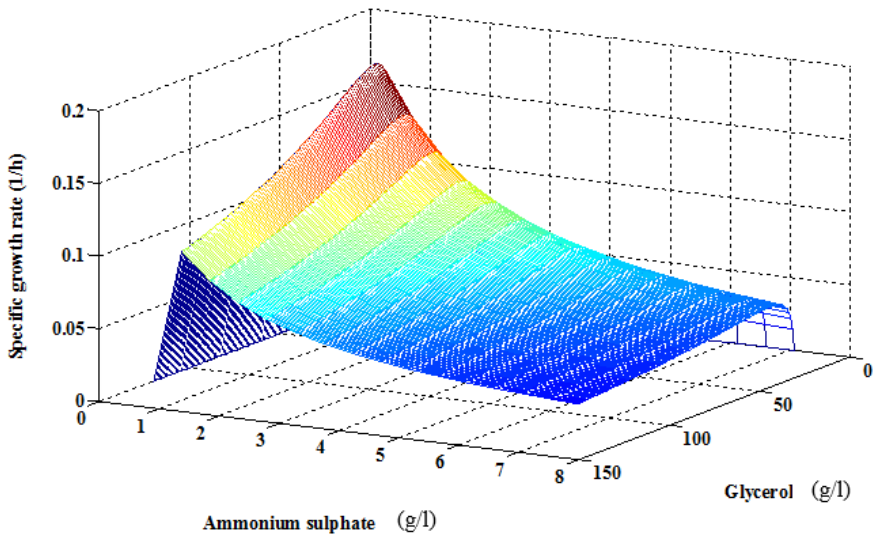

Figure 6-9: Contour plot of predicted specific growth rate for *C. necator* as a function of the nitrogen and carbon concentrations in the fermentation broth.

The model can also be used to asses other type of optimization problems, for example, to evaluate suitable end times for a batch fermentation. For this, it is necessary to first specify the criteria to define a suitable end point, *e.g.* maximum product concentration, maximum productivity, maximum consumptions of substrate. As shown in Figure 6-10, PHB production rate is slow during the very early stages of fermentation but it quickly rises following a sigmoidal trend, so that, the increase in PHB concentration is small towards the end. Thereby, after a certain period of time, a very small increase in PHB concentration is achieved at the expenses of continued operation. The product concentration over time (productivity) reaches its maximum when PHB concentration is only half of the value at the end of the fermentation (see dotted line in Figure 6-10). However, the product of productivity and concentration shows a maximum much closer to the final achievable PHB concentration and might therefore be a more sensible indicator of when to stop the process (see dashed line).

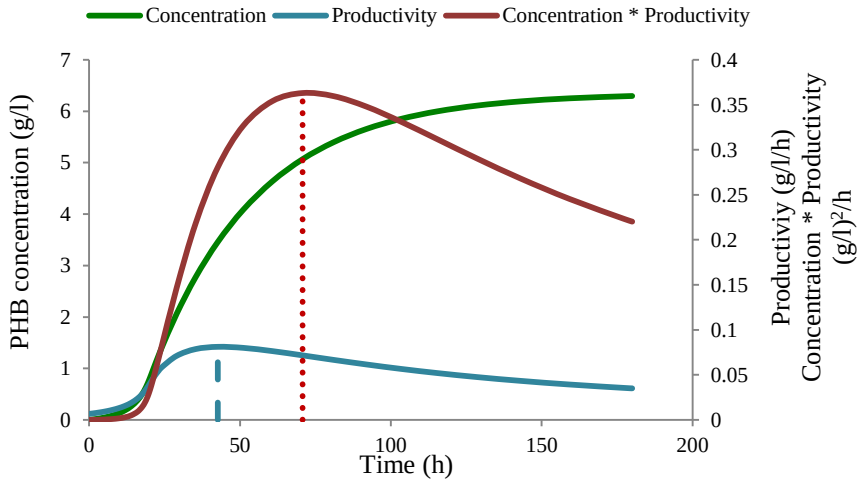

Figure 6-10: Simulations of PHB production during glycerol fermentation by *C. necator* started with x_A=0.15 g/l, AS=0,25 g/l, Gly=30 g/l.

Optimization of the system´s performance can be attempted by maximizing different functions. The results for maximum PHB concentration and maximum total biomass concentration (TB) are summarized in Table 6-3. The different initial conditions reflect the trade between growth and PHB production when higher concentrations of nitrogen are present. This can be seen in the 3D Figure 6-8.

Table 6-3: Optimization results performed at different objective functions: maximization of PHB and total biomass.

Variable (g/l)	Max PHB	Max TB
N_o	0.17	0.40
Gly	28.00	33.62
PHB	6.60	5.44
x_A	1.16	2.55

The above analysis helps us with the design of a batch bioreactor system but ultimately, the model could be used for control purposes, *i.e.*, to compare measured and predicted values and adapt conditions accordingly. As an example, if glycerol concentration, based on a measurement, was predicted by the model to be depleted in 5 hours, an addition of it could be planned within that timeframe. This in an example of predictive control as illustrated in Figure 6-11:

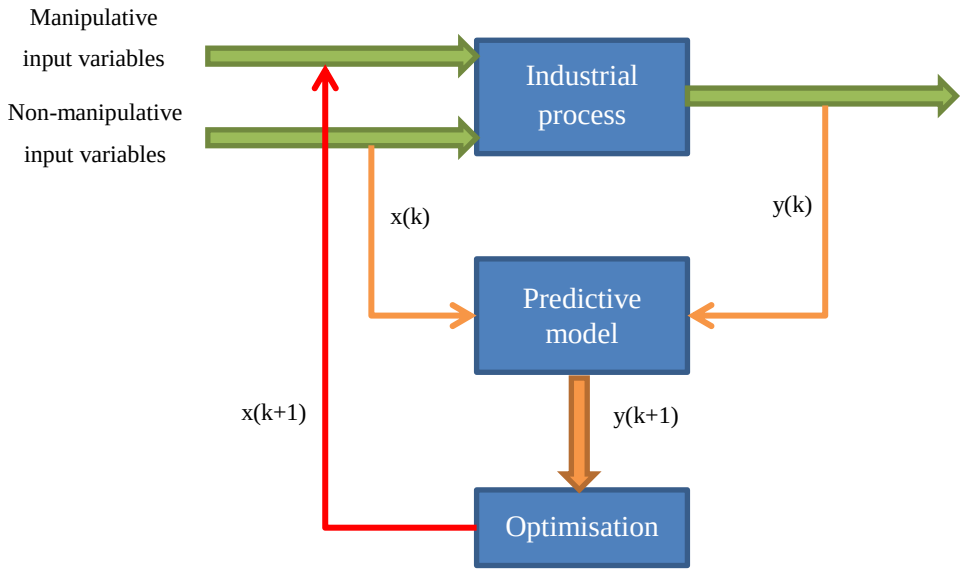

Figure 6-11: Schematic representation of model predictive control applied to a generic industrial process.

To realize such a predictive control application of the model, it must first be tested in a bioreactor where control systems could potentially be implemented. The next section presents the computational and experimental studies performed in a bioreactor, aimed at improving performance metrics (PHB concentration and/or productivity) and also investigating mode of operation.

6.3 Bioreactor studies

The potential applications of this type of modelling have been shown in flask studies. However, bioreactors provide a very different environment from flasks and also potentially enable different modes of operation and control systems to be tested. The differences between fermentations conducted in flasks and bioreactors are therefore considered below in order to refine the model and also to identify those aspects that have a major impact on the fermentation. To investigate the extent of the differences between the two systems, an experiment that could be comparable to those conducted in flask was carried out in a bioreactor. The fermentation profiles are shown in Figure 6-12. Conditions, within the optimal range, determined for shake flasks where tested in a 2 l bench-top reactor, where aeration gas was added through a diffuser.

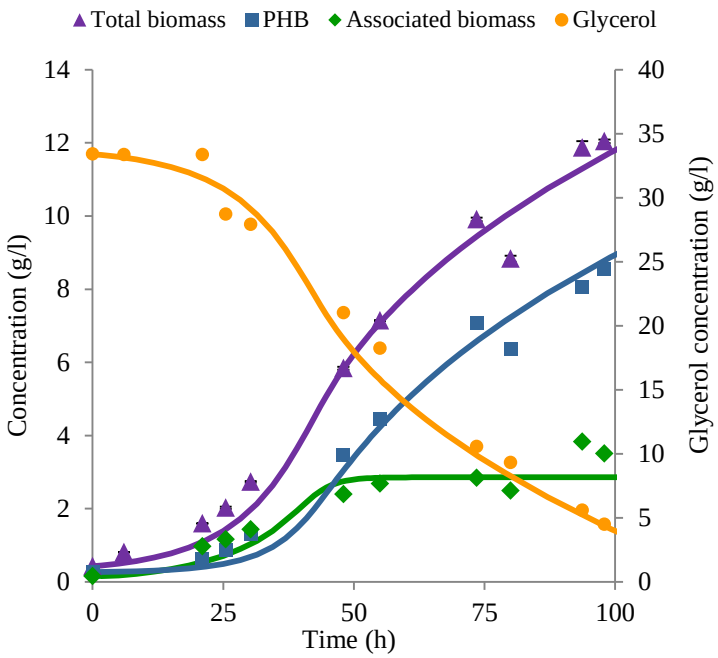

Figure 6-12: Model results from the bioreactor model (lines) and experimental data (symbols) for a batch glycerol fermentation by *C. necator* conducted in bench-top reactor. Experimental results served to estimate the model parameters.

Significantly higher total biomass was achieved in this case when compared to data previously presented. Total biomass, of which 70 % was PHB, reached more than 12 g/l by the 100th hour of fermentation. Although the shapes of the curves for substrate and product concentrations were reasonably similar (*e.g.* growth entered a stationary phase when nitrogen had been depleted and the PHB curve started to flatten as glycerol was almost exhausted), in order for the model to fit reasonably, the carrying capacity calculated for the flask experiment (8 g/l) would clearly need to be different. The higher total biomass achieved in the bioreactor suggests a higher value of K_x

The carrying capacity constant has been removed from the modified version of the model and another constant, with an easier determination value, was introduced in the differential equation for PHB. P^{max} represents the maximum content that total biomass can accumulate and relates to the fact that PHB synthesis can be inhibited by increasing intracellular mass fraction of PHB (steric disturbing effect). By doing so, a term that regulates PHB productions, as the Hill coefficients used in the preliminary model, has been introduced and reduces degrees of freedom (n and k_d were previously necessary) and brings more realistic physical meaning. All the rest, remains the same, see Table 6-4. Kinetic constants were calculates as explained in section 6.2.1 with the experimental results shown in Figure 6-12.

Table 6-4: Equations and computed parameter values for the model adapted to fermentations conducted in bioreactor.

Associated biomass growth rate	$\frac{dx_A}{dt} = \frac{\mu_m N}{k_N + N} \cdot \frac{1}{1 + \frac{N}{k_{IN}}} \cdot \frac{Gly}{Gly \cdot \left(1 + \frac{Gly}{k_{IG}}\right) + k_G} \cdot x_A$	$\mu_m = 0.35\ h^{-1}$ $k_N = 0.2\ g/l$ $k_{IN} = 0.7\ g/l$ $k_{IG} = 40\ g/l$ $k_G = 10\ g/l$
PHB production rate	$\frac{dPHB}{dt} = \frac{\beta \cdot Gly}{Gly + k_P + \frac{N^2}{k_{INP}}} \cdot x_A \cdot \left(1 - \frac{PHB}{(x_A + PHB) \cdot P^{max}}\right)$	$\beta = 0.15\ h^{-1}$ $k_P = 0.10\ g/l$ $k_{INP} = 0.001 \left(\frac{g}{l}\right)^2$ $P^{max} = 0.9$
Glycerol consumption rate	$-\frac{dGly}{dt} = \left(\frac{1}{Y_{x_A/Gly}} \cdot \mu_{x_A} + \frac{1}{Y_{PHB/Gly}} \cdot \mu_p\right) \cdot x_A$	$Y_{x_A/Gly} = 0.35\ g/g$ $Y_{PHB/Gly} = 0.40\ g/g$
Nitrogen consumption rate	$-\frac{dN}{dt} = \frac{1}{Y_{x_A/N}} \cdot \mu_{x_A} \cdot x_A$	$Y_{x_A/N} = 7.5\ g/g$

6.3.1 Sensitivity analysis

A sensitivity analysis was performed in order to investigate which kinetic parameters had a greater influence on an objective function. The chosen function was the sum of squared differences between predicted and experimental values for a set of experiments. Each parameter was varied by a 5% of its initial value while the other parameters remained constant and the objective function was then calculated. The evaluation of the degree of change was represented as the relative sensitivity, which is the % of increase in the objective function, and is represented in Figure 6-13.

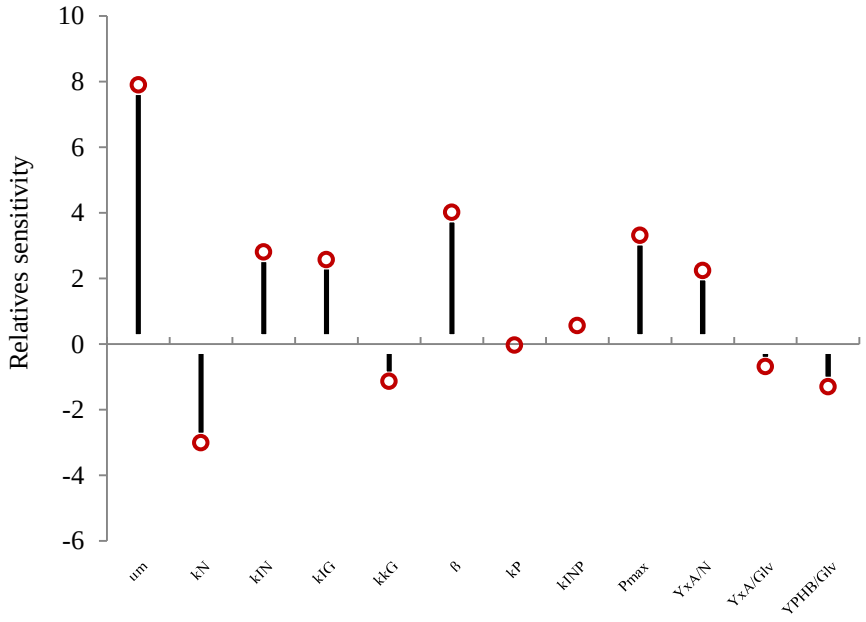

Figure 6-13: Sensitivity analysis on the objective function by 5% variation around the stated value for the kinetic parameters.

It can be seen from Figure 6-13 that the biggest impact on the function is caused by changing μ_m, β and P^{max}. Also, altering the values of $k_{N,}$ k_{IN}, k_{IG}, and $Y_{x_{A/N}}$ induced to an increase in the function between 2.5 and 3.5%. Very small changes are observed when varying k_G, k_P, k_{INP}, $Y_{x_{A/Gly}}$ and $Y_{PHB/Gly}$.

6.3.2 Studies on the mode of operation

Ammonium sulphate and glycerol are inhibitory compounds for growth and PHB formation when exceeding certain concentrations. Also, as seen in Chapter 5, nutrients can be 'wasted' when converted to products different to those of interest. Fed-batch configuration can overcome these problems by supplying the nutrients over the course of the fermentation, at appropriate times. For example a pulse of nutrients can be added when initial nutrients have been exhausted and this can be repeated several or many times. Alternatively, a continuous feed can be started at a strategic time and maintained at either a constant rate or other, variable rate, as appropriate. Combinations can also be envisaged, where nutrients are supplied separately and in the manner most appropriate to each.

Clearly, there are many options for operation in fed-batch mode. Several such fed-batch scenarios have been simulated and then tested experimentally in order to evaluate how well the model could predict different modes of operation and which had greater potential for PHB production.

The first attempt, with the objective to increase PHB production, was done by injecting both nutrients (glycerol and ammonium sulphate) before the initial glycerol had been completely consumed. The addition of glycerol was targeted to provide a non-limiting source of carbon that would allow a continued production of PHB at high rate whereas the supply of nitrogen would, in principle, ensure sustained residual growth (Grousseau *et al.*, 2013).

The model predictions, represented by lines in Figure 6-14, were obtained by running the model with the appropriate initial conditions from 0 to the time of injection. For subsequent hours, the model was run with the final concentrations from the first part used as initial values and including the addition of nutrients in the respective variables. As observed from the figure, the simulations show an increase in PHB and associated biomass starting just after the injection. As a result, total biomass underwent a significant increase with respect to the batch phase. The glycerol provided at the moment of injection was rapidly consumed according to the model, and determined the moment PHB and total biomass entered stationary phase. Nitrogen seemed to be rapidly assimilated given the short transition phase between the x_A levels before and after the injection.

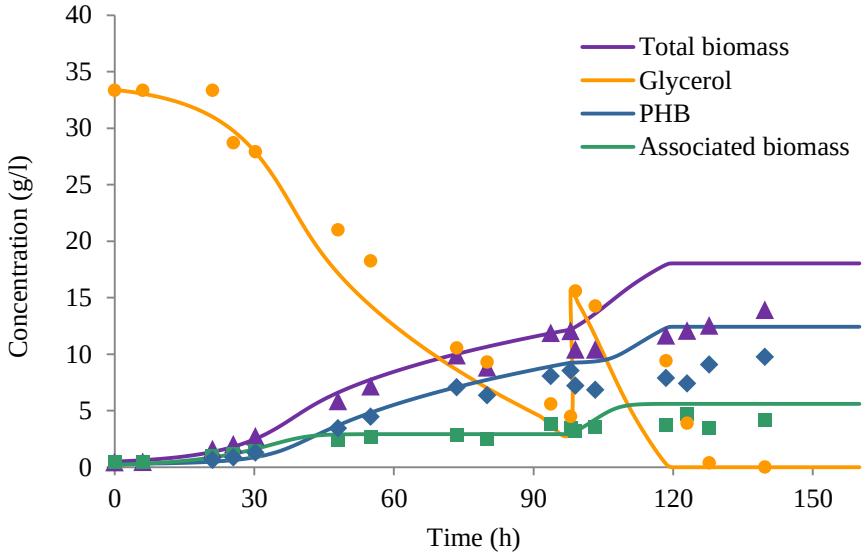

Figure 6-14: Model predictions (lines) and experimental results (symbols) for a glycerol fermentation by *C. necator* in which a pulse of nutrients was added just prior to the 100th hour of culture in bioreactor.

Compared to the simulations, the experimental results, represented as data points in Figure 6-14, showed a good similarity for glycerol consumption, albeit after an apparent adaptation period. PHB and total biomass concentration, on the other hand, decreased shortly after the injection. The reason for this decrease is uncertain; dilution effects have been accounted for in the data treatment and were not the cause. It is more likely that the optical density conversion into concentration measurements (total biomass and PHB, which is calculated as a percentage of the first) is unreliable during the sudden changes associated with the injection. Changes in the media composition and/or chemical reactions between components may result in changes to the turbidity, and thereby to misleading values on conversion to concentration.

After the slight decrease, PHB resumed production and although the data points all fall below the model line, the experimental overall increase in PHB after injection (2.9 g/l) was not far from the predicted increase (3.1 g/l). Associated biomass concentration increased after the injection but it oscillated and always stayed below predicted values after the disturbance. The fact that cellular death might have occurred could explain that the addition of nitrogen did not lead to a population increase as would be expected. Total biomass, the sum of PHB and associated biomass, which were both overpredicted, was indeed much lower than what had been simulated and did not reach a constant value as the model suggested. The reason behind this could be that glycerol consumption was not as prompt as anticipated. Hence, there is residual glycerol until almost 130 h. In other words, it would take more time for the concentration to reach stationary state than 120 h, which was the time when lines become horizontal in the figure.

A very late injection may not result in the benefits foreseen if nutrients become scarce before the injection occurs; in practice, some irreversible deterioration may have already occurred in the culture. The history

of the fermentation and its consequences on the physiological condition of cells is not considered in the model. In any case, time of injection is clearly an important parameter in the fed-batch system and further simulation studies were conducted in order to investigate its impact and determine a suitable value. As previously described, fermentations conducted with an injection of nutrients were simulated with the only difference being that the injections were made at different times. Results are shown in Figure 6-15:

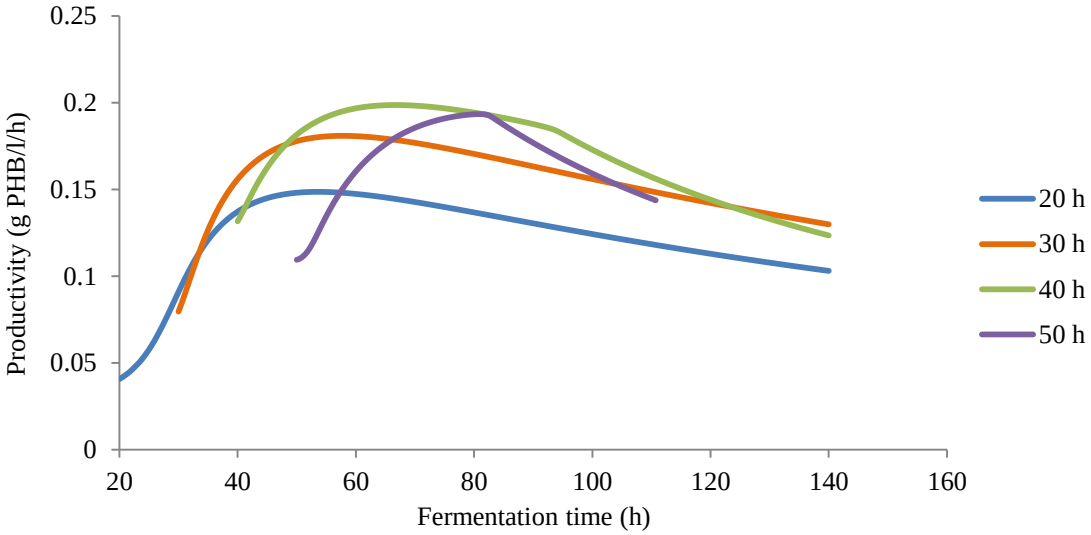

Figure 6-15: Simulations of glycerol fermentations by *C. necator* in which an injection of glycerol was done at different times.

As observed in the graph, the lowest productivities correspond to the fermentations in which the injections were made earliest. These early injections (20, 30 h) might have led to glycerol accumulation exceeding the inhibitory concentration, *i.e.*, a concentration that negatively affected specific growth rate. Injection at 40 and 50 h reached similar high values of productivity. However, from 50 to 110 h, the area below the 40 h line shows that 11.22 g of PHB were produced per litre of reactor compared to 10.07 g PHB for the 50 h line. Thereby, for a fermentation conducted under the same conditions as those simulated, the optimal injection time was 40 h.

In terms of composition, the effect of injecting nitrogen together with glycerol was also evaluated as a means of generating high density cultures. Two different flow rates and a single injection for the feeding of nitrogen were compared. The amount of nitrogen provided through the injection was calculated to be the same as that supplied in the simulation with one of the steady feeding regimes (including also the initial nitrogen). The predicted fermentation profiles are shown in Figure 6-16:

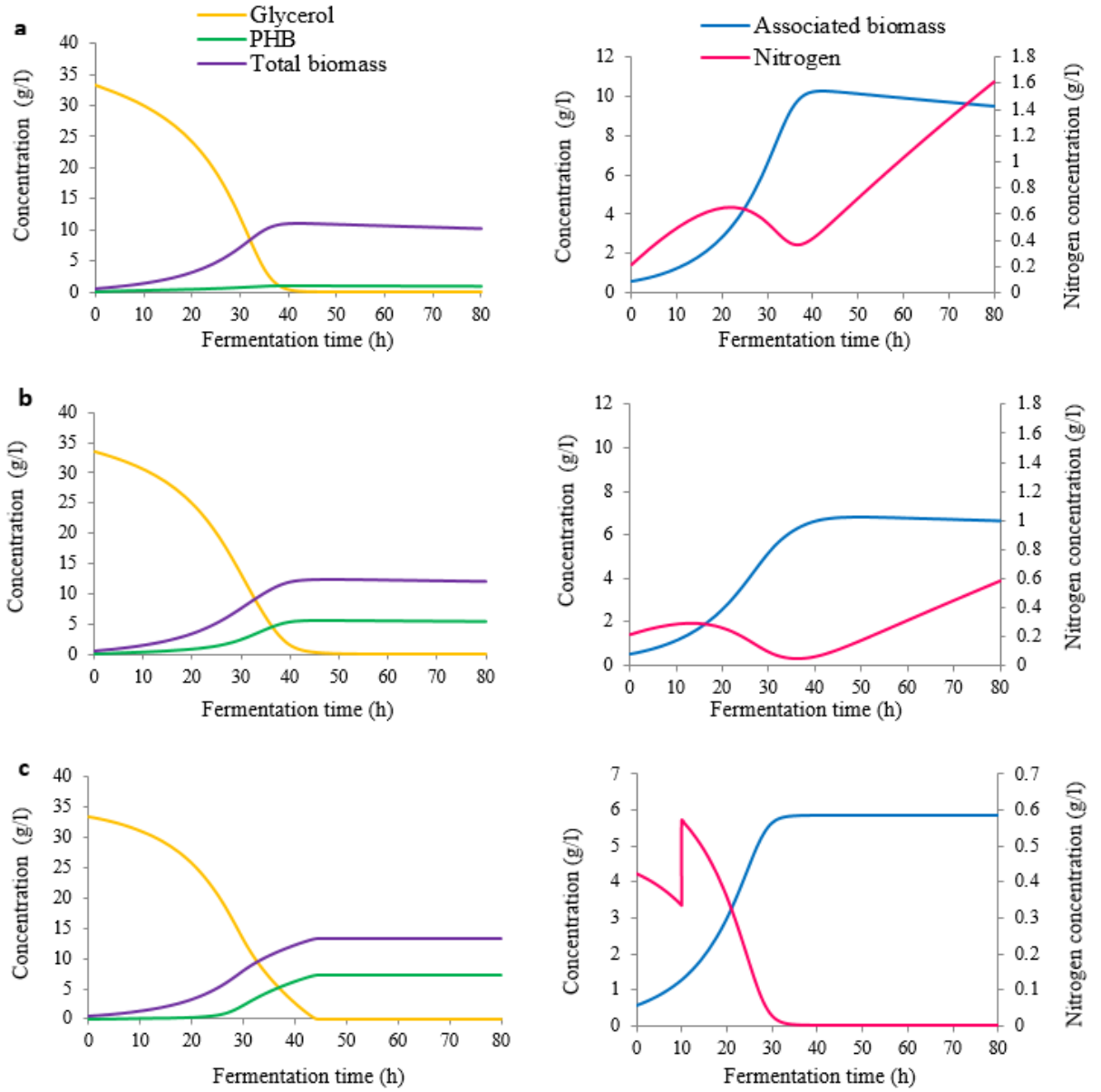

Figure 6-16: Simulations of glycerol fermentations by *C. necator* conducted with different feeding strategies for the nitrogen: (a) nitrogen feeding at a flow rate of 0.0025 l/h; (b) nitrogen feeding at a flow rate of 0.001 l/h; (c) single pulse of nitrogen.

For the flow rate of 0.0025 l/h (Figure 6-14 a), nitrogen was predicted to accumulate, blocking the synthesis of PHB. With the lower flow rate, 0.001 l/h (Figure 6-14 b), the accumulation of nitrogen was less significant and PHB was produced. However, comparing the fermentation for the lower flow rate with that of the injection, it can be observed that more associated biomass could be produced in the first case, and this resulted in less PHB synthesized for the limited amount of carbon available. Although it looks like the injection has no effect on the rest of variables, without it less associated biomass and lower specific growth rate during a certain period of time would result. Figure 6-17 shows the summarized results. It is apparent that either a very low flow rate of nitrogen or the injection would be the most

sensible methods for supplying additional nitrogen. Of these two, an injection is the most practical way to do it in the laboratory.

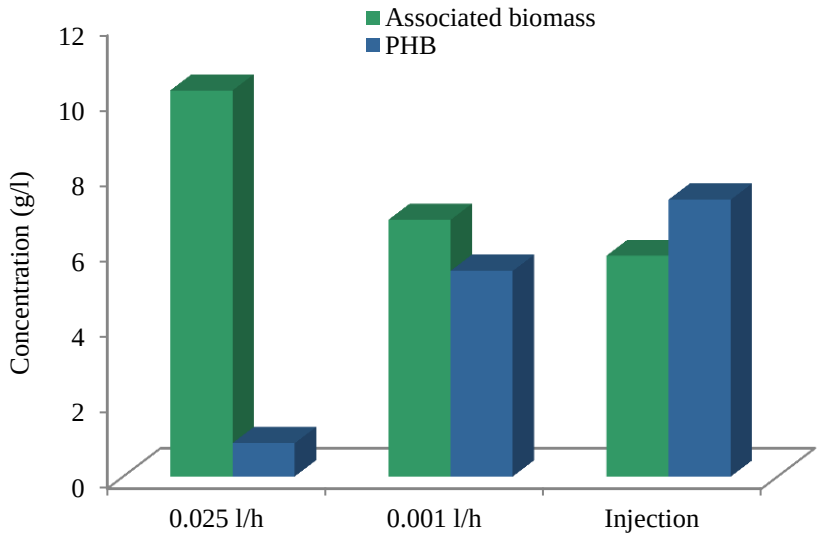

Figure 6-17: Summary of results obtained from fermentations simulated with different feeding strategies for the supply of nitrogen.

Based on the last two sets of results, a fermentation with an addition of glycerol at an appropriate time, along with injections of nitrogen, should improve product concentration. In order to test this, a fermentation with a pulse of ammonium sulphate during exponential growth phase and a pulse of glycerol plus ammonium sulphate before the 50th hour was simulated. A second pulse of glycerol was planned once the carbon had been totally consumed. A bioreactor with all these features was then conducted in the laboratory. The results of this fermentation are shown as data points superimposed on the simulations in Figure 6-17.

Based on the predictions shown in Figure 6-18, higher PHB production and total biomass can be achieved through this configuration compared to any other previous case presented. The higher availability of nitrogen enhanced higher associated biomass, which in turn influenced production. A continued growth was obtained throughout the first 50 hours and the addition of nitrogen at that time induced a second and shorter stage of growth. The two injections of carbon source extended PHB production until the 125th hour. Nonetheless, the slope of the PHB curve was not as steep as it was for the first forty hours. As glycerol was predicted to be totally consumed before the injection, there was a time region where production stopped and was not resumed until more glycerol was supplied. The whole amount of glycerol provided at the second injection was forecast to be consumed and yielded a PHB content of 77%.

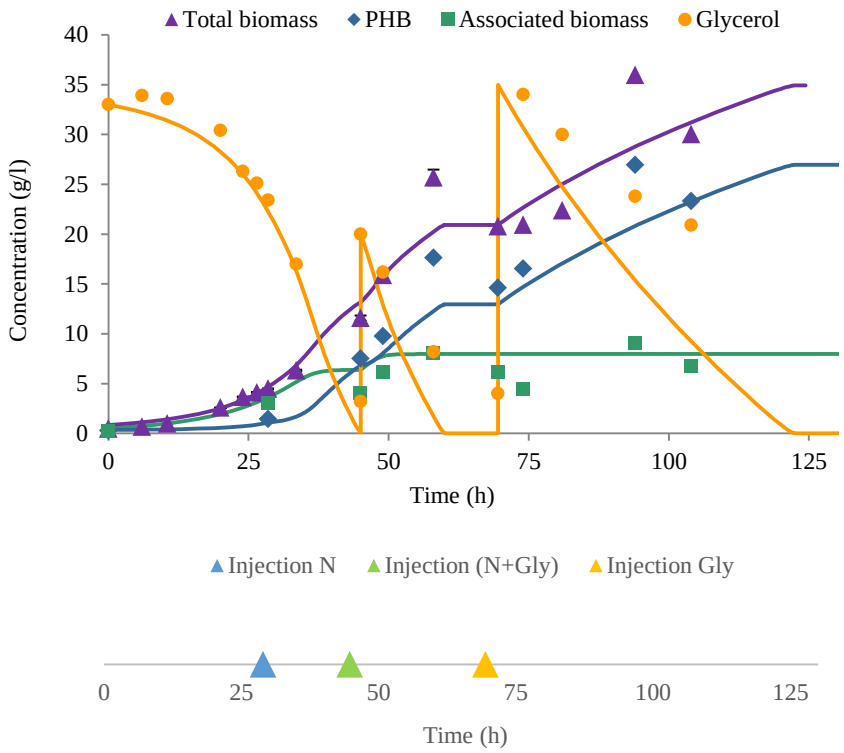

Figure 6-18: Model predictions (lines) and experimental results (symbols) for a glycerol fermentation by *C. necator* in which pulses of nutrients were done during fermentation. Fermentation was started with 33 g/l glycerol and 0.68 g N.

In line with the simulation, the experimental results show sustained growth (albeit with some minor oscillations) throughout the fermentation reaching a maximum of 9 g/l of associated biomass by the 94th hour. PHB production occurred almost uninterruptedly during the culture with two notable rogue points at 70 and 94 hours. These could just be an indicator of the inaccuracy of practical measurements or might indicate an oscillatory nature of PHB production followed by consumption. Overall, total biomass was very close, if not exceeding, 30 g/l, which is more than three times the maximum concentration obtained in a flask culture. Glycerol results followed nicely the model prediction for the batch period, and seemed to agree for the period in between glycerol injections. However, after the second addition, measurements drifted away from the model results. Interestingly, PHB concentration was exactly what should be based on the model, even though the "required" glycerol had not being consumed. It is useful to know whether beyond this time, PHB production would continue or the cells would start to degrade the PHB, so the fermentation was continued and the results are presented in Figure 6-19. For a better understanding of potential PHB degradation, the extension beyond 100 hours was conducted with several further additions of nitrogen but no more carbon. No simulations are shown alongside the results since degradation is a phenomenon not included in the current model.

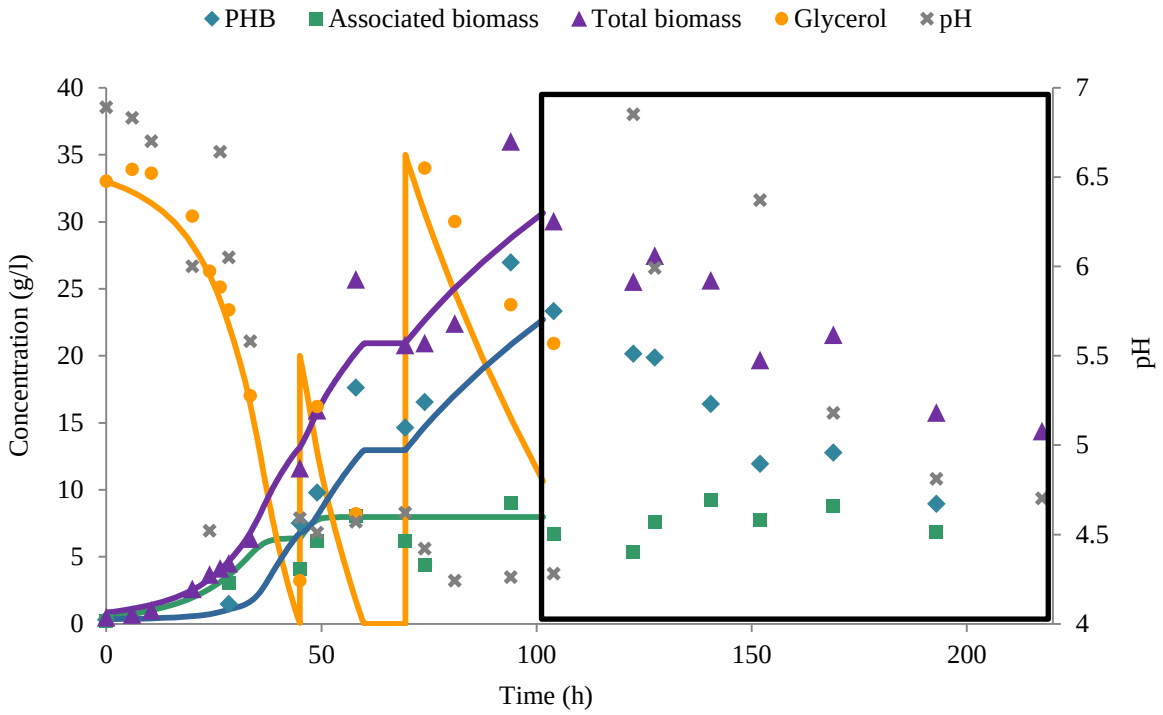

Figure 6-19: Experimental results for a glycerol fermentation by *C. necator* in which pulses of nutrients were done during fermentation. PHB degradation was induced after the 100th hour by the addition of nitrogen. Results within this period are inside the box.

It is apparent that total biomass and PHB concentration decreased significantly within the framed region, while associated biomass concentration seemed to stay rather stable. The nitrogen provided during the extended fermentation was taken up by the cells, which can be induced by the drop in pH during that time. It appears that PHB degradation occurred despite there being significant amounts of glycerol in the medium. It also appears that this PHB degradation occurs at a constant rate and is hence proportional to the amount of associated biomass, *i.e*. the number of cells.

The above results show the effects of successive injections of nutrients, but the same total addition could have been achieved by continuously feeding fresh medium. It was therefore decided to simulate and test continuous feeding that would provide the same amount of nutrients as in the case with multiple injections. In order to simulate this, the flow terms needed to be incorporated to the mass balance equations as indicated in Table 6-5:

Table 6-5: Equations and computed parameter values for the model adapted to fed-batch operation.

Associated biomass growth rate	$\frac{dx_A}{dt} = \frac{\mu_m N}{k_N + N} \cdot \frac{1}{1 + \frac{N}{k_{IN}}} \cdot \frac{Gly}{Gly \cdot \left(1 + \frac{Gly}{k_{IG}}\right) + k_G} - D \cdot x_R$	$\mu_m = 0.35\ h^{-1}$ $k_N = 0.2\ g/l$ $k_{IN} = 0.7\ g/l$ $k_{IG} = 40\ g/l$ $k_G = 10\ g/l$
PHB production rate	$\frac{dPHB}{dt} = \frac{\beta \cdot Gly}{Gly + k_P + \frac{N^2}{k_{INP}}} \cdot x_A \cdot \left(1 - \frac{PHB}{(x_R + PHB) \cdot P^{max}}\right) - D \cdot PHB$	$\beta = 0.15\ h^{-1}$ $k_P = 0.10\ g/l$ $k_{INP} = 0.001 \left(\frac{g}{l}\right)^2$ $P^{max} = 0.9$
Glycerol consumption rate	$-\frac{dGly}{dt} = \left(\frac{1}{Y_{x_A/Gly}} \cdot \mu_{x_A} + \frac{1}{Y_{PHB/Gly}} \cdot \mu_p\right) \cdot x_A + D \cdot (Gly_f - Gly)$	$Y_{x_A/Gly} = 0.35\ g/g$ $Y_{PHB/Gly} = 0.40\ g/g$
Nitrogen consumption rate	$-\frac{dN}{dt} = \frac{1}{Y_{x_A/N}} \cdot \mu_{x_A} \cdot x_A + D \cdot N$	$Y_{x_A/N} = 7.5\ g/g$
Variable volume	$\frac{dV}{dt} = F$	
Dilution rate	$D = \frac{F}{V}$	

Once a suitable configuration was determined through model simulations, it was implemented in the bioreactor. Figure 6-20 illustrates the feeding strategy along with the simulation results. Superimposed on those, the empirical results are shown as data points. Simulations show smooth growth that continued for a few hours after the feeding began, before the associated biomass reached a constant value. PHB production was less significant than growth for the first hours of fermentation and entered an exponential-type-phase after 30 hours of culture. Production progressively slowed down once the feeding was over and PHB concentration reached a plateau concurrent with glycerol depletion.

In practice (see data points), total biomass exhibited a steady growth which ended up with more than 35 g/l. Actually, the total biomass exceeded the prediction but reached its maximum value around the time predicted by the simulation. Regarding glycerol, its concentration decreased in the first hours of fermentation, increased during the feeding stage and decreased again afterwards, as predicted.

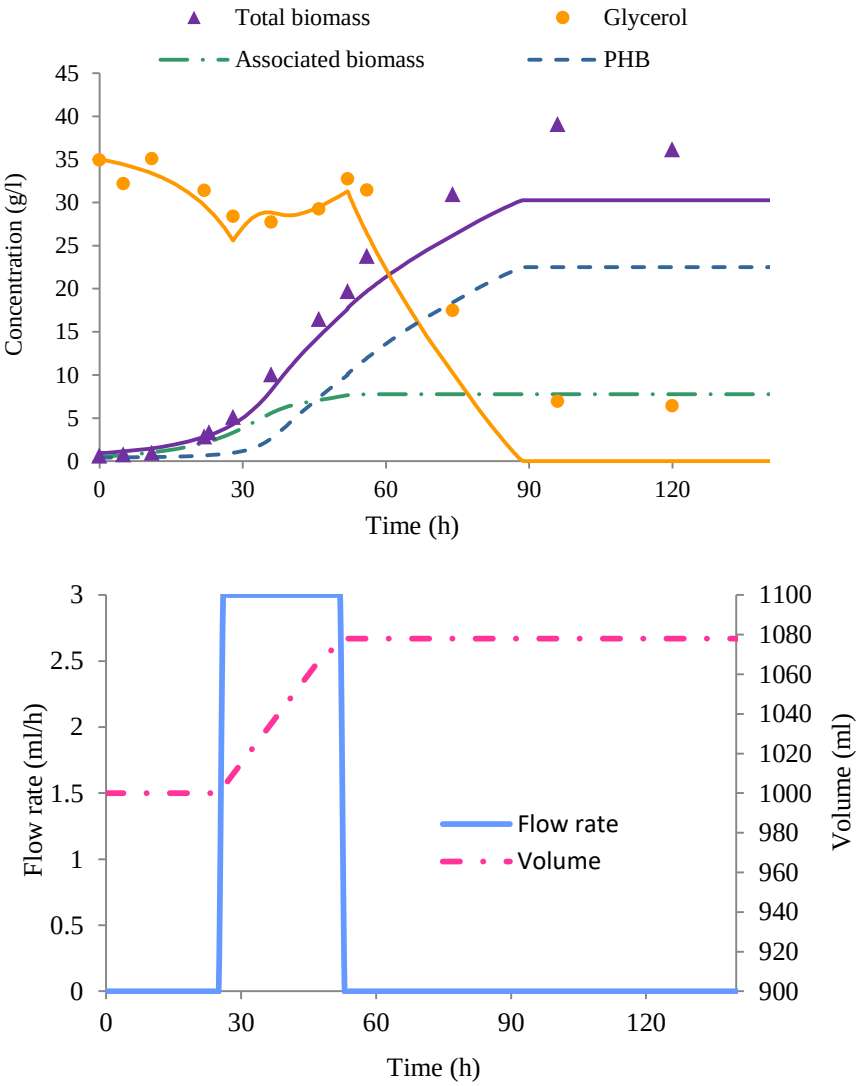

Figure 6-20: Model predictions (lines) and experimental results (symbols) for a glycerol fermentation by *C. necator* with continuous feeding of nutrients.

Model predictions were a good indicator of the fermentation profiles for biomass and glycerol during the first 60 hours of fermentation. Beyond that, total biomass was under-predicted since the simulation peaks at 30 g/l and then becomes constant. It is interesting to note that, during the same period, glycerol was forecast to be completely consumed although data suggests consumption was actually slower. The effect of the continuous feeding seemed beneficial in maintaining active metabolic rates and the process overall seems more efficient. This could suggest that the decline in cellular activity observed in the fermentation in which nutrients were fed through injections could be avoided through a continuous supply of nutrients. Having said that, the PHB content, productivity and even PHB concentration were found to be higher in the fermentation with multiple injections, see Figure 6-21:

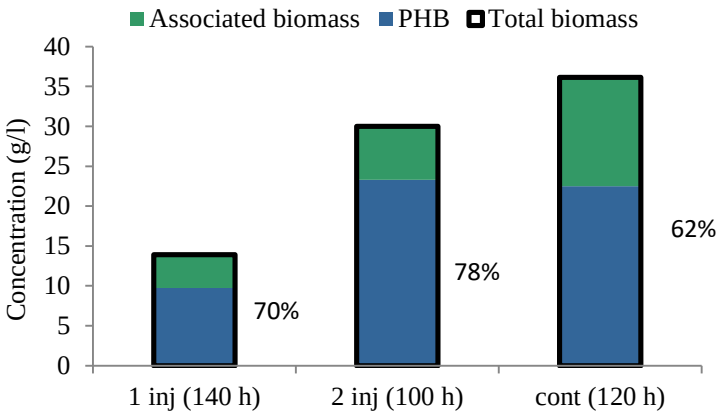

Figure 6-21: Comparison in terms of PHB, associated biomass and total biomass and PHB content (% of total biomass) of three extended batches with different feeding schemes. The time in brackets on the x-axis indicates the moment at which the measurements of concentrations were made.

Clearly, the feeding strategy affects the fermentation results obtained. When comparing the specific growth and production rate for the fermentation performed with multiple injections to that conducted with continuous feeding over a period of time (see Figure 6-22), it can be appreciated how the latter method avoids the sharp changes and hence maintains better conditions between the extreme of substrate limitation and substrate inhibition.

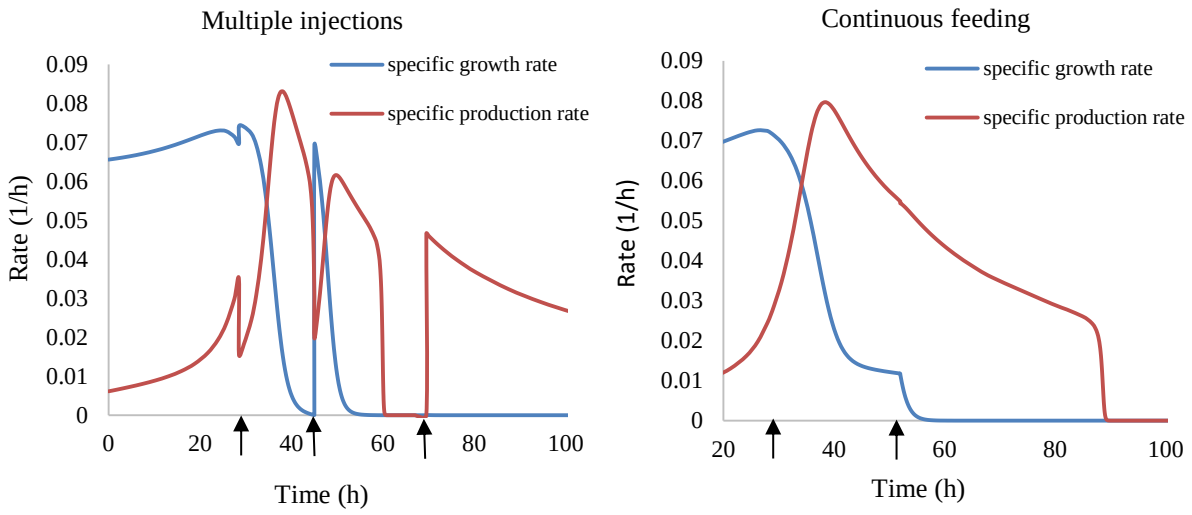

Figure 6-22: Predicted fermentation rates for glycerol fermentations by *C. necator* conducted with different feeding regimes. The arrows indicate the times when the injections were made (plot on the left) and the interval during which the continuous feeding took place (plot on the right).

6.4 Discussion

Glycerol fermentations by *C. necator* conducted in small flasks have shown to yield a limited amount of biomass, composed by PHB and associated biomass. This means, for example, that vigorous growth occurred in the early hours of fermentation, will lead to low PHB production. To account for this competition effect between PHB and associated biomass, the carrying capacity concept was introduced in the model formulation in the form of a constant K_x. In this way, the updated model was able to describe a wide range of situations characterized by the initial conditions for a fixed set of kinetic constants. Other uses for the model included the optimization of operation conditions or the evaluation of fermentation metrics based on the carbon and nitrogen concentrations through 3D plots.

Results from fermentation conducted in bioreactor showed that higher concentrations were possible for the same medium composition. This suggests that the better agitation and oxygen enables larger growth and production. In order to avoid an empirical constant as K_x within the model (which would be more difficult to determine in bioreactor as they can be operated in a much wider range of conditions), the limitation in PHB production was imposed by the increasing proportion of PHB within biomass, *i.e*. PHB content, when carbon is abundant. PHB degradation was observed within cells with high biopolymer content provided with nitrogen source. Its mechanism seems to be directly proportional to the associated biomass, responsible for the production of the enzymes involved in depolymerization, for a certain time period.

It is essential to design a feeding strategy to prevent overfeeding or underfeeding of substrate to the culture. This is especially complicated when the roles of carbon and nitrogen are the induction of PHB synthesis and growth respectively but they also are inhibitory substrates for the other phenomenon. The model, with the range of parameters fixed for bioreactor operation, enabled the simulation of different fed-batch regimes. Continuous feeding of nutrients seemed to be, based on simulated and tested experiments, the best and safest configuration to enhance high dense cultures. Successive feeding by injection would not be a practical configuration to implement at an industrial scale, where very high volumes would have to be added during fermentation. Oxygen has already demonstrated its importance in laboratory-based experiments and it would be crucial at a larger scale. Nonetheless, the role of oxygen has not yet being described and requires of tailored experiments to achieve a better understanding. Oxygen mass transfer limitations seem to set an upper bound the fermentation performance. Oxygen transfer rate (OTR) is considered to be the most important parameter implicated in the design, operation and scale-up of aerobic fermentation process in bioreactor, and the knowledge of k_La, characteristic of the OTR, is essential for stablishing a mathematical model for the dynamic simulation of a microbial fermentation process. Therefore, the mechanisms involved in the oxygen uptake during fermentation will be the subject of the next chapter.

Chapter 7

Preliminary studies into the influence of aeration

7.1 Introduction and theoretical background

Oxygen is critical for growth and survival of aerobic organisms. In aerobic respiration, oxygen acts as terminal electron acceptor for the electron-transport chain, which generates energy. Oxygen requirements are not only are strain dependent but also vary with the type of substrate to be oxidized, as illustrated in Table 7-1.

Table 7-1: Oxygen requirement for some bacteria and carbon substrates.

Substrate	Organism	Oxygen requirement (g O_2 ·g^{-1} CDM)	Reference
Glucose	*E.coli*	0.4	(1)
Methanol	*Pseudomonas C.*	1.2	(2)
Octane	*Pseudomonas CB*	1.7	(3)

(1) Schulze & Lipe, 1964 ; (2) Goldberg, 1976 *Pseudomonas C.* isolated from methanol; (3) Wodzinski & Johnson, 1968 *Pseudomonas CB* isolated from pristine.

Due to its low solubility in aqueous media, oxygen is usually supplied continuously during aerobic fermentations conducted in bioreactors. When oxygen requirements are met, maximum biomass production can be achieved and substrates totally oxidized. On the other hand, if the dissolved oxygen concentration (DO) in the culture broth falls below a critical level (C_{crit}), cell metabolism may be disturbed. As a consequence, substrates might be only partially oxidized and by-products might be segregated to allow for the energy generation and to balance the cellular redox metabolism. Some of these critical values are listed in Table 7-2:

Table 7-2: Critical dissolved oxygen values for certain microbial strain (Heldman 2003).

Organism	T (°C)	C_{crit} (mg·l^{-1})
Aspergillus oryzae	30	0.64
Azotobacter vinelandii	30	1.07
E. coli	38	0.26
E. coli	15	0.10
Penicillium chrysogenum	24	0.70
Penicillium chrysogenum	30	0.29
Pseudomonas denitrificans	30	0.29
Saccharomyces cerevisae	35	0.15
Saccharomyces cerevisae	20	0.12
Serratia marcescens	31	0.48

Variation in oxygen requirements can occur during fermentation. Specifically, for the case of PHB synthesis by *C. necator*, it has been reported that optimal oxygen concentration during the growth

phase should be higher than that during the production stage (Mozumder *et al.,* 2016). In fact, the limitation of oxygen can be used to trigger PHB formation as mentioned in the literature review. Figure 7-1 shows that maximum specific growth and production rates are achieved at different concentrations of oxygen in the medium.

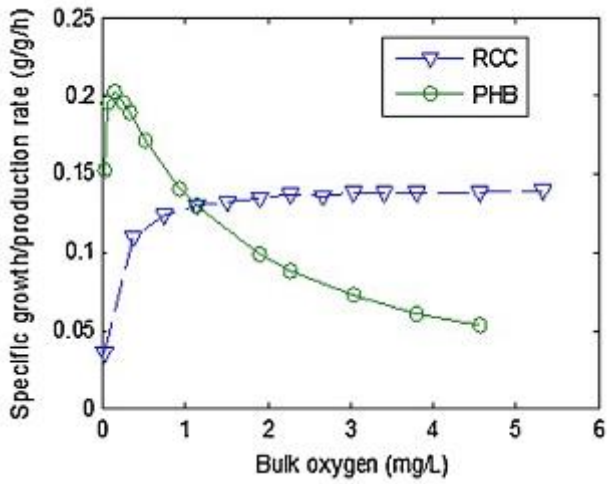

Figure 7-1: Specific biomass growth rate (RCC) and specific PHB production rate (PHB) as function of the dissolved oxygen in the bulk medium (Mozumder *et al.*, 2016).

In order to satisfy the oxygen demand by the cells and/or impose the desired limitations when appropriate, it is necessary to know the rate at which oxygen is being transferred to the media and utilized by the biomass. These two terms allow determining the dynamics of oxygen in the broth as represented by Eq. 7- 1:

$$\frac{\mathrm{d}c_L}{dt} = \mathrm{OTR} - \mathrm{OUR} \qquad \textbf{Eq. 7- 1}$$

where c_L is the concentration of dissolved oxygen, OTR, the oxygen transfer rate from the gas to the liquid and OUR the oxygen uptake rate by the cells in the liquid phase

7.1.1 Oxygen transfer rate

The nature of the oxygen mass transfer phenomena in a cellular culture can be described as follows. A low soluble gas (O_2) is transported from a gas bubble to a liquid phase containing the cells. To reach the cytosol, the oxygen crosses several resistances as shown in Figure 7-2.

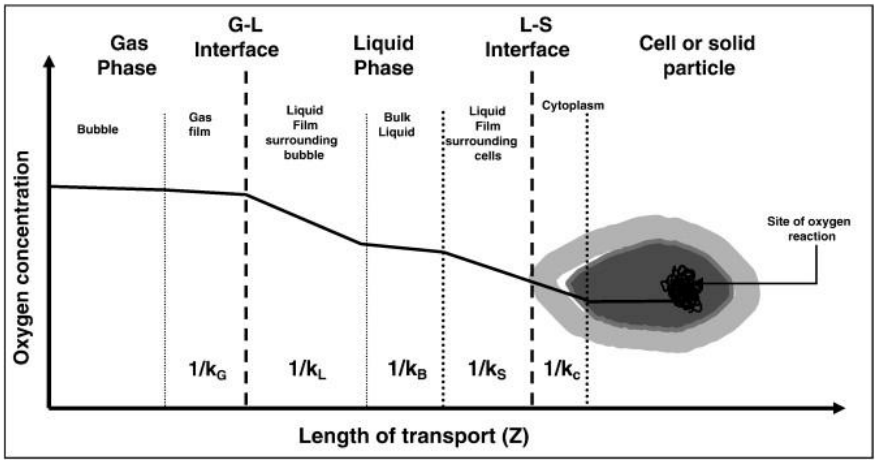

Figure 7-2: **Overview of steps in the overall transfer of oxygen from a gas bubble to the reaction site inside the individual cell (Garcia-Ochoa & Gomez 2009).**

Oxygen transfer rate is the rate at which oxygen is supplied on a volumetric basis. This is the oxygen transferred from the gas bubble to the bulk liquid. The flux of oxygen across the boundary separating the two phases is proportional to the driving force for mass transfer. Since oxygen is only sparingly soluble in water, the mass transfer is assumed to be liquid phase controlled and the flux if described by Eq. 7- 2:

$$\Phi = \mathrm{K_L} \cdot (\mathrm{c_l^*} - \mathrm{c_l}) \qquad \textbf{Eq. 7- 2}$$

where $\mathrm{K_L}$ is the overall mass transfer coefficient and $\mathrm{c_l^*}$ the saturation concentration in the liquid phase. It is generally accepted that the greatest resistance is on the liquid side, thus $\mathrm{K_L} \cong k_L$. The oxygen transfer rate is related to flux by interfacial area per unit of volume, *a*, is typically lumped with the mass transfer coefficient so that OTR becomes Eq. 7- 3:

$$\mathrm{OTR} = k_L a \cdot (\mathrm{c_l^*} - \mathrm{c_l}) \qquad \textbf{Eq. 7- 3}$$

The maximum OTR occurs when the liquid phase concentration is zero: such situation would occur when all oxygen entering the bulk solution is rapidly consumed: $OTR_{max} = k_L \mathrm{a} \cdot \mathrm{c_l^*}$.

There are different methods for determining the volumetric mass transfer coefficient, $(k_L a)$. These can be classified as chemical or physical methods. Within the chemical methods, the most popular is the sulphite oxidation technique. In this method, the oxygen uptake by the cells is mimicked by a chemical reaction in which oxygen is the limiting substrate. As soon as it dissolves, oxygen is used in the oxidation of sodium sulphite to sodium sulphate in the presence of Cu^{2+} or Co^{3+}. By following the evolution of the reaction, *i.e.* measuring the sulphite concentration, $k_L a$ can be determined. In this case, the reaction rate is equivalent to the oxygen transfer rate. However, the rate of absorption is enhanced by the chemical reaction and measured values are normally higher than the actual ones (Sikyta 1995).

The most extensively used physical techniques are the gassing out technique and the oxygen balance technique. Gassing out technique requires the measurement of dissolved oxygen and can be carried out in fermentative as well as non-fermentative systems. For the former, oxygen is firstly scrubbed from the system by sparging with nitrogen. Then the system is aerated and agitated so that the change in dissolved oxygen concentration can be directly correlated with the OTR. When dynamic gassing out method is carried out in a fermentation system, aeration is simply interrupted for a period of time and resumed before DO levels fall below critical. By plotting the dissolved oxygen with time, OUR can be determined as the slope of the first region, and once known, used to determine OTR from the slope of the second region as illustrated in Figure 7-3. A variation of this method involves introducing a step change in the air flow rate instead of stopping it.

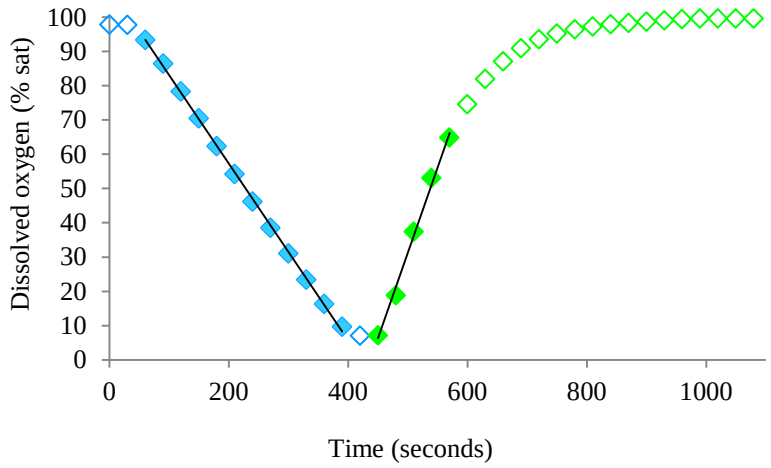

Figure 7-3: Graph of experimental data obtained during dynamic gassing-out technique for OUR and OTR determination. Blue symbols represent the region where the air supply is off and green, where it is on.

In addition to measurements of dissolved oxygen, the oxygen balance technique also requires the measurement of the oxygen content in the inlet and outlet gas streams so that an oxygen mass balance under steady-state conditions (Eq. 7- 4) can be solved to determine $k_L a$:

$$F_{O_2}^{in} - F_{O_2}^{out} - \mathrm{V} \cdot \mathrm{OUR} = 0 \qquad \textbf{Eq. 7- 4}$$

where $F_{O_2}^{in}$, $F_{O_2}^{out}$ are the oxygen flow rates measured at the inlet and outlet of a bioreactor of volume V.

Empirical correlations have also been developed to calculate OTR, where $k_L a$ is a function of different variables, including intrinsic characteristics of the system, such as medium density or surface tension, as well as operational conditions (agitation speed and gas flow rate). Table 7-3 shows some of the existing correlations that can be found in the literature.

Table 7-3: Correlations for the calculation of volumetric mass transfer coefficient; copied from Gill *et al.*, (2008).

References	Vessel diameter (m)	Impeller characteristics		Proposed correlation and type of fluid
		Type	d_i/d_T	
This work	0.06	Rushton turbine	0.33	Air–water with ions: $k_La = 0.224\left(\frac{P_g}{V}\right)^{0.35} u_s^{0.52}$
van't Riet (1979)	Various	Various	Various	Air–water with ions: $k_La = 2 \times 10^{-3}\left(\frac{P_g}{V}\right)^{0.7} u_s^{0.2}$
Vilaca et al. (2000)	0.21	Rushton turbine	0.4	Air–water–sulfite solution $k_La = 6.76 \times 10^{-3}\left(\frac{P_g}{V}\right)^{0.94} u_s^{0.65}$
Linek et al. (2004)	0.29	Rushton turbine	0.33	Air–water: $k_La = 0.01\left(\frac{P_g}{V}\right)^{0.699} u_s^{0.581}$
Smith et al. (1977)	0.61–1.83	Disc turbine	0.5–0.33	Air–water: $k_La = 0.01\left(\frac{P_g}{V}\right)^{0.475} u_s^{0.4}$
Zhu et al. (2001)	0.39	Disc turbine	0.33	Air–water: $k_La = 0.031\left(\frac{P_g}{V}\right)^{0.4} u_s^{0.5}$

7.1.2 Oxygen uptake rate

OUR is defined as the rate at which oxygen is consumed on a volumetric basis. As already mentioned, in bioreactor design, it is useful to know whether oxygen transfer or oxygen uptake dominates. If OTR is found to be lower than OUR, the aeration/mixing conditions can be changed in order to increase it. If the OTR is known, then the OUR can be determined by measuring changes in DO with time (Eq 7-1).

Alternatively, OUR can be calculated from biomass kinetics and the corresponding respective yields of biomass and product formation ($Y_{x/O}$, $Y_{P/O}$):

$$OUR = m_o \cdot x + \frac{\mu \cdot x}{Y_{x/O}} + \frac{Q_p}{Y_{P/O}} \qquad \textbf{Eq. 7- 5}$$

where m_o specific oxygen demand for maintenance and Q_p is the production rate.

Generally the first and third terms in the equation are negligible or ignored. Thereby, the equation is simplified to the cell growth term; in other words, it is assumed that oxygen is only consumed for the purposes of growth:

$$OUR = \frac{\mu \cdot x}{Y_{x/O}} \qquad \textbf{Eq. 7- 6}$$

If OUR is much smaller than OTR_{max}, then c_l and c_l^* are practically the same and the rate of oxygen consumed by the cells is limited by microbial metabolism. If OUR is equal to OTR_{max}, then $c_l = 0$ and the rate of oxygen consumed by cells is limited by the supply of oxygen. This can be potentially

overcome by increasing agitation rate, flow rate, oxygen content in the gas (enriched air) or by using pure oxygen.

It is important to recall that, as in the case of the sulphite oxidation method, oxygen uptake rate and oxygen transfer rate affect each other. In this way the absorption rate of oxygen in the liquid can be enhanced due to its consumption within the cell.

7.1.3 Kinetics of specific oxygen consumption

In spite of being an essential nutrient in many fermentation systems, oxygen is not very often included in the macroscopic description of microbial kinetics. The production of penicillin is one of the systems where the effect of oxygen has been better studied. Oxygen limitation on growth and product formation has been modelled through double substrate kinetics based on the Contois type model (Bajpai & Reuß 2007; Birol *et al.,* 2002). The same kinetic expression has also been used to describe the conversion of glucose into gluconic acid by *Aspergillus niger*, a filamentous fungus (Niger *et al.,* 2004). More recently, double substrate Monod expressions have been adapted to express the influence of oxygen together with other different substrates on growth rate of biofilms (Gonzo *et al.,* 2014).

As reported in chapter 6, the larger biomass achieved in bioreactor experiments depicts the importance of aeration for *C. necator* fermentation. The objective of this chapter is to describe, mathematically, dissolved oxygen profiles as has been done for other essential nutrients in previous chapters. Oxygen transfer and uptake rate were evaluated along the course of fermentation in order to set the basis for modelling oxygen dynamics.

7.2 Methodology: Dynamic method

Batch fermentations were conducted in bioreactors with the same set-up as presented in section 3.2.3. A dissolved oxygen probe allowed online measurements of the DO in the broth. Aeration was interrupted for a short period of time at different fermentation times. The dissolved oxygen concentration was recorded during those disturbances and until the system reached a pseudo steady state once aeration had been resumed. By applying the gassing-out technique, OUR and OTR determinations were possible.

As illustrated in Figure 7-3, a graphical method was used to determine OUR and OTR. When the air supply was switched off (*i.e.* OTR = 0), OUR was obtained from the slope of the straight line fit to the dissolved oxygen data points over time:

$$OUR = -\frac{dc_L}{dt} \qquad \textbf{Eq. 7- 7}$$

As air supply was switched back on, both oxygen transfer rate and oxygen uptake rate occurred. The OTR could be then calculated as follows:

$$OTR = \frac{dc_L}{dt} + OUR \qquad \textbf{Eq. 7- 8}$$

where $\frac{dc_L}{dt}$ was obtained from the slope of the straight line fitted to the data following resumption of aeration.

The culture medium was saturated with oxygen, prior to inoculation, in order to calibrate the oxygen probe (100% saturation). The saturation percentages were then converted into concentration by assuming the oxygen solubility in the medium to be 0.00754 g/l at 30°C as in water at atmospheric pressure (Garcia-Ochoa & Gomez 2009).

7.3 Results and discussion

7.3.1 Determination of OUR by dynamic method

In order to determine OUR at various times throughout the fermentation, the gassing-out technique was used prior to each sample withdrawal in two separate bioreactor experiments. Dissolved oxygen measurements were obtained as percentage of saturation based on calibration measurements before inoculation. The results for oxygen uptake rate along with experimental fermentation data for total biomass are plotted together with predicted biomass profiles in Figure 7-4. The predictions are based on the latest version of the model presented in chapter 6 (Table 6-4). It should be noted that this model does not consider the availability of oxygen, assuming it a non-limiting component.

During the time region indicated by the shaded area in Figure 7-4, the low values of DO within the bioreactor vessel (<10 % sat) prevented normal measurements of OUR by the gassing-out method. To overcome this, DO was artificially increased to 30% saturation by increasing the agitation for a few seconds and concentration monitored until it reached a low level again.

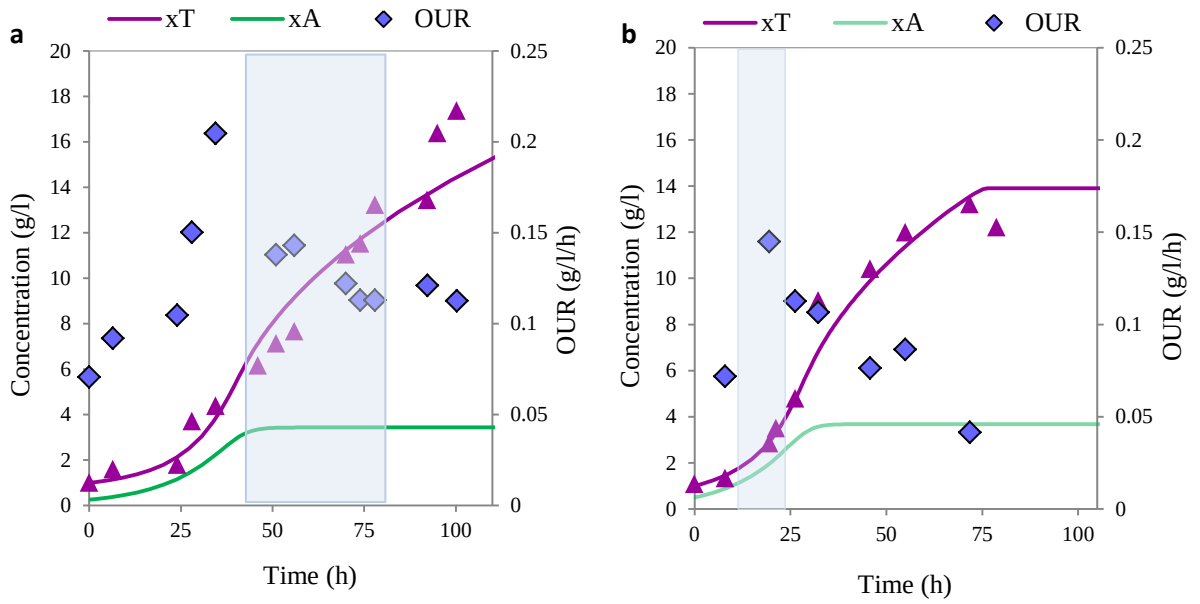

Figure 7-4: Oxygen uptake rates (OUR) and experimental values for total biomass concentration (symbols) and predicted biomass profiles (lines) for two bioreactor fermentations by *C. necator* with different initial glycerol concentrations :(a) 45 g/l and (b) 30 g/l for that on the right.

The figure shows that oxygen uptake rates clearly increased over the first forty hours of fermentation. The maximum value measured corresponded to 0.2 g 0_2/l/h, which is equivalent to an specific oxygen consumption, q_{O_2}, of 0.063 h^{-1} based on the associated biomass predicted by the model. After that, OUR decreased quickly and all the remaining values seemed to vary around an average of about 0.12 g 0_2/l/h. It appears that this coincides with the stationary phase of the cells, suggesting that growth related activities generated a greater oxygen demand than those activities associated with product formation and maintenance. Results from a second experiment (see Figure 7-4b), exhibited ales obvious but still similar trend. OUR values were higher in the early hours of fermentation (exponential growth phase) and tended to decrease as fermentation progressed. In this case, however, oxygen uptake rates were lower than in the previous case which may be a consequence of the difference in initial glycerol concentration between the experiments. The slower growth rate of the first experiment (see green line in Figure 7-4) suggests that a higher initial glycerol concentration induced concurrent growth and production for a longer period. The combined requirements for growth and production could result in overall higher OUR.

Ienczak *et al.*, (2011) proposed a high cell density strategy for PHB production by *C. necator* and investigated the oxygen demand to achieve that. A maximum value of 25 mg O_2/g cell/h was observed at the 10th hour of culture (when $\mu = \mu_{max}$). Specific oxygen uptake rate continually decreased after that, reaching a value of 3 mg O_2/g cell/h at the 55th hour. The trend is consistent with data presented above but the reported values are lower than those obtained for the present study: 113.7 mg O_2/g cell/h and 35.5 mg O_2/g cell/h in Figure 7-4a and 72.5 mg O_2/g cell/h and 10.8 mg O_2/g cell/h in Figure 7-4b.

Grunwald *et al.*, (2015) obtained the specific oxygen uptake rates, in a formic acid limited continuous culture by *R. eutropha*, by using the stoichiometric model developed by Grousseau *et al.* (2013). They obtained a very similar value 125.4 mg/g/h to their experimental data 128.3 mg/g/h. These values, from a chemostat culture, are higher but of a similar magnitude to those presented here for a batch culture. In the continuous culture, it is not possible to observe separately growth and production, so the significant switch in OUR observed in the present work has not been reported.

Considering the directly proportional increase of OUR with growth and the quick decrease to an approximate constant value once cell concentration enters stationary phase, an equation of the following form could potentially fit the data:

$$OUR = \left(\frac{\mu}{Y_{x_A/O}} + m\right) \cdot x_A \qquad \textbf{Eq. 7- 9}$$

where $Y_{x_A/O}$ is the biomass yielded per oxygen consumed and *m*, specific oxygen demand for maintenance.

Plots generated, using this equation are shown in Figure 7-5. These satisfactorily fit the two sets of data, but only by using different values for the parameters.

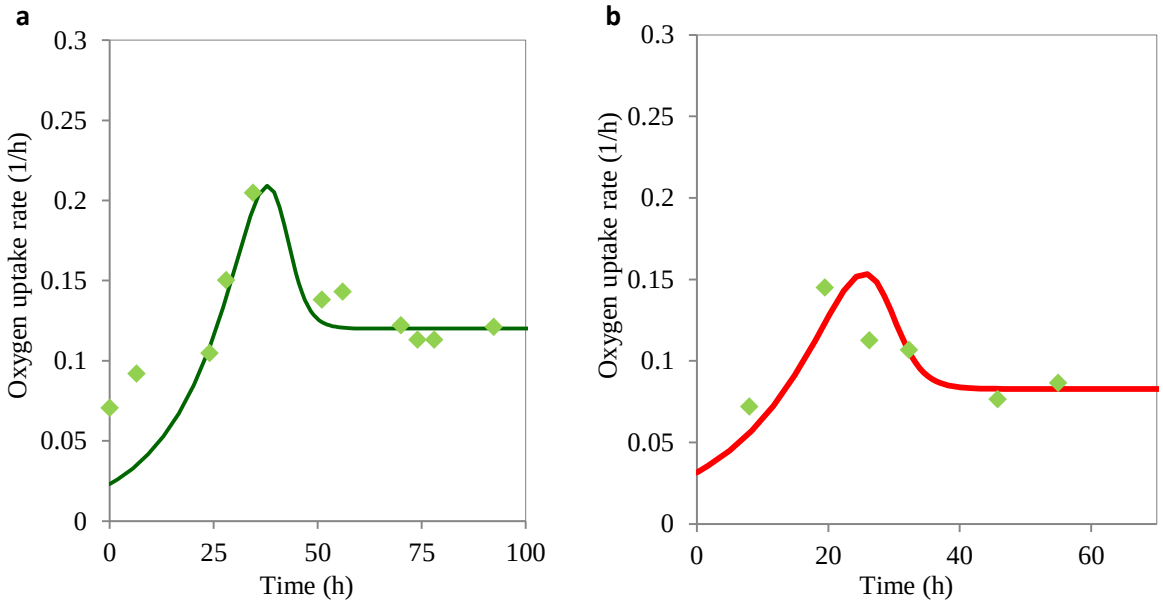

Figure 7-5: OUR experimental values (symbols) and model predictions using Eq. 7- 9 and $Y_{ox_A} = 1.1$ g/g and $m = 0.04$ h^{-1} in a and $Y_{ox_A} = 1.7$ g/g and $m = 0.0225$ h^{-1} for b.

7.3.2 Relationship between specific oxygen consumption and dissolved oxygen

Besides the apparent effect of the predominant cellular activity (growth, production, maintenance), it was questioned whether the concentration of dissolved oxygen would influence the rate of oxygen consumption. From the graphs of experimental data obtained during the dynamic gassing-out technique, plots of the specific oxygen consumption against dissolved oxygen concentration were generated as illustrated in Figure 7-6:

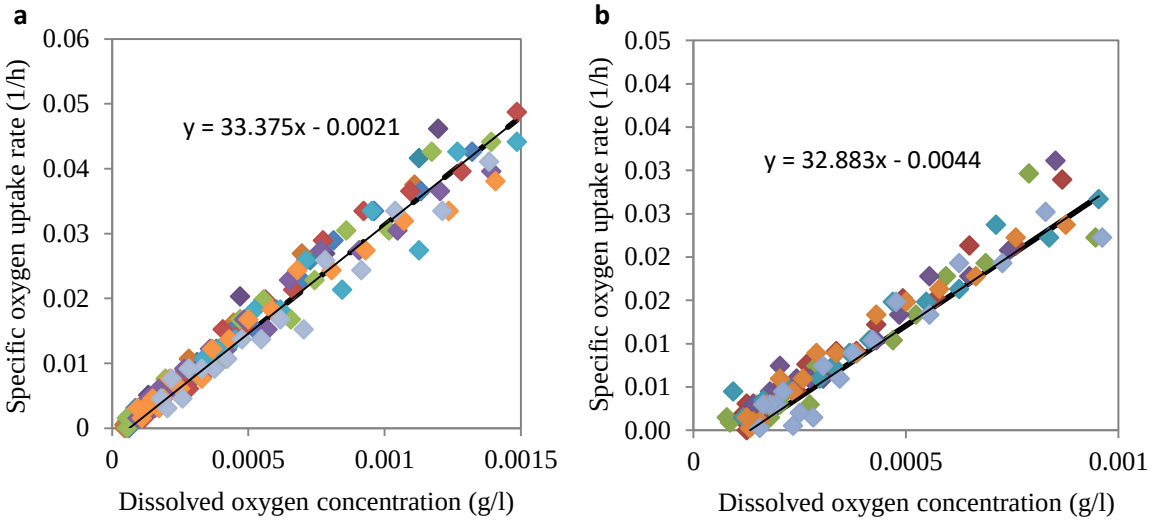

Figure 7-6: Relationship between specific oxygen uptake and dissolved oxygen concentrations for two bioreactor fermentations by *C. necator* with different initial glycerol concentrations: (a) 45 g/l and (b) 30 g/l .

By considering the variation with DO for all the measurements performed, specific oxygen uptake rate seemed to follow a linear relationship with DO at least for low oxygen concentrations. This seems to indicate that oxygen uptake rate depends largely on the concentration of oxygen in the bulk liquid phase rather than on the demand for oxygen within the cell.

Eq.7-10 and Eq.7-10b, characteristic of a reaction between a substrate and an enzyme, have been used to describe oxygen kinetics. k_1 and k_2 represent the kinetic constants :

$$q_{O_2} = \frac{c_L}{k_1 c_L + k_2} \qquad \textbf{Eq. 7- 10}$$

$$q_{O_2} = \frac{k_1 \cdot c_L}{c_L + k_2} \qquad \textbf{Eq. 7- 10b}$$

For both of them, the specific oxygen uptake becomes linear with oxygen concentration in the following cases:

Eq. 7-10: $k_1 c_L << k_2$, $q_{O_2} \sim 1/k_2\, c_L$

Eq. 7-10b: $c_L << k_2$, $q_{O_2} \sim k_1 / k_2\, c_L$

This type of relationship suggests that concentration of oxygen in the medium governs the rate at which oxygen is incorporated into the cell, possibly until a certain concentration inside the cell is

attained. It could be that it is the intracellular concentration that regulates the kinetics of bioreactions; in other words, increasing the dissolved oxygen in the medium (external concentration) might not necessarily increase the metabolic reaction rate.

7.3.3 Determination of k_La

In addition to the graphical method, previously described, two further strategies were implemented to estimate k_La and to compare results between the methods. Based on the value of OUR obtained from the graphical method (slope during oxygen depletion), the volumetric mass transfer coefficient can be calculated as follows:

$$k_La = \frac{\frac{dc_L}{dt} + OUR_{graph}}{c^* - c_L} \qquad \textbf{Eq. 7- 11}$$

where $\frac{dc_L}{dt}$ is the change in oxygen concentration during absorption. The denominator in Eq. 7-11 changes as c_L increases with time. Two values of k_La were calculated. The first one was calculated using the **minimum** c_L value *i.e.* when aeration was resumed. The second one was an average of all the k_La values calculated.

Based on the value of OUR predicted by a simple **Monod**-type model fitted to the data. The difference between this and the previous strategy is that the value of OUR instead of being assumed constant, is calculated with respect to dissolved oxygen concentration.

$$k_La = \frac{\frac{dc_L}{dt} + OUR_{Monod}}{c^* - c_L} \qquad \textbf{Eq. 7- 12}$$

$$OUR_{Monod} = q_{O_2} \cdot x_A \qquad \textbf{Eq. 7- 13}$$

$$q_{O_2} = \frac{q_{max} \cdot c_L}{k_s + c_L} \qquad \textbf{Eq. 7- 14}$$

The kinetic constants in the Monod expression were fitted for each set of data (every time k_La was determined) and x_A was assumed to remain constant value during the time the gassing out was carried out. An average value for k_La was then computed.

By assuming **steady-state**, *i.e* no change in the concentration of oxygen, the oxygen uptake rate would equal the transfer rate. In this case, k_La can be calculated from the values once the steady state has been reestablished after applying the gassing out technique *i.e.* when the values of concentration can be assumed to be constant again.

$$k_L a = \frac{q_{o_2} \cdot x_A}{c^* - c_{Lss}} \qquad \textbf{Eq. 7-15}$$

$k_L a$ values determined by the three methods throughout the fermentation are presented in Figure 7-7. for the two fermentation experiments already introduced.

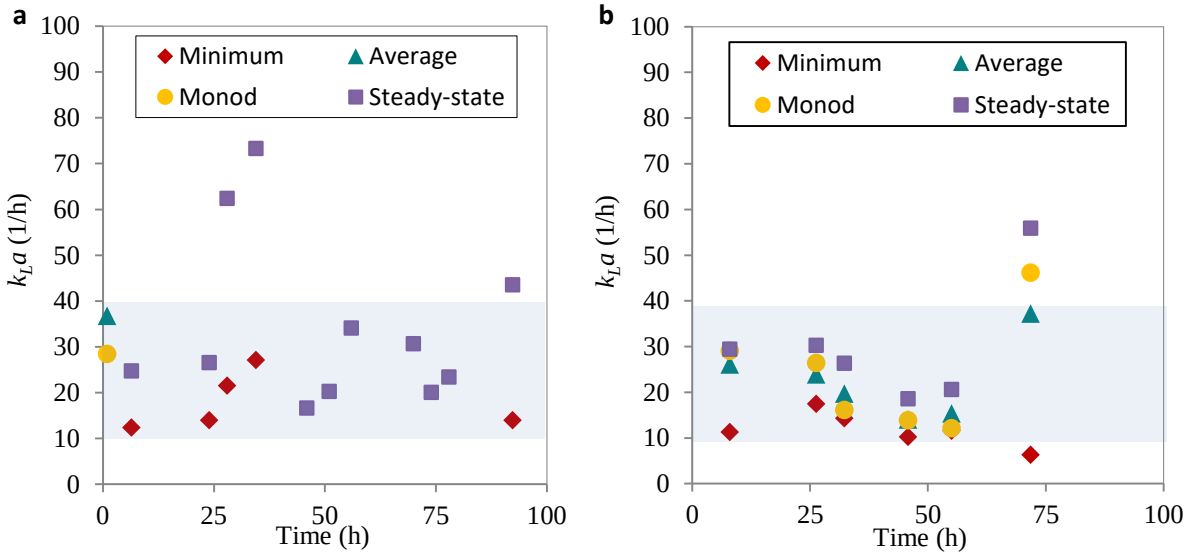

Figure 7-7: Evaluation of $k_L a$ using various methods. Values are presented for different times, during glycerol fermentation by *C. necator*, for two separate systems with different initial glycerol concentrations (a) 45 g/l and (b) 30 g/l .As can be seen, for both fermentations, most of the data fall within a broad horizontal band.

$k_L a$ values obtained varied throughout the fermentation and also with the calculation method employed. The values that resulted from using the minimum concentration of oxygen (when aeration was resumed) in Eq. 7-11 are effectively the lowest values overall. The highest values were obtained from the assumption of steady state.

$k_L a$ can also be calculated from measurements conducted in the fermentation medium without cells , *i.e.*, before inoculation. Then OTR in Eq. 7- 8 equals dc/dt and by continuously measuring O2 concentration in the liquid as in the other methods, $k_L a$ is thus obtained solving the differential equation. Thus, a plot of the $\ln(c^* - c_L)/(c^* - c_o)$ vs time should give a straight light, the slope of which, corresponds to $k_L a$, this is shown in Figure 7-8.

$$k_L a = -\frac{\ln \frac{(c^* - c_L)}{(c^* - c_o)}}{t} \qquad \textbf{Eq. 7-16}$$

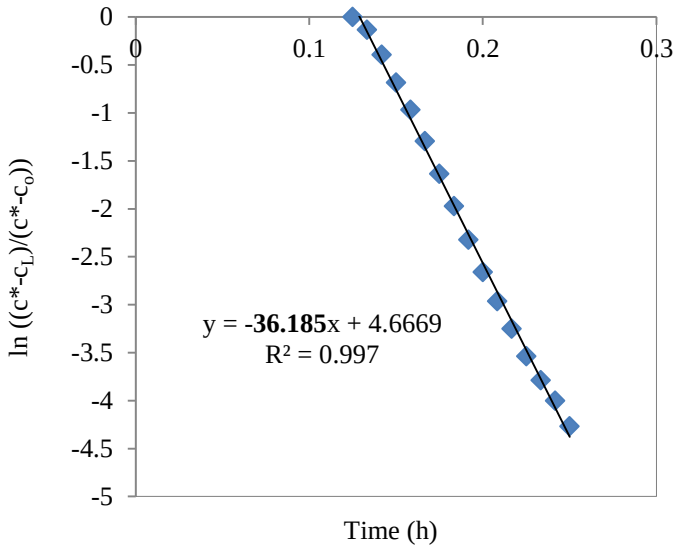

Figure 7-8: Plot of the ln((c*-cl)/(c*-co)) against time of aeration, the slope of which equals – k_La.

As can be seen from Figure 7-8, the value of k_La when there is no uptake of oxygen is 36 1/h which is in the same range of values shown in Figure 7-7.

All methods presented are based on assumptions that can compromise their accuracy. Those related to the degassing (air turn-off) technique require for the probe response time to be lower than the rate of change. Although this is assumed to be the case in the experimental setup (fast response time for the DO probe), more accurate determinations would take into account the sensor lag constant. Furthermore, it is considered that the interruption has no effect on the fermentation and cells maintain a constant uptake rate during the degassing period. However, it could be argued that, even in such a short time, they 'adapt' to the restricted conditions by reducing the uptake levels (maybe they reduce their consumption in order to preserve the oxygen). If concentration falls below a critical level, anaerobic metabolism will occur rather than the aerobic metabolism. After aeration is returned to the initial value, oxygen concentration usually increases and returns to values similar to the ones before the start. As soon as the profile is reestablished, dissolved oxygen values start changing again and the quasi steady state is disrupted, so the assumption used for calculation of k_La (*i.e.* true steady-state) never really applies. Lastly, determining k_La when no cells are present gives a measurement under artificial conditions that might substantially differ from those of the broth. On top of that, in all the calculations, it is assumed that physical properties (solubility, viscosity, surface tension, etc.) remain constant throughout the fermentation, even though the composition of the medium is known to vary. For instance, it has been observed that the solubility of oxygen increased from 6.8 to 7.8 mg/l in an aerobic bacteria fermentation (Vendruscolo *et al.*, 2012).

As introduced in theoretical background section for the chapter, there are empirical correlations to estimate the value of k_La in different systems. For example, Eq. 7-17 is applicable for stirred tank

reactors containing air-water systems agitated by Rushton impeller, which was the type of impeller used in the experimental work presented here. This correlation was used to estimate k_La and compare the value obtained with the experimental data and thus, evaluate its applicability for the bioreactor system described in this research.

$$k_La = 0.04\left(\frac{P_g}{V}\right)^{0,47} u_g{}^{0,6} \qquad \textbf{Eq. 7-17}$$

where P_g is the power exerted by the stirrer to the aerated liquid in Watts, V the volume in litre and u_g the superficial gas velocity in m/s. P was calculated from the adimesional number, Np, obtained from Figure 7-9 , for a Re_i = 26666 (curve 1). The resulting k_La equals 9 1/h.

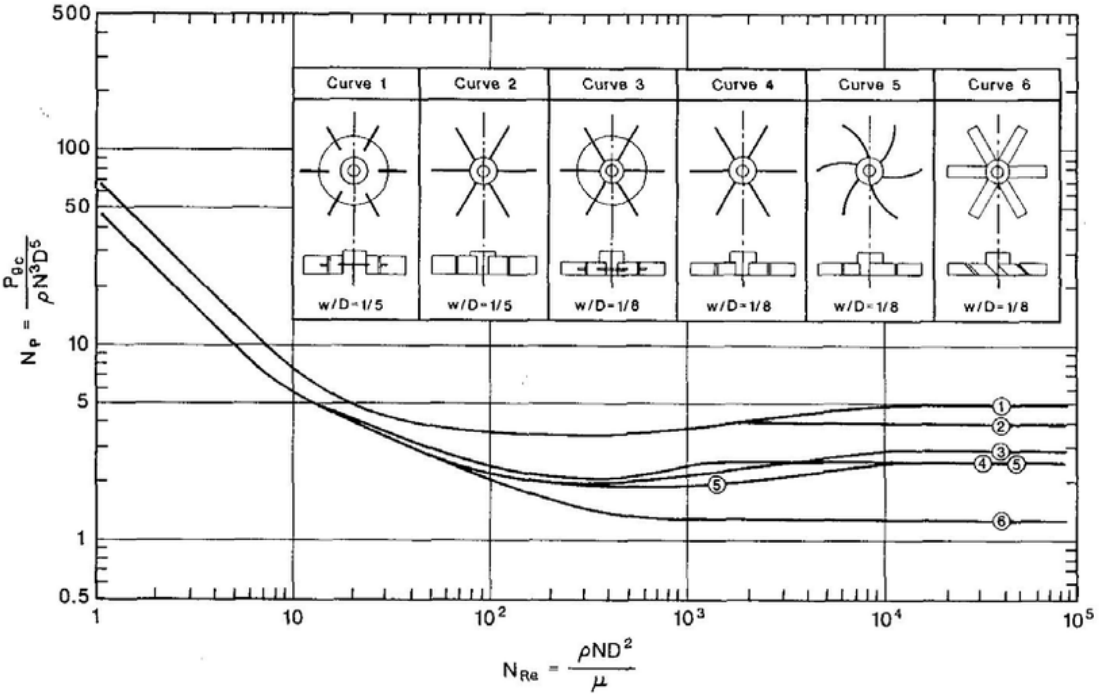

Figure 7-9: Reynold number-power number curve for different types of impellers (Padron 2001).

$$Re_i = \frac{D_i^2 \cdot n \cdot \rho}{\mu} = \frac{(0.08\,m)^2 \cdot \left(\frac{250}{60}s^{-1}\right) \cdot \left(1000\frac{kg}{m^3}\right)}{0.01\,Pa \cdot s} = 26666.6$$

$$P = N_p \rho n^3 D^5 = 5 \cdot \left(1000\frac{kg}{m^3}\right) \cdot \left(\frac{250}{60}s^{-1}\right)^3 \cdot (0.08\,m)^5 = 1.185\,W$$

$$k_La = 0.04 \cdot \left(\frac{1.185\,W}{1\,l}\right)^{0,47} \cdot \left(\frac{\frac{0.001m^3}{60\,s}}{\pi\,(0.025\,m)^2}\right)^{0,6} = 2.5\,10^{-3}s^{-1}$$

7.3.4 Variation of k_La with agitation and flow rate

In order to gain a preliminary insight into the effect of other factors on volumetric mass-transfer coefficient, agitation and flow rate were varied so that k_La determinations could be made during a certain time during fermentation. Results are shown in Figure 7-10:

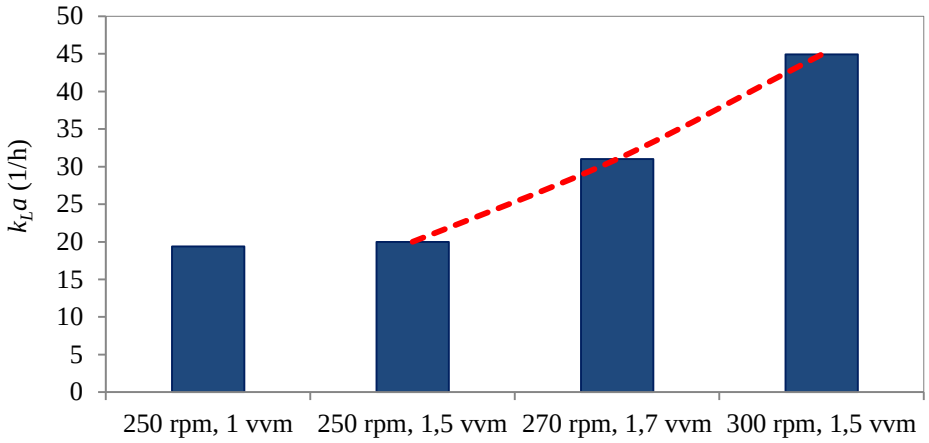

Figure 7-10: k_La estimations based on the OUR values obtained by the graphical method for different operational conditions.

Based on the results presented in Figure 7-10, increasing agitation seems to have a stronger effect than increasing flow rate. This has been reported in literature for different systems (Oh *et al.*, 1993). The values from Figure 7-7 (experimental values) were compared to the values that would be obtained using the empirical correlation *(*calculated values). Results are shown in Figure 7-11.

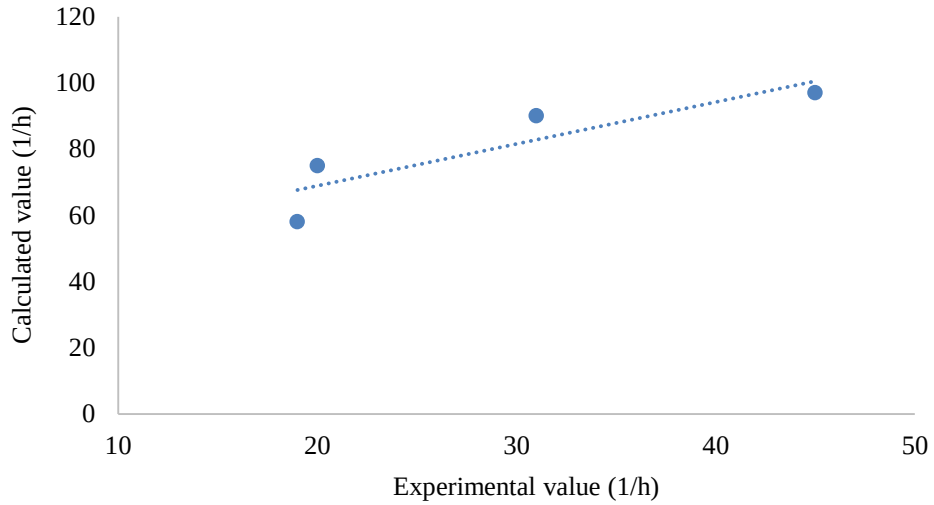

Figure 7-11: Experimental (gassing-out) and calculated values (correlation) for different operational conditions.

7.4 Conclusions

The level of oxygen in the fermentation broth is a parameter that, even though is not yet considered as a substrate in the model that represents the bioreactor kinetics, has effectively demonstrated an important role by imposing an upper bound on the fermentation performance. This chapter considered, in greater detail, the phenomena related to the oxygen dynamics, namely, oxygen uptake rate and oxygen transfer rate. Although this constituted a preliminary study in the influence of aeration, some relevant conclusion can be drawn.

The oxygen uptake rate by *C. necator* cells throughout fermentation varies depending on the predominant cellular stage. This can be mathematically expressed through a yield of associated biomass based on oxygen coupled to growth rate and a maintenance term proportional to associate biomass concentration. The data obtained suggests that these parameters are function of some other properties of the system, *e.g.* dissolved oxygen, and took different values when fitted to the two sets of data presented. Further studies would be required to establish meaningful values for the parameters or, if not constants, describe their variation as function of measured properties.

The oxygen requirement by *C. necator* is 1.3 g O_2/g x_A, which is within the typical range of aerobic bacteria (Heldman & Moraru 2010) but cannot be dismissed when operating with high cell density cultures. The fact that specific oxygen consumption can be modeled with a Monod type equation and exhibits a linear region up to 1.5 mg/0_2, implies that whenever dissolved oxygen concentration exceeds a such concentration, oxygen is no longer a limiting nutrient (and μ depends on other substrates). With the aeration system used, (OTR), DO should just be maintained above this C_{crit} (1.5 mg O_2/l) in order to provide the cells with the stoichiometric amount of oxygen required for growth until associated biomass concentration stop increasing. After that, the oxygen supply could be decreased, providing the maintenance requirements are fulfilled.

OUR cannot be studied without also considering OTR. Methods to estimate a range for the volumetric mass coefficient were thus employed, yielding an average k_La of 29 1/h. An increase of the agitation speed is preferred over an increase of the flow rate as a means of increasing k_La. This can avoid situations where the dissolved oxygen in the medium is zero. Empirical correlations have also been tested and gave an estimation just at the bottom of the band obtained from experimental measurements (9 1/h). Considering they are not developed for biological system and small vessels, the approximation is still within the range obtained.

In terms of modeling the role of oxygen, a distinction in terms of the oxygen levels in the reactor that yields different growth rates could be formulated. Still, to get a more realistic representation, further studies would be required to obtain meaningful values for the parameters involved. This would be

useful in order to define scenarios in which oxygen could become the limiting nutrient instead of nitrogen and prevents growth, but also, to establish the minimum (optimum) amount to air require during production.

Chapter 8

Conclusions and recommendations

8.1 Introduction

As introduced in the first chapter, bioprocesses are gaining importance and, eventually, the current oil-based economy will give up terrain in favor of a bio-based economy. To favor the transition, bioprocesses need to be sustainable and cost-effective. The so-called circular economy, where resources are exploited to their maximum potential, falls within this framework. Taking as example the biofuel sector, large amounts of resources are disposed as residues when they still possess potential high value as microbial feedstock. In this way, the glycerol cogenerated with biodiesel can be a suitable carbon source in biotechnology. Waste glycerol can be converted into numerous chemicals, including plastics, and energy sources (*e.g.* hydrogen) through fermentation. The design of a bioprocess for the synthesis of PHB from glycerol has been the case-study developed in this thesis. PHB is well known for being a biodegradable plastic that blended with different polymers (hydroxyvalerate, hydroxyoctanoate, lactic acid) exhibits mechanical properties comparable to commercial petroleum plastics, *e.g.* polypropylene (PP). In a biochemical sense, PHB is a carbon storage compound. In particular, *C. necator* cells synthesis PHB in nutrient-limited situations. Although PHB is already being produced at industrial scale, its costs are more than three times that of PP (1€/kg). This underlines the need for improving the efficiency of fermentation technologies.

There is an increasing number of research works that aim at integrating the experimental work necessary for characterizing biological systems with computational studies that look at *in-silico* optimization. Obtaining a macroscopic representation of the kinetics of a bioprocess can be attempted in numerous ways. In the present thesis, an iterative methodology supported by experiments and model predictions was implemented. In order to do so, raw batch data from bioreactor cultivation was used to propose relationships for the production and consumption rates. The model proposal was tested against different batch data to refine the model until good agreement between experiments and predictions was reached. The model was then extrapolated to fed–batch cultivation by addition of dilution terms and used to design operational strategies for experimental implementation. Within this approach, the values of the kinetic parameters were assumed to be absolute. In other words, they were maintained constant once the model was validated and not tuned with each new set of data. This enabled forecasting the fermentation results before conducting the experiment or even generating the data for conditions not tested in the lab. The ‘suck it and see’ approach, often used with biological experiments was significantly simplified as the range of operation was defined by other means and the hypotheses in which the model was based were continuously re-assessed.

8.2 Conclusions

The choice of PHB as the target product enabled an in-depth study of a relatively common yet not well understood system involving intracellular products with significant mass (up to 90% of the total).

C. necator is a wild type bacteria strain and was chosen as the PHB producer due to its ability to accumulate PHB under nutrient limiting conditions. Like most strains, *C. necator* 545 is capable of metabolising a variety of sugars but prefers glucose. Its growth on glycerol is relatively slow if unadapted. As a consequence, glycerol cannot be used directly as fermentation feedstock without a significant increase in the operation times or without a period of acclimatization. In order to establish the experimental set-up on which model hypotheses could be based, an acclimatization process of the microbial strain to the substrate was performed and is reported in **chapter 4**. This was planned as a preliminary piece of work to ensure a good microbial performance on the selected substrate. However, very important implications derived from the data analysis were found. For example, it became clear that serial sub-cultivation in glycerol as sole carbon source, along with a nitrogen source, is an effective way of adapting cells. A reduction of undesirable lag times and an increase in the specific growth and uptake rate were observed as results from the adaptation process.

It was also discovered that the changes occurring during adaptation have a degree of permanence and are maintained throughout lengthy storage periods. It is likely that either modifications in the transport systems that enable glycerol entry into the cytosol or a switch on the enzymes produced for the metabolism of the carbon source is the reason for this adaptation. What is certain is that the presence of glucose alongside the glycerol delays the adaptation, but once adapted to glycerol, cells prefer it as the substrate. Experiments with both carbon sources confirmed that the original glucose repression can be reverted. To determine whether the main resistance for glycerol uptake is transportation through the membrane or the activation of the metabolic regulation that targets the consumption of glycerol, it could be useful to carry out studies on the protein expressed by adapted cells.

The number of generations was used as an indicator of the adaptation progress and it was found that serial subcultivation should allow a minimum number of 15 generations to ensure the desirable cell performance. A possible mechanism for the adaptation was formulated through the inclusion of an inhibition term in the growth rate expression based on glycerol which decreased with the exposure time of cells to glycerol. Other types of models, such as population based models or models accounting for enzyme activities could also prove useful if the corresponding information were available. For the purpose of testing the system's versatility and potential concerning industrial implementation, where concentrations above 40 g/l are probable, a bio-training process of cells adapted to 20 g/l glycerol was carried out. As glycerol was gradually increased when cells had already acclimatized to the previous concentration, cells demonstrated the ability to grow on 100 g/l glycerol without a significant increase in doubling time. In fact, cultures performed with initial glycerol concentrations ranging from 30 to 100 g/l showed coincident growth curves. Without undergoing the bio-training, growth on such high concentrations occurred more slowly.

PHB was produced from bio-trained cells using an inexpensive culture medium. PHB was obtained as the main fermentation product with a yield of 0.16 g/g (34% maximum theoretical yield according to Moralejo-Garate *et al.*, 2011). Despite the low yield, glycerol was completely consumed by the end of the fermentation. Rapid screening of PHB was done through sudan staining on agar plates and fresh culture samples fixed on microscope slides, whereas a more detailed representation of PHB granules was obtained through TEM images. The quantification of PHB was done in GC-FID. This enabled the important differentiation between PHB and associated biomass (the biomass fraction other than PHB). It was initially thought that optical density could not be used as a direct indicator biomass concentration because of the presence of inclusion bodies. Nevertheless, although OD changes faster than cell dry mass for the first hours of fermentation (maybe due to larger differences in transparency/size than in mass), an almost linear correlation was still found between the two (see Figure 5-5). It was therefore concluded that OD values could be successfully converted to CDM to represent biomass in this system.

A kinetic model was built using empirical knowledge and was shown to be suitable to describe the fermentation profiles under different conditions and modes of operation. To keep the model relative simple, several assumptions, based on observations, were made. For example, it was assumed that growth and production were effectively separate processes governed by different variables. In fact, growth and product formation rates always peak at different times during the fermentation. Carbon (glycerol) was assumed to be the major contributing factor for PHB formation whereas nitrogen, which has a key influence on the dynamics of cellular growth, was also taken into account for biomass formation. It was also assumed that oxygen was provided in excess of the need for metabolism.

A comprehensive study of the effects of carbon and nitrogen was reported in **chapter 5** with a view to establishing the kinetics of substrate consumption and product formation. It is widely accepted that a surplus of the carbon source over the limiting nutrient encourages PHB production. It was found in this study that PHB production increases with initial glycerol concentration up to 40 g/l. Exceeding this concentration led to organic acid production alongside PHB. Formic, acetic and other organic acids were detected as fermentation by-products when very large concentrations of glycerol were used. This causes a decrease in the pH of the media and a reduction in overall PHB yield but does not affect the associated biomass. Very high glycerol concentrations should therefore be avoided.

Ammonium sulphate was preferred as nitrogen source because it is defined and therefore easily quantifiable. Nitrogen was, for the systems of study presented here, the element that triggered PHB production whenever it was reduced beyond a critical concentration (around 25 ml/l). When a nutrient such as nitrogen is scarce, high levels of NADH or NADPH are generated. High ratios of those over the oxidized forms, NAD and NADPH, inhibit the citrate synthase which favours the metabolic flux of acetyl-coA to the PHB synthesis pathway. As expected, nitrogen was found to be the element that

controls replication and maximum amount of associated biomass (limiting nutrient). Thereby, by limiting its availability, the extent of biosynthesis can be restricted. Normally, ammonium sulphate dropped below detectable levels within the first 30 hours of fermentation so that the culture became nitrogen limited and carbon utilization shifted. But the effect of nitrogen was found to go beyond that. There seems to be a minimum amount of nitrogen (or minimum amount of biomass) for PHB production to start and also a limit to the amount of ammonium sulphate that can be used. Concentrations exceeding 3 g/l were found to cause growth inhibition. The phenomenon could be related to the fact that the enzyme system, responsible for assimilating ammonium, is repressed by high concentrations of cations. The effect has been incorporated into the model as a non-competitive inhibition term (as if some enzyme has been removed from the pool). It was also found that pH evolution can be used to follow growth evolution in non controlled pH fermentations. A simple differential equation was successfully incorporated into the model using a constant proportional to the nitrogen consumption rate when pH profiles are required. Comparative studies with peptone yielded a very similar amount of biomass to that one obtained with ammonium sulphate. The pattern of cell growth was however different (linear) from the expected one (exponential). Other nutrient limitation, when cell growth is based on easily assimilable organic sources, could explain the restricted proliferation.

A basic form of the kinetic model was seen to be adequate for the description of fermentations conducted with low nitrogen concentrations ($\leq$ 2 g/l). This model includes a double substrate equation with inhibition terms due to nitrogen and glycerol for growth and a saturation expression with nitrogen inhibition for PHB. Nitrogen is utilised exclusively for growth while carbon is used both in growth and product formation. It was necessary to include glycerol in the equation that depicts growth to account for inhibition at high glycerol concentrations. Other by-products would also have to be accounted for in the model formulation and carbon mass balances if high glycerol amounts were to be used.

During model testing reported in chapter 6, it was found that while the preliminary form of the model worked well for conditions of low nutrient concentrations, it could not be extrapolated successfully for nutrient rich conditions beyond about 3 g/l ammonium sulphate (Figure 6-4). Nitrogen supply regulates the amount of cells that can be formed but to effectively form that amount of x_A, a certain concentration of carbon is also required. The remaining carbon would be the potential precursor for PHB. When increasing the nitrogen concentration, a greater amount of x_A can be achieved but only at the expense of consuming further glycerol, leaving a smaller fraction for PHB synthesis. However, a simple constitutive relationship for substrates (glycerol and ammonium sulphate) and products (PHB and associated biomass) cannot describe the experimental data. The exhaustion of other nutrients or a poor conversion of substrates under favorable conditions for growth was therefore assumed in order to set a threshold in the amount of total biomass (x_A + PHB) that can be formed. As in the logistic model,

the concept of a carrying capacity was introduced to describe the trade-off between having vigorous growth or abundant PHB accumulation. The addition of this term does a good job in mapping the interaction between ammonium sulphate and glycerol concentration and the contour maps generated with the reformulated model are an easy way to view the conditions that favour growth and production. By using this model, an estimation of the best harvesting time becomes possible. In order to achieve high PHB content without unnecessarily extending the fermentation, a stopping criterion based on the maximum value resulting from multiplying concentration and productivity was proposed.

Larger amounts of biomass were produced when fermentations were performed in bench-top bioreactors instead of flasks. The forced aeration (sparging) *vs* the convective mass transfer of air in flasks contributed to a better oxygenation of the broth, so that the maximum biomass obtainable in flasks (carrying capacity) was easily surpassed. The model was adapted by removing the carrying capacity but retaining the same key principles (Table 6-4). As a result of a sensitivity analysis, changes in values of the maximum specific growth rate and the non-growth associated constant for PHB production were found to be the most influential variables in the model.

High density cellular cultures (>30 g/l) were achieved through the successive addition of nutrients based predictions from computational studies. The rates of supply of carbon and nitrogen are critical to enhance PHB production. There should be sufficient, but not excess of, carbon to promote cell growth, and a reasonable shortage, but no cessation, of nitrogen to initiate PHB synthesis and sustain the cellular activity during the production phase. In this way, the feeding of both carbon and nitrogen was identified as a better strategy than the simple addition of glycerol.

PHB degradation was observed in PHB-containing cells provided with nitrogen source. The rate of degradation was found to be proportional to the number of cells. Although it is a phenomenon that would normally be avoided in the fermenter, it could be useful to further establish the degradation kinetics in order to forecast possible biodegradation times for PHB-made objects.

As suggested by Bailey (1986), mathematical modeling does not make sense without defining, before making the model, what its intended use is and what problem it is intended to help to solve. Extending this logic further, the degree of complexity of the model should be in agreement with the role it is intended to play. A more sophisticated version of a macroscopic model would include other (secondary) variables affecting production. In this context, in **chapter 7,** the role of oxygen was preliminarily examined. Oxygen uptake rates were observed to change during the course of a fermentation. OUR was directly proportional to growth and rapidly decreased to an approximately constant value once cell concentration entered stationary phase. A simple increase in the agitation (and consequently, OTR) could prevent physical limitations at the end of the exponential growth phase. Nonetheless, it still needs to be determined if a dual limitation (nitrogen + oxygen) benefits or

hampers PHB production. It was concluded that, provided oxygen concentration exceeded the critical value (1.5 mg/l), there was no requirement for additional consideration in the existing equations. It is however important to consider that for other cases (*e.g.* microbial growth on organic source, systems started with larger inoculum size, etc.), oxygen could set an upper bound on the fermentation performance and should then not be ignored in the optimization of the process operation.

In summary, the experimental data collected have been presented in a consistent way through the formulation of mathematical equations and the resultant model is ready for other researchers to make use of. In the case of carbon storage compounds, the selection of the operational conditions that yield high productivities is not trivial. However, the model has demonstrated its worth in defining operational conditions and assisting the researcher in the process design. The iterative process of testing and further developing the model is believed to be a useful tool to reach a good understanding of the system when compared to simply tuning parameters. As all models, it has its limitations and some suggestions for improvements and further work are presented in the next section.

8.3 Recommendations

The limitations of the model can potentially be overcome in different ways. For example, off-gas analysis and measurement of organic carbon in the biomass would allow to formulate more accurate carbon balances. Other restrictions on the versatility of the model arise from neglecting endogenous respiration or cell death/age. These could be studied systematically in microbiological experiments to gain more insights into their influence on overall performance.

One of the main aims of fermentation modeling is “to design large-scale fermentations processes using data obtained from small scale fermentations” (Sinclair & Cantero 1990).The system of study was well mixed, but it is important to note that as the working scale increases, mass transfer phenomena may start to become rate limiting. This is not only the case for oxygen, but limitation in the diffusion of other nutrients can also occur. It is therefore important that the scaling up process goes hand in hand with further model development.

To relate macroscopic observations to microscopic phenomena, the model developed in this thesis could be complemented with metabolic approaches. For example, metabolites analysis could indicate which pathways are being used under different types of stress. It should be pointed out that the design of a bioprocess by a chemical engineer depends on the knowledge and insight of the bioprocess, in which microbiologists, molecular biologists and biochemists are involved. Until now, microscopic (metabolic) and macroscopic approaches have developed along separate tracks but it is desirable to work on reducing the gap between those to a reach to a better overall understanding of the biological process.

The design of a bioprocess requires of many other factors not considered in this thesis but that should be analysed next in the process development: process control, economic feasibility studies and life cycle analysis. Adaptive control strategies could be implemented to regulate the distribution of nutrients. Optimization functions based on costs attributed to different variables, *e.g.* biomass (separation), PHB (purity), unconsumed glycerol (disposal costs) would be a practical thing to do. The carbon dioxide released when PHB naturally degrades should be balanced with the CO_2 captured by biomass (the fermentation feedstock for PHB synthesis) to ensure that the carbon footprint could be very close to zero.

The design exercise presented here is an abstraction from reality and thus does not account for other aspects that would be involved in the process development. Glycerol has been used in its pure form to elaborate fundamental relationships, but crude glycerol would be the actual feedstock of a real process. The impact of recent developments in molecular biology in the field of bioprocess engineering is considerable. In fact, the metabolic models mentioned above aim generally at optimizing the strain and that could lead to improved yields. Regarding the downstream operations, the extraction technique would need to be revised to guarantee meeting green technology practices. The properties of the PHB obtained would require of proper characterization for establishing suitable application or blending. Last but not least, an integrated biorefinery can be further enhanced by the bioprocessing not only of glycerol but also of other by-products *e.g.* cereal cake (López-Gómez *et al.*, 2016). An example of such biorefineries is illustrated in Figure 8-1:

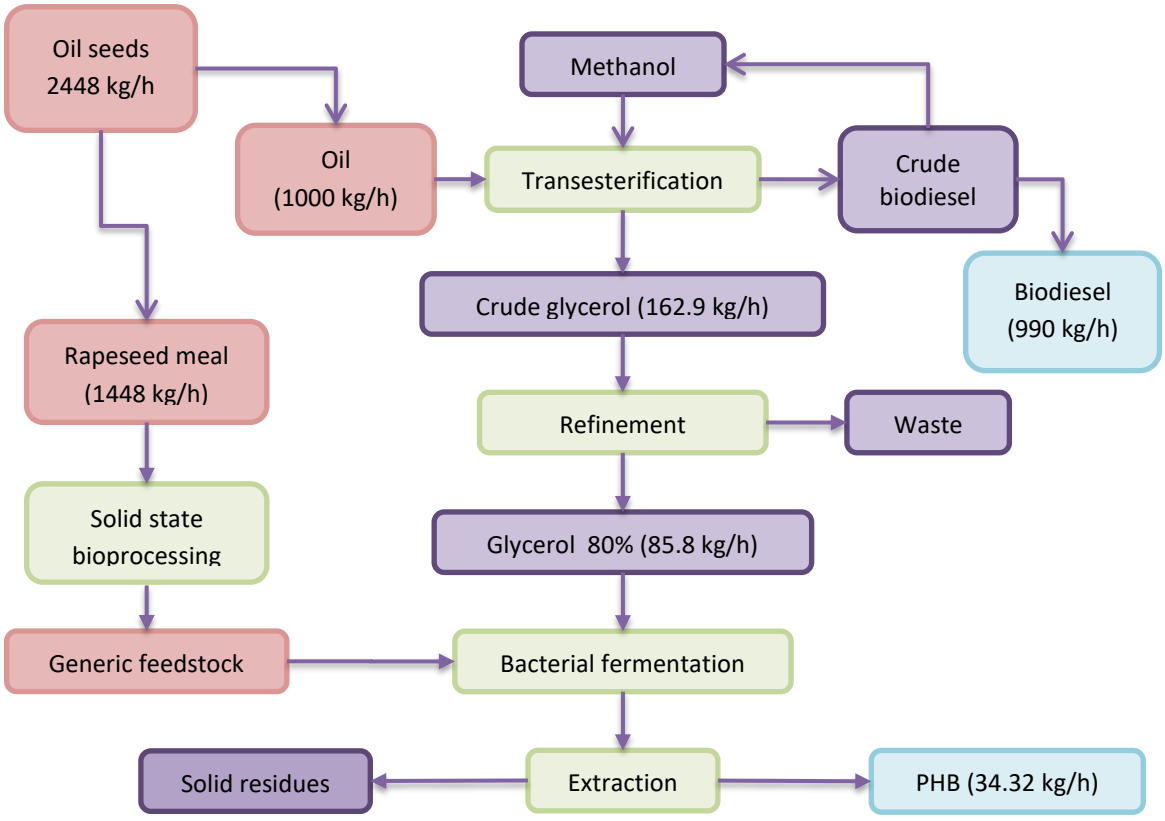

Figure 8-1: Schematics of an integrated biorefinery for the co-production of biodiesel and PHB from rapeseed oil. The mass flow rates are based on those from a small biodiesel plant.

Associated publications

Publications derived from the research presented in this thesis:

Pérez-Rivero, C., Sun, C., Theodoropoulos, C., & Webb, C. (2016). Building a predictive model for PHB production from glycerol. *Biochemical Engineering Journal*, *116*, 113–121. https://doi.org/10.1016/j.bej.2016.04.016

Pérez-Rivero, C. P., Hu, Y., Kwan, T. H., Webb, C., Theodoropoulos, C., Daoud, W., & Lin, C. S. K. (2017). 1 – Bioplastics From Solid Waste. In *Current Developments in Biotechnology and Bioengineering* (pp. 1–26). https://doi.org/10.1016/B978-0-444-63664-5.00001-0

Pleissner, D., Qi, Q., Gao, C., Pérez-Rivero, C. P., Webb, C., Lin, C. S. K., & Venus, J. (2016). Valorization of organic residues for the production of added value chemicals: A contribution to the bio-based economy. *Biochemical Engineering Journal*, *116*, 3–16. https://doi.org/10.1016/j.bej.2015.12.016

Pérez-Rivero, C., Sun, C., Theodoropoulos, C., & Webb, C. Exploring microbial adaptation for enhanced glycerol utilization by *Cupriavidus necator* (under preparation).

Publications produced during a stay at City University of Hong Kong:

Gao, C., Yang, X., Wang, H., Pérez-Rivero, C. P., Li, C., Cui, Z., Qi, Q., Lin, C. S. K. (2016). Robust succinic acid production from crude glycerol using engineered Yarrowia lipolytica. Biotechnology for Biofuels, 9(1), 179. https://doi.org/10.1186/s13068-016-0597-8

Bibliography

Abernathy, D. G., Spedding G. & Starcher B. (2009). Analysis of Protein and Total Usable Nitrogen in Beer and Wine Using a Microwell Ninhydrin Assay. Journal of the Institute of Brewing 115 (2). Blackwell Publishing Ltd: 122–27. doi:10.1002/j.2050-0416.2009.tb00356.x.

Abou-Zeid, D.-M., Müller, R.-J., & Deckwer, W.-D. (2001). Degradation of natural and synthetic polyesters under anaerobic conditions. Tailored Biopolymers, 86(2), 113–126. https://doi.org/10.1016/S0168-1656(00)00406-5

Akiyama, M., Tsuge, T., & Doi, Y. (2003). Environmental life cycle comparison of polyhydroxyalkanoates produced from renewable carbon resources by bacterial fermentation. Polymer Degradation and Stability, 80(1), 183–194. https://doi.org/10.1016/S0141-3910(02)00400-7

Albuquerque, M., Eiroa, M., Torres, C., Nunes, B., & Reis, M. (2007). Strategies for the development of a side stream process for polyhydroxyalkanoate (PHA) production from sugar cane molasses. Journal of Biotechnology, 130(4), 411–421.

American Society for Microbiology. (1964). Bergey's Manual of Determinative Bacteriology (7th ed.). Baltimore,Williams & Wilkins Co.

Anderson, A. J., & Dawes, E. A. (1990). Occurrence, metabolism, metabolic role, and industrial uses of bacterial polyhydroxyalkanoates. Microbiological Reviews, 54(4), 450–472.

Anderson, A. J., & Dawes, E. A. (1990). Occurrence, metabolism, metabolic role, and industrial uses of bacterial polyhydroxyalkanoates. Microbiological Reviews, 54(4), 450–72. Retrieved from http://www.ncbi.nlm.nih.gov/pubmed/2087222

Asrar, J., & Gruys, K. J. (2011). Biodegradable polymer (BIOPOL®). Biopolymers Online.

Atlić, A., Koller, M., Scherzer, D., Kutschera, C., Grillo-Fernandes, E., Horvat, P., Chiellini, E., Braunegg, G. (2011). Continuous production of poly ([R]-3-hydroxybutyrate) by Cupriavidus necator in a multistage bioreactor cascade. Applied Microbiology and Biotechnology, 91(2), 295–304.

Aziz, N. A., Sipaut, C. S., & Abdullah, A. A.-A. (2012). Improvement of the production of poly(3-hydroxybutyrate- co -3-hydroxyvalerate- co -4-hydroxybutyrate) terpolyester by manipulating the culture condition. Journal of Chemical Technology & Biotechnology, 87(11), 1607–1614. https://doi.org/10.1002/jctb.3817

Babel, W., Ackermann, J.-U., & Breuer, U. (2001). Physiology, regulation, and limits of the synthesis of poly (3HB). In Biopolyesters (pp. 125–157). Springer.

Bader, F. G. (1978). Analysis of double-substrate limited growth. Biotechnology and Bioengineering, 20(2), 183–202. https://doi.org/10.1002/bit.260200203

Bailey, J. E. Ollis, D. F. (1976). Biochemical Engineering Fundamentals. Chemical Engineering Education. Retrieved from https://eric.ed.gov/?id=EJ151863

Bailey, J. E. (1986). Biochemical engineering fundamentals / (2nd ed.). New York : McGraw-Hill,. Retrieved from https://searchworks.stanford.edu/view/1200573

Bailey, J. E. (1998). Mathematical Modeling and Analysis in Biochemical Engineering: Past Accomplishments and Future Opportunities. Biotechnology Progress, 14(1), 8–20. https://doi.org/10.1021/bp9701269

Bajpai, R. K., & Reuß, M. (2007). A mechanistic model for penicillin production. Journal of Chemical Technology and Biotechnology, 30(1), 332–344. https://doi.org/10.1002/jctb.503300140

Ballard, D. G. H., Holmes, P. A., & Senior, P. J. (1987). Formation of Polymers of ß-Hydroxybutyric Acid in Bacterial Cells and a Comparison of the Morphology of Growth with the Formation of Polyethylene in the Solid State. In Recent Advances in Mechanistic and Synthetic Aspects of Polymerization (pp. 293–314). Dordrecht: Springer Netherlands. https://doi.org/10.1007/978-94-009-3989-9_22

Belal, E. B. (2013). Production of Poly-β-Hydroxybutyric Acid (PHB) by Rhizobium elti and Pseudomonas stutzeri. Current Research Journal of Biological Sciences, 273–284.

Bellgardt, K.-H. (2000). Introduction. In Bioreaction Engineering (pp. 1–18). Berlin, Heidelberg: Springer Berlin Heidelberg. https://doi.org/10.1007/978-3-642-59735-0_1

BioEnergy Genome Center. (2011). Microbial Resources Group. Retrieved April 17, 2017, from http://www.bioenergychina.org/mr/ABOUT.html

Bionique® Testing Laboratories, I. (2016). Bionique.com. Retrieved April 11, 2017, from http://www.bionique.com/mycoplasma-resources/technical-articles/certified-working-cell-bank.htm

Birol, G., Ündey, C., & Çinar, A. (2002). A modular simulation package for fed-batch fermentation: penicillin production. Computers & Chemical Engineering, 26(11), 1553–1565. https://doi.org/10.1016/S0098-1354(02)00127-8

Braunegg, G., Lefebvre, G., & Genser, K. F. (1998). Polyhydroxyalkanoates, biopolyesters from renewable resources: physiological and engineering aspects. Journal of Biotechnology, 65(2), 127–161.

Bresan, S., Sznajder, A., Hauf, W., Forchhammer, K., Pfeiffer, D., & Jendrossek, D. (2016). Polyhydroxyalkanoate (PHA) Granules Have no Phospholipids. Scientific Reports, 6.

Brigham, C. J., & Kurosawa, K. (2011). Bacterial Carbon Storage to Value Added Products. Journal of Microbial & Biochemical Technology, s3. https://doi.org/10.4172/1948-5948.S3-002

Brooks, A. N., Turkarslan, S., Beer, K. D., Yin Lo, F., & Baliga, N. S. (2011). Adaptation of cells to new environments. Wiley Interdisciplinary Reviews: Systems Biology and Medicine, 3(5), 544–561. https://doi.org/10.1002/wsbm.136

Bugnicourt, E., Cinelli, P., Lazzeri, A., & Alvarez, V. (2014). Polyhydroxyalkanoate (PHA): Review of synthesis, characteristics, processing and potential applications in packaging. Express Polymer Letters, 8(11), 791–808. https://doi.org/10.3144/expresspolymlett.2014.82

Buzzini, P., & Margesin, R. (2014). Cold-Adapted Yeasts: A Lesson from the Cold and a Challenge for the XXI Century. In Cold-adapted Yeasts (pp. 3–22). Berlin, Heidelberg: Springer Berlin Heidelberg. https://doi.org/10.1007/978-3-642-39681-6_1

Cavalheiro, J. M. B. T., Almeida, M. C. M. D. de, Fonseca, M. M. R. da, & Carvalho, C. C. C. R. de. (2013). Adaptation of Cupriavidus necator to conditions favoring polyhydroxyalkanoate production. Journal of Biotechnology, 164(2), 309–317. https://doi.org/10.1016/j.jbiotec.2013.01.009

Cavalheiro, J. M. B. T., de Almeida, M. C. M. D., Grandfils, C., & da Fonseca, M. M. R. (2009a). Poly(3-hydroxybutyrate) production by Cupriavidus necator using waste glycerol. Process Biochemistry, 44(5), 509–

515. https://doi.org/10.1016/j.procbio.2009.01.008

Chakraborty, P., Gibbons, W., & Muthukumarappan, K. (2009). Conversion of volatile fatty acids into polyhydroxyalkanoate by Ralstonia eutropha. Journal of Applied Microbiology, 106(6), 1996–2005. https://doi.org/10.1111/j.1365-2672.2009.04158.x

Chanprateep, S. (2010). Current trends in biodegradable polyhydroxyalkanoates. Journal of Bioscience and Bioengineering, 110(6), 621–632. https://doi.org/10.1016/j.jbiosc.2010.07.014

Chee, J.-Y., Yoga, S.-S., Lau, N.-S., Ling, S.-C., Abed, R. M., & Sudesh, K. (2010). Bacterially produced polyhydroxyalkanoate (PHA): converting renewable resources into bioplastics. Current Research, Technology and Education Topics in Applied Microbiology and Microbial Biotechnology, 2, 1395–1404.

Chen, G.-Q., & Wu, Q. (2005). The application of polyhydroxyalkanoates as tissue engineering materials. Biomaterials, 26(33), 6565–6578.

Choi, J., & Lee, Y. S. (1997). Process analysis and economic evaluation for Poly(3-hydroxybutyrate) production by fermentation. Bioprocess Engineering, 17(6), 335–342. https://doi.org/10.1007/s004490050394

Cohen, S. N., Chang, A. C., Boyer, H. W., & Helling, R. B. (1973). Construction of biologically functional bacterial plasmids in vitro. Proceedings of the National Academy of Sciences of the United States of America, 70(11), 3240–4. Retrieved from http://www.ncbi.nlm.nih.gov/pubmed/4594039

Collander, R. (1937). The permeability of plant protoplasts to non-electrolytes. Transactions of the Faraday Society, 33(0), 985. https://doi.org/10.1039/tf9373300985

Collier, D. N., Hager, P. W., & Phibbs, P. V. (1996). Catabolite repression control in the Pseudomonads. Research in Microbiology, 147(6-7), 551–561. https://doi.org/10.1016/0923-2508(96)84011-3

Contois, D. E. (1959). Kinetics of Bacterial Growth: Relationship between Population Density and Specific Growth Rate of Continuous Cultures. Journal of General Microbiology, 21(1), 40–50. https://doi.org/10.1099/00221287-21-1-40

Davis, D. H., Doudoroff, M., Stanier, R. Y., & Mandel, M. (1969). Proposal to reject the genus Hydrogenomonas: Taxonomic implications. International Journal of Systematic Bacteriology, 19(4), 375–390. https://doi.org/10.1099/00207713-19-4-375

De Jong, E., Higson, A., Walsh, P., & Wellisch, M. (2012). Bio-based Chemicals Value Added Products from Biorefineries Report. Retrieved from www.ieabioenergy.com

Dhanasekar, R., Viruthagiri, T., & Sabarathinam, P. (2003). Poly (3-hydroxy butyrate) synthesis from a mutant strain Azotobacter vinelandii utilizing glucose in a batch reactor. Biochemical Engineering Journal, 16(1), 1–8.

Dias, J. M. L., Lemos, P. C., Serafim, L. S., Oliveira, C., Eiroa, M., Albuquerque, M. G. E., … Reis, M. A. M. (2006). Recent Advances in Polyhydroxyalkanoate Production by Mixed Aerobic Cultures: From the Substrate to the Final Product. Macromolecular Bioscience, 6(11), 885–906. https://doi.org/10.1002/mabi.200600112

DiSalvo, A. (2010). Filamentous Fungi.

Duchars, M. G., & Attwood, M. M. (1989). The Influence of C:N Ratio in the Growth Medium on the Cellular Composition and Regulation of Enzyme Activity in Hyphomicrobium X. Microbiology, 135(4), 787–793. https://doi.org/10.1099/00221287-135-4-787

Erickson, B., & Winters, P. (2012). Perspective on opportunities in industrial biotechnology in renewable chemicals. Biotechnology Journal, 7(2), 176–185.

European Bioplastics e.V. (2015). French law introduces measures to strengthen bioplastics market Biobased, biodegradable fruit and vegetable bags mandatory as of January 2017. Retrieved April 17, 2017, from http://www.european-bioplastics.org/pr_150723/

Faccin, D. J. L., Martins, I., Cardozo, N. S. M., Rech, R., Ayub, M. A. Z., Alves, T. L. M., Gambetta, R., Secchi, A. R. (2009). Optimization of C:N ratio and minimal initial carbon source for poly(3-hydroxybutyrate) production by Bacillus megaterium. Journal of Chemical Technology and Biotechnology, 84(12), 1756–1761. https://doi.org/10.1002/jctb.2240

Falkowski, P. G., & Owens, T. G. (1980). Light-Shade Adaptation : TWO STRATEGIES IN MARINE PHYTOPLANKTON. Plant Physiology, 66(4), 592–5. Retrieved from http://www.ncbi.nlm.nih.gov/pubmed/16661484

Ferenci, T. (2007). Bacterial Physiology, Regulation and Mutational Adaptation in a Chemostat Environment. Advances in Microbial Physiology, 53, 169–315. https://doi.org/10.1016/S0065-2911(07)53003-1

Foster, J. W. (1947). Some introspections of mold metabolism. Bacteriological Reviews, 11(3), 167–88. Retrieved from http://www.ncbi.nlm.nih.gov/pubmed/16350111

Gahlawat, G., Sengupta, B., & Srivastava, A. K. (2012). Enhanced production of poly(3-hydroxybutyrate) in a novel airlift reactor with in situ cell retention using Azohydromonas australica. Journal of Industrial Microbiology & Biotechnology, 39(9), 1377–1384. https://doi.org/10.1007/s10295-012-1138-5

García, I. L., López, J. A., Dorado, M. P., Kopsahelis, N., Alexandri, M., Papanikolaou, S., Villar, M.A., Koutinas, A. A. (2013). Evaluation of by-products from the biodiesel industry as fermentation feedstock for poly(3-hydroxybutyrate-co-3-hydroxyvalerate) production by Cupriavidus necator. Bioresource Technology, 130, 16–22. https://doi.org/10.1016/j.biortech.2012.11.088

Garcia-Ochoa, F., & Gomez, E. (2009). Bioreactor scale-up and oxygen transfer rate in microbial processes: An overview. Biotechnology Advances, 27(2), 153–176. https://doi.org/10.1016/j.biotechadv.2008.10.006

Gavrilescu, M., & Chisti, Y. (2005). Biotechnology—a sustainable alternative for chemical industry. Biotechnology Advances, 23(7), 471–499. https://doi.org/10.1016/j.biotechadv.2005.03.004

Giannattasio, S., Guaragnella, N., Corte-Real, M., Passarella, S., & Marra, E. (2005). Acid stress adaptation protects Saccharomyces cerevisiae from acetic acid-induced programmed cell death. Gene, 354, 93–98. https://doi.org/10.1016/j.gene.2005.03.030

Gill, N. K., Appleton, M., Baganz, F., & Lye, G. J. (2008). Quantification of power consumption and oxygen transfer characteristics of a stirred miniature bioreactor for predictive fermentation scale-up. Biotechnology and Bioengineering, 100(6), 1144–1155. https://doi.org/10.1002/bit.21852

Goldberg, I. (1976). Purification and Properties of a Methanol-Oxidizing Enzyme in Pseudomonas C. European Journal of Biochemistry, 63(1), 233–240. https://doi.org/10.1111/j.1432-1033.1976.tb10225.x

Gonzo, E. E., Wuertz, S., & Rajal, V. B. (2014). The continuum heterogeneous biofilm model with multiple limiting substrate Monod kinetics. Biotechnology and Bioengineering, 111(11), 2252–2264.

https://doi.org/10.1002/bit.25284

Gouda, M. K., Swellam, A. E., & Omar, S. H. (2001). Production of PHB by a Bacillus megaterium strain using sugarcane molasses and corn steep liquor as sole carbon and nitrogen sources. Microbiological Research, 156(3), 201–207.

Grothe, E., Moo-Young, M., & Chisti, Y. (1999). Fermentation optimization for the production of poly (β-hydroxybutyric acid) microbial thermoplastic. Enzyme and Microbial Technology, 25(1), 132–141.

Grousseau, E., Blanchet, E., Déléris, S., Albuquerque, M. G. E., Paul, E., & Uribelarrea, J.-L. (2013). Impact of sustaining a controlled residual growth on polyhydroxybutyrate yield and production kinetics in Cupriavidus necator. Bioresource Technology, 148, 30–38. https://doi.org/10.1016/j.biortech.2013.08.120

Grunwald, S., Mottet, A., Grousseau, E., Plassmeier, J. K., Popović, M. K., Uribelarrea, J-L., Gorret, J., Guillouet, N., Sinskey, A. (2015). Kinetic and stoichiometric characterization of organoautotrophic growth of Ralstonia eutropha on formic acid in fed-batch and continuous cultures. Microbial Biotechnology, 8(1), 155–63. https://doi.org/10.1111/1751-7915.12149

Haas, R., Jin, B., & Zepf, F. T. (2008). Production of poly (3-hydroxybutyrate) from waste potato starch. Bioscience, Biotechnology, and Biochemistry, 72(1), 253–256.

Hafuka, A., Sakaida, K., Satoh, H., Takahashi, M., Watanabe, Y., & Okabe, S. (2011). Effect of feeding regimens on polyhydroxybutyrate production from food wastes by Cupriavidus necator. Bioresource Technology, 102(3), 3551–3553.

Hahn, S. K., Chang, Y. K., & Lee, S. Y. (1995). Recovery and characterization of poly(3-hydroxybutyric acid) synthesized in Alcaligenes eutrophus and recombinant Escherichia coli. Applied and Environmental Microbiology, 61(1), 34–9. Retrieved from http://www.ncbi.nlm.nih.gov/pubmed/7887612

Heinzle, E., & Lafferty, R. M. (1980a). A kinetic model for growth and synthesis of poly-?-hydroxybutyric acid (PHB) in Alcaligenes eutrophus H 16. European Journal of Applied Microbiology and Biotechnology, 11(1), 8–16. https://doi.org/10.1007/BF00514072

Heldman, D. R. (Ed.). (2003). Encyclopedia of Agricultural, Food, and Biological Engineering (6th Editio). New York: Marcel Dekker.

Heldman, D. R., & Moraru, C. I. (2010). Encyclopedia of Agricultural, Food, and Biological Engineering. CRC Press.

Hrabak, O. (1992). Industrial production of poly-β-hydroxybutyrate. FEMS Microbiology Letters, 103(2-4), 251–255.

Huang, C., Chen, X., Xiong, L., Chen, X., Ma, L., & Chen, Y. (2013). Single cell oil production from low-cost substrates: The possibility and potential of its industrialization. Biotechnology Advances, 31(2), 129–139. https://doi.org/10.1016/j.biotechadv.2012.08.010

Huang, T.-Y., Duan, K.-J., Huang, S.-Y., & Chen, C. W. (2006). Production of polyhydroxyalkanoates from inexpensive extruded rice bran and starch by Haloferax mediterranei. Journal of Industrial Microbiology and Biotechnology, 33(8), 701–706.

Ibrahim, M. H., & Steinbüchel, A. (2009). Poly (3-hydroxybutyrate) production from glycerol by Zobellella

denitrificans MW1 via high-cell-density fed-batch fermentation and simplified solvent extraction. Applied and Environmental Microbiology, 75(19), 6222–6231.

Ienczak, J. L., Quines, L. K., Melo, A. A. de, Brandellero, M., Mendes, C. R., Schmidell, W., & Aragão, G. M. F. (2011). High cell density strategy for poly(3-hydroxybutyrate) production by Cupriavidus necator. Brazilian Journal of Chemical Engineering, 28(4), 585–596. https://doi.org/10.1590/S0104-66322011000400004

Inui, M., Vertès, A. A., & Yukawa, H. (1996). Reverse catabolite repression and the regulation of CO2 fixation in Rhodobacter and related bacteria. Research in Microbiology, 147(6-7), 562–566. https://doi.org/10.1016/0923-2508(96)84012-5

Iordanskii, A., Bonartseva, G., Pankova, Y., Rogovina, S., Gumargalieva, K., Zaikov, G., & Berlin, A. (2014). Current Status and Biomedical Application Spectrum of Poly (3-Hydroxybutyrate) as a Bacterial Biodegradable Polymer. In Key Engineering Materials, Volume 1 (Vol. 1, pp. 143–183). Apple Academic Press. https://doi.org/10.1201/b16588-13

Ishizaki, A., & Tanaka, K. (1991). Production of poly-β-hydroxybutyric acid from carbon dioxide by Alcaligenes eutrophus ATCC 17697T. Journal of Fermentation and Bioengineering, 71(4), 254–257. https://doi.org/10.1016/0922-338X(91)90277-N

Jacquel, N., Lo, C.-W., Wei, Y.-H., Wu, H.-S., & Wang, S. S. (2008). Isolation and purification of bacterial poly(3-hydroxyalkanoates). Biochemical Engineering Journal, 39(1), 15–27. https://doi.org/10.1016/j.bej.2007.11.029

Jari, M., Khatami, S. R., Galehdari, H., & Shafiei, M. (2015). Cloning and Expression of Poly 3-Hydroxybutyrate Operon Into Escherichia coli. Jundishapur Journal of Microbiology, 8(2), e16318. https://doi.org/10.5812/jjm.16318

Jendrossek, D., Schirmer, A., & Schlegel, H. G. (1996). Biodegradation of polyhydroxyalkanoic acids. Appl Microbiol Biotechnol, 46. https://doi.org/10.1007/s002530050844

Kalaiyezhini, D., & Ramachandran, K. B. (2015). Biosynthesis of Poly-3-Hydroxybutyrate (PHB) from Glycerol by Paracoccus denitrificans in a Batch Bioreactor: Effect of Process Variables. Preparative Biochemistry and Biotechnology, 45(1), 69–83. https://doi.org/10.1080/10826068.2014.887582

Kalia VC, ed. (2017) Microbial Applications Vol.2. Cham: Springer International Publishing. doi:10.1007/978-3-319-52669-0.

Karamerou, E. E., Theodoropoulos, C., & Webb, C. (2016). A biorefinery approach to microbial oil production from glycerol by Rhodotorula glutinis. Biomass and Bioenergy, 89, 113–122. https://doi.org/10.1016/j.biombioe.2016.01.007

Khanna, S., & Srivastava, A. K. (2005a). Recent advances in microbial polyhydroxyalkanoates. Process Biochemistry, 40(2), 607–619. https://doi.org/10.1016/j.procbio.2004.01.053

Khanna, S., & Srivastava, A. K. (2005b). Statistical media optimization studies for growth and PHB production by Ralstonia eutropha. Process Biochemistry, 40(6), 2173–2182. https://doi.org/10.1016/j.procbio.2004.08.011

Khanna, S., & Srivastava, A. K. (2008). A Simple Structured Mathematical Model for Biopolymer (PHB) Production. Biotechnology Progress, 21(3), 830–838. https://doi.org/10.1021/bp0495769

Kim, B. S., Lee, S. C., Lee, S. Y., Chang, H. N., Chang, Y. K., & Woo, S. I. (1994). Production of poly(3-hydroxybutyric acid) by fed-batch culture ofAlcaligenes eutrophus with glucose concentration control. Biotechnology and Bioengineering, 43(9), 892–898. https://doi.org/10.1002/bit.260430908

Koller, M., Atlić, A., Dias, M., Reiterer, A., & Braunegg, G. (2010). Microbial PHA production from waste raw materials. In Plastics from bacteria (pp. 85–119). Springer.

Koller, M., & Braunegg, G. (2015). Potential and Prospects of Continuous Polyhydroxyalkanoate (PHA) Production. Bioengineering, 2(2), 94–121.

Koller, M., Horvat, P., Hesse, P., Bona, R., Kutschera, C., Atlić, A., & Braunegg, G. (2006). Assessment of formal and low structured kinetic modeling of polyhydroxyalkanoate synthesis from complex substrates. Bioprocess and Biosystems Engineering, 29(5), 367–377. https://doi.org/10.1007/s00449-006-0084-x

Koyama, N., & Doi, Y. (1995). Continuous production of poly (3-hydroxybutyrate-co-3-hyhroxyvalerate) byAlcaligenes eutrophus. Biotechnology Letters, 17(3), 281–284.

Krishna, C., & Van Loosdrecht, M. C. M. (1999). Effect of temperature on storage polymers and settleability of activated sludge. Water Research, 33(10), 2374–2382. https://doi.org/10.1016/S0043-1354(98)00445-X

Kulpreecha, S., Boonruangthavorn, A., Meksiriporn, B., & Thongchul, N. (2009). Inexpensive fed-batch cultivation for high poly (3-hydroxybutyrate) production by a new isolate of Bacillus megaterium. Journal of Bioscience and Bioengineering, 107(3), 240–245.

Kunasundari, B., & Sudesh, K. (2011). Isolation and recovery of microbial polyhydroxyalkanoates. Express Polymer Letters, 5(7), 620–634. https://doi.org/10.3144/expresspolymlett.2011.60

Landaeta, R., Aroca, G., Acevedo, F., Teixeira, J. A., & Mussatto, S. I. (2013). Adaptation of a flocculent Saccharomyces cerevisiae strain to lignocellulosic inhibitors by cell recycle batch fermentation. Applied Energy, 102, 124–130. https://doi.org/10.1016/j.apenergy.2012.06.048

Lapage, S. P., Sneath, P. H., Lessel, E. F., Skerman, V., Seeliger, H., & Clark, W. (1992). International code of nomenclature of bacteria: bacteriological code, 1990 revision. ASM Press.

Lathwal, P., Nehra, K., Singh, M., Jamdagni, P., & Rana, J. S. (2015). Optimization of Culture Parameters for Maximum Polyhydroxybutyrate Production by Selected Bacterial Strains Isolated from Rhizospheric Soils. Polish Journal of Microbiology, 64(3), 227–39. Retrieved from http://www.ncbi.nlm.nih.gov/pubmed/26638531

Lee, S. Y. (1996). Bacterial Polyhydroxyalkanoates. Biotechnology and Bioengineering, 49, 1–14.

Lehninger, A. L. (1959). Respiratory-Energy Transformation. Reviews of Modern Physics, 31(1), 136–146. https://doi.org/10.1103/RevModPhys.31.136

Lemoigne, M. (1926). Produits de Dehydration et de Polymerisation de l'Acide ß-oxobutyrique. Bull Soc Chim Biol, 8, 770–782.

Li, R., Chen, Q., Wang, P. G., & Qi, Q. (2007). A novel-designed Escherichia coli for the production of various polyhydroxyalkanoates from inexpensive substrate mixture. Appl Microbiol Biotechnol, 75. https://doi.org/10.1007/s00253-007-0903-2

Lopar, M., Špoljarić, I. V., Cepanec, N., Koller, M., Braunegg, G., & Horvat, P. (2014). Study of metabolic network of Cupriavidus necator DSM 545 growing on glycerol by applying elementary flux modes and yield

space analysis. Journal of Industrial Microbiology & Biotechnology, 41(6), 913–930. https://doi.org/10.1007/s10295-014-1439-y

López-Gómez, J. P., Blanco-Rosete, S., & Webb, C. (2016). Extending shelf life of wheat based animal feed using solid state bioprocessing. Chemical Engineering Research and Design, 107, 147–152. https://doi.org/10.1016/j.cherd.2015.10.049

Luedeking, R., & Piret, E. L. (1959). A kinetic study of the lactic acid fermentation. Batch process at controlled pH. Journal of Biochemical and Microbiological Technology and Engineering, 1(4), 393–412.

Luo X, Hu S, Zhang X, Li Y. (2013). Thermochemical conversion of crude glycerol to biopolyols for the production of polyurethane foams. Bioresour Technol. 2013;139:323-329. doi:10.1016/j.biortech.2013.04.011.

Luong, J. (1987). Generalization of Monod kinetics for analysis of growth data with substrate inhibition. Biotechnology and Bioengineering, 29(2), 242–248.

Luong, J., Mulchandani, A., & LeDuy, A. (1988). Kinetics of biopolymer synthesis: a revisit. Enzyme and Microbial Technology, 10(6), 326–332.

Macrae, R., & Wilkinson, J. (1958). Poly-β-hyroxybutyrate metabolism in washed suspensions of Bacillus cereus and Bacillus megaterium. Microbiology, 19(1), 210–222.

Makkar, N., & Casida Jr, L. (1987). Cupriavidus necator gen. nov., sp. nov.; a Nonobligate bacterial predator of bacteria in soil†. International Journal of Systematic and Evolutionary Microbiology, 37(4), 323–326.

Marchessault, R., Bluhm, T., Deslandes, Y., Hamer, G., Orts, W., Sundararajan, P., … Holden, D. (1988). Poly (β-hydroxyalkanoates): Biorefinery polymers in search of applications (Vol. 19, pp. 235–254). Wiley Online Library.

Marchessault, R., Monasterios, C., Jesudason, J., Ramsay, B., Saracovan, I., Ramsay, J., & Saito, T. (1994). Chemical, enzymatic and microbial degradation of bacterial and synthetic poly-β-hydroxyalkanoates. Polymer Degradation and Stability, 45(2), 187–196.

Marzan, L. W., & Shimizu, K. (2011). Metabolic regulation of Escherichia coli and its phoB and phoR genes knockout mutants under phosphate and nitrogen limitations as well as at acidic condition. Microbial Cell Factories, 10(1), 1.

Meher, L., Sagar, D. V., & Naik, S. (2006). Technical aspects of biodiesel production by transesterification—a review. Renewable and Sustainable Energy Reviews, 10(3), 248–268.

Mendenhall, J., Li, D., Frey, M., Hinestroza, J., Babalola, O., Bonnasar, L., & Batt, C. A. (2007). Piezoelectric poly (3-hydroxybutyrate)-poly (lactic acid) three dimensional scaffolds for bone tissue engineering (Vol. 1025, pp. 1025–B12). Cambridge Univ Press.

Meng, X., Yang, J., Xu, X., Zhang, L., Nie, Q., & Xian, M. (2009). Biodiesel production from oleaginous microorganisms. Renewable Energy, 34(1), 1–5. https://doi.org/10.1016/j.renene.2008.04.014

Mokhtari-Hosseini, Z. B., Vasheghani-Farahani, E., Heidarzadeh-Vazifekhoran, A., Shojaosadati, S. A., Karimzadeh, R., & Darani, K. K. (2009). Statistical media optimization for growth and PHB production from methanol by a methylotrophic bacterium. Bioresource Technology, 100(8), 2436–2443.

Mothes, G., Schnorpfeil, C., & Ackermann, J.-U. (2007). Production of PHB from Crude Glycerol. Engineering

in Life Sciences, 7(5), 475–479. https://doi.org/10.1002/elsc.200620210

Mozumder, M. S. I., Garcia-Gonzalez, L., De Wever, H., & Volcke, E. I. (2016a). Model-based process analysis of heterotrophic-autotrophic poly (3-hydroxybutyrate)(PHB) production. Biochemical Engineering Journal, 114, 202–208.

Mozumder, M. S. I., Goormachtigh, L., Garcia-Gonzalez, L., De Wever, H., & Volcke, E. I. P. (2014). Modeling pure culture heterotrophic production of polyhydroxybutyrate (PHB). Bioresource Technology, 155, 272–280. https://doi.org/10.1016/j.biortech.2013.12.103

Mravec, F., Obruca, S., Krzyzanek, V., Sedlacek, P., Hrubanova, K., Samek, O., Kucera D., Nebesarova, J. (2016). Accumulation of PHA granules in Cupriavidus necator as seen by confocal fluorescence microscopy. FEMS Microbiology Letters, 363(10).

Mulchandani, A., Luong, J. H. T., & Groom, C. (1989). Substrate inhibition kinetics for microbial growth and synthesis of poly-β-hydroxybutyric acid by Alcaligenes eutrophus ATCC 17697. Applied Microbiology and Biotechnology, 30(1), 11–17. https://doi.org/10.1007/BF00255990

Mulchandani, A., Luong, J., & Leduy, A. (1988). Batch kinetics of microbial polysaccharide biosynthesis. Biotechnology and Bioengineering, 32(5), 639–646.

Naranjo, J. M., Posada, J. A., Higuita, J. C., & Cardona, C. A. (2013). Valorization of glycerol through the production of biopolymers: The PHB case using Bacillus megaterium. Bioresource Technology, 133, 38–44. https://doi.org/10.1016/j.biortech.2013.01.129

Nikel, P. I., Pettinari, M. J., Méndez, B. S., & Galvagno, M. A. (2010). Statistical optimization of a culture medium for biomass and poly (3-hydroxybutyrate) production by a recombinant Escherichia coli strain using agroindustrial byproducts. International Microbiology, 8(4), 243–250.

Novak, M. (2015). Mathematical Modelling as a Tool for Optimized PHA Production. Chemical and Biochemical Engineering Quarterly 29 (2): 183–220. doi:10.15255/CABEQ.2014.2101.

O'Toole, G., Kaplan, H. B., & Kolter, R. (2000). Biofilm Formation as Microbial Development. Annual Review of Microbiology, 54(1), 49–79. https://doi.org/10.1146/annurev.micro.54.1.49

OECD. (2005). Statistical Definition of Biotechnology. Retrieved October 11, 2016, from http://www.oecd.org/sti/biotech/statisticaldefinitionofbiotechnology.htm

Oh, S.-H., O, Py.-S., & Lee, C.-H. (1993). Effect of Aeration and Agitation Conditions on the Production of Glucoamylase with Aspergillus niger No. PFST-38. Journal of Microbiology and Biotechnology (Vol. 3). Korean Society for Applied Microbiology. Retrieved from http://www.koreascience.or.kr/article/ArticleFullRecord.jsp?cn=E1MBA4_1993_v3n4_292

Oil-price.net. (2016). Oil-price.net. Retrieved September 27, 2016, from http://www.oil-price.net/

Okpokwasili, G., & Nweke, C. (2005). Microbial growth and substrate utilization kinetics. African Journal of Biotechnology, 5(4), 305–317.

Padron, G. A. (2001). Measurement and Comparison of Power Draw in Batch Rotor-Stator Mixers. University of Maryland.

Pagliaro, M., & Rossi, M. (2010). The future of glycerol. Royal Society of Chemistry.

Pallerla, S. R., Knebel, S., Polen, T., Klauth, P., Hollender, J., Wendisch, V. F., & Schoberth, S. M. (2005). Formation of volutin granules in Corynebacterium glutamicum. FEMS Microbiology Letters, 243(1), 133–140. https://doi.org/10.1016/j.femsle.2004.11.047

Palleroni, N. J., & Palleroni, A. V. (1978). Alcaligenes latus, a new species of hydrogen-utilizing bacteria. International Journal of Systematic and Evolutionary Microbiology, 28(3), 416–424.

Parche, S., Jacobs, D., Arigoni, F., Titgemeyer, F., & Jankovic, I. (2006). Lactose-over-Glucose Preference in Bifidobacterium longum NCC2705: glcP, Encoding a Glucose Transporter, Is Subject to Lactose Repression†. Society, 188(4), 1260–1265. https://doi.org/10.1128/JB.188.4.1260

Patnaik, P. R. (2008). Response coefficient analysis of a fed-batch bioreactor to dissolved oxygen perturbation in complementary cultures during PHB production. Journal of Biological Engineering, 2(1), 1–11. https://doi.org/10.1186/1754-1611-2-4

Patwardhan, P., & Srivastava, A. (2004). Model-based fed-batch cultivation of R. eutropha for enhanced biopolymer production. Biochemical Engineering Journal, 20(1), 21–28.

Pereira, S. M., Sánchez, R. J., Rieumont, J., & Cabrera, J. G. (2008). Synthesis of biodegradable polyhydroxyalcanoate copolymer from a renewable source by alternate feeding. Polymer Engineering & Science, 48(10), 2051–2059.

Pérez Rivero, C., Sun, C., Theodoropoulos, C., & Webb, C. (2016). Building a predictive model for PHB production from glycerol. Biochemical Engineering Journal, 116, 113–121. https://doi.org/10.1016/j.bej.2016.04.016

Petrides, D., Harrison, R. G., Todd, P. W., Rudge, S. R., & Petrides, D. P. (2015). Bioprocess Design and Economics Bioseparations Science and Engineering (2 nd Edition). Retrieved from http://www.intelligen.com

Philip, S., Keshavarz, T., & Roy, I. (2007). Polyhydroxyalkanoates: biodegradable polymers with a range of applications. Journal of Chemical Technology and Biotechnology, 82(3), 233–247.

Posada, J. A., Naranjo, J. M., López, J. A., Higuita, J. C., & Cardona, C. A. (2011). Design and analysis of poly-3-hydroxybutyrate production processes from crude glycerol. Process Biochemistry, 46(1), 310–317. https://doi.org/10.1016/j.procbio.2010.09.003

Prieto, A., Escapa, I. F., Martínez, V., Dinjaski, N., Herencias, C., de la Peña, F., Tarazona, N., Revelles, O. (2014). A holistic view of polyhydroxyalkanoate metabolism in Pseudomonas putida. Environmental Microbiology.

Quagliano, C. J., & Miyazaki, S. S. (1997). Effect of aeration and carbon/nitrogen ratio on the molecular mass of the biodegradable polymer poly-β-hydroxybutyrate obtained from Azotobacter chroococcum 6B. Applied Microbiology and Biotechnology, 48(5), 662–664. https://doi.org/10.1007/s002530051112

Quispe, C. A. G., Coronado, C. J. R., & Carvalho Jr., J. A. (2013). Glycerol: Production, consumption, prices, characterization and new trends in combustion. Renewable and Sustainable Energy Reviews, 27, 475–493. https://doi.org/10.1016/j.rser.2013.06.017

Radakovits, R., Jinkerson, R. E., Darzins, A., & Posewitz, M. C. (2010). Genetic engineering of algae for enhanced biofuel production. Eukaryotic Cell, 9(4), 486–501. https://doi.org/10.1128/EC.00364-09

Raje, P., & Srivastava, A. K. (1998). Updated mathematical model and fed-batch strategies for poly-β-Hydroxybutyrate (PHB) production by Alcaligenes eutrophus. Bioresource Technology, 64(3), 185–192. https://doi.org/10.1016/S0960-8524(97)00173-9

Ramadas, N. V., Soccol, C. R., & Pandey, A. (2010). A Statistical Approach for Optimization of Polyhydroxybutyrate Production by Bacillus sphaericus NCIM 5149 under Submerged Fermentation Using Central Composite Design. Applied Biochemistry and Biotechnology, 162(4), 996–1007. https://doi.org/10.1007/s12010-009-8807-5

Ramadas, N. V, Singh, S. K., Soccol, C. R., & Pandey, A. (2009). Polyhydroxybutyrate production using agro-industrial residue as substrate by Bacillus sphaericus NCIM 5149. Brazilian Archives of Biology and Technology, 52(1), 17–23.

Riis, V., & Mai, W. (1988). Gas chromatographic determination of poly-β-hydroxybutyric acid in microbial biomass after hydrochloric acid propanolysis. Journal of Chromatography A, 445, 285–289. https://doi.org/10.1016/S0021-9673(01)84535-0

Roy, H., Dare, K., & Ibba, M. (2009). Adaptation of the bacterial membrane to changing environments using aminoacylated phospholipids. Molecular Microbiology, 71(3), 547–550. https://doi.org/10.1111/j.1365-2958.2008.06563.x

Russell, N. J., Harrisson, P., Johnston, I. A., Jaenicke, R., Zuber, M., Franks, F., & Wynn-Williams, D. (1990). Cold Adaptation of Microorganisms [and Discussion]. Philosophical Transactions of the Royal Society B: Biological Sciences, 326(1237), 595–611. https://doi.org/10.1098/rstb.1990.0034

Salakkam, A. (2012). Bioconversion of biodiesel by-products to value added chemicals. [Thesis]. Manchester, UK:The University of Manchester; 2012. The University of Manchester, Manchester, UK. Retrieved from https://www.escholar.manchester.ac.uk/uk-ac-man-scw:169207

Sangkharak, K., & Prasertsan, P. (2008). Nutrient optimization for production of polyhydroxybutyrate from halotolerant photosynthetic bacteria cultivated under aerobic-dark condition. Electronic Journal of Biotechnology, 11(3), 0–0. https://doi.org/10.2225/vol11-issue3-fulltext-2

Santimano, M., Prabhu, N. N., & Garg, S. (2009). PHA Production Using Low—Cost Agro—Industrial Wastes by Bacillus sp. Strain COLl/Afi. Research Journal of Microbiology, 4(3), 89–96.

Schué, F. (2000). Biopolymers from renewable resources. Edited by DL Kaplan Springer-Verlag, Heidelberg, 1998. pp 417, Price DM278. 00 ISBN 3-540-63567-X. Polymer International, 49(5), 472–473.

Schulze, K. L., & Lipe, R. S. (1964). Relationship between substrate concentration, growth rate, and respiration rate of Escherichia coli in continuous culture. Archiv Fuer Mikrobiologie, 48(1), 1–20. https://doi.org/10.1007/BF00406595

Scopus. (2016). Number of publications related to biobased polymers over recent years.

Sengupta, D., & Pike, R. W. (2013). Chemicals from biomass : integrating bioprocesses into chemical production complexes for sustainable development. CRC Press.

Shang, L., Fan, D. Di, Kim, M. Il, Choi, J., & Chang, H. N. (2007). Modeling of poly(3-hydroxybutyrate) production by high cell density fed-batch culture of Ralstonia eutropha. Biotechnology and Bioprocess

Engineering, 12(4), 417–423. https://doi.org/10.1007/BF02931065

Sharma, M., & Dhingra, H. K. (2015). Isolation and optimization of culture conditions for PHB production by bacillus megaterium. Int J Pharm Bio Sci, 6(4), 724–734. Retrieved from http://www.ijpbs.net/cms/php/upload/4749_pdf.pdf

Shino Yamada, Yi Wang, Naoki Asakawa, Naoko Yoshie, and, & Inoue*, Y. (2001). Crystalline Structural Change of Bacterial Poly(3-hydroxybutyrate-co-3-hydroxyvalerate) with Narrow Compositional Distribution. https://doi.org/10.1021/MA002120X

Shively, J. (1974). Inclusion bodies of prokaryotes. Annual Reviews in Microbiology, 28(1), 167–188.

Shively, J. M. (2006). Inclusions in prokaryotes (Vol. 1). Springer Science & Business Media.

Sikyta, B. (1995). Techniques in Applied Microbiology. Elsevier Science.

Silva, L. F. da, Gomez, J. G. C., Rocha, R. C. S., Taciro, M. K., & Pradella, J. G. da C. (2007). Produção biotecnológica de poli-hidroxialcanoatos para a geração de polímeros biodegradáveis no Brasil. Química Nova, 30(7), 1732–1743. https://doi.org/10.1590/S0100-40422007000700040

Sinclair, C. G., & Cantero, D. (1990). Fermentation modelling. In L. Harvey & B. McNeil (Eds.), Fermentation: a practical approach (pp. 65–112). Oxford: Oxford University Press.

Smolke, C. D. (2010). The metabolic pathway engineering handbook : tools and applications. CRC Press.

Society for General Microbiology. (1992). Prokaryotic structure and function : a new perspective. Cambridge University Press. Retrieved from https://books.google.fr/books/about/Prokaryotic_Structure_and_Function.html?id=o_U4cVeqIIQC&redir_esc=y

Solaiman, D. K., Ashby, R. D., Foglia, T. A., & Marmer, W. N. (2006). Conversion of agricultural feedstock and coproducts into poly (hydroxyalkanoates). Applied Microbiology and Biotechnology, 71(6), 783–789.

Sonnleitner, B., Heinzle, E., Braunegg, G., & Lafferty, R. (1979). Formal kinetics of poly-β-hydroxybutyric acid (PHB) production in Alcaligenes eutrophus H 16 and Mycoplana rubra R 14 with respect to the dissolved oxygen tension in ammonium-limited batch cultures. European Journal of Applied Microbiology and Biotechnology, 7(1), 1–10.

Špoljarić, I. V., Lopar, M., Koller, M., Muhr, A., Salerno, A., Reiterer, A., & Horvat, P. (2013). In silico optimization and low structured kinetic model of poly[(R)-3-hydroxybutyrate] synthesis by Cupriavidus necator DSM 545 by fed-batch cultivation on glycerol. Journal of Biotechnology, 168(4), 625–635. https://doi.org/10.1016/j.jbiotec.2013.08.019

Špoljarić, I. V., Lopar, M., Koller, M., Muhr, A., Salerno, A., Reiterer, A., Malli, K.,Angerer, H., Strohmeier, K.,Schober, S.,Mittelbach, M., Horvat, P. (2013). Mathematical modeling of poly[(R)-3-hydroxyalkanoate] synthesis by Cupriavidus necator DSM 545 on substrates stemming from biodiesel production. Bioresource Technology, 133, 482–494. https://doi.org/10.1016/j.biortech.2013.01.126

Stal, L. J. (1992). Poly (hydroxyalkanoate) in cyanobacteria: an overview. FEMS Microbiology Reviews, 9(2-4), 169–180.

Stanier, R. Y. (1951). Enzymatic Adaptation in Bacteria. Annual Review of Microbiology, 5(1), 35–56. https://doi.org/10.1146/annurev.mi.05.100151.000343

Steinmetz, S. A., Herrington, J. S., Winterrowd, C. K., Roberts, W. L., Wendt, J. O., & Linak, W. P. (2013). Crude glycerol combustion: Particulate, acrolein, and other volatile organic emissions. Proceedings of the Combustion Institute, 34(2), 2749–2757.

Suzuki, T., Yamane, T., & Shimizu, S. (1986). Mass production of poly-β-hydroxybutyric acid by fed-batch culture with controlled carbon/nitrogen feeding. Applied Microbiology and Biotechnology, 24(5), 370–374.

Szymanowska-Powałowska, D. (2015). The effect of high concentrations of glycerol on the growth, metabolism and adaptation capacity of Clostridium butyricum DSP1. Electronic Journal of Biotechnology, 18(2), 128–133. https://doi.org/10.1016/j.ejbt.2015.01.006

Tamdoğan, N., & Sidal, U. (2011). Investigation of Poly-β-Hydroxybutyrate (PHB) Production by Bacillus subtilis ATCC 6633 Under Different Conditions. Kafkas Üniversitesi Veteriner Fakültesi Dergisi, 17(173), 173–176. Retrieved from http://search.ebscohost.com/login.aspx?direct=true&db=a9h&AN=66697193&lang=es&site=ehost-live\nhttp://search.ebscohost.com/login.aspx?direct=true&db=a9h&AN=62294075&lang=es&site=ehost-live

Tan, G.-Y. A., Chen, C.-L., Li, L., Ge, L., Wang, L., Razaad, I. M. N., Li, Y., Zhao, L., Mo, Y., Wang, J.-Y. (2014). Start a research on biopolymer polyhydroxyalkanoate (PHA): a review. Polymers, 6(3), 706–754.

Tanadchangsaeng, N., & Yu, J. (2012). Microbial synthesis of polyhydroxybutyrate from glycerol: Gluconeogenesis, molecular weight and material properties of biopolyester. Biotechnology and Bioengineering, 109(11), 2808–2818. https://doi.org/10.1002/bit.24546

Tessier, G. (1936). Les lois quantitatives de la croissance. Annales de Physiologie et de Physiochimie Biologique, 12, 527–573.

Thauer, R. K., Jungermann, K., & Decker, K. (1977). Energy conservation in chemotrophic anaerobic bacteria. Bacteriological Reviews, 41(1), 100–80. Retrieved from http://www.ncbi.nlm.nih.gov/pubmed/860983

Tian, J., Sinskey, A. J., & Stubbe, J. (2005). Kinetic studies of polyhydroxybutyrate granule formation in Wautersia eutropha H16 by transmission electron microscopy. Journal of Bacteriology, 187(11), 3814–24. https://doi.org/10.1128/JB.187.11.3814-3824.2005

Tohyama, M., Patarinska, T., Qiang, Z., & Shimizu, K. (2002). Modeling of the mixed culture and periodic control for PHB production. Biochemical Engineering Journal, 10(3), 157–173.

Tokiwa, Y., Calabia, B. P., Ugwu, C. U., & Aiba, S. (2009). Biodegradability of Plastics. International Journal of Molecular Sciences, 10(9), 3722–3742. https://doi.org/10.3390/ijms10093722

Tripathi, A. D., Srivastava, S. K., & Singh, R. P. (2013). Statistical optimization of physical process variables for bio-plastic (PHB) production by Alcaligenes sp. Biomass and Bioenergy, 55, 243–250.

Tsoularis, A., & Wallace, J. (2002). Analysis of logistic growth models. Mathematical Biosciences, 179(1), 21–55. https://doi.org/10.1016/S0025-5564(02)00096-2

Vadlja, D., Koller, M., Novak, M., Braunegg, G., & Horvat, P. (2016). Footprint area analysis of binary imaged Cupriavidus necator cells to study PHB production at balanced, transient, and limited growth conditions in a cascade process. Applied Microbiology and Biotechnology, 100(23), 10065–10080. https://doi.org/10.1007/s00253-016-7844-6

Valappil, S. P., Misra, S. K., Boccaccini, A. R., & Roy, I. (2006). Biomedical applications of polyhydroxyalkanoates, an overview of animal testing and in vivo responses. Expert Review of Medical Devices, 3(6), 853–868.

van Gemerden, H., & Kuenen, J. G. (1984). Strategies for Growth and Evolution of Micro-Organisms in Oligotrophic Habitats. In Heterotrophic Activity in the Sea (pp. 25–54). Boston, MA: Springer US. https://doi.org/10.1007/978-1-4684-9010-7_2

Vandamme, P., & Coenye, T. (2004). Taxonomy of the genus Cupriavidus: a tale of lost and found. International Journal of Systematic and Evolutionary Microbiology, 54(6), 2285–2289.

Vaneechoutte, M. (2004). Wautersia gen. nov., a novel genus accommodating the phylogenetic lineage including Ralstonia eutropha and related species, and proposal of Ralstonia [Pseudomonas] syzygii (Roberts et al. 1990) comb. nov. International Journal of Systematic and Evolutionary Microbiology, 54(2), 317–327. https://doi.org/10.1099/ijs.0.02754-0

Van-Thuoc, D., Quillaguaman, J., Mamo, G., & Mattiasson, B. (2008). Utilization of agricultural residues for poly (3-hydroxybutyrate) production by Halomonas boliviensis LC1. Journal of Applied Microbiology, 104(2), 420–428.

Vendruscolo, F., Rossi, M. J., Schmidell, W., & Ninow, J. L. (2012). Determination of Oxygen Solubility in Liquid Media. ISRN Chemical Engineering, 2012, 1–5. https://doi.org/10.5402/2012/601458

Venkataramanan, K. P., & Scholz, C. (2014). Chapter 11 – Integrated Production of Butanol from Glycerol. In Biorefineries (pp. 225–233). https://doi.org/10.1016/B978-0-444-59498-3.00011-7

Verlinden, R. A., Hill, D. J., Kenward, M. A., Williams, C. D., Piotrowska-Seget, Z., & Radecka, I. K. (2011). Production of polyhydroxyalkanoates from waste frying oil by Cupriavidus necator. AMB Express, 1(1), 11. https://doi.org/10.1186/2191-0855-1-11

Vlysidis, A., Binns M., Webb C. & Theodoropoulos C. (2011). Glycerol Utilisation for the Production of Chemicals: Conversion to Succinic Acid, a Combined Experimental and Computational Study. Biochemical Engineering Journal 58-59 (1). Elsevier: 1–11. doi:10.1016/j.bej.2011.07.004.

Wei, Y.-H., Chen, W.-C., Huang, C.-K., Wu, H.-S., Sun, Y.-M., Lo, C.-W., & Janarthanan, O.-M. (2011). Screening and Evaluation of Polyhydroxybutyrate-Producing Strains from Indigenous Isolate Cupriavidus taiwanensis Strains. International Journal of Molecular Sciences, 12(12), 252–265. https://doi.org/10.3390/ijms12010252

Whitaker, W. B., Parent, M. A., Naughton, L. M., Richards, G. P., Blumerman, S. L., & Boyd, E. F. (2010). Modulation of Responses of Vibrio parahaemolyticus O3:K6 to pH and Temperature Stresses by Growth at Different Salt Concentrations. Applied and Environmental Microbiology, 76(14), 4720–4729. https://doi.org/10.1128/AEM.00474-10

Wilkinson, J. (1959). The problem of energy-storage compounds in bacteria. Experimental Cell Research, 7, 111–130. https://doi.org/10.1016/0014-4827(59)90237-X

Wittenberger, C. L., & Repaske, R. (1958). Studies on the electron transport system in Hydrogenomonas Eutropha. Bacteriological Procedures, (106).

Wodzinski Ad, R. S., & Johnson, M. J. (1968). Yields of Bacterial Cells from Hydracarbons, 16(12), 1886–1891.

Wu, Q., Huang, H., Hu, G., Chen, J., Ho, K., & Chen, G.-Q. (2001). Production of poly-3-hydroxybutyrate by Bacillus sp. JMa5 cultivated in molasses media. Antonie van Leeuwenhoek, 80(2), 111–118.

Yabuuchi, E., Kosako, Y., Yano, I., Hotta, H., & Nishiuchi, Y. (1995). Transfer of Two Burkholderia and An Alcaligenes Species to Ralstonia Gen. Nov. Microbiology and Immunology, 39(11), 897–904. https://doi.org/10.1111/j.1348-0421.1995.tb03275.x

Yamane, T. (1993). Yield of poly-D(-)-3-hydroxybutyrate from various carbon sources: A theoretical study. Biotechnology and Bioengineering, 41(1), 165–170. https://doi.org/10.1002/bit.260410122

Yu, S.-T., Lin, C., & Too, J. (2005). PHBV production by Ralstoniaeutropha in a continuous stirred tank reactor. Process Biochemistry, 40(8), 2729–2734.

Zhu, C., Nomura, C. T., Perrotta, J. A., Stipanovic, A. J., & Nakas, J. P. (2009). Production and characterization of poly-3-hydroxybutyrate from biodiesel-glycerol by Burkholderia cepacia ATCC 17759. Biotechnology Progress, NA–NA. https://doi.org/10.1002/btpr.355

Znad, H., Blažej, M., Báleš, V., & Markoš, J. (2004). A Kinetic Model for Gluconic Acid Production by Aspergillus niger. Chemicals Papers, 58(1), 23–28.